UNIVERSITY OF BIRMINGHAM

INVESTIGATING THE IMPACT OF SINGLE BOUTS OF EXERCISE ON THE NUMBER AND FUNCTION OF PERIPHERAL BLOOD IMMUNE CELLS

By

FENDI PRADANA

A thesis submitted to the University of Birmingham for the degree of

DOCTOR OF PHILOSOPHY

School of Sport, Exercise and Rehabilitation Sciences

College of Life and Environmental Sciences

University of Birmingham

May 2024

Abstract

Single bouts of exercise elicit changes to the number of immune cells within the bloodstream of humans. The initial transient increase in cell types including haemopoietic and progenitor cells (HSPCs) may offer relevance in the context of peripheral blood stem cell donations, which are used to collect HSPCs to treat various haematological disorders. The composition of the collected HSPC-rich immune graft is equally important, with higher numbers of cytolytic natural killer (NK) cells predicting better health outcomes in patients, and strikingly, these cells are mobilised up to 10-fold during exercise. Mobilisation of immune cells during exercise forms part of a dynamic response in recovery, that may drive immune remodelling when repeated over time. The mechanisms underpinning this are not well understood, but recent work has started to examine bioenergetic responses within the total peripheral blood mononuclear cell (PBMC) fraction. PBMCs are a highly heterogeneous population of T and B lymphocytes and monocytes, each with various subsets with distinct bioenergetic profiles. Given that single bouts of exercise evoke marked compositional changes to PBMCs, providing single cell resolution of immunometabolic changes is crucial to facilitate understanding of the acute immune response to exercise.

Chapter 2 investigated differences in HSPC and cytolytic NK cell concentrations during and after continuous and interval-based cycling bouts utilising high intensity interval exercise (HIIE). We demonstrated that 2 x 2-minute bouts of HIIE (90-95% HR_{max}) were sufficient to increase peripheral blood HSPC concentrations above rest, but not in response to 30 minutes of continuous cycling at moderate intensity. Furthermore,

peripheral blood was enriched with higher numbers of cytolytic NK cells following bouts of high and low volume HIIE, compared to moderate intensity cycling. These data indicate that a very low volume of cycling at a high intensity can potentiate peripheral blood HSPC concentrations and provides a rationale for exploring whether intermittent cycling during PBSC collections can increase the yield of HSPCs for transplant.

Chapter 3 developed methods using extracellular flux analysis to examine the metabolic phenotype and real time responses to *ex vivo* activation of enriched naïve Helper and Cytotoxic T cells vs. PBMCs. Conditions were optimised for nutrient assay conditions (i.e., glucose and glutamine concentrations) and blood collection procedures (anticoagulant and blood 'sitting' time) to provide a robust experimental model for chapter 4 of this thesis.

Chapter 4 utilised an innovative human study design and methodology to investigate the impact of prolonged moderate intensity cycling on the energy metabolism of naïve T cells. This study provided detailed analysis at the single cell level for both naïve $CD4^+$ and $CD8^+$ T cell subsets. This chapter showed that a 2-hour session of cycling at a moderate intensity (define by a power output that reaches 95% of the lactate threshold-1) did not cause any changes in the metabolic profiles of naïve $CD4^+$ and $CD8^+$ T cells, or peripheral blood mononuclear cells (PBMCs), immediately after or 2 hours into recovery, compared to rest. This included comprehensive measures of mitochondrial respiration, glycolytic flux, and ATP synthesis rates. Furthermore, there were no differences in the bioenergetic responses to *ex vivo* activation of PBMCs or enriched naïve T cells based on sampling before, immediately after or 2 hours following cycling

completion. These data indicate that the metabolism of PBMCs and naïve T cells are unaltered within 2 hours of prolonged moderate intensity cycling.

Overall, this thesis presents novel data on acute changes in circulating immune cell number and function within peripheral blood.

Acknowledgments

I would like to begin my acknowledgements by first thanking to those closest to me, Mama and Papa, thank you for countless sacrifices you both made throughout my life. I hope You both are happy there and know that I was able to finish this thesis. I will forever love you.

Next, to the most inspiring duo to me, my Supervisors. To Dr Alex, I could not thank you enough for your patience, support, understanding, and being like big brother to me over 4 years of my PhD. I have learnt so much from you. I was impressed by the level of attention in science you have shown me and it has consistently inspired me to grow more as a scientist. To Professor Gareth, thank you so much for always offering help during my study. I am fortunate and thankful to have you both as my supervisors. I hope in the future we can all continue working together.

I would like to thank my best friends: Phoebe, Megan, Tim, Israel, Rita, Barny, Jack, Rachel and all colleagues and SportExR's staffs who have supported me during my study. Thank you for always checking on me and giving me valued advice over the past three years.

Finally, I would like to thank Indonesian Government through Kementerian Keuangan Republik Indonesia that allowed me to achieve my dream.

List of conference communications, publications, and awards

Conference Communications

The 27th Annual Congress of the European College of Sports Science (ECSS). Sevilla, August 2022. Oral presentation. Young Investigator category. Investigating Changes in Hematopoietic Stem and Progenitor Cell Concentrations during and after continuous vs. interval-based exercise bouts.

Publications in Peer Reviewed Journals

Pradana, F., Nijjar., T., Cox, P.A., Morgan, P.T., Podlogar, T., Lucas, S.E., Drayson, M.T., Kinsella, F.A.M., Wadley, A.J., (2024). Brief cycling intervals incrementally increase the number of hematopoietic stem & progenitor cells in human peripheral blood, *Frontiers in Physiology.* *https://doi.org/10.3389/fphys.2024.1327269*.

Wadley, A.J., **Pradana, F.,** Nijjar, T.S., Drayson, M.T., Lucas, S.E., Kinsella, F.A.M., Cox, P.A., (2024). Intra-Apheresis Cycling to Improve the Clinical Efficacy of Peripheral Blood Stem Cell Donations: A Narrative Review, *Sports Medicine (submitted).*

Pradana, **F.,** Barlow, J.P., Shayler, J., Dimeloe, S.K., Gudgeon, N., Podlogar, T., Wallis, G.A., Wadley, A.J., (2024). Immunometabolic profiling of isolated and mixed T cell populations in response to prolonged moderate intensity cycling in humans *Exercise Immunology Review (in preparation).*

Cox, P.A., **Pradana, F.,** Noble, E., Lucas, S.E., Stathi, A., Pratt, G., Drayson, M.T., Amin, K., Kinsella, F.A.M., Wadley, A.J., (2024). Intermittent high and moderate intensity cycling intervals over 3-hours sustain higher concentrations of hematopoietic stem and natural killer cells vs. time-matched rest, *Stem Cell Research and Therapy (in preparation).*

Awards

1. 2024 - Associate Fellowship - Advance Higher Education (HE), Associate Fellow of the Higher Education Academy (AFHEA).
2. 2022 - Turing Scheme grant, Short-term Global Placement (student mobility programme).
3. 2020 – 2024 - Scholarship for PhD studies at the University of Birmingham, United Kingdom, Republic of Indonesia.

COVID-19 statement:

The COVID-19 pandemic had a significant impact on the amount of work included in this thesis. Due to restrictions, there was no access to facilities or participants for 8 months during the four-year PhD process, but multiple pilot work was required to optimise methods and resulted ethics amendment. Unfortunately, besides COVID-19 restriction, ethical approval took again a long delay to start the study in Chapter 2 and 4.

Table of Contents

List of Figures

List of Tables

List of Abbreviations

β2 = beta 2

2-DG = 2-deoxy-D-glucose

7-AAD = 7-Aminoactinomycin D

ANOVA = Analysis of variance

ATP = adenosine triphosphate

AUC = area under the curve

CD = cluster differentiation

CM = central memory

CO_2 = carbon dioxide

CXCL-12 = C-X-C motif chemokine 12

CXCR-4 = C-X-C chemokine receptor 4

D-PBS = dulbecco's phosphate-buffered saline

DPFC = double platform flow cytometry

ECAR = extracellular acidification rate

EDTA = ethylene-diamine-tetra-acetic acid

EFA = extracellular flux analysis

EM = effector memory

FBS = fetal bovine serum

FMO = fluorescence minus one

FSC-A = forward side scatter-area

FSC-H = forward side scatter-height

G-CSF = granulocyte colony stimulating factor

GPPAQ = general practice physical activity questionnaire

GvHD = graft-versus-host disease

HGlu = high glucose

HIIE = high intensity interval exercise

HLA = human leukocyte antigen

HR = heart rate

HR_{max} = maximum heart rate

HSC = hematopoietic stem cell

HSPC = haematopoietic stem and progenitor cell

HSCT= haematopoietic stem cell transplantation

HV-HIIE = high volume-high intensity interval exercise

ISHAGE = The International Society of Hematotherapy and Graft Engineering

K_2EDTA = potassium ethylene-diamine-tetra-acetic acid

LGlut = low glutamine

LV-HIIE = low volume-high intensity interval exercise

MACS = magnetic activated cell sorting

MFI = median fluorescence intensity

MICE = moderate intensity continuous exercise

MS = mass spectrophotometry

NGlu = normal glucose

NGlut = normal glutamine

NK cell = natural killer cell

OCR = oxygen consumption rate

PBMC = peripheral blood mononuclear cell

PBSC = peripheral blood stem cell

PE = phycoerythrin

PER = proton efflux rate

RNA = ribonucleic acid

RPE = ratings of perceived exertion

RPM = rotations/minute

RPMI = roswell park memorial institute

SD = standard deviation

SI =stain index

SPFC = single platform flow cytometry

SS = single stained

Temp = temperature

TEMRA = T effector memory re-expressing CD45RA

US = unstained

VCAM-1 = vascular cellular adhesion molecule 1

VLA-4 = Very Late antigen 4

$Watt_{max}$ = maximal power

WBC = white blood cell

ZGlu = zero glucose

ZGlut = zero glutamine

Thesis Outline

This thesis is composed of 5 chapters and begins with Chapter 1 providing general introduction to immunology in the context of exercise. This chapter forms a narrative review discussing how single sessions of exercise impact the number and function of immune cells in peripheral blood.

Chapter 2 aimed to investigate the impact of continuous vs. interval exercise on HSPC concentration and function. This provides the rational of the feasibility and clinical implementation of interval cycling in a PBSC donation context.

Chapter 3 elucidates the details of method development to implement in experimental Chapter 4. Chapter 3 optimised experimental methods to examine real-time immunometabolic processes in T cells using EFA assays in a Jurkat cell line and enriched primary naïve $CD4^+$ and $CD8^+$ T cells.

Chapter 4 investigates the effect of prolonged moderate intensity exercise on T cell bioenergetics in isolated vs. mixed cell populations (PBMCs). Chapter 4 examined whether 2-hour moderate intensity cycling can have effect on how immune cell modulate bioenergetics.

Finally, Chapter 5 outlines key findings from the experimental chapters and presents directions for future research.

Chapter 1: General Introduction

1.1 Thesis Overview

The immune system is a complex network of proteins, cells, and organs, that defend the body against infection, repair tissues and prevent disease (1). The immune system responds to multiple physiological cues and adapts or degrades depending on the magnitude and duration of the exposure. Over a century ago, a landmark paper reported a marked increase in peripheral white blood cell concentration after a single bout of exercise (2). A wave of investigations on the immune system's response to both acute (single bout) and chronic (repeated bouts) exercise have since been undertaken in populations across the spectrum of human health. These include athletes (3–5), older adults (6–8) and people with communicable and non-communicable disease (9), thus sparking interest in the combined disciplines of exercise immunology with sports nutrition, athlete well-being and more recently clinical health.

Alterations in substrate availability within immune cells during exercise is responsible for mediating the movement of the cells towards the bloodstream that may indicate a stimulation for substrate uptake to meet their energy demand (10–12). However, these claims require further study due to a series of factors, notably limited data at a single cell level. This is important given that the immune system is highly heterogeneous with specific roles and metabolic profiles; however, novel methodologies are now offering huge potential to unravel this complex picture and analyse immune cell function with a high degree of sensitivity and accuracy at the single cell level (13–18). The field of

immunometabolism is a rapidly expanding field in immunological research, with rewiring of cellular metabolism now linked with modulating multiple immune processes (19). Despite the high energy demands of a bout of prolonged moderate intensity exercise, its impact on the metabolism of immune cells at a single cell level has yet to be investigated.

As well as understanding how the function of immune cells changes with acute exercise, there has been much interest in exploiting changes in the number and composition of immune cells after exercise in clinical practice, such as peripheral blood stem cell (PBSC) donations. A single bout of exercise enriches peripheral blood with cells capable of killing viruses and tumour cells (e.g., natural killer cells), as well as stem cell populations (e.g., haemopoietic stem and progenitor cells (HSPCs) and mesenchymal stem cells (MSCs) that repair and regenerate tissues, notably the immune system. This dynamic physiological response is thus hugely attractive to clinicians and patients for the potential treatment of people with a variety of illnesses characterised by impaired immunity. Despite the strength of the underpinning science supporting this concept, the practicalities of how this might feasibly work have yet to addressed. Given the transient nature of the increase of these cells in peripheral blood (<15 minutes) and the length of time taken to undertake a peripheral blood stem cell donation (3–4 hours), intermittent exercise is perhaps the only feasible strategy to maximise the concentrations of these cell types over time. The optimal intensity and duration of these intervals for different types of donors and how exercise impacts the quality of these cells are however far from clear.

This thesis aims to address two primary research questions through the design of acute exercise studies: 1) can intermittent exercise sustain peripheral blood concentrations of HSPCs compared to steady state exercise and 2) how does a single bout of prolonged moderate intensity exercise impact bioenergetics in mixed vs. isolated immune cell populations.

This thesis is composed of 5 chapters, beginning with a background to immunology in the context of exercise, with a primary focus on how single sessions of exercise impact the number and function of immune cells in peripheral blood (Chapter 1). Chapter 2 evaluates the impact of continuous vs. interval exercise on HSPC concentration and function. Chapter 3 provides details of the development of methods for implementation in experimental chapter 4 that investigates the effect of prolonged moderate intensity exercise on T cell bioenergetics in isolated vs. mixed cell populations. Finally, Chapter 5 outlines key findings from the experimental chapters and presents directions for future research.

1.2 The Immune System

The human body is consistently under exposure of pathogenic agents, such as parasites, virus, bacteria, and fungi (20). The immune system is a complex array of cells that defend the body against these pathogens and coordinate the repair and turnover of bodily tissues by exhibiting various effector functions (21,22). Immune cells express unique combinations of molecules on their cell surface (e.g., cluster of differentiation (CD) and pattern recognition receptors (PRR), which indicate their stage of lineage-specific differentiation, phenotype and/ or current functional state (e.g.,

activation) (23). Fluorescently conjugated monoclonal antibodies are commonly used to detect these molecules to identify and classify immune cell populations using flow cytometry (23). Mature immune cells are produced from the bone marrow derived haematopoietic stem cell (HSC) lineage. HSCs differentiate into cells of the myeloid or lymphoid lineage and form the two key components of cellular and humoral immunity, namely innate (non-specific or natural) and adaptive (specific or acquired) respectively (24). These cells and chemicals are circulated via the lymphatic system - a group of tissues (lymph nodes and tonsils), vessels (lymphatic capillaries) and organs (bone marrow, spleen, and thymus) that work together to gather excess fluids, filter out waste products, and initiate specialised immune responses (25).

1.2.1 Haematopoietic Stem Cell Lineage

The majority of specialised cells present in mammalian blood have varying yet restricted lifespans and require continuous replenishment that relies on a group of precursor cells. These cells are pluripotent able to self-renew and develop into diverse types of blood cells including immune cells (26). During fetal stage, the migratory capabilities of HSCs have been associated with their function to undergo multiple modifications and differentiate into haematopoietic progenitor cells (HPCs) (27). However, HSCs progressively lose the ability to differentiate into certain cell lineages upon entering aging phase (28). The loss of self-renewal potential of HSCs into a specific cell lineage leads to the commitment of HPCs to differentiate into different cell lineages (29). HPCs can differentiate into blood cells, which fall under lymphoid or myeloid lineage. The lymphoid lineage consists of T, B, and natural killer (NK) cells,

whereas the myeloid lineage comprises megakaryocytes and erythrocytes, as well as granulocytes and macrophages (30,31).

1.2.2 Innate Immunity

The ability of innate immune cells to recognise foreign molecules is programmed in the specialised cell lineage (germline) responsible for carrying and transferring genetic information between generations. As a result, this system is highly conserved in humans and has been historically defined as having no memory function, although this notion has recently been challenged (32). Cells of the innate immune system include dendritic cells (DC), macrophages, monocytes, neutrophils and NK cells, and use pattern recognition receptors (PRRs), including Toll-like receptors (TLRs), C-type lectin receptors (CLRs), and galectin family proteins to detect pathogen-associated molecular patterns (PAMPs) (32) which are conserved molecular structures found in several types of bacteria, such as endotoxin or lipopolysaccharides (LPS), teichoic acids, or bacterial DNA (33).

Innate immunity is the first system of body defence employed by the host immediately or within hours of encountering a pathogen and for governing tissue repair (34). The innate immune system comprises four types of defensive lines: anatomic or physical barriers (skin and mucous membrane), physiological (temperature, acidity, and chemical mediators), phagocytic (dendritic cells, neutrophils, monocytes, macrophages, basophils, and eosinophils) and soluble inflammatory molecules (interleukins (IL), interferons (IFN), tumour necrosis factors (TNF), colony-stimulating factors and histamine) (35). Notably, mucosal surfaces are responsible for protecting

the respiratory tract, nasal passages, and intestines from opportunistic pathogens triggering an infection (36). Failing this, innate immune cells comprising granulocytes (neutrophils, eosinophils, and basophils), monocytes/macrophages, DC, and NK cells) are the next line of defence against these pathogens. Granulocytes are a type of white blood cell containing small granules that secrete proteins such as cytokines, chemokines, and digestive enzymes to rapidly break down pathogens (37). Different from the other innate immune cells, NK cells are lymphocytes (one cell group in adaptive immune system) that are able to release cytokines upon activation and play a vital part in the elimination of cancer cells as well as the clearing of virally infected cells (38,39) by enhancing their lysis properties (cytolytic activity) towards virus infected or transformed cells (40,41). Since NK has non-specific response to an antigen, it provides antigen-independent defence mechanism leading to generate non immunologic memory response and therefore cannot recognise subsequence infection of the same pathogen in the future (20).

1.2.3 Adaptive Immunity

Operating in conjunction with the innate immune system are organs, cells and chemicals of the adaptive immune system. The solitary cells of the adaptive immune system are called lymphocytes, composed of T and B cells. T cells are activated through interaction with Antigen Presenting Cells (APCs) such as dendritic cells that ingest pathogens and present antigens to T cells via the major histocompatibility complex (MHC) within lymph nodes (19). B cells can also be activated in this manner, as well as via T cell dependent mechanisms that results in their differentiation into plasma cells to manufacture antibodies (immunoglobulins, Ig) (20). Immature T and B

cells undergo antigen receptor gene rearrangements during development (negative selection), resulting in an extremely diversified repertoire of antigen-specific receptors capable of identifying all possible antigens (42). The early lymphocytes (T and B cells), like those of other blood cells, come from HPCs produced in bone marrow (43). As they are highly mobile, T cells specifically travel to thymus glands (primary lymphoid organ) for maturation and migrate to secondary lymphoid organs like lymph nodes and spleen where they capture circulating antigens from lymph and blood. Lymphocytes emigrating from the spleen and lymph nodes moreover can subsequently perform effector roles (antigen-attacking ability) at a variety of locations throughout the body such as common sites of infection (44).

T cells are broadly grouped into two subpopulations including $CD8^+$ T cells known as killer or cytotoxic T cells that elicit immune response against intracellular pathogens such as virus-infected or cancerous cells (45), and CD4+ T cells, also known as helper T cells, which coordinate immune responses (e.g., activation of B cells and macrophages by producing cytokines) against different types of pathogens (46). Moreover, each T cell subpopulation has different subsets including naïve T cells which are novel to antigen exposure and defined by cell surface receptor expression of $CD45RA^+CCR7^+$. Federica *et al*. (1999) reported that naïve T cells have uniform expression of CCR7 which mediates their homing to primary lymphoid tissues (47). Memory T cells are developed after antigen exposure and are commonly distinguished by the presence or absence of CD45RA and CCR7 receptor expression, subcategorised into central memory (CM) T cells ($CD45RA^-CCR7^+$) which traffic to lymphoid tissues, effector memory (EM) T cells ($CD45RA^-CCR7^-$) which migrate to

multiple peripheral tissue sites and terminally differentiated effector memory (TEMRA) T cells ($CD45RA^{+}CCR7^{-}$) (47,48). Different from naïve subsets, memory subsets have experience of a diverse range of antigen exposures over the course of person's life and facilitate more rapid immune responses to infections caused by the same pathogen (49).

B cells have a variety of activities in the immune system, including antigen presentation, cytokine secretion, and establishing the architecture of lymphoid organs, but their principal function is their differentiation into plasma cell producing antibodies (50). Unlike T cells, B cells have unique antibodies on their cell surface that allow them to identify antigens without the use of APCs (20).

When the body is exposed to infection, tissue damage, inflammation, or dysregulation of immune system, a sequence of biochemical and physiological events evokes the mobilisation of both innate and adaptive immune cells into peripheral blood. It is well established that single bouts of physical exercise elicit mobilisation of all the main types of white blood cells (leukocytes) into the bloodstream, a response termed leukocytosis. Repeated exposure to exercise-induced leukocytosis over periods of exercise training are then believed able to drive a series of adaptations to the immune system that enhance immune surveillance, improve health, and lower risk of illness (51–53).

1.3 Exercise and Immune System

1.3.1 Chronic Exercise and the Immune System

Current evidence indicates that engaging in regular physical activity and/ or structured bouts of exercise lowers the risk of both communicable (e.g. bacterial and viral or diseases all characterised by compromised immunity) (9,52). Studies have demonstrated that regular exercise training elicits a range of anti-inflammatory effects. For example, regular exercise stimulates the hypothalamic-pituitary-adrenal axis and sympathetic nervous system (SNS) (54), which heightens the release of plasma cortisol and adrenaline that downregulate the production of pro-inflammatory cytokines (e.g., TNF-α and IL-1β in immune cells) (55,56). Moreover, increased secretion of myokines (specifically IL-6) from skeletal muscle can lower the systemic inflammatory profile with regular training (53). Changes to the composition of inflammatory immune cells within peripheral blood (57) and tissues (e.g., adipose tissue-resident macrophages (58)) have also been reported with regular exercise training. Timmerman *et al.* (2008) reported that a 12-week exercise programme substantially decreased the percentage of pro-inflammatory monocytes in the peripheral blood of physically inactive older adults (57). There is also data to indicate that exercise training can reduce the expression of receptors on cell membranes that control the function, mobility, and production of inflammatory cytokines by immune cells (53). At present, the contribution of changes in body composition that accompany training (59) and direct changes to cells of the immune system (58) on the anti-inflammatory effects of exercise are unclear in humans. Nonetheless, regular exercise training improves aspects of immune function, and this has been eloquently demonstrated by studies

reporting improvements in *in vivo* immunity, notably wound healing (60), vaccination responses (61,62), and a lower incidence and severity of common upper respiratory tract infections (URTI) (9,52,63,64).

A consistent narrative in the literature over the past 40 years has been that high training loads can impair immune function and increase susceptibility to URTIs (64–66). The J-shaped model was first proposed following a study reporting a higher incidence of URTIs in runners after the Los Angeles marathon (66). Coupled to this, studies have reported relationships between URTIs and immune outcomes measured in the bloodstream, including the number, frequency and/ or function of immune cell populations, and the concentration of proteins released from immunological cells or tissues (e.g., cytokines and antibodies) (53,66–71). However, recent limitations have been emphasised with regards to this body of literature (52).

Many studies investigating the effect of exercise on immune cell function had been conducted by collecting data from self-reported incidence of URTI and not a clinically confirmed infection (9,52). With regards to analysis at the level of the immune system, laboratory methods have mostly examined functional changes (e.g., proliferation and cytokine production) within the PBMC fraction, which is a heterogenous mix of lymphocytes and monocytes (63,68,69,72,73). In fact, the composition of cell types within peripheral blood (74) and tissues (75) has been reported to change after periods of exercise training (9,52,63). These shifts in cell composition are more marked in response to individual bouts of exercise, which are regularly used to examine and model the influence of exercise on the immune system (76). The next section will

overview the impact of single (or 'acute') bouts of exercise on the immune system before then focussing on two applications for this thesis: 1) the potential to harvest certain cells as a result of this acute response **(section 1.4)** and 2) examining functional changes, namely immunometabolic, underpinning the mobilisation of immune cells during bouts of exercise **(section 1.7).**

1.3.2 Acute Exercise and the Immune System

One of the most reproduced discoveries in exercise immunology since 1902 (2) is the rapid increase in peripheral blood leukocytes during exercise (77,78). Single bouts of exercise cause remargination of all major leukocytes, which is mediated by an increase in hemodynamic shear forces and the release of catecholamines resulting a striking leukocytosis. This response is not uniform, with a substantial intensity-dependent increase in antigen experienced effector cells observed, notably non-classical monocytes (79), gamma-delta T cells (80–82), cytotoxic T cells (80,81) and NK cells (79,80). The latter are the most sensitive to mobilisation with exercise, specifically the cytolytic subset expressing low amount of CD56 (termed $CD56_{dim}$ NK cells), due to their higher density of β_2-adrenergic receptors compared to other subsets (83,84). This increase in count is also matched by a rise of NK cytolytic activity (85–87), indicating that exercise-induce leukocytosis is likely a functional response indicative of enhanced immunity.

Within minutes of exercise cessation, lymphocytes and monocytes rapidly egress from the peripheral blood compartment (80), either becoming remarginalised or later (1-3 hours) migrating to peripheral tissues mediated by glucocorticoid signalling (61). NK

cells, B cells and T cells exhibit this biphasic pattern (80,88–91), exemplified by a rapid increase in peripheral blood concentration during (92) and a decrease below resting concentration within hours of the bout (80). It is now widely accepted that this decrease in concentration results from the redistribution of these cells to peripheral tissues (discussed in **section 1.6** below), particularly those that mount vast effector functions. Indeed, effector memory $CD8^+$ T cells and $CD56_{dim}$ NK cells are essential in eradicating malignant or virus infected cells (1,61,93) and these lymphocytes are the most responsive to mobilisation during exercise (1,79,93,94). Unlike T and NK cells, Turner *et al*. (2016), reported that B cell mobilisation during exercise was not influenced by effector status, yet immature cells, which could benefit in the detection of new pathogens (95). Similarly, neutrophil numbers, which increase in peripheral blood during exercise and continue to increase in recovery, result from the appearance of immature neutrophils from the bone marrow (96–98). Although circulating in substantially lower numbers, concentrations of different lineages of stem cells (i.e., endothelial (ESC), hematopoietic (HSC), and mesenchymal (MSC)) also increase in peripheral blood during and after bouts of exercise (99). Together with the enrichment of NK cells and effector lymphocytes (100), this has led to an emerging interest in whether exercise could be a powerful adjuvant to isolate stem cells, particularly HSCs, for clinical benefit (100,101).

1.4 Exercise and Immune Cell Harvest

HSPCs play an important role in processes of cell regeneration in the human body. The bone marrow is a rich source of HSPCs, which are principally involved in the maintenance of hematopoietic system, namely formation of cells of the innate and

adaptive immune system (102,103). The importance of HSPCs in the regeneration of the immune system makes their utility paramount for the treatment of various haematological malignancies and other blood disorders (100,101,104). Every year approximately 90,000 people worldwide receive hematopoietic stem cell transplants (HSCT) (105), with approximately 2,000 of these taking place in the United Kingdom (106).

In transplantation setting, HSPCs can be obtained from a variety of sources, including mobilised peripheral blood (mPB) termed PBSC, umbilical cord blood (CB), and bone marrow (BM) (107,108). However, HSPC collection from PBSC is favourable because it allows for faster recipient reconstitution than CB and easier access than BM. PBSC HSPCs therefore are currently used in nearly all autologous transplants and 75% of allogeneic transplants (107,108). PBSC collections are carried out by the patient requiring the HSCT prior to their treatment (autologous donor) or a human leukocyte antigen (HLA)-matched donor (allogeneic donor).

Bone marrow-derived HSPCs circulate in modest numbers in peripheral blood under homeostatic settings (109). Since HSPCs are limited in peripheral blood circulation, pharmacological intervention is mandatory to mobilise HSCs from the bone marrow for PBSC collections (107). Intradermal injections of granulocyte-colony stimulating factor (G-CSF) for 4–5 days are administered to stimulate proliferation of HSPCs in the bone marrow and migration into peripheral blood. This raises the concentration to the required HSPC collection threshold, and enables commencement of apheresis, the process of extracting the immune cell fraction from blood (108,110). Despite the fact

that G-CSF has been utilised during PBSC collections since the 1980s, there are still significant therapeutic hurdles for both autologous and allogeneic donors.

With up to 40% of autologous donors classified as "poor mobilizers" during PBSC collections, engraftment failure is more common for autologous HSCT (111). Because these individuals do not respond well to pharmacological treatments, it is difficult to harvest enough HSPCs for transplantation. In some individuals, therefore prolonged apheresis, numerous mobilisation attempts, or alternate HSPC collection methods are required, leading in higher health-care expenses and significant psychological impacts on patients (112). Moreover, side effects of G-CSF administration such us bone pain and nausea have been identified as factors that may dissuade potential HSPC donors (110,113). As a result, improved techniques for HSPC mobilisation in an autologous HSCT setting are required.

On the other hand, with less than 5% failure (114), allogeneic donations are largely successful with regards to harvesting sufficient HSPCs. However, the composition of other cells (such as NK and T cells) within the HSPC-rich graft from the allogeneic donor can result in significant health issues following the HSCT, namely a medical condition known as Graft vs. Host Disease (GvHD) (115,116). GvHD causes damage to immunodeficient tissues, such as the skin, digestive system, and liver, in individuals who have received an allogeneic graft. Acute GvHD can long up to 100 days with around 50% occurrence rate, whereas chronic GvHD can range from 6% to 80% (117). This condition leads to death in approximately 15% of recipient (118). The composition

of other cells in the graft such as cytolytic natural killer ($CD56_{dim}$ NK) cells have been associated with a lower risk of GvHD (115,116).

High intensity exercise without G-CSF administration results in peak concentrations of HSPCs at around 5 cells/μL in the bloodstream which is equivalent to an estimated dose of about 320,000 HSPCs/kg (120,121). However, 10–150 HSPCs/μL are achieved after 5 days of G-CSF therapy which is superior to non-pharmaceutical treatment, and it remains at that level for several days (122). HSPCs can be mobilised without the need of pharmaceutical drugs, but to a lesser extent. Moreover, the amount of HSPCs in peripheral blood varies throughout the day and is influenced by circadian rhythms (123). Similarly, acute physiological stress can raise HSPC levels in the peripheral circulation quickly and transiently (124). Exercise, as a type of physiological stress has been demonstrated to mobilise hematopoietic progenitor cells, which may aid in the repair of tissue injured during the activity (125–127). HSPCs concentration increases transiently by 1–2.5-fold over resting levels (120,121,128) and for $CD56_{dim}$ NK cells, this can be up to 10-fold (83).

Table 1.1 Research on Exercise-induced HSPC Mobilisation.

Author	Subject	Study Design	Key Finding
Callanan *et al*., 2021 (129)	16 healthy males (aged 20 – 39 years)	Cycling for 20 minutes.	There was a significant increase in $CD34^+$ cells (3.9 ± 2.0 to 5.3 ± 2.8 cells/μL, $P < 0.001$) following exercise.

Author	Subject	Study Design	Key Finding
Wu *et al*., 2020 (130)	22 healthy males (aged 25 – 62 years)	Participants practiced the day easy exercise (DEE) twice a day, 30 min each time for 3 months.	DEE increased the proportion of CD34+ circulating in peripheral blood of adults after 1-month practice (4.7 ± 2.31 to 8.8 ± 4.73 cells/μL, P = 0.007).
Nederveen *et al*., 2020 (105)	16 healthy males (aged 21.5 – 69.9 years)	Subjects completed 10 × 60 s intervals of high intensity interval training (HIIT) on cycle ergometer at a workload which elicited ~90% maximal HR (HRmax)	CD34+ cells per millilitre of blood increased immediately post-exercise, older males (~ 101%, P < 0.05) and young males (~ 352%, P < 0.05)
O'Carroll *et al*., 2019 (131)	12 participants (aged 29 ± 2 years)	Participants completed a 45-min bout of continuous (CONTEX) and 6 x 20 s sprint interval exercise (SPRINT) on a cycle ergometer	Circulating CD34+CD45 dim progenitor cells were higher immediately post-exercise in SPRINT (1,515 ± 206 to 2,496 ± 443 cells/mL, P = 0.03), but unchanged in CONTEX.
Anz *et al*., 2019 (132)	20 healthy subjects (aged 21- 45 years)	A 20-minute vigorous exercise regimen on an upright stationary bike at 70% to 85% of maximum target heart rate.	Concentration of mobilized hematopoietic stem cells was significantly higher following exercise, from 1.7/μL to 2.7/μL, P = 0.043).
Agha *et al*., 2018 (102)	15 healthy runners (aged 28.3 ± 7.8 years)	On separate days in random order, perform a single bout of treadmill running exercise consisting of either 30-min of steady state running at +15% of ventilatory threshold (VT) (vigorous) or 90-min of steady state running at -5% of VT (moderate).	A significant ($p < 0.05$) increase in the number of $CD34^+$ HSCs at 15-min of vigorous vs 1h moderate intensity (4.2 ± 1.42 vs 3.25 ± 1.43, P < 0.001) and immediately post-exercise for vigorous vs moderate intensity (4.40 ± 1.37 vs 2.78 ± 1.15; P < 0.001).
Niemiro *et al.*, 2017 (133)	7 healthy men (aged 25.3 ± 2.4 years)	A maximal exercise test on a motorized treadmill increases of 1% per minute until volitional exhaustion.	The circulating progenitor cells (CPCs) are significantly increased 2.7 and 2.4-fold, respectively, at 20 and 40 minutes into exercise compared with Pre values.

Author	Subject	Study Design	Key Finding
Baker *et al.*, 2017 (134)	11 healthy men (aged 23.5 ± 2.9 years)	Healthy individuals were exercised on a cycle ergometer at 70% of their peak work rate (WR_{peak}) until volitional fatigue and at 30% of their WR peak work matched to the 70% WRpeak bout.	The 70% WR_{peak} exercise group showed greater mobilization immediately post-exercise (98.4%, $P < 0.05$), while there was no observable increase in mobilization in the work matched 30% WR_{peak} exercise group.
Ribeiro *et al*., 2017 (135)	38 women (aged 20.87 ± 1.3 years)	A resistance exercise session at an intensity of 60% (n = 13), 70% (n = 12) or 80% (n = 13) of one repetition maximum.	Circulating CD34+ cells was significantly higher after exercise (49.3%, $P < 0.001$) and the change from baseline was greatest in the 80% group (81.1%, $P < 0.001$), reaching the highest at 6 hours post-exercise.
Harris *et al*., 2017 (136)	15 healthy postmenopausal women (aged 63 ± 4 years)	30 min acute moderate-intensity continuous (CON), interval (MOD-INT), and heavy-intensity interval (HEAVY-INT) exercise.	CD34+ number did not change post exercise regardless of exercise type ($P > 0.05$).
Marycz *et al*., 2016 (137)	12 healthy runners (aged 20 – 28 years)	Long-distance running for one year, six times per week.	Endurance exercise increased the number of HSPCs circulating in peripheral blood ($P < 0.05$).
Lutz *et al*., 2016 (138)	45 older men and women adults (aged 60 – 64 years)	A 30-min bout of submaximal exercise on a treadmill.	No statistically significant changes in CD34+ hematopoietic progenitor cell number after acute submaximal exercise.
Krüger *et al*., 2015 (120)	36 healthy subjects (aged 21- 29 years)	Subjects were divided into 3 exercise groups: concentric endurance test group (CET), a resistance exercise test group (RET), and an eccentric endurance test group (ECC) and performed the exercise for about 90 ± 5 min.	Not only CET but also acute bouts of RET and ECC increased in HPCs ($P < 0.05$).

Author	Subject	Study Design	Key Finding
Kroepfl *et al*., 2012 (139)	10 healthy men (aged 25.3 ± 4.4 years)	A standardized cycle incremental ergometry test protocol (3-min resting phase, 40-W starting load, increasing 20 W/min) until exhaustion.	A significant increase of Circulating hematopoietic cells (CPCs/mL) release after 10 min of exercise under normoxic (1,073.5 ± 162.3 to 1,982.2 ± 290.4, P < 0.01) as well as hypoxic (1,242.7 ± 214.8 to 2,059.3 ± 268.0, P < 0.01) conditions
Bonsignore *et al*., 2010 (121)	10 healthy male runners (aged 43.5 ± 11.25 years)	Subjects performed a marathon and 1.5-km field run protocols.	CD34+ cells increased significantly following the field run protocols (P < 0.005).
Craenenbroeck *et al*., 2010 (140)	41 chronic heart failure (CHF) patients (aged 62.5 ± 2.6 years) and 13 healthy subjects (aged 55.7 ± 1.6 years)	Cardiopulmonary exercise testing (CPET)	No significant change in circulating CD34+ cells following a single exercise bout in both CHF group (P = 0.18) and healthy control group (P = 0.79)
Mobius-Winkler *et al*., 2009 (128)	18 healthy men (32.4 ± 2.3 years)	One cycle ergometer test with an individualized power of 70% of the individual anaerobic threshold (IAT), for 4 hours.	Strenuous activity in healthy individuals leads to a 3.1-fold time-dependent increase of circulating CD34+ cells/mL blood (P < 0.001) relative to baseline.
Craenenbroeck *et al*., 2008 (137)	25 healthy subject (aged 20 – 50 years)	A single bout of exercise test until exhaustion on a graded bicycle ergometer.	A maximal bout of exercise induces a significant increase in CD34+ cells, cohort 1 by 76% (15.4 ± 10.7 cells/mL to 27.2 ± 13.7 cells/mL, P = 0.01) and cohort 2 by 69% (30.9 ± 14.6 cells/mL to 52.5 ± 42.6 cells/mL, P = 0.03)
Wardyn *et al*., 2008 (142)	37 healthy subjects (aged 19 – 35 years)	Exercised on a treadmill to maximum fatigue.	Exercise can increase the presence of HSPCs in blood circulation (25.1 ± 41.9 cells/mL to 38.2 ± 43.8 cells/mL, P = 0.03).

Author	Subject	Study Design	Key Finding
Zaldivar *et al*., 2007 (143)	14 early pubertal (EP, age 10.3 ± 0.3 y) and 13 late pubertal (LP, age 16.5 ± 0.4 y)	Intermittent high-intensity exercise: 10 two-minute bouts of constant work rate cycle ergometry, with a one-minute rest interval between each bout of exercise.	Substantially and significantly increase in circulating levels of CD34+ stem cells, in EP from 112 ± 21 to 182 ± 30 cells/μL, P = 0.0007 and LP from 63 ± 8 to 152 ± 21, P = 0.0008.
Thijssen *et at*., 2006 (144)	24 men divided into 2 groups: young (aged 18 – 28 years) and old (67 – 76 years)	A single maximal exercise bout on a cycling ergometer.	Acute exercise significantly increased HSCs (P < 0.01) in young and older men.
Morici *et al*., 2005 (145)	20 young competitive rowers (aged 17.1 ± 2.1 years)	Supramaximal ("1000 m") exercise.	Supramaximal exercise acutely doubled circulating CD34+ cells (rest: 7.6 ± 3.0, all-out: 16.3 ± 9.1 cells/μL, P < 0.001).
Rehman *et al*., 2004 (146)	22 patients (aged 54 ± 10 years)	Exhaustive dynamic exercise.	Circulating hematopoietic stem/ progenitor cells) increased nearly in peripheral blood from 1,743 ± 272 cells/mL to 2,455 ± 253 cells/mL following exercise.
Bonsignore *et al*., 2002 (147)	16 runners (aged 41.3 ± 13.4 years)	Marathon (M) and half-marathon (HM).	HPC counts were increased in peripheral blood of runners 3- to 4-fold higher than in controls at baseline and did not change immediately after a M or HM race.
Heal and Brightman, 1987 (148)	15 healthy people (aged 24 – 41 years)	A brief period of intense exercise.	A significant increase in the absolute number of circulating hematopoietic progenitor cells from 164 ± 27 to 240 ± 46 cells/mL. However, all values returned to baseline within 15 minutes.

Table 1.1 presents a comprehensive list of the studies that have measured changes in HSPCs in peripheral blood in response to single bouts of exercise. HSPC

concentration increases within the peripheral blood compartment during exercise as cells are mobilised from marginal pools via physiological (blood pressure and shear stress) and biochemical mechanisms (catecholamines and cytokines) **(Figure 1.1)**. Following an initial increase, there is a further rise occurring between 3-24 hours later. This is due to HSPCs leaving the bone marrow and entering the bloodstream. These HSPCs replace other immune cells that have exited the peripheral blood and migrated to areas of inflammation. The underpinning mechanisms are attributed to these proses may include the increase in blood flow to the bone marrow, and G-CSF production within the bone marrow niche, the reduction of C-X-C chemokine receptor type 4 (CXCR-4) and very late antigen-4 (VLA-4) dependent HSPC adhesion, and chemoattractant gradients facilitating the movement of HSPCs from bone marrow into peripheral blood circulation. There is data to indicate that the latter is governed by the release of chemokines from skeletal muscle that may draw HSPCs into peripheral blood (149), although other tissues could contribute.

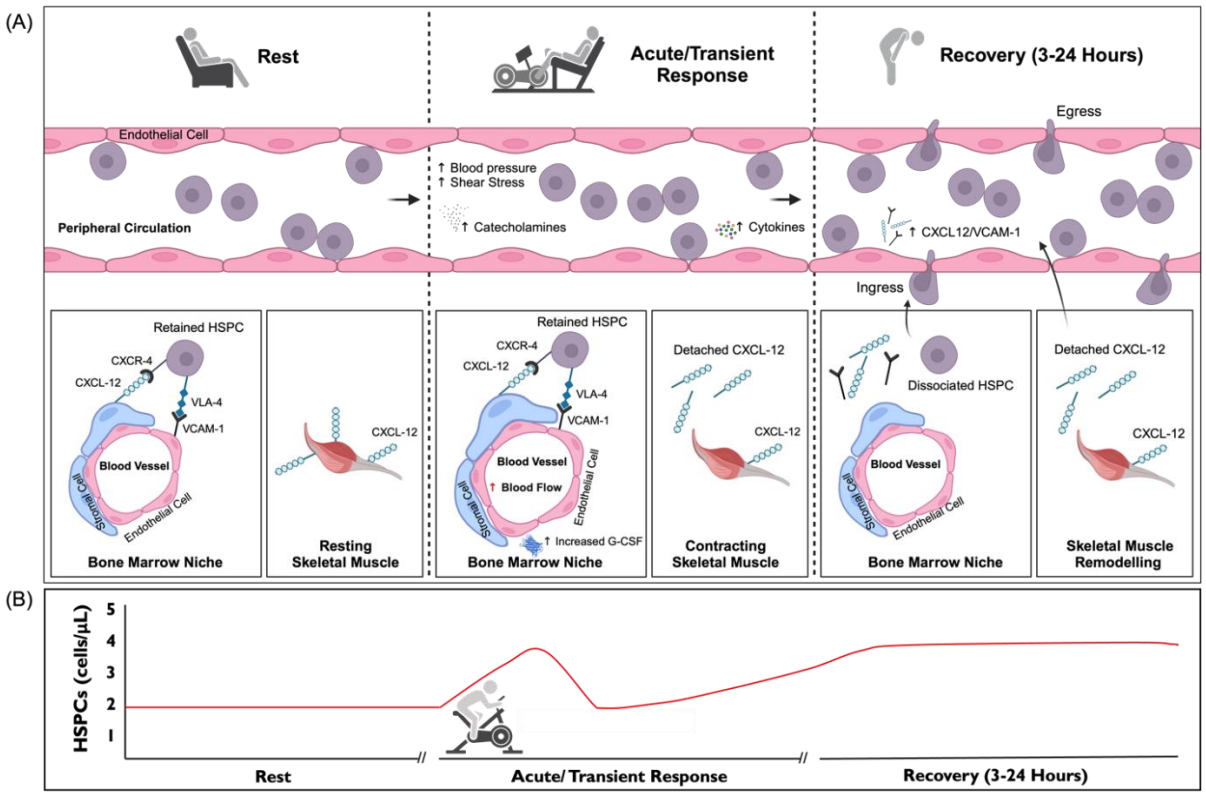

Figure 1.1 Time course and mechanisms underpinning the biphasic increase in peripheral blood HSPC concentrations. (A) Illustrates the interactions between peripheral blood (depicted as 1μL volume), the bone marrow niche, and skeletal muscle at rest (left), during the transient increase in response to exercise (middle) and during recovery (right). (B) Illustrates the predicted timecourse of HSPC concentrations in peripheral blood in response to bouts of exercise based on the available studies. This will vary depending on the intensity and duration of the bout and degree of muscle damage. HSPC = haemopoietic stem cell, CXCL-12 = C-X-C motif chemokine 12, VCAM-1 = vascular cell adhesion molecule 1, CXCR-4 = C-X-C chemokine receptor type 4, and VLA-4 = very late antigen-4. Created with BioRender.com.

Together with recent studies establishing the safety of exercise for patients undergoing HSCT (150,151), exercise could be used as an adjuvant therapy to promote HSPC mobilisation and collection to achieve a HSPC collection threshold (> 10 cells/µL) to initiate apheresis and shorten the donation procedure (134). The protocols used however have largely been too long to feasibly implement in a donation setting (133,134). Studies showed that single bouts of exercise transiently enrich peripheral blood with HSPCs (120,121). However, the presence of more stem cells in the blood appears to be influenced by a combination of exercise volume and intensity (100,102,120,131,134) which remains unclear. Therefore, it is necessary to determine the best intensity and duration of exercise for maximal mobilisation of HSPCs, as well as different sampling timepoints to examine the time course of HSPC mobilization in response to exercise. High intensity interval exercise (HIIE) entails working out at a higher intensity for a shorter period of time and with a lower overall exercise volume compares to steady state exercise. HIIE has been shown to mobilise HSPCs to the same extent (120,131) as steady state exercise (100) Whereas it must be noted that the concentration of HSPCs achieved during HIIE without G-CSF administration is still below the HSPC collection threshold used for PBSC donations, it could be hypothesised that implementing HIIE as a complementary therapy after G-CSF infusion would maximise HSPC concentrations during the donation process (120,131,133,152,153).

Since the rising usage of mPB HSPCs in the context of HSCT as they are preferable alternative to BM, it has become obvious that a sensitive, fast, and repeatable technique for planning apheresis procedures and quality control of apheresis products

ahead to transplant is required to reliably assess the engraftment potential of such collections (154). Using $CD34^+$ surface marker antigen expressed by HSPCs (155) can help to enumerate these cells circulating in blood. $CD34^+$ is a transmembrane glycoprotein found on lymphohematopoietic stem cells, progenitor cells, and endothelial cells in the early stages of development. $CD34^+$ expression in HSPCs is linked to multilineage engraftment following transplantation (156–158). Although, several flow cytometric techniques have been established to count $CD34^+$ HSPCs, the lack of a defined procedure has resulted in significantly inconsistent data (159). The International Society of Hematotherapy and Graft Engineering (ISHAGE), now known as the International Society for Cellular Therapy (ISCT), formed a stem cell enumeration committee in early 1995 with the mission of validating a simple, quick, and sensitive flow cytometric approach for accurately quantifying $CD34^+$ cells in peripheral blood and apheresis products (159).

1.5 The Landscape of Exercise Immunology

As mentioned above in **section 1.3.1**, the J-shaped model has been a mainstay within the discipline of exercise immunology since the late 1980's. Although limitations have been emphasised with regards some of the literature supporting this model (53), there are some data to support the notion that strenuous bouts of exercise or periods of intense training may compromise components of cellular and humoral immunity (96,160,161). It is important to note that the immune system is sensitive to many factors when examining over a period of exercise training, including diet, anxiety, travel, sleep disorders, temperature fluctuations, genetic polymorphisms, and prior infection and/or immunisation, which makes these studies challenging to conduct (162–164). This is

currently a contentious issue in the discipline of exercise immunology. However, the immune system is evidently very sensitive to effects of single bouts of exercise **(section 1.3.2)**, and there is clear consensus that the acute redistribution of immune cells after exercise translates into chronic adaptations. Whether this is favourable or not for immunity is not a direct aim of this thesis. Instead, Chapters 3 and 4 were designed to implement novel methods to examine immunometabolic mechanisms underpinning the trafficking of immune cells after exercise, which are not well understood.

1.6 Redistribution of T Cells from Peripheral Blood

It is well known that exercise elicits a bi-phasic change in the number of lymphocytes (primarily T and NK cells) in peripheral blood, an initial rapid increase within minutes that is followed by a decrease within 1-2 hours (81). This phenomenon is in conjunction with changes in cell function such as cytokine production, proliferation, migration capability, and cytotoxicity, leading to some speculation over the years that immune competency is temporally compromised, termed the ‘open window’ hypothesis (12). However, according to animal research conducted by Kruger *et al.* using fluorescence probes to track T cell redistribution after exercise, T cells are known to migrate to lymphoid tissues, such as the gut, lungs, and bone marrow during the time that concentrations fall in peripheral blood (76). This indicates increased immune surveillance at areas where infections are likely to be encountered (gut and lungs) and amplified immuno-regulatory activities (in bone marrow). In humans, a limited number of apoptotic lymphocytes are found within 24 hours of exercise cessation to explain the drop in T cell number within peripheral blood and this also coincides with the

mobilisation of HSCs from the bone marrow (165). This supports the idea that exercise may mobilise senescent T cells to undergo apoptosis (166), and the development and/or survival of naïve T cells is therefore triggered, which may be aided by myokine release from contracting skeletal muscle (167).

The trafficking of T cells from the peripheral blood compartment in this biphasic manner makes analysis of the functional processes underpinning these changes challenging. Recent studies have used single cell RNA sequencing to report that $CD4^+$ and $CD8^+$ T cells modulate their metabolic phenotype during a bout of maximal exercise (92). This has sparked interest in whether shifts in T cell energy metabolism underpin their acute redistribution during exercise recovery.

1.7 Immunometabolism

Immunometabolism is a branch of contemporary biology that investigates the interplay between immunology and metabolism, namely, bioenergetic mechanisms underpinning divergent shifts in immune cell function. These functions include 1) energy usage for motor activities such as migration and phagocytosis (168,169), 2) processing and presentation of antigenic peptides (170,171), 3) cell signalling, proliferation, and differentiation (172,173), and 4) execution of effector roles such as antibody production, cytokine secretion, and cytotoxicity (172,174). In response to signalling cues/ activation, immune cells undergo metabolic reprogramming to provide the energy required to fulfil these functions.

T cells are one of the main components of the adaptive immune system which exhibit highly specific and long-lasting immune responses against pathogens (175). In the setting of both acute and chronic viral infection, T cell function is tightly regulated by nutrition sensing to balance ongoing co-stimulatory and co-inhibitory signals (176). The availability of nutrients is an essential factor for the metabolic regulation of principal T cell functions such as maturation, activation, proliferation, and differentiation (177). As a reminder, T cells are composed of distinct subpopulations, classified by their degree of antigen experience and defined by the expression of cell surface receptors CCR7 and CD45RA including naïve, CM, EM and TEMRA. These T cells varying cytokine profiles (178) were governed by unique metabolic phenotype (179–181).

Chapman *et al*. reported that naïve T cells rely largely on oxidative phosphorylation (OXPHOS) to drive ATP synthesis (179–181). Because naïve T cells do not undergo clonal division or secrete significant amounts of cytokines, they remain in a quiescent state in terms of metabolic activity. As a result, the stimulation of anabolic pathways required for the *de novo* production of DNA, lipids, and proteins is minimal in naïve T cells.

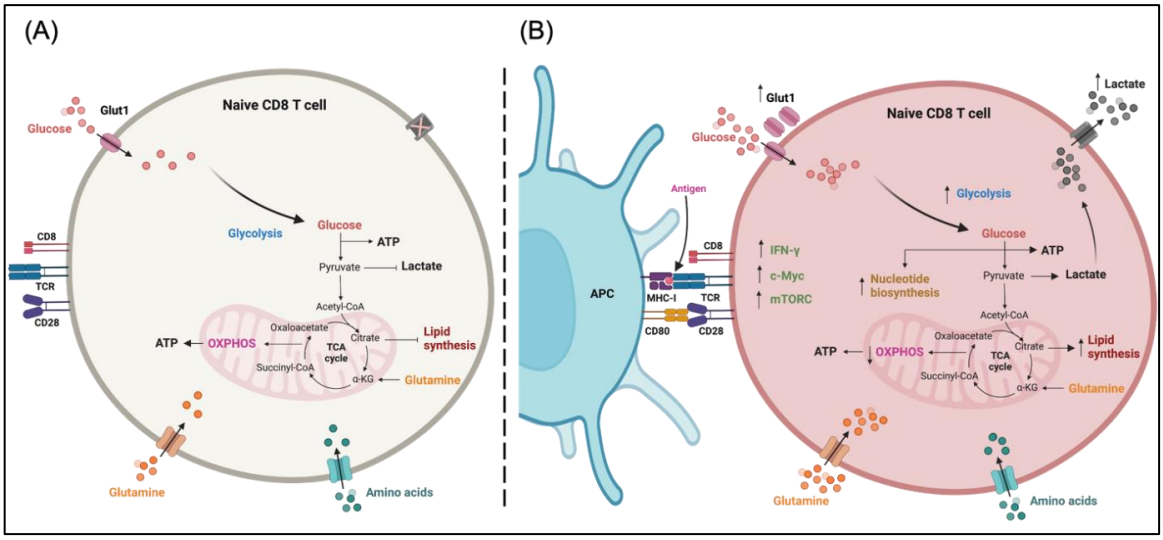

Figure 1.2 Shifted metabolism in $CD8^+$ T cells in respond to activation. (A) Naïve $CD8^+$ T cells rely essentially on oxidation of glucose and fatty acids to support energy demand. (B) Activated CD8+ T cells prefer to run anabolic pathway (upregulation of glycolysis) to support cell growth, proliferation, antiviral activities. Created with BioRender.com.

Following antigen and co-stimulatory stimulation, the metabolism of T cells dramatically shifts to favour glycolysis over OXPHOS, which supplies ATP more rapidly to activated T cells (182,183). Glycolysis provides a higher rate of ATP production per unit time compared to than mitochondrial respiration and allows T cells to adapt to hypoxic environments more effectively (184,185), thus enabling rapid T cell growth, proliferation, cytokine production, and other effector functions (182). Specifically, TCR receptor engagement, combined with CD28-mediated co-stimulation initiates the uptake of glucose, glutamine, and amino acids and the upregulation of glycolytic genes (186–188). Activation of the phosphatidylinositol 3-kinase (PI3K)-Akt transduction pathway in human peripheral blood T cells (189) suppresses key enzymes of tricarboxylic acid (TCA) cycle (190), resulting in rapid overexpression of Glucose Transporter-1 (GLUT-1) to increase in glucose uptake (189). In addition, transcriptional mediators c-Myc and mammalian target of rapamycin complex (mTORC) are upregulated after T cell activation to facilitate glycolytic reprogramming (186) and nutrient sensing (191) respectively. The integrated stimulation of early signalling events enables enhanced absorption of nutrients, particularly glucose, for the metabolic reprogramming of T cells after activation.

After being exposed to antigen and co-stimulatory signals, naïve T cells emerge from their dormancy and multiply rapidly into effector T cells, which is linked to changes in their metabolic processes. Changes in cell diameter, increased expression of activation-associated markers (e.g., CD44, CD25, and CD154), and proliferation are all signs of T cell activation. Activated T cells adopt a more anabolic programme to support cell growth and proliferation, whereas naïve T cells are more catabolic **(Figure 1.2A)** (186). Antigen-specific T cells increase over time, but most die in a process known as contraction. If there is exposure to the same antigen, residual memory T cells can rapidly re-expand from mediastinal lymph nodes and regain effector functions (181). Based on the expression of distinct trafficking receptors and functional features, memory T cells are further categorised into CM, EM, and TEMRA T cells. Several theories have been presented to explain how $CD8^+$ T cells become memory or effector cells (192). Due to increased expression of CD36, long-chain fatty acid absorption is stronger in effector T cells than in naïve or memory T cells. Subsequently, lipids are kept as neutral lipids like triacylglycerol or cholesterol esters that can be broken down by memory T cells in the lysosome because the cells express larger levels of lysosomal acid lipase (LAL) than effector T cells, providing an inherent substrate for fatty acid oxidation (FAO) (193). Glycolysis and glutaminolysis are preferred over FAO by effector T cells, while FAO and OXPHOS are preferred by memory T cells (193–195). Glycolysis increases in effector T cells due to increased expression of glycolytic enzymes such as aldolase C, α-enolase, and hexokinase 2 (HK2), however mitochondrial metabolism and FAO genes are downregulated associated with mitochondrial fission (195,196). Unlike effector T cells, a large proportion of fused

mitochondria is contained in memory T cells, providing higher levels of OXPHOS and spare respiratory capacity (SRC) as their characteristics (196,197).

1.8 Exercise Immunometabolism

The regulation of cellular metabolism is critical for driving important T cell functions, with each memory subset exhibiting a unique metabolic phenotype. The ability of humans to exercise depends on the conversion of chemical energy in the form of adenosine triphosphate (ATP) to mechanical energy in working skeletal muscle, which relies on the utilisation of glucose and other metabolites. Immune cells also rely on these substrates, but how T cells modulate their energy metabolism to meet this energy demand is far from clear. Recent studies have started examining immunometabolic changes in circulating peripheral blood mononuclear cells (PBMCs) after bouts of exercise (11,16,198–201). However, examining the total PBMC fraction is complicated by the aforementioned **(section 1.3.1)** fluctuations in the number and type of T cells within peripheral blood at the time of sampling. With technology available to purify single cell T cell populations and perform extracellular flux analysis of oxygen consumption rate (OCR) and extracellular acidification rate (ECAR) in live cells, there is an opportunity to conduct studies that interrogate the metabolic phenotype of T cells with single cell resolution.

1.9 Summary and Aims of the Thesis

PBSC donation is the primary procedure used to collect HSPCs for transplantation in individuals with various medical conditions, but there is an increasing need to improve HSPC mobilisation and the quality of the immune cell fraction for better health

outcomes following HSCT. The mobilisation of HSPCs and cytolytic natural killer (NK) cells during bouts of exercise may provide the efficiency of collection and patient outcomes following transplantation; however, practical steps to facilitate this for PBSC collections have not been taken. Chapter 2, therefore aims to investigate differences in HSPC and NK cell concentrations during and after continuous vs. interval-based cycling bouts. The latter included a comparison of low and high volume HIIE to examine how the intensity and duration of cycling intervals impacts HSPC kinetics over a detailed timecourse.

Single bouts of exercise evoke marked shifts in the number and function of peripheral blood T cells. These changes may underpin enhanced T cell trafficking and longer-term adaptations to the immune system; however, the mechanisms underpinning this are not understood. The development of techniques employing extracellular flux analysis have revealed multiple T cell functions governed by shifts in cellular metabolism. Chapter 3 aims to optimise experimental techniques for evaluating T cell bioenergetics in human acute exercise studies. The work in Chapter 3 developed methods using magnetic activated cell sorting and extracellular flux analysis to examine the metabolic phenotype and real time responses to *ex vivo* activation of enriched naïve Helper and Cytotoxic T cells vs. PBMCs including the optimisation for nutrient assay conditions (i.e., glucose and glutamine concentrations) and blood collection procedures (anticoagulant and blood 'sitting' time) to provide a robust experimental model for chapter 4 of this thesis to examine the impact of prolonged moderate intensity cycling on bioenergetic profiles of PBMCs and isolated naïve $CD4^+$ and $CD8^+$ T cells.

List of References

1. Baker FL, Simpson RJ. Exercise to Support Optimal Immune Function. ACSMs Health Fit J. 2021;25(1):5–8.

2. Larrabee RC. Leucocytosis after violent Exercise. J Med Res [Internet]. 1902;7(1):76–82. Available from: http://www.pubmedcentral.nih.gov/articlerender.fcgi?artid=2105828&tool=pmcentrez&rendertype=abstract

3. Weidner TG, Sevier TL. Sport, exercise, and the common cold. J Athl Train [Internet]. 1996;31(2):154–9. Available from: http://www.ncbi.nlm.nih.gov/pubmed/16558389%0Ahttp://www.pubmedcentral.nih.gov/articlerender.fcgi?artid=PMC1318446

4. Gleeson M. Mucosal immunity and respiratory illness in elite athletes. International Journal of Sports Medicine, Supplement. 2000;21(1).

5. Gleeson M, Williams C. Intense exercise training and immune function. Nestle Nutr Inst Workshop Ser. 2013;76:39–50.

6. Spielmann G, Bollard CM, Bigley AB, Hanley PJ, Blaney JW, LaVoy ECP, et al. The effects of age and latent cytomegalovirus infection on the redeployment of CD8+ T cell subsets in response to acute exercise in humans. Brain Behav Immun [Internet]. 2014;39:142–51. Available from: http://dx.doi.org/10.1016/j.bbi.2013.05.003

7. Simpson RJ, Cosgrove C, Ingram LA, Florida-James GD, Whyte GP, Pircher H, et al. Senescent T-lymphocytes are mobilised into the peripheral blood compartment in young and older humans after exhaustive exercise. Brain Behav Immun. 2008;22(4):544–51.

8. Duggal NA, Pollock RD, Lazarus NR, Harridge S, Lord JM. Major features of immunesenescence, including reduced thymic output, are ameliorated by high levels of physical activity in adulthood. Aging Cell. 2018;17(2).

9. Simpson R, Campbell J, Gleeson M, Krüger K, Nieman D, Pyne D, et al. Can exercise affect immune function to increase susceptibility to infection? J Appl Sport Psychol. 2015;27(2):216–34.

10. Batatinha HAP, Biondo LA, Lira FS, Castell LM, Rosa-Neto JC. Nutrients, immune system, and exercise: Where will it take us? Nutrition. 2019;61:151–6.

11. Theall B, Stampley J, Cho E, Granger J, Johannsen NM, Irving BA, et al. Impact of acute exercise on peripheral blood mononuclear cells nutrient sensing and mitochondrial oxidative capacity in healthy young adults. Physiol Rep. 2021 Dec 1;9(23).

12. Lancaster GI, Khan Q, Drysdale PT, Wallace F, Jeukendrup AE, Drayson MT, et al. Effect of prolonged exercise and carbohydrate ingestion on type 1 and type 2 T lymphocyte distribution and intracellular cytokine production in humans. J Appl Physiol. 2005;98(2):565–71.

13. Nieman DC, Lila MA, Gillitt ND. Immunometabolism: A Multi-Omics Approach to Interpreting the Influence of Exercise and Diet on the Immune System. Annu Rev Food Sci Technol. 2019;10:341–63.

14. La Rocca C, Carbone F, De Rosa V, Colamatteo A, Galgani M, Perna F, et al. Immunometabolic profiling of T cells from patients with relapsing-remitting multiple sclerosis reveals an impairment in glycolysis and mitochondrial respiration. Metabolism. 2017 Dec 1;77:39–46.

15. Nielsen BR, Ratzer R, Börnsen L, von Essen MR, Christensen JR, Sellebjerg F. Characterization of naïve, memory and effector T cells in progressive multiple sclerosis. J Neuroimmunol. 2017 Sep 15;310:17–25.

16. Janssen JJE, Lagerwaard B, Porbahaie M, Nieuwenhuizen AG, Savelkoul HFJ, Van Neerven RJJ, et al. Extracellular flux analyses reveal differences in mitochondrial PBMC metabolism between high-fit and low-fit females. Am J Physiol Endocrinol Metab. 2022 Feb 1;322(2).

17. Janssen JJE, Lagerwaard B, Bunschoten A, Savelkoul HFJ, van Neerven RJJ, Keijer J, et al. Novel standardized method for extracellular flux analysis of oxidative and glycolytic metabolism in peripheral blood mononuclear cells. Sci Rep [Internet]. 2021;11(1):1–15. Available from: https://doi.org/10.1038/s41598-021-81217-4

18. Lee HT, Lin CS, Pan SC, Wu TH, Lee CS, Chang DM, et al. Alterations of oxygen consumption and extracellular acidification rates by glutamine in PBMCs of SLE patients. Mitochondrion [Internet]. 2019;44(July 2017):65–74. Available from: https://doi.org/10.1016/j.mito.2018.01.002

19. Dimeloe S, Burgener A, Grählert J, Hess C. T-cell metabolism governing activation, proliferation and differentiation; a modular view. Immunology [Internet]. 2017 Jan 23;150(1):35–44. Available from: https://onlinelibrary.wiley.com/doi/10.1111/imm.12655

20. Marshall JS, Warrington R, Watson W, Kim HL. An introduction to immunology and immunopathology. Allergy, Asthma and Clinical Immunology [Internet]. 2018;14(s2):1–10. Available from: https://doi.org/10.1186/s13223-018-0278-1

21. Nicholson LB. The immune system. Essays Biochem. 2016 Oct 31;60(3):275–301.

22. Forlin R, James A, Brodin P. Making human immune systems more interpretable through systems immunology. Vol. 44, Trends in Immunology. Elsevier Ltd; 2023. p. 577–84.

23. Wilkerson MJ, Springer NL. Cluster of Differentiation (CD) Antigens. In: Schalm's Veterinary Hematology [Internet]. John Wiley & Sons, Ltd; 2022. p. 41–7. Available from: https://onlinelibrary.wiley.com/doi/abs/10.1002/9781119500537.ch6

24. Randolph GJ, Ivanov S, Zinselmeyer BH, Scallan JP. The lymphatic system: Integral roles in immunity. Vol. 35, Annual Review of Immunology. Annual Reviews Inc.; 2017. p. 31–52.

25. Moore JE, Bertram CD. Lymphatic System Flows. 2017; Available from: https://doi.org/10.1146/annurev-fluid-122316-

26. Cumano A, Godin I. Ontogeny of the hematopoietic system. Vol. 25, Annual Review of Immunology. 2007. p. 745–85.

27. Grinenko T, Eugster A, Thielecke L, Ramasz B, Krüger A, Dietz S, et al. Hematopoietic stem cells can differentiate into restricted myeloid progenitors before cell division in mice. Nat Commun. 2018 Dec 1;9(1).

28. Seita J, Weissman IL. Hematopoietic stem cell: Self-renewal versus differentiation. Vol. 2, Wiley Interdisciplinary Reviews: Systems Biology and Medicine. 2010. p. 640–53.

29. Waclawovsky G, Umpierre D, Figueira FR, De Lima ES, Alegretti AP, Schneider L, et al. Exercise on progenitor cells in healthy subjects and patients with type 1 diabetes. Med Sci Sports Exerc. 2016;48(2):190–9.

30. Kondo M, Wagers AJ, Manz MG, Prohaska SS, Scherer DC, Beilhack GF, et al. Biology of hematopoietic stem cells and progenitors: Implications for clinical application. Vol. 21, Annual Review of Immunology. 2003. p. 759–806.

31. Weissman IL. Translating Stem and Progenitor Cell Biology to the Clinic: Barriers and Opportunities [Internet]. Available from: https://www.science.org

32. Romani L. Immunity to fungal infections. Vol. 11, Nature Reviews Immunology. 2011. p. 275–88.

33. Beutler Bruce, Rietschel ET. Innate immune sensing and its roots: the story of endotoxin. Nat Rev Immunol. 2003;3:169–76.

34. Park JE, Barbul A. Understanding the role of immune regulation in wound healing. Am J Surg. 2004;187(5 SUPPL. 1):S11–6.

35. Dewitt JC, Rockwell CE, Bowman CC. Immunotoxicity Testing. Methods in Molecular Biology [Internet]. 2018. Available from: http://www.springer.com/series/7651

36. Bishop NC, Walker GJ, Gleeson M, Wallace FA, Hewitt CRA. Human T lymphocyte migration towards the supernatants of Human Rhinovirus infected

airway epithelial cells: Influence of exercise and carbohydrate intake. Exerc Immunol Rev. 2009;15:127–44.

37. Woods JA, Davis JM, Smith JA, Nieman DC. Exercise and cellular innate immune function. Vol. 31, Medicine and Science in Sports and Exercise. 1999. p. 57–66.

38. Grégoire C, Chasson L, Luci C, Tomasello E, Geissmann F, Vivier E, et al. The trafficking of natural killer cells. Immunol Rev. 2007;220(1):169–82.

39. Vivier E, Tomasello E, Baratin M, Walzer T, Ugolini S. Functions of natural killer cells. Nat Immunol. 2008;9(5):503–10.

40. Ham H, Billadeau DD. Human immunodeficiency syndromes affecting human natural killer cell cytolytic activity. Front Immunol. 2014;5(JAN):1–17.

41. Kiladjian JJ, Bourgeois E, Lobe I, Braun T, Visentin G, Bourhis JH, et al. Cytolytic function and survival of natural killer cells are severely altered in myelodysplastic syndromes. Leukemia. 2006;20(3):463–70.

42. Dimeloe S, Burgener AV, Grählert J, Hess C. T-cell metabolism governing activation, proliferation and differentiation; a modular view. Immunology. 2017;150(1):35–44.

43. Mirzaei HR. Adaptive Immunity. In: Reference Module in Biomedical Sciences [Internet]. Elsevier; 2020. Available from: https://www.sciencedirect.com/science/article/pii/B9780128187319000288

44. Cooper MD, Alder MN. The evolution of adaptive immune systems. Cell. 2006;124(4):815–22.

45. Bonilla FA, Oettgen HC. Adaptive immunity. Journal of Allergy and Clinical Immunology [Internet]. 2010;125(2 SUPPL. 2):S33–40. Available from: http://dx.doi.org/10.1016/j.jaci.2009.09.017

46. Gerritsen B, Pandit A. The memory of a killer T cell: models of CD8(+) T cell differentiation. Immunol Cell Biol [Internet]. 2016 Mar;94(3):236–41. Available from: http://www.ncbi.nlm.nih.gov/pubmed/26700072

47. Lee GR. Molecular Mechanisms of T Helper Cell Differentiation and Functional Specialization. Vol. 23, Immune Network. Korean Association of Immunologists; 2023.

48. Sallusto F, Lenig D, Förster R, Lipp M, Lanzavecchia A. Two subsets of memory T lymphocytes with distinct homing potentials and effector functions. Nature. 1999;401(6754):708–12.

49. Turner JE, Wadley AJ, Aldred S, Fisher JP, Bosch JA, Campbell JP. Intensive Exercise Does Not Preferentially Mobilize Skin-Homing T Cells and NK Cells. Med Sci Sports Exerc. 2016;48(7):1285–93.

50. Farber DL, Yudanin NA, Restifo NP. Human memory T cells: Generation, compartmentalization and homeostasis. Nat Rev Immunol. 2014;14(1):24–35.

51. Merlo LMF, Mandik-Nayak L. Adaptive Immunity: B Cells and Antibodies [Internet]. Second Edi. Cancer Immunotherapy: Immune Suppression and Tumor Growth: Second Edition. Elsevier; 2013. 25–40 p. Available from: http://dx.doi.org/10.1016/B978-0-12-394296-8.00003-8

52. Rundqvist H, Veliça P, Barbieri L, Gameiro PA, Bargiela D, Gojkovic M, et al. Cytotoxic t-cells mediate exercise-induced reductions in tumor growth. Elife. 2020;9:1–25.

53. Campbell JP, Turner JE. Debunking the Myth of Exercise-Induced Immune Suppression: Redefining the Impact of Exercise on Immunological Health Across the Lifespan. Front Immunol [Internet]. 2018 Apr 16;9(APR):1–21. Available from: http://journal.frontiersin.org/article/10.3389/fimmu.2018.00648/full

54. Gleeson M, Bishop NC, Stensel DJ, Lindley MR, Mastana SS, Nimmo MA. The anti-inflammatory effects of exercise: Mechanisms and implications for the prevention and treatment of disease. Nat Rev Immunol. 2011;11(9):607–10.

55. Galbo D. Hormonal and metabolic adaptation to exercise. 1983.

56. Cupps TR, Fauci AS. Corticosteroid-Mediated Immunoregulation in Man. Vol. 65, Immunological Rev. 1982.

57. Bergmann M, Gornikiewicz A, Sautner T, Waldmann E, Weber T, Mittlböck M, et al. Attenuation of catecholamine-induced immunosuppression in whole blood from patients with sepsis. Shock. 1999;12(6).

58. Timmerman KL, Flynn MG, Coen PM, Markofski MM, Pence BD. Exercise training-induced lowering of inflammatory (CD14+CD16+) monocytes: a role in the anti-inflammatory influence of exercise? J Leukoc Biol. 2008 Nov 1;84(5):1271–8.

59. Wadley AJ, Cullen T, Vautrinot J, Keane G, Bishop NC, Coles SJ. High intensity interval exercise increases the frequency of peripheral PD-1+ CD8+ central memory T-cells and soluble PD-L1 in humans. Brain Behav Immun Health [Internet]. 2020;3(January):100049. Available from: https://doi.org/10.1016/j.bbih.2020.100049

60. Bishop NC, Wadley AJ, Hamrouni M, Roberts MJ. Inactivity and obesity: Consequences for macrophage-mediated inflammation and the development of cardiometabolic disease. Proceedings of the Nutrition Society. Cambridge University Press; 2022.

61. Goh J, Ladiges WC. Exercise enhances wound healing and prevents cancer progression during aging by targeting macrophage polarity. Mech Ageing Dev

[Internet]. 2014;139(1):41–8. Available from: http://dx.doi.org/10.1016/j.mad.2014.06.004

62. Simpson RJ, Kunz H, Agha N, Graff R. Exercise and the Regulation of Immune Functions [Internet]. 1st ed. Vol. 135, Progress in Molecular Biology and Translational Science. Elsevier Inc.; 2015. 355–380 p. Available from: http://dx.doi.org/10.1016/bs.pmbts.2015.08.001

63. Wong GCL, Narang V, Lu Y, Camous X, Nyunt MSZ, Carre C, et al. Hallmarks of Improved Immunological Responses in the Vaccination of More Physically Active Elderly Females.

64. Peake JM, Neubauer O, Walsh NP, Simpson RJ. Recovery of the immune system after exercise. J Appl Physiol. 2017;122(5):1077–87.

65. Matthews CE, Ockene IRAS, Freedson PS, Rosal MC, Merriam PA, Hebert JR. Moderate to vigorous physical activity and risk of upper-respiratory tract infection. 1998;(February 1997).

66. Zhang Z, Zhang L, Xu J. The effects of different exercise training mode on interleukin. Life Sci J. 2007;4.

67. Nieman DC, Johanssen LM, Lee JW, Arabatzis K. Infectious episodes in runners before and after the Los Angeles Marathon. Journal of Sports Medicine and Physical Fitness. 1990;30(3):316–28.

68. Fahlman MM, Engels HJ. Mucosal IgA and URTI in American college football players: A year longitudinal study. Med Sci Sports Exerc. 2005;37(3):374–80.

69. Nieman DC. Exercise, infection, and immunity. Int J Sports Med. 1994 Oct;15 Suppl 3:S131-41.

70. Nieman DC, Johanssen LM, Lee JW. Infectious episodes in runners before and after a roadrace. J Sports Med Phys Fitness. 1989 Sep;29(3):289–96.

71. Nieman DC, Henson DA, Dumke CL, Lind RH, Shooter LR, Gross SJ. Relationship between salivary IgA secretion and upper respiratory tract infection following a 160-km race. J Sports Med Phys Fitness. 2006 Mar;46(1):158–62.

72. Nieman DC, Nehlsen-Cannarella SL, Markoff PA, Balk-Lamberton AJ, Yang H, Chritton DBW, et al. The effects of moderate exercise training on natural killer cells and acute upper respiratory tract infections. Int J Sports Med. 1990;11(6):467–73.

73. Field CJ, Gougeon R, Marliss EB. Circulating mononuclear cell numbers and function during intense exercise and recovery. J Appl Physiol. 1991;71(3):1089–97.

74. Verde T, Thomas S, Shephard RJ. Potential markers of heavy training in highly trained distance runners. Br J Sports Med. 1992;26(3):167–75.

75. Kawanishi N, Yano H, Yokogawa Y, Suzuki K. Exercise training inhibits inflammation in adipose tissue via both suppression of macrophage infiltration and acceleration of phenotypic switching from M1 to M2 macrophages in high-fat-diet-induced obese mice.

76. Krüger K, Lechtermann A, Fobker M, Völker K, Mooren FC. Exercise-induced redistribution of T lymphocytes is regulated by adrenergic mechanisms. Brain Behav Immun. 2008;22(3):324–38.

77. Simpson RJ, Kunz H, Agha N, Graff R. Exercise and the Regulation of Immune Functions. 1st ed. Vol. 135, Progress in Molecular Biology and Translational Science. Elsevier Inc.; 2015. 355–380 p.

78. Krüger K, Mooren FC. T cell homing and exercise. Exerc Immunol Rev. 2007;13:37–54.

79. Gleeson M. Immune function in sport and exercise. J Appl Physiol. 2007;103(2):693–9.

80. Graff RM, Kunz HE, Agha NH, Baker FL, Laughlin M, Bigley AB, et al. β2-Adrenergic receptor signaling mediates the preferential mobilization of differentiated subsets of CD8+ T-cells, NK-cells and non-classical monocytes in response to acute exercise in humans. Brain Behav Immun. 2018;74(July):143–53.

81. Rooney B V., Bigley AB, LaVoy EC, Laughlin M, Pedlar C, Simpson RJ. Lymphocytes and monocytes egress peripheral blood within minutes after cessation of steady state exercise: A detailed temporal analysis of leukocyte extravasation. Physiol Behav [Internet]. 2018;194(June):260–7. Available from: https://doi.org/10.1016/j.physbeh.2018.06.008

82. Gabriel H, Schwarz L, Born P, Kindermann W. Differential mobilization of leucocyte and lymphocyte subpopulations into the circulation during endurance exercise. Vol. 65, European .ouo, o, Applied Physiology and Occupational Physiology. Springer-Verlag; 1992.

83. Anane LH, Edwards KM, Burns VE, Drayson MT, Riddell NE, van Zanten JJCSV, et al. Mobilization of γδ T lymphocytes in response to psychological stress, exercise, and β-agonist infusion. Brain Behav Immun. 2009 Aug;23(6):823–9.

84. Kappel M, Tvede N, Galbo H, Haahr PM, Kjaer M, Linstow M, et al. Evidence that the effect of physical exercise on NK cell activity is mediated by epinephrine. J Appl Physiol. 1991;70(6):2530–4.

85. Nieman D, Miller A, Henson D a, Warren B, Gusewitch G, Jhonson R, et al. Effects of High- vs Moderate-Intensity Exercise on Natural Killer Cell Activity. 1993. p. 1126–34.

86. Shephard RJ. Physical Activity, Training and the Immune Response. Carmel, IN, Cooper Publications Group. 1997;

87. Gannon GA, Rhind SG, Suzui M, Zamecnik J, Sabiston BH, Shek PN, et al. β-endorphin and natural killer cell cytolytic activity during prolonged exercise. Is there a connection? Am J Physiol Regul Integr Comp Physiol. 1998;275(6 44-6):1725–34.

88. Brown FF, Campbell JP, Wadley AJ, Fisher JP, Aldred S, Turner JE. Acute aerobic exercise induces a preferential mobilisation of plasmacytoid dendritic cells into the peripheral blood in man. Physiol Behav [Internet]. 2018;194(April):191–8. Available from: https://doi.org/10.1016/j.physbeh.2018.05.012

89. Hoffman-Goetz L, Simpson JR, Cipp N, Arumugam Y, Houston ME. Lymphocyte subset responses to repeated submaximal exercise in men. J Appl Physiol. 1990;68(3):1069–74.

90. Gabriel H, Schwarz L, Born P, Kindermann W. Differential mobilization of leucocyte and lymphocyte subpopulations into the circulation during endurance exercise. Eur J Appl Physiol Occup Physiol. 1992;65(6):529–34.

91. Arroyo E, Tagesen EC, Hart TL, Miller BA, Jajtner AR. Comparison of the lymphocyte response to interval exercise versus continuous exercise in recreationally trained men. Brain Behav Immun Health [Internet]. 2022;20(December 2021):100415. Available from: https://doi.org/10.1016/j.bbih.2022.100415

92. Batatinha H, Diak DM, Niemiro GM, Baker FL, Smith KA, Zúñiga TM, et al. Human lymphocytes mobilized with exercise have an anti-tumor transcriptomic profile and exert enhanced graft-versus-leukemia effects in xenogeneic mice. Front Immunol [Internet]. 2023 Apr 3;14(April):1–14. Available from: https://www.frontiersin.org/articles/10.3389/fimmu.2023.1067369/full

93. Walsh NP, Gleeson M, Shephard RJ, Gleeson M, Woods JA, Bishop NC, et al. Position statement part one: Immune function and exercise. Exerc Immunol Rev. 2011;17:6–63.

94. Bigley AB, Rezvani K, Chew C, Sekine T, Pistillo M, Crucian B, et al. Acute exercise preferentially redeploys NK-cells with a highly-differentiated phenotype and augments cytotoxicity against lymphoma and multiple myeloma target cells. Brain Behav Immun [Internet]. 2014 Jul;39:160–71. Available from: https://linkinghub.elsevier.com/retrieve/pii/S0889159113005291

95. Campbell JP, Riddell NE, Burns VE, Turner M, van Zanten JJCSV, Drayson MT, et al. Acute exercise mobilises CD8+ T lymphocytes exhibiting an effector-memory phenotype. Brain Behav Immun [Internet]. 2009;23(6):767–75. Available from: http://dx.doi.org/10.1016/j.bbi.2009.02.011

96. Turner JE, Spielmann G, Wadley AJ, Aldred S, Simpson RJ, Campbell JP. Exercise-induced B cell mobilisation: Preliminary evidence for an influx of immature cells into the bloodstream. Physiol Behav [Internet]. 2016;164:376–82. Available from: http://dx.doi.org/10.1016/j.physbeh.2016.06.023

97. Robson PJ, Blannin AK, Walsh NP, Castell LM, Gleeson M. Effects of exercise intensity, duration and recovery on in vitro neutrophil function in male athletes. Int J Sports Med. 1999;20(2):128–35.

98. Peake JM. Exercise-induced alterations in neutrophil degranulation and respiratory burst activity: possible mechanisms of action. Exerc Immunol Rev. 2002;8:49–100.

99. McCarthy DA, Dale MM. The Leucocytosis of Exercise. Sports Medicine. 1988;6(6):333–63.

100. Schmid M, Kröpfl JM, Spengler CM. Correction to: Changes in Circulating Stem and Progenitor Cell Numbers Following Acute Exercise in Healthy Human Subjects: a Systematic Review and Meta-Analysis. Stem Cell Rev Rep. 2021;17(4):1511.

101. Simpson RJ, Bigley AB, Agha N, Hanley PJ, Bollard CM. Mobilizing immune cells with exercise for cancer immunotherapy. Exerc Sport Sci Rev. 2017;45(3):163–72.

102. Agha NH, Baker FL, Kunz HE, Graff R, Azadan R, Dolan C, et al. Vigorous exercise mobilizes CD34+ hematopoietic stem cells to peripheral blood via the β2-adrenergic receptor. Brain Behav Immun [Internet]. 2018;68:66–75. Available from: https://www.sciencedirect.com/science/article/pii/S0889159117304543

103. Boppart MD, De Lisio M, Witkowski S. Exercise and Stem Cells. In: Progress in Molecular Biology and Translational Science. Elsevier B.V.; 2015. p. 423–56.

104. Ratajczak MZ. A novel view of the adult bone marrow stem cell hierarchy and stem cell trafficking. Vol. 29, Leukemia. Nature Publishing Group; 2015. p. 776–82.

105. Nederveen JP, Baker J, Ibrahim G, Ivankovic V, Percival ME, Parise G. Hematopoietic Stem and Progenitor Cell (HSPC) Mobilization Responses to Different Exercise Intensities in Young and Older Adults. Journal of Science in Sport and Exercise [Internet]. 2020;2(1):47–58. Available from: https://doi.org/10.1007/s42978-019-00050-4

106. Gyurkocza B, Rezvani A SRF. Allogeneic hematopoietic cell transplantation: the state of the art. Expert Rev Hematol. 2010;3(3):285–299. 2011;3(3):285–99.

107. Saraiva L, Wang L, Kammel M, Kummrow A, Atkinson E, Lee JY, et al. Comparison of Volumetric and Bead-Based Counting of CD34 Cells by Single-Platform Flow Cytometry. Cytometry B Clin Cytom. 2019;96(6):508–13.

108. To LB, Levesque JP, Herbert KE. How I treat patients who mobilize hematopoietic stem cells poorly. Blood [Internet]. 2011;118(17):4530–40. Available from: http://dx.doi.org/10.1182/blood-2011-06-318220

109. Marquez-Curtis LA, Turner AR, Sridharan S, Ratajczak MZ, Janowska-Wieczorek A. The Ins and Outs of Hematopoietic Stem Cells: Studies to Improve Transplantation Outcomes. Stem Cell Rev Rep. 2011;7(3):590–607.

110. Wright DE, Wagers AJ, Pathak Gulati A, Johnson FL, Weissman IL. Physiological migration of hematopoietic stem and progenitor cells. Science (1979). 2001;294(5548):1933–6.

111. Bonig H, Papayannopoulou T. Mobilization of hematopoietic stem/progenitor cells: General principles and molecular mechanisms. Methods in Molecular Biology. 2012;904:1–14.

112. Goker H, Etgul S, Buyukasik Y. Optimizing mobilization strategies in difficult-to-mobilize patients: The role of plerixafor. Transfusion and Apheresis Science [Internet]. 2015;53(1):23–9. Available from: http://dx.doi.org/10.1016/j.transci.2015.05.011

113. Emmons R, Niemiro GM, De Lisio M. Exercise as an Adjuvant Therapy for Hematopoietic Stem Cell Mobilization. Stem Cells Int. 2016;2016.

114. Brockmann F, Kramer M, Bornhäuser M, Ehninger G, Hölig K. Efficacy and side effects of granulocyte collection in healthy donors. Transfusion Medicine and Hemotherapy. 2013;40(4):258–64.

115. Bazinet A, Popradi G. A general practitioner's guide to hematopoietic stem-cell transplantation. Current Oncology. 2019;26(3):187–91.

116. Loschi M, Porcher R, Peffault de Latour R, Vanneaux V, Robin M, Xhaard A, et al. High Number of Memory T Cells Is Associated with Higher Risk of Acute Graft-versus-Host Disease after Allogeneic Stem Cell Transplantation. Biology of Blood and Marrow Transplantation. 2015 Mar 1;21(3):569–74.

117. Amsen D. T cells take directions from supporting cast in graft-versus-host disease. Vol. 127, Journal of Clinical Investigation. American Society for Clinical Investigation; 2017. p. 1215–7.

118. Justiz Vaillant A, Modi P, Mohammadi O, Pin TM. Graft Versus Host Disease.

119. Kerry Atkinson B, Horowitz MM, Peter Gale R, van Bekkum DW, Gluckman E, Good RA, et al. Risk Factors for Chronic Graft-Versus-Host Disease After HLA-Identical Sibling Bone Marrow Transplantation. 1990.

120. Krüger K, Pilat C, Schild M, Lindner N, Frech T, Muders K, et al. Progenitor cell mobilization after exercise is related to systemic levels of G-CSF and muscle damage. Scand J Med Sci Sports. 2015;25(3):e283–91.

121. Bonsignore MR, Morici G, Riccioni R, Huertas A, Petrucci E, Veca M, et al. Hemopoietic and angiogenetic progenitors in healthy athletes: Different responses to endurance and maximal exercise. J Appl Physiol. 2010;109(1):60–7.

122. Stroncek DF, Clay ME, Herr G, Smith J, Jaszcz WB, Ilstrup S, et al. The kinetics of G-CSF mobilization of CD34+ cells in healthy people. Transfusion Medicine. 1997;7(1):19–24.

123. Méndez-Ferrer S, Battista M, Frenette PS. Cooperation of β2- and β3-adrenergic receptors in hematopoietic progenitor cell mobilization. Ann N Y Acad Sci. 2010;1192:139–44.

124. Barrett AJ, Longhurst P, Sneath P, Watson JG. Mobilization of CFU-C by exercise and ACTH induced stress in man. Exp Hematol [Internet]. 1978 Aug;6(7):590—594. Available from: http://europepmc.org/abstract/MED/211045

125. Camargo FD, Green R, Capetenaki Y, Jackson KA, Goodell MA. Single hematopoietic stem cells generate skeletal muscle through myeloid intermediates. Nat Med. 2003;9(12):1520–7.

126. Palermo AT, LaBarge MA, Doyonnas R, Pomerantz J, Blau HM. Bone marrow contribution to skeletal muscle: A physiological response to stress. Dev Biol. 2005;279(2):336–44.

127. Wahl P, Bloch W, Schmidt A. Exercise has a positive effect on endothelial progenitor cells, which could be necessary for vascular adaptation processes. Int J Sports Med. 2007;28(5):374–80.

128. Möbius-Winkler S, Hilberg T, Menzel K, Golla E, Burman A, Schuler G, et al. Time-dependent mobilization of circulating progenitor cells during strenuous exercise in healthy individuals. J Appl Physiol. 2009;107(6):1943–50.

129. Callanan MC, Christensen KD, Plummer HA, Torres J, Anz AW. Elevation of Peripheral Blood CD34+ and Platelet Levels After Exercise With Cooling and Compression. Arthrosc Sports Med Rehabil [Internet]. 2021;3(2):e399–410. Available from: https://doi.org/10.1016/j.asmr.2020.10.003

130. Wu TY, Kung CC, Kao TY, Sun WH. Innovative Mind–Body Intervention Day Easy Exercise Increases Peripheral Blood CD34+ Cells in Adults. Cell Transplant. 2020;29(155):1–9.

131. O'Carroll L, Wardrop B, Murphy RP, Ross MD, Harrison M. Circulating angiogenic cell response to sprint interval and continuous exercise. Eur J Appl Physiol. 2019 Mar 6;119(3):743–52.

132. Anz AW, Parsa RS, Romero-Creel MF, Nabors A, Tucker MS, Harrison RM, et al. Exercise-Mobilized Platelet-Rich Plasma: Short-Term Exercise Increases Stem Cell and Platelet Concentrations in Platelet-Rich Plasma. Arthroscopy - Journal of Arthroscopic and Related Surgery. 2019 Jan 1;35(1):192–200.

133. Niemiro GM, Parel J, Beals J, Van Vliet S, Paluska SA, Moore DR, et al. Kinetics of circulating progenitor cell mobilization during submaximal exercise. J Appl Physiol. 2017;122(3):675–82.

134. Baker JM, Nederveen JP, Parise G. Aerobic exercise in humans mobilizes HSCs in an intensity-dependent manner. J Appl Physiol. 2017;122(1):182–90.

135. Ribeiro F, Ribeiro IP, Gonçalves AC, Alves AJ, Melo E, Fernandes R, et al. Effects of resistance exercise on endothelial progenitor cell mobilization in women. Sci Rep. 2017;7(1):1–9.

136. Harris E, Rakobowchuk M, Birch KM. Interval exercise increases angiogenic cell function in postmenopausal women. BMJ Open Sport Exerc Med. 2017;3(1).

137. Marycz K, Mierzejewska K, ̄mieszek A, Suszynska E, Malicka I, Kucia M, et al. Endurance exercise mobilizes developmentally early stem cells into peripheral blood and increases their number in bone marrow: Implications for tissue regeneration. Stem Cells Int. 2016;2016.

138. Lutz AH, Blumenthal JB, Landers-Ramos RQ, Prior SJ. Exercise-induced endothelial progenitor cell mobilization is attenuated in impaired glucose tolerance and type 2 diabetes. J Appl Physiol. 2016;121(1):36–41.

139. Kroepfl JM, Pekovits K, Stelzer I, Fuchs R, Zelzer S, Hofmann P, et al. Exercise increases the frequency of circulating hematopoietic progenitor cells, but reduces hematopoietic colony-forming capacity. Stem Cells Dev. 2012;21(16):2915–25.

140. Van Craenenbroeck EM, Beckers PJ, Possemiers NM, Wuyts K, Frederix G, Hoymans VY, et al. Exercise acutely reverses dysfunction of circulating angiogenic cells in chronic heart failure. Eur Heart J. 2010;31(15):1924–34.

141. Van Craenenbroeck EMF, Vrints CJ, Haine SE, Vermeulen K, Goovaerts I, Van Tendeloo VFI, et al. A maximal exercise bout increases the number of circulating CD34+/KDR+ endothelial progenitor cells in healthy subjects. Relation with lipid profile. J Appl Physiol. 2008;104(4):1006–13.

142. Wardyn GG, Rennard SI, Brusnahan SK, McGuire TR, Carlson ML, Smith LM, et al. Effects of exercise on hematological parameters, circulating side population cells, and cytokines. Exp Hematol. 2008;36(2):216–23.

143. Zaldivar F, Eliakim A, Radom-Aizik S, Leu SY, Cooper DM. The effect of brief exercise on circulating CD34+ stem cells in early and late pubertal boys. Pediatr Res. 2007;61(4):491–5.

144. Thijssen DHJ, Vos JB, Verseyden C, Van Zonneveld AJ, Smits P, Sweep FCGJ, et al. Haematopoietic stem cells and endothelial progenitor cells in healthy men: Effect of aging and training. Aging Cell. 2006;5(6):495–503.

145. Morici G, Zangla D, Santoro A, Pelosi E, Petrucci E, Gioia M, et al. Supramaximal exercise mobilizes hematopoietic progenitors and reticulocytes in athletes. Am J Physiol Regul Integr Comp Physiol. 2005;289(5 58-5):1496–503.

146. Rehman J, Li J, Parvathaneni L, Karlsson G, Panchal VR, Temm CJ, et al. Exercise acutely increases circulating endothelial progenitor cells and monocyte-/macrophage-derived angiogenic cells. J Am Coll Cardiol [Internet]. 2004;43(12):2314–8. Available from: http://dx.doi.org/10.1016/j.jacc.2004.02.049

147. Bonsignore MR, Morici G, Santoro A, Pagano M, Cascio L, Bonanno A, et al. Circulating hematopoietic progenitor cells in runners. J Appl Physiol. 2002;93(5):1691–7.

148. Heal JM, Brightman A. Exercise and circulating hematopoietic progenitor cells (CFU-GM) in humans. Transfusion (Paris). 1987;27(2):155–8.

149. Strömberg A, Rullman E, Jansson E, Gustafsson T. Exercise-induced upregulation of endothelial adhesion molecules in human skeletal muscle and number of circulating cells with remodeling properties. J Appl Physiol [Internet]. 2017;122:1145–54. Available from: http://www.jappl.org

150. Wiskemann J, Huber G. Physical exercise as adjuvant therapy for patients undergoing hematopoietic stem cell transplantation. Bone Marrow Transplant. 2008;41(4):321–9.

151. Kuehl R, Feyer J, Limbach M, Pahl A, Stoelzel F, Beck H, et al. Prehabilitative high-intensity interval training and resistance exercise in patients prior allogeneic stem cell transplantation. Sci Rep. 2023 Dec 1;13(1).

152. Weston KS, Wisløff U, Coombes JS. High-intensity interval training in patients with lifestyle-induced cardiometabolic disease: A systematic review and meta-analysis. Br J Sports Med. 2014;48(16):1227–34.

153. Taylor JL, Holland DJ, Spathis JG, Beetham KS, Wisløff U, Keating SE, et al. Guidelines for the delivery and monitoring of high intensity interval training in clinical populations. Prog Cardiovasc Dis [Internet]. 2019;62(2):140–6. Available from: https://doi.org/10.1016/j.pcad.2019.01.004

154. Keeney M, Chin-Yee I, Weir K, Popma J, Nayar R, Robert Sutherland D. Single platform flow cytometric absolute CD34+ cell counts based on the ISHAGE guidelines. Communications in Clinical Cytometry. 1998;34(2):61–70.

155. Naeim F. Principles of Immunophenotyping. Hematopathology. 2008;27–55.

156. Basquiera AL, Abichain P, Damonte JC, Ricchi B, Sturich AG, Palazzo ED, et al. The number of CD34+ cells in peripheral blood as a predictor of the CD34+ yield in patients going to autologous stem cell transplantation. J Clin Apher. 2006 Jul;21(2):92–5.

157. Remberger M, Törlén J, Ringdén O, Engström M, Watz E, Uhlin M, et al. Effect of total nucleated and CD34+ cell dose on outcome after allogeneic hematopoietic stem cell transplantation. Biology of Blood and Marrow Transplantation [Internet]. 2015;21(5):889–93. Available from: http://dx.doi.org/10.1016/j.bbmt.2015.01.025

158. Hénon PH, Sovalat H, Bourderont D. Importance of CD34+ cell subsets in autologous PBSC transplantation: the mulhouse experience using CD34+CD38- cells as predictive tool for hematopoietic engraftment. J Biol Regul Homeost Agents. 2001;15(1):62–7.

159. Sutherland DR, Anderson L, Keeney M, Nayar R, Chin-Yee I. The ISHAGE guidelines for CD34+ cell determination by flow cytometry. J Hematother Stem Cell Res. 1996;5(3):213–26.

160. Tvede N, Kappel M, Galbo H, Pedersen BK. The Effect of Light, Moderate and Severe Bicycle Exercise on Lymphocyte Subsets, Natural and Lymphokine Activated Killer Cells, Lymphocyte Proliferative Response and Interleukin 2 Production.

161. Gleeson M, Pyne DB. Exercise effects on mucosal immunity. Immunol Cell Biol. 2000;78(5):536–44.

162. Gleeson M. Immunological aspects of sport nutrition. Immunol Cell Biol. 2016;94(2):117–23.

163. Svendsen IS, Taylor IM, Tønnessen E, Bahr R, Gleeson M. Training-related and competition-related risk factors for respiratory tract and gastrointestinal infections in elite cross-country skiers. Br J Sports Med. 2016;50(13):809–15.

164. Schwellnus MP, Derman WE, Jordaan E, Page T, Lambert MI, Readhead C, et al. Elite athletes travelling to international destinations >5 time zone differences from their home country have a 2-3-fold increased risk of illness. Br J Sports Med. 2012;46(11):816–21.

165. Mooren FC, Krüger K. Apoptotic lymphocytes induce progenitor cell mobilization after exercise. J Appl Physiol. 2015;119(2):135–9.

166. Simpson RJ. Aging, persistent viral infections, and immunosenescence: Can exercise “make space”? Exerc Sport Sci Rev. 2011;39(1):23–33.

167. Duggal NA, Niemiro G, Harridge SDR, Simpson RJ, Lord JM. Can physical activity ameliorate immunosenescence and thereby reduce age-related multi-morbidity? Nat Rev Immunol [Internet]. 2019;19(9):563–72. Available from: http://dx.doi.org/10.1038/s41577-019-0177-9

168. Jones GE. Cellular signaling in macrophage migration and chemotaxis [Internet]. Available from: http://www.jleukbio.org

169. Pixley FJ, Stanley ER. CSF-1 regulation of the wandering macrophage: Complexity in action. Vol. 14, Trends in Cell Biology. 2004. p. 628–38.

170. Kotsias F, Cebrian I, Alloatti A. Antigen processing and presentation. In: International Review of Cell and Molecular Biology. Elsevier Inc.; 2019. p. 69–121.

171. Pishesha N, Harmand TJ, Ploegh HL. A guide to antigen processing and presentation. Vol. 22, Nature Reviews Immunology. Nature Research; 2022. p. 751–64.

172. Guy CS, Vignali KM, Temirov J, Bettini ML, Overacre AE, Smeltzer M, et al. Distinct TCR signaling pathways drive proliferation and cytokine production in T cells. Nat Immunol. 2013;14(3):262–70.

173. Li X, Jiang S, Tapping RI. Toll-like receptor signaling in cell proliferation and survival. Vol. 49, Cytokine. 2010. p. 1–9.

174. Russell JH, Ley TJ. Lymphocyte-mediated cytotoxicity. Vol. 20, Annual Review of Immunology. 2002. p. 323–70.

175. Fabbri M. T lymphocytes. Int J Biochem Cell Biol [Internet]. 2003 Jul;35(7):1004–8. Available from: https://linkinghub.elsevier.com/retrieve/pii/S1357272503000372

176. Pallett LJ, Schmidt N, Schurich A. T cell metabolism in chronic viral infection. Clin Exp Immunol. 2019;197(2):143–52.

177. Buck MD, Sowell RT, Kaech SM, Pearce EL. Metabolic Instruction of Immunity. Cell [Internet]. 2017;169(4):570–86. Available from: http://dx.doi.org/10.1016/j.cell.2017.04.004

178. LaVoy EC, Bosch JA, Lowder TW, Simpson RJ. Acute aerobic exercise in humans increases cytokine expression in CD27- but not CD27+ CD8+ T-cells. Brain Behav Immun. 2013 Jan;27(1):54–62.

179. Golubovskaya V, Wu L. Different subsets of T cells, memory, effector functions, and CAR-T immunotherapy. Cancers (Basel). 2016;8(3).

180. Bishop EL, Gudgeon N, Dimeloe S. Control of T Cell Metabolism by Cytokines and Hormones. Front Immunol. 2021;12(April):1–15.

181. Almeida L, Lochner M, Berod L, Sparwasser T. Metabolic pathways in T cell activation and lineage differentiation. Semin Immunol [Internet]. 2016;28(5):514–24. Available from: http://dx.doi.org/10.1016/j.smim.2016.10.009

182. Maciver NJ, Michalek RD, Rathmell JC. Metabolic regulation of T lymphocytes. Annu Rev Immunol. 2013;31(December 2012):259–83.

183. Kumar V. T cells and their immunometabolism: A novel way to understanding sepsis immunopathogenesis and future therapeutics. Eur J Cell Biol [Internet]. 2018;97(6):379–92. Available from: https://doi.org/10.1016/j.ejcb.2018.05.001

184. Zhang Y, Ertl HCJ. Starved and asphyxiated: How can CD8+ T cells within a tumor microenvironment prevent tumor progression. Front Immunol. 2016;7(FEB):1–7.

185. Vander Heiden MG, Cantley LC TCB. Understanding the Warburg Effect: The Metabolic Requirements of Cell Proliferation. Science (1979). 2009;324:1029–33.

186. Wang R, Dillon CP, Shi LZ, Milasta S, Carter R, Finkelstein D, et al. The Transcription Factor Myc Controls Metabolic Reprogramming upon T Lymphocyte Activation. Immunity [Internet]. 2011;35(6):871–82. Available from: http://dx.doi.org/10.1016/j.immuni.2011.09.021

187. Sinclair L V., Rolf J, Emslie E, Shi YB, Taylor PM, Cantrell DA. Control of amino-acid transport by antigen receptors coordinates the metabolic reprogramming essential for T cell differentiation. Nat Immunol. 2013;14(5):500–8.

188. Macintyre AN, Gerriets VA, Nichols AG, Michalek RD, Rudolph MC, Deoliveira D, et al. The glucose transporter Glut1 is selectively essential for CD4 T cell activation and effector function. Cell Metab [Internet]. 2014;20(1):61–72. Available from: http://dx.doi.org/10.1016/j.cmet.2014.05.004

189. O'Neill LA, Kishton RJ RJ. The CD28 Signaling Pathway Regulates Glucose Metabolism. Immunity. 2002;16:769–77.

190. Tyrakis PA, Yurkovich ME, Sciacovelli M, Papachristou EK, Bridges HR, Gaude E, et al. Fumarate Hydratase Loss Causes Combined Respiratory Chain Defects. Cell Rep [Internet]. 2017;21(4):1036–47. Available from: https://doi.org/10.1016/j.celrep.2017.09.092

191. O'Neill LA, Kishton RJ RJ. A guide to immunometabolism for immunologists. Nat Rev Immunol. 2016;16(9):553–65.

192. Kaech SM, Cui W. Transcriptional control of effector and memory CD8+ T cell differentiation. Nat Rev Immunol. 2012;12(11):749–61.

193. O'Sullivan D, vanderWindt GWJ, Huang SCC, Curtis JD, Chang CH, Buck MDL, et al. Memory CD8+ T Cells Use Cell-Intrinsic Lipolysis to Support the Metabolic Programming Necessary for Development. Immunity [Internet]. 2014;41(1):75–88. Available from: http://dx.doi.org/10.1016/j.immuni.2014.06.005

194. Cham CM, Gajewski TF. Glucose Availability Regulates IFN-γ Production and p70S6 Kinase Activation in CD8 + Effector T Cells . The Journal of Immunology. 2005;174(8):4670–7.

195. Sukumar M, Liu J, Ji Y, Subramanian M, Crompton JG, Yu Z, et al. Inhibiting glycolytic metabolism enhances CD8+ T cell memory and antitumor function. Journal of Clinical Investigation. 2013;123(10):4479–88.

196. Buck MDD, O'Sullivan D, Klein Geltink RII, Curtis JDD, Chang CH, Sanin DEE, et al. Mitochondrial Dynamics Controls T Cell Fate through Metabolic Programming. Cell [Internet]. 2016;166(1):63–76. Available from: http://dx.doi.org/10.1016/j.cell.2016.05.035

197. van der Windt GJW, Everts B, Chang CH, Curtis JD, Freitas TC, Amiel E, et al. Mitochondrial Respiratory Capacity Is a Critical Regulator of CD8 + T Cell Memory Development. Immunity. 2012 Jan 27;36(1):68–78.

198. Stampley JE, Cho E, Wang H, Theall B, Johannsen NM, Spielmann G, et al. Impact of maximal exercise on immune cell mobilization and bioenergetics. Physiol Rep [Internet]. 2023 Jun 13;11(11):1–10. Available from: https://physoc.onlinelibrary.wiley.com/doi/10.14814/phy2.15753

199. Palmowski J, Gebhardt K, Reichel T, Frech T, Ringseis R, Eder K, et al. The Impact of Exercise Serum on Selected Parameters of CD4+ T Cell Metabolism. Immuno. 2021;1(3):119–31.

200. Lin ML, Hsu CC, Fu TC, Lin YT, Huang YC, Wang JS. Exercise Training Improves Mitochondrial Bioenergetics of Natural Killer Cells. Med Sci Sports Exerc. 2022 May 1;54(5):751–60.

201. Liepinsh E, Makarova E, Plakane L, Konrade I, Liepins K, Videja M, et al. Low-intensity exercise stimulates bioenergetics and increases fat oxidation in mitochondria of blood mononuclear cells from sedentary adults. Physiol Rep. 2020 Jun 1;8(12).

Chapter 2: Brief cycling intervals incrementally increase the number of hematopoietic stem & progenitor cells in human peripheral blood

Work presented within this chapter has been published:

Pradana, F., Nijjar., T., Cox, P.A., Morgan, P.T., Podlogar, T., Lucas, S.E., Drayson, M.T., Kinsella, F.A.M., Wadley, A.J., (2024). Brief cycling intervals incrementally increase the number of hematopoietic stem & progenitor cells in human peripheral blood, *Frontiers in Physiology.* https://doi.org/10.3389/fphys.2024.1327269.

2.1 Abstract

Peripheral blood stem cell (PBSC) donation is the primary procedure used to collect hematopoietic stem and progenitor cells (HSPCs) for hematopoietic stem cell transplantation. Single bouts of exercise transiently enrich peripheral blood with HSPCs and cytolytic natural killer cells ($CD56^{dim}$), which are important in preventing post-transplant complications. To provide a rationale to investigate the utility of exercise in a PBSC donation setting (≈3 hours), this study aimed to establish whether interval cycling increased peripheral blood HSPC and $CD56^{dim}$ concentrations to a greater degree than continuous cycling. In a randomised crossover study design, eleven males (mean ± SD: age 25 ± 7 years) undertook bouts of moderate intensity continuous exercise (MICE, 30 min, 65-70% maximum heart rate (HR_{max})), high-volume high intensity interval exercise (HV-HIIE, 4 x 4 min, 80-85% HR_{max}) and low-volume HIIE (LV-HIIE, 4 x 2 min, 90-95% HR_{max}). The cumulative impact of each interval on circulating HSPC ($CD34^{+}CD45^{dim}SSC^{low}$) and $CD56^{dim}$ concentrations, and the bone marrow homing potential of HSPCs (expression of CXCR-4 and VLA-4) were

determined. There was an increase in HSPC concentration after two intervals of LV-HIIE (Rest: 1.84 ± 1.55 vs. Interval 2: 2.94 ± 1.34, P = 0.01) and three intervals of HV-HIIE only (Rest: 2.05 ± 0.86 vs. Interval 3: 2.51 ± 1.05, P = 0.04). The concentration of all leukocyte subsets increased after each trial, with this greatest for $CD56^{dim}$ NK cells, and in HIIE vs. MICE (LV-HIIE: 4.77 ± 2.82, HV-HIIE: 4.65 ± 2.06, MICE: 2.44 ± 0.77, P < 0.0001). These patterns were observed for concentration, not frequency of CXCR-4^{+} and VLA-4^{+} HSPCs, which was unaltered. There was a marginal decrease in VLA-4, but not CXCR-4 expression on exercise-mobilised HSPCs after all trials (P < 0.0001). The results of the present study indicate that HIIE caused a more marked increase in HSPC and $CD56^{dim}$ NK cell concentrations than MICE, with mobilised HSPCs maintaining their bone marrow homing phenotype. LV-HIIE evoked an increase in HSPC concentration after just 2 x 2-minute intervals. The feasibility and clinical utility of interval cycling in a PBSC donation context should therefore be evaluated.

2.2 Introduction

Single bouts of exercise evoke rapid increases in the concentration of various subsets of immune cells in peripheral blood (1,2). This is part of a dynamic response that transiently enriches blood with cells that govern skeletal muscle repair and immunosurveillance in exercise recovery (3). Notably, the number of effector immune cells (e.g., cytolytic natural killer (NK) cells ($CD56^{dim}$) and cytotoxic T cells) increase between ~4–10-fold during exercise, whereas pluripotent cells such as haematopoietic stem and progenitor cells (HSPCs) increase by ~2-3 fold (4,5). There has subsequently been an emerging clinical interest in the potential of exercise to enrich the immune cell

fraction or ‘graft’ during peripheral blood stem cell (PBSC) donations (6,7), which are used to treat conditions such as multiple myeloma and lymphoma (7–9) and rare blood, autoimmune and congenital metabolic diseases (10).

Exceeding the HSPC collection threshold (>2 x 10^6 cells/kg) is critical for patients undergoing PBSC donations (termed ‘autologous donors’) (11). In response to standard mobilisation therapy using granulocyte colony stimulating factor (G-CSF), many autologous donors are classified as ‘poor mobilisers’ (≈40%) due to prior treatments damaging the bone marrow (e.g., myeloablative chemotherapy). This results in delayed and compromised engraftment of HSPCs, repeated hospital visits, inability to deliver further treatments and poorer health outcomes. HSPC mobilisation failure is much less common (≈5%) in healthy human leukocyte antigen (HLA)-matched donors (termed ‘allogenic donors’). However, the collection of effector immune cells such as $CD56^{dim}$ cells alongside HSPCs is of paramount importance to reduce this risk of disease relapse in the recipient after transplant (12). Although the magnitude (~4 cells/µL) of the HSPC response to exercise falls short of the collection threshold needed to begin apheresis (>10 cells/µL), a forward-thinking hypothesis has been that exercise in combination with G-CSF may help to achieve the HSPC dosing threshold required for successful engraftment and expedite the PBSC donation process (13). Furthermore, enrichment of the graft with $CD56^{dim}$ and other effector immune cells may offset the risk of post-transplant viral infections and graft-versus-host disease (GvHD) by priming adaptive immune responses in the recipient (7).

In addition to the number of harvested HSPCs, the engraftment phenotype of these cells is critical for predicting clinical endpoints following transplant, and some evidence indicates that exercise may modulate this. For example, non-lineage pluripotent hematopoietic stem cells (HSCs: $CD34^+$ $CD38^-$) are known to predict trilineage engraftment success following autologous transplants with the ability to repopulate (self-renewal) the bone marrow with colony-forming cells (CFC) and sustain haematopoiesis. However, the engraftment phenotype called late-lineage committed hematopoietic progenitor cells (HPCs: $CD34^+$ $CD38^+$) can differentiate into blood cells including lymphoid and myeloid lineages (14). Furthermore, higher expression of bone marrow homing receptors C-X-C chemokine receptor type 4 (CXCR-4) (15) and Very Late Antigen-4 (VLA-4) (16) on HSPCs promotes their successful engraftment in animal models and some human data indicate an association between CXCR-4 expression and engraftment success (17). Exercise can mobilise $CXCR\text{-}4^+$ HSPCs (+500 cells/mL) (18) and $CD34^+$ $CD38^-$ (+3000 cells/mL) (13,19); however, this largely reflects the typical leukocytosis associated with exercise, and the impact of different types of exercise on the cell surface expression of these receptors has not been reported. The complementary ligands to these receptors C-X-C motif chemokine 12 (CXCL-12) and vascular cellular adhesion molecule-1 (VCAM-1) increase in the circulation immediately after exercise in humans (20,21) and the expression of CXCL-12 is upregulated in skeletal muscle within 15 minutes of exercise onset in mice (22). These changes may provide chemoattractant cues for HSPCs to egress from vascular walls or the bone marrow into peripheral blood (23), thus making them available for harvest during PBSC donations.

Before addressing the feasibility of translating this concept into a clinical setting, the optimal dose of exercise to maximise HSPC and $CD56^{dim}$ NK cell concentrations needs to first be established. During exercise, HSPCs and $CD56^{dim}$ NK cells are rapidly mobilised from marginal pools within the circulation and tissues by shear stress and beta 2 (β2) adrenergic dependent mechanisms (24), with resting cell numbers restored within 5 (25) and 20 (26) minutes, respectively. Although many studies have reported increases in HSPCs after bouts of steady-state exercise lasting 30-45 minutes (13,22,24), this duration does not align with the timeline of a PBSC donation session, which often lasts 3-4 hours and often extends to multiple days. Given the known mechanisms underpinning HSPC mobilisation and rapid margination in response exercise, adopting periods of rest between intervals of high intensity exercise might therefore be a feasible approach. High intensity interval exercise (HIIE) of both high volume (5 x 3-minute cycling intervals at 90% peak power) and low volume (6 x 20 second 'all-out' cycling sprints) (27) have been reported to increase HSPC concentrations after the final interval relative to rest. However, one study evaluating moderate volume HIIE (≈10 minutes of total intervals at 90% of maximal heart rate) reported no change (19). In contrast, there are consistent data reporting increases in circulating $CD56^{dim}$ NK cell concentrations after HIIE, ranging from 10 to 15 intervals (60–90 seconds) at 85–90% peak oxygen consumption (26,28,29). More prominent NK mobilisation compared to HSPCs is explained by higher β2 adrenergic receptor expression on the surface of NK cells.

Evidently, there is a complex interplay between the intensity, duration, and total work of intervals needed to maximise circulating HSPC concentrations, and this is not fully

understood. Previous studies typically compare changes before and after the last interval of HIIE, rather than monitoring cumulative changes after each interval. Enumerating HSPCs using guidance set out by the International Society of Hematotherapy and Graft Engineering (ISHAGE) (30) would facilitate such an approach. This single platform flow cytometric (SPFC) approach uses small volumes of whole blood (100 µL) to enable rapid and accurate quantification of peripheral blood HSPC concentrations. The advantage of using the SPFC approach compared to the previous exercise-based studies that have mostly used a double platform flow cytometry (DPFC) approach (i.e., flow cytometry coupled with automated haematology analysis) is that less blood is needed, processing times are shorter and both inter- and intra- laboratory variances are significantly less with SPFC than DPFC (31).

Understanding how different volumes of HIIE impact the 'quantity' and 'quality' of HSPCs in peripheral blood over a suitable time course is a clear knowledge gap that needs addressing to evaluate the potential of exercise to work in combination with PBSC donations. For future adoption of this approach clinically, evaluation of HIIE protocols that are feasible for the donor are critical. Therefore, criteria outlined for utilising HIIE in clinical populations based on a percentage of maximal heart rate were used to guide protocol design (32,33). Accordingly, the primary aim of this study was to compare changes in peripheral blood HSPC concentrations before and after each of four consecutive intervals of low volume HIIE (LV-HIIE) and high-volume HIIE (HV-HIIE) vs. a time-matched continuous cycling bout (control). Secondary aims included quantifying changes in $CD56^{dim}$ NK cell concentrations, characterising the bone

marrow homing potential of HSPCs mobilised with exercise, and contrasting single vs. double platform quantitative HSPC methods.

2.3 Materials and Methods

2.3.1 Participants

Eleven healthy males were recruited into this study (mean ± SD: age 25 ± 7 years; body mass index: 25.7 ± 3.0 kg/m^2). Participants underwent screening prior to enrolment and were deemed eligible if they were 18–45 year-old, not highly active (as defined by the General Practice Physical Activity Questionnaire (GPPAQ) (34), non-smokers, not currently taking medication, and had no previous history of cardiovascular, metabolic, neurological, or inflammatory diseases. All participants gave written informed consent before participating and the study was given favourable ethical opinion by the Science, Technology, Engineering and Mathematics ethical committee at the University of Birmingham (ERN_19-1574PA2).

2.3.2 Preliminary Testing

Participants undertook four laboratory visits, including 3 randomised cycling trials at the School of Sport, Exercise and Rehabilitation Sciences at the University of Birmingham, conforming to the Declaration of Helsinki. On the first visit, participants initially rested for a period of 30 minutes followed by measurements of resting blood pressure (*Thuasne BP 3W1-A, Taipei, Taiwan*), height (*Seca Alpha, Hamburg, Germany*) and body mass (*Ohaus CD31, New Jersey, USA*). Participants then undertook a maximal power ($Watt_{max}$) ramp test on an electromagnetically braked cycle

ergometer (*Excalibur, Lode, The Netherlands*). After a warm-up for 5 minutes at 50 watts, the test started at 70 watts and then 25 watts increments were added every minute until volitional exhaustion. Heart rate (HR) was monitored continuously throughout (*H10, Polar Electro, Finland*). Participants were asked to maintain a cadence of ~60 rotations/minute (RPM). Following a 15-minute rest period, participants were familiarised with the exercise protocols used in the three main trials. The intensity of these trials was based on a percentage of their maximal heart rate (HR_{max}).

2.3.3 Experimental Sessions

The 3 main cycling trials were separated by at least one week and carried out at the same time of day (8:00–9.00 AM start time) and under stable climatic conditions (temperature: 19–20^{o}C, humidity: 30–55% and Barometric pressure: 1000–1050 hPa). Prior to each laboratory visit, participants were asked to undertake an overnight fast, refrain from vigorous exercise, and the consumption of caffeine and alcohol for 48 hours. In the morning of each trial, participants were asked to drink 0.5 L of water within 4 hours and 0.25 L within 15 minutes of commencing the trial. Questionnaires evaluating state and trait anxiety (35) and sleep efficiency (percentage of time asleep relative to the amount of time spent in bed) (36) were completed during a 30-minute period of rest where blood pressure and body mass were also measured. Following this a catheter (*Becton, Dickson & Company, Oxford, UK*) was inserted into the antecubital vein of the forearm and a baseline blood sample was taken (Rest). The catheter was kept patent through regular flushes with saline (0.9% NaCl*, Becton, Dickson & Company, Oxford, UK*,). Each trial commenced with a 5-minute warm-up at 50 watts and then one of three randomised 30 minute trials: 1) Moderate intensity

continuous exercise (MICE) consisting of 30-minutes of cycling at 65–70% HR_{max}, 2) High volume-high intensity interval exercise (HV-HIIE) consisting of 4 x 4-minute cycling intervals at 80–85% HR_{max} with 3 minutes of passive rest between each interval or 3) Low volume-high intensity interval exercise (LV-HIIE), consisting of 4 x 2-minute interval at 90–95% HR_{max} with 5 minutes of passive rest between each interval. HR was monitored continuously alongside ratings of perceived exertion (RPE) (37) and the affective response using the Feeling Scale (38) every minute. Total energy expenditure from each trial was estimated from power output using an equation proposed by Ettema et al, 2009 (39). Six further blood samples were taken during each trial, one after each of the four intervals (and matched timepoints for MICE), and two samples in recovery (5 and 10 minutes following cycling completion).

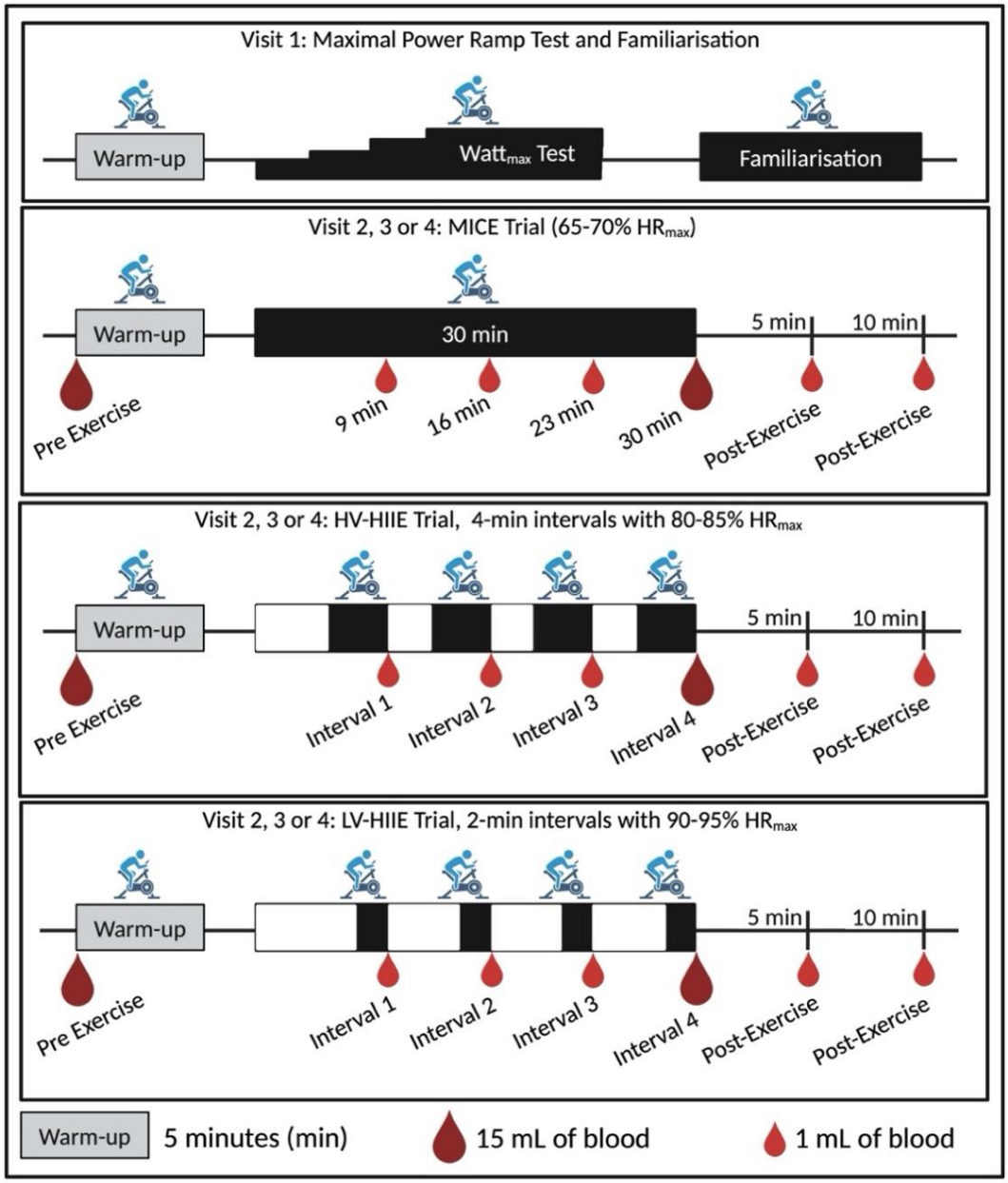

Figure 2.1 Study design illustrating a time axis of the warmup, intervals/ steady state, and recovery cycling periods for the 4 laboratory visits and 3 randomised trials: MICE, Moderate intensity continuous exercise, HV-HIIE, High volume-high intensity interval exercise, LV-HIIE, Low volume-high intensity interval exercise. Blood sampling is indicated with small droplets (1mL) for whole blood analysis, and large droplets (15mL) for PBMC and plasma analyses. Created with BioRender.com.

The 7 samples were therefore named: Rest, Interval 1 (9 min), Interval 2 (16 min), Interval 3 (23 min), Interval 4 (30 min), Recovery 1 (35 min) and Recovery 2 (40 min). No fluid intake was permitted throughout the trials so as not to influence blood volume independent of the exercise itself; however, corrections were made (outlined below). A total of 35 mL of blood was taken during each trial, including 7 x 1-mL containing potassium ethylene-diamine-tetra-acetic acid (K_2EDTA) vacutainers (*Greiner Bio-One, Frickenhausen, Germany*) for whole blood HSPC and complete blood counts (*Yumizen H500, Horiba, Kyoto, Japan*) at every timepoint. At Rest and after Interval 4 (30 min) only, 15-mL of blood was collected in K_2EDTA vacutainers (*Becton, Dickson & Company, Oxford, UK*) for complete blood counts and then plasma and peripheral blood mononuclear cell (PBMC) isolation **(Figure 2.1)**. The complete blood count was used to determine total white blood cell, neutrophil, monocyte, and lymphocyte concentrations (cells/µL), with haematocrit (L/L) and haemoglobin concentration (g/dL) also determined.

2.3.4 Blood Processing

Plasma was obtained through centrifugation of 4 mL K_2EDTA blood for 10 minutes at 1525 x *g* at 4ºC and stored at -80ºC. PBMCs were isolated by gradient density centrifugation by first diluting 10 mL of whole blood with Dulbecco's phosphate-buffered saline (*D-PBS, Thermo Fisher Scientific, Massachusetts, USA*) in a 1:1 ratio. Diluted blood was gently layered on the top of Histopaque-1077 separating medium (*Sigma Aldrich, Missouri, USA*) and centrifuged for 40 min, at 300 x *g* (brake off) and 21ºC. PBMCs were harvested by removing the PBMC interphase and washing 3 times with D-PBS before counting on a Cellometer 2000 dual fluorescence cell counter

(*Nexcelom Bioscience, Massachusetts, USA*). PBMCs were cryopreserved in freezing medium (RPMI (Roswell Park Memorial Institute) supplemented with 20% FBS (Fetal bovine serum) and 10% Dimethylsulfoxide) and stored in liquid nitrogen at the Human Biomaterials and Resource Centre at the University of Birmingham until analysis.

2.3.5 Flow Cytometry Data Acquisition and Analysis

Four colour flow cytometry analyses were undertaken using a CytoFlex-S flow cytometer (*Beckman Coulter, California, USA*): Analyses included determining: 1) concentration (cells/µL) of HSPCs in whole blood, 2) frequency of HSPCs, $CD3^{+}$, $CD56^{dim}$, and $CD56^{bright}$ NK cells in the PBMC fraction and 3) frequency (%) and cell surface expression (Geometric Mean Fluorescence Intensity) of bone marrow homing receptor positive HSPCs (CXCR-4 and VLA-4) in the purified PBMC fraction. All antibodies used were purchased from BioLegend (*San Diego, CA*) or R&D Systems (*Minneapolis, USA*) and data were analysed with CytExpert v2.5 Software (*Beckman Coulter, California, USA*). Presentation of gating strategies was carried out using FlowJo™ v10.9 Software (*Becton, Dickson & Company, Ashland, USA*). Gates were formed using fluorescence minus one (FMO) controls, and compensation was applied for each trial/participant using single stained controls. Dead cells were excluded using a viability exclusion dye.

2.3.6 Single Platform Flow Cytometry

A SPFC method validated by the International Society of Hematotherapy and Graft Engineering (ISHAGE) was used to identify HSPCs (defined as $CD34^{+}CD45^{dim}SSC^{low}$) in whole blood. Whole blood (100 µL) was stained with anti-human CD34-PE (clone

581), anti-human CD45-FITC (clone 2D1), CD38-BV421 (clone HB-7), and a viability exclusion dye (7-amino-actinomycin D, 7-AAD) at room temperature, in the dark, for 30 minutes and then 2 mL of red blood cell lysis buffer added for 10 minutes. All samples were analysed within 1 hour. HSPCs were enumerated using a Boolean gating strategy based on three key criteria: positive expression of CD34, moderate expression of CD45 and low side scatter **(Figure 2.2)**.

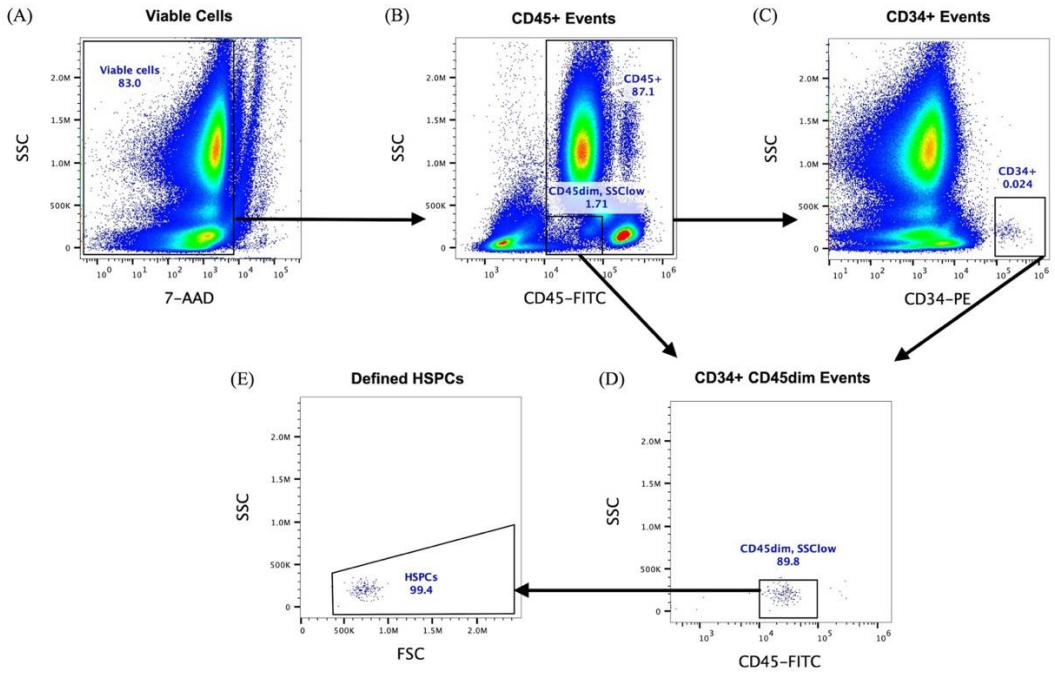

Figure 2.2 A Boolean gating strategy was used to enumerate HSPCs following guidelines validated by the International Society of Hematotherapy and Graft Engineering (ISHAGE) using whole blood (single platform, presented herein) or PBMCs (double platform). $CD34^+$ cells were first identified by sequential gating of (A) viable cells using 7-AAD exclusion, (B) $CD45^+$ events and then (C) $CD34^+$ events. (D) A gate on plot B defining viable cells with low to moderate (dim) expression of CD45 and low side scatter properties was combined with $CD34^+$ cells using Boolean gating.

(E) Finally, debris was removed and viable HSPCs defined as $CD34^{+}CD45^{dim}SSC^{low}$ on a FSC vs SSC plot.

A minimum of 100 HSPC events were acquired in the final gate in accordance with ISHAGE guidelines and data expressed as the concentration of HSPCs in whole blood (cells/µL), fold change or total area under the curve (AUC), calculating using the Trapezoid method (40). The frequency of HSPCs expressing CD38 was also calculated.

2.3.7 Double Platform Flow Cytometry

Cryopreserved PBMCs were thawed by submerging half of the vials containing approximately ≈20 million cells for 1 minute and then gently pouring the cells into sterile 15-mL falcon tubes. Cells were washed 3 times with RPMI supplemented with 20% FBS, 100 U/mL Pen-Strep, and 2 mM Glutamine. PBMCs (2×10^6) were stained with anti-human CD45-FITC (clone 2D1), anti-human CD34-PE (clone 581), anti-human CXCR4-APC (clone 12G5), anti-human VLA4-AF (clone Hu114), anti-human CD3-FITC (clone UCHT1), anti-human CD56-PE (clone 5.1H11) and anti-human CD16-APC (clone 3G8) and 7-AAD on ice, in the dark for 30 minutes. These cells were then washed three times in FACS buffer (500 mL of D-PBS, 2 mM EDTA, 0.1% Sodium Azide, and 1 mM FBS) for 5 minutes at 500 x *g* and 4ºC before data acquisition.

A DPFC approach was used to calculate the concentration of HSPCs, $CD3^{+}$ T cells, $CD56^{dim}$ and $CD56^{bright}$ NK cells in peripheral blood by coupling their frequency in the PBMC fraction determined by flow cytometry **(Figure 2.3)** to a whole blood lymphocyte

count from the same sample using an automated haematology analyser (*Yumizen H500, Horiba, Kyoto, Japan*).

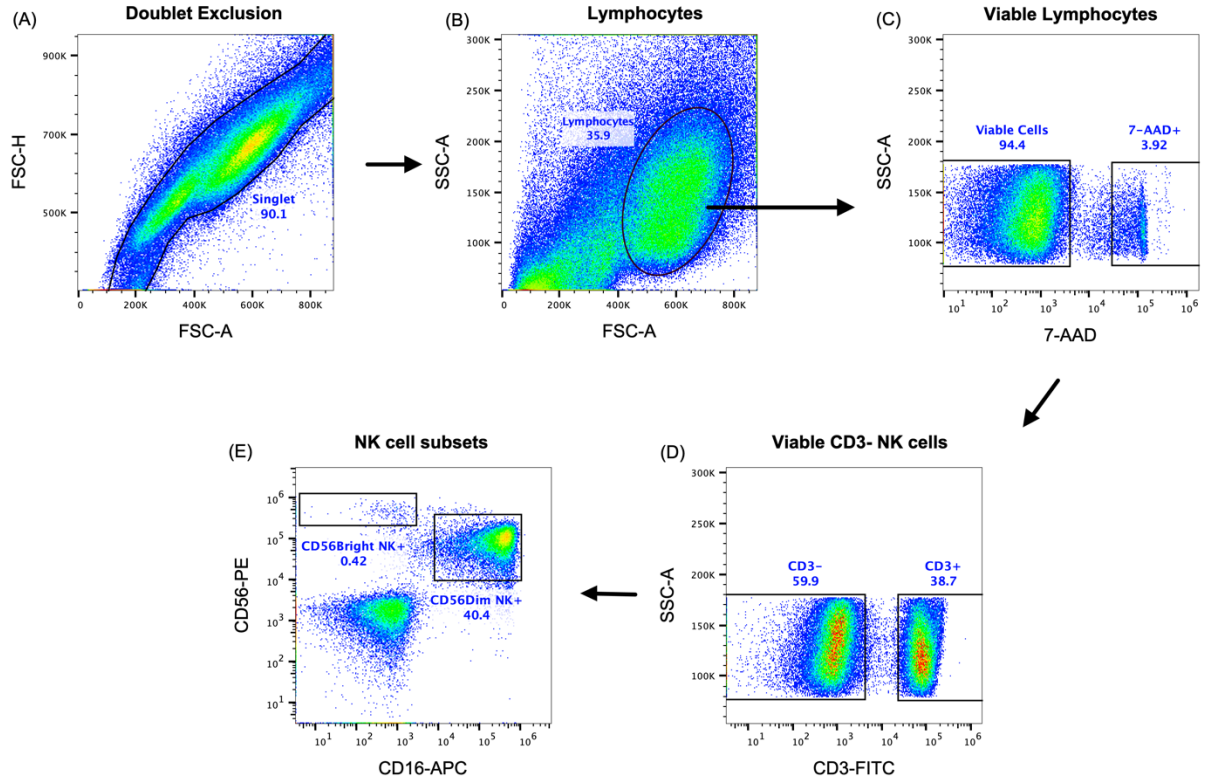

Figure 2.3 Gating strategy to identify CD56^{dim} and CD56^{bright} NK cells within PBMCs using flow cytometry. (A) Single cells were gated by forward scatter area (FSC-A) vs. forward scatter height (FSC-H) to exclude doublets. (B) Lymphocytes were identified by forward scatter (FSC) vs. side scatter (SSC), and then (C) dead cells excluded by sequential gating of viable cells using 7-AAD exclusion. (D) CD3+ and CD3^{-} events were determined from viable lymphocytes and, (E) CD3- events gated on a bivariate plot between CD16 and CD56 to define cytolytic (CD16^{+} CD56^{dim}) and regulatory (CD16^{-} CD56^{bright}) natural killer (NK) cells.

Titrations antibody volumes were conducted to determine the optimal conditions for flow cytometry analysis of CXCR-4+ or VLA-4+ HSPCs **(Figure 2.4)**. Eight volumes (0, 0.3125, 0.625, 1.25, 2.5, 5, 10 and 20 µL) of CXCR-4 and VLA-4 antibodies were each added to 200 x 10^3 PBMCs (50 µL). A stain index (SI) was calculated for the titrated volumes of each antibody. SI represents the level of separation between positive and negative cell populations and is calculated by dividing the difference between the median fluorescence intensity (MFI) of positive and negative populations by 2 times the standard deviation of the negative population. The red boxes and * in the dot and line graphs respectively indicate the volume of CXCR-4-APC or VLA-AF that gave the highest SI and therefore, optimal separation between positive and negative cell population of CXCR-4 or VLA **(Figure 2.4)**. The SI was 5 µL for 200 x 10^3 PBMCs stained with either CXCR-4-APC or VLA-AF.

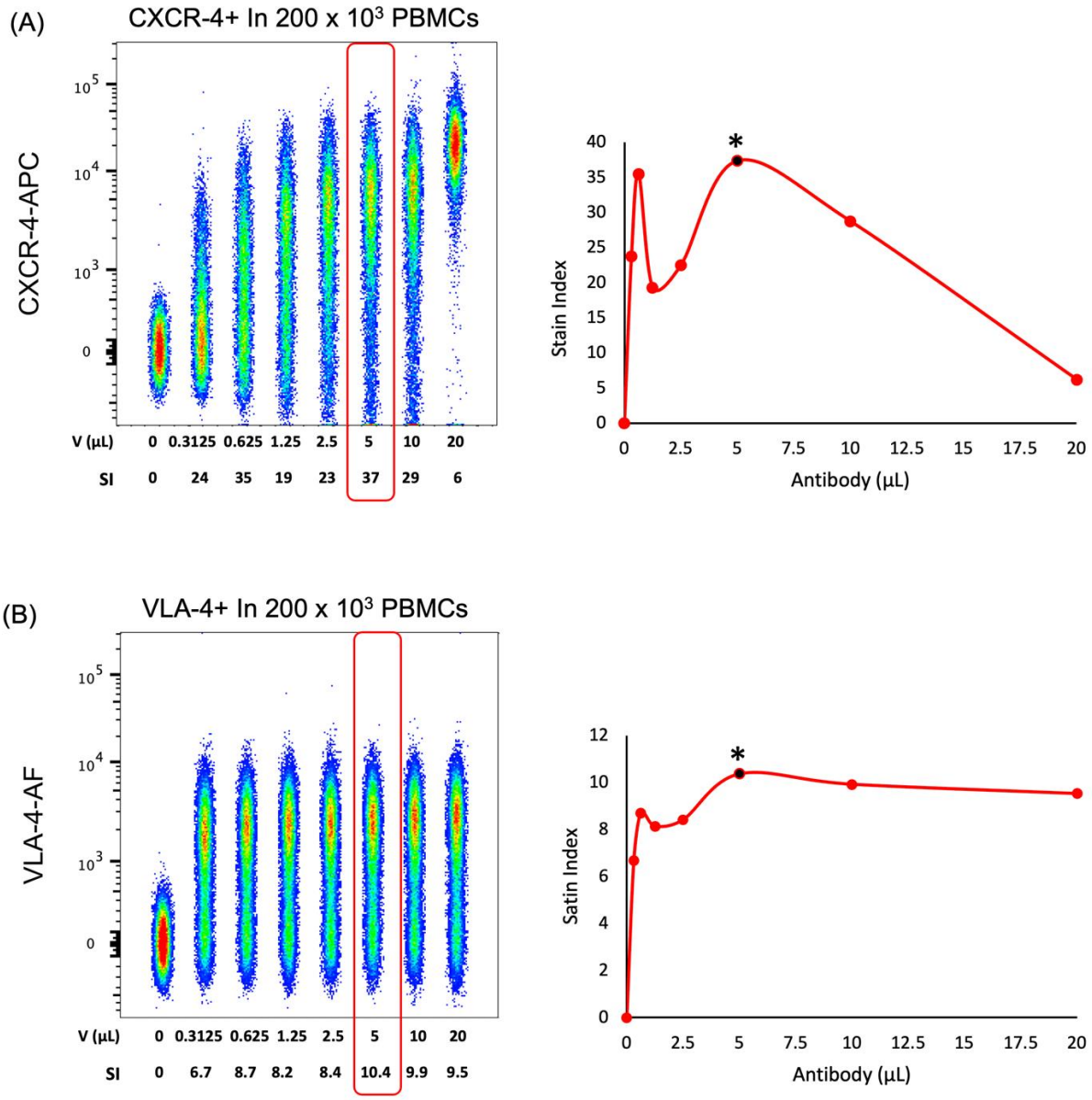

Figure 2.4 Antibody titration in 200 x 10^3 PBMCs stained with 0, 0.3125, 0.625, 1.25, 2.5, 5, 10 and 20 µL of CXCR-4-APC or VLA-AF. The dot plots (left) display the separation of (A) CXCR-4+ and CXCR-4- and (B) VLA-4+ and VLA-4- cells and the line graph the stain index of each antibody volume (right).

A minimum of 1 x 10^6 lymphocyte events were acquired, resulting in approximately 1 x 10^3, 1 x 10^6, 5 x 10^4, and 1 x 10^3 events in the HSPC, $CD3^+$, $CD56^{dim}$ and $CD56^{bright}$

gates, respectively. Data were expressed as concentration in peripheral blood (cells/µL) or fold change. Within the HSPC gate, the frequency (%) of CXCR-4^{+} and VLA-4^{+} HSPCs were calculated and used to determine a peripheral blood concentration (cells/µL) for each cell type **(Figure 2.5)**. The cell surface expression of CXCR-4 and VLA-4 on gated HSPCs was then determined using the Geometric Mean Fluorescence Intensity (GeoMean)**.**

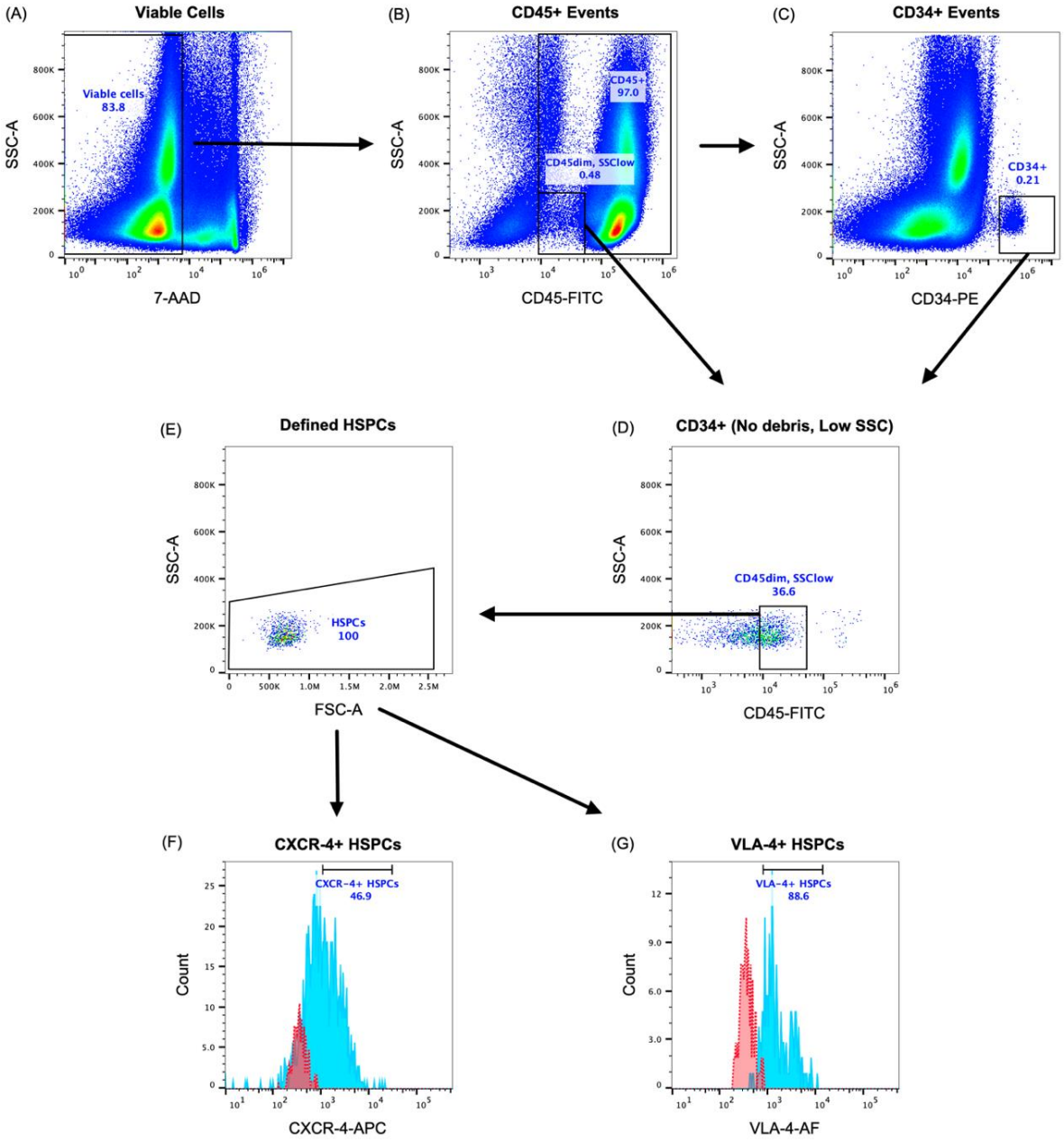

Figure 2.5 Validated gating strategy to enumerate CXCR-4$^+$ and VLA-4$^+$ HSPCs in flow cytometry. (A) Dead cells were excluded by sequential gating of viable cells using 7-AAD exclusion. CD34$^+$ cells were identified by sequential gating of (B) CD45$^+$ events and then (C) CD34$^+$ events. (D) A gate on plot B defining viable cells with low to moderate (dim) expression of CD45 and low side scatter properties was combined with CD34$^+$ cells using Boolean gating. (E) Debris was removed and viable HSPCs defined as CD34$^+$CD45^{dim}SSC^{low} on a FSC vs SSC plot. Finally, (F) CXCR-4$^+$ and (G) VLA-4$^+$ HSPCs were identified (solid line-blue histogram) using a fluorescence minus one (FMO) control (dotted line-red histogram) to establish the positive population.

2.3.8 Correction of Cell Concentrations for Changes in Blood Volume

Changes in cell concentrations vs. rest measured using DPFC (T cells, NK cell subsets, HSPCs, CXCR-4$^+$ HSPCs and VLA-4$^+$ HSPCs), automated haematology analysis (total white blood cells, neutrophils, lymphocytes, monocyte), and SPFC (HSPCs) were adjusted for changes in blood volume using the formula proposed by Matomäki et al, 2000 (41).

2.3.9 Enzyme-Linked Immunosorbent Assays

The concentration of soluble adhesion molecules CXCL-12/SDF-1 (stromal cell-derived factor-1) and VCAM-1 (Vascular cell adhesion molecule-1) were determined in plasma using enzyme-linked immunosorbent assay (ELISA) kits purchased from Bio-techne (*Minneapolis, USA, assay sensitivity, CXCL-12: 18 pg/mL and VCAM-1: 0.6 ng/mL*). All samples were analysed in duplicate and concentrations were obtained from a standard curve of known CXCL-12 and VCAM-1 concentrations and adjusted

for changes in plasma volume (42). The manufacturer reported intra- (*CXCL-12: 3.6% and VCAM-1:* 0.6%) and inter-assay (*CXCL-12: 10.3% and VCAM-1:* 7.0%) variability that aligned with our laboratory.

2.3.10 Statistical analysis

Statistical analyses were performed using GraphPad Prism 10.0.3 analysis software (*San Diego, CA*). Data at all timepoints were checked for normal distribution using the Shapiro-Wilk test. Normally distributed variables were analysed over time (Rest, End of intervals 1–4, 5-minute and 10-minute post exercise) and across Trials (MICE, HV-HIIE, and LV-HIIE) by mixed-effects two-way analysis of variance (Two-way ANOVA). Data that weren't normally distributed were analysed using Wilcoxon or Kruskal-Wallis's test. Post hoc analyses of any interaction effects (Time x Trial) were performed by a test of multiple comparisons, with either Tukey or Dunn's test, depending on variable normality. All values are presented as means ± standard deviation (SD). Statistical significance was accepted at the $P < 0.05$ level. AUC for HSPC concentration determined by SPFC was calculated using Trapezoid method that approximates the region under the graph of a function as a trapezoid by dividing the total area into smaller trapezoids (40). The Cohen's *d* effect sizes (*d*) were calculated where appropriate by dividing the difference between the means by the pooled standard deviations. An effect size of 0.2 was considered the minimal value for a meaningful difference, 0.5 for moderate and 0.8 for large (43). The relationship between HSPC concentrations determined by SPFC and DPFC methods was evaluated by calculating a Pearson correlation coefficient and agreement of these methods by formulating a Bland-Altman plot. For the latter, mean concentrations of

both methods (x-axis) were plotted against the difference between these values (SPFC – DPFC, y-axis). This enabled identification of systemic differences between these two quantitative methods, including degree of bias and outliers. The limits of agreement ('lower limit' = mean difference – (1.96 x standard deviation of difference) and 'upper limit' = mean difference + (1.96 x standard deviation of difference) were calculated according to 95% confidence intervals.

2.4 Results

2.4.1 Physiological Responses and Subjective Perceptions During Experimental Trials

There were no significant differences in resting HR ($F(2, 30) = 0.09$, $P = 0.91$) and participants weight remained stable across all 3 experimental trials ($F(2, 30) = 0.01$, $P < 0.99$). There was no difference between anxiety and sleep quality between the three experimental trials **(Table 2.1)**. These variables were therefore not used as covariates in subsequent ANOVA analyses.

Table 2.1 Sleep efficiency and state and trait anxiety prior to each experimental trial.

	Cycling Trial			
Parameter	**MICE**	**HV-HIIE**	**LV-HIIE**	**P-Value**
Anxiety State ($S_{anxiety}$)	45.18 ± 3.49	44.91 ± 3.83	44.55 ± 3.80	> 0.05
Anxiety Trait ($T_{anxiety}$)	44.36 ± 3.61	45.27 ± 4.32	44.09 ± 3.70	> 0.05
Sleep Efficiency (%)	87.36 ± 8.36	86.84 ± 10.50	86.27 ± 8.14	> 0.05

Data displayed as mean ± SD.
P > 0.05 indicates no significant differences between trials.

A repeated measures ANOVA revealed no significant differences in state (F (2, 30) = 0.08, P = 0.92) and trait (F (2, 30) = 0.28, P = 0.76) anxiety levels or sleep efficiency (F (2, 30) = 0.04, P = 0.96) before undertaking the three experimental trials.

Abbreviations: MICE, moderate intensity continuous exercise; HV-HIIE, high volume-high intensity interval exercise; LV-HIIE, low volume-high intensity interval exercise.

By design, average power output (F (2, 30) = 46.54, P < 0.0001), peak HR (HR_{peak}) (F (2, 30) = 115.50, P < 0.0001), HR_{max} (F (2, 30) = 354.00 P < 0.0001) and average RPE (F (2, 30) = 25.08, P < 0.0001) were greater throughout LV-HIIE > HV-HIIE > MICE **(Table 2.2)** and estimated total energy expenditure was greater in MICE > HV-HIIE > LV-HIIE (F (2, 30) = 25.48 P < 0.0001).

Table 2.2 Physiological responses during each experimental trial.

	Cycling Trial			
Parameter	**MICE**	**HV-HIIE**	**LV-HIIE**	**P-Value**
Average Power output (W)	132 ± 19.79[1,2]	215 ± 32.2[1,3]	271 ± 45.3[2,3]	< 0.0001
Relative Maximal Power (%)	42.44 ± 4.68[1,2]	68.77 ± 3.35[1,3]	86.57 ± 3.08[2,3]	< 0.0001
HR_{peak} (bpm)	131 ± 6.78[1,2]	162 ± 7.32[1,3]	175 ± 6.84[2,3]	< 0.0001
HR_{max} (%)	69.73 ± 2[1,2]	84.18 ± 3	94.45 ± 2[2,3]	< 0.0001
Estimated Energy Expenditure (kcal)	221.60 ± 42.79[1,2]	151.50 ± 45.68	86.55 ± 44.71[2,3]	< 0.01
Average RPE	12 ± 0.59[1,2]	14 ± 0.87[1,3]	17 ± 1.04[2,3]	< 0.0001

Average Feeling Scale	2.96 ± 1.47	2.37 ± 1.74	1.69 ± 2.41	> 0.05

Data displayed as mean ± SD.
[1], significant difference between MICE and HV-HIIE (P < 0.05)
[2], significant difference between MICE and LV-HIIE (P < 0.05)
[3], significant difference between HV-HIIE and LV-HIIE (P < 0.05)

Abbreviations: MICE, moderate intensity continuous exercise; HV-HIIE, high volume-high intensity interval exercise; LV-HIIE, low volume-high intensity interval exercise; HR_{peak}, peak heart rate; RPE, rating of perceived exertion.

A repeated measures ANOVA indicated significant differences in average HR after each interval (Time x Trial Interaction: F (6, 90) = 2.60, P = 0.02). *Post-hoc* analysis revealed that heart rate peaked after the second interval during HV-HIIE (155.60 ± 7.78, P < 0.0001), the third interval during LV-HIIE (171.90 ± 6.43, P < 0.0001) and remained stable above rest during MICE (125.18 ± 5.33, P > 0.99). Within each trial, power output and RPE remained consistent over the 30-minute trial or between intervals (Time x Trial Interaction: P > 0.05). There was no significant difference in the affective response between the three trials measured by the feeling scale (F (2, 30) = 1.21, P = 0.31) **(Table 2.2)**.

2.4.2 SPFC to Determine Peripheral Blood HSPC Concentrations

Changes in peripheral blood HSPC concentrations in response to trials determined by SPFC are shown in **Figure 2.6**. A Time x Trial interaction effect was observed (F (12, 180) = 2.31, P = 0.01), indicating no change in HSPC concentration during MICE and a significant increase after two intervals of LV-HIIE (Rest: 1.84 ± 1.55 vs. Interval 2: 2.94 ± 1.34, P = 0.005), and three intervals of HV-HIIE (Rest: 2.05 ± 0.86 vs. Interval

3: 2.51 ± 1.05, P = 0.04), although this was only sustained through to the end of Interval 4 during LV-HIIE.

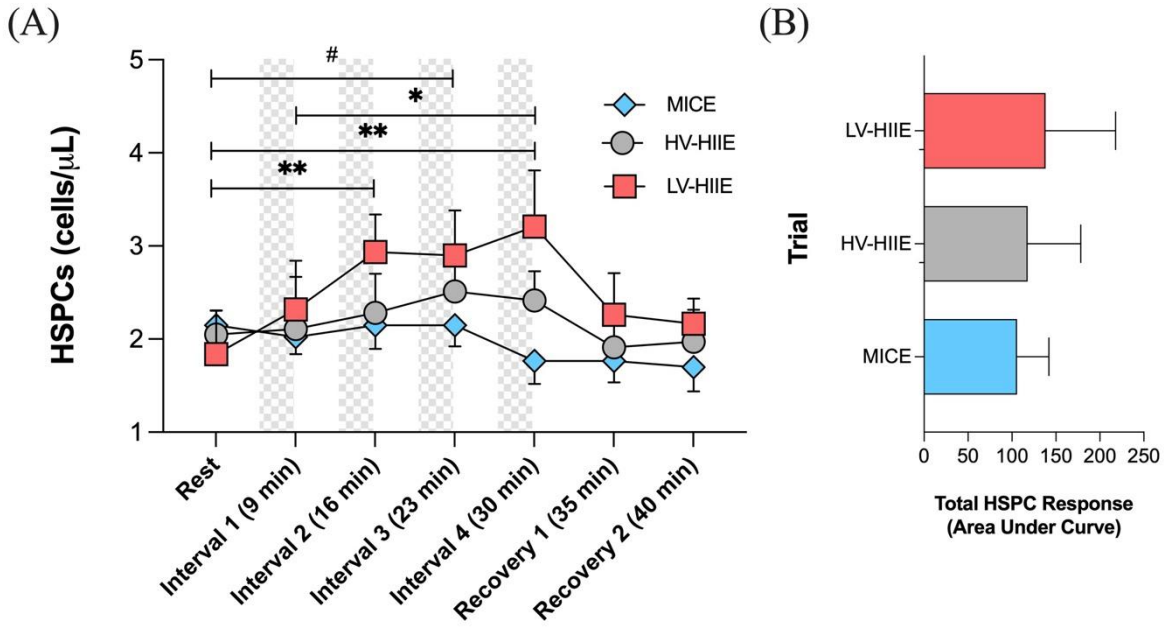

Figure 2.6 (A) Changes in peripheral blood HSPC concentrations (B) and total area under the curve HSPC response across seven timepoints of MICE (blue bars), HV-HIIE (grey bars) and LV-HIIE (red bars) enumerated by SPFC. Values are means ± SD. * and # indicate significant differences between timepoints in LV-HIIE and HV-HIIE respectively: *P < 0.05, **P < 0.01, #P < 0.05.

A cumulative increase was observed during LV-HIIE only, with HSPC concentration significantly greater following Interval 4 (3.21 ± 2.00) than Interval 1 (2.32 ± 1.73, P = 0.03). A *post hoc* analysis comparing peak HSPC concentrations at Interval 4 (30 minutes) demonstrated a significant difference between LV-HIIE vs. MICE (LV-HIIE: 3.21 ± 2 vs. MICE: 1.76 ± 0.82, *d* = 0.95, P = 0.02). In all trials, HSPC concentrations

decreased to resting levels within 5 minutes of cycling cessation. Analysis of changes in HSPC concentrations over time by calculating AUC revealed no statistically significant differences between trials (LV-HIIE: 138 ± 79.71, HV-HIIE: 117.90 ± 60.46, MICE: 105.90 ± 36.23) **(Figure 2.6B)**. The Cohen's *d* effect size for MICE vs. LV-HIIE was 0.3, whereas comparisons between other trials were < 0.2.

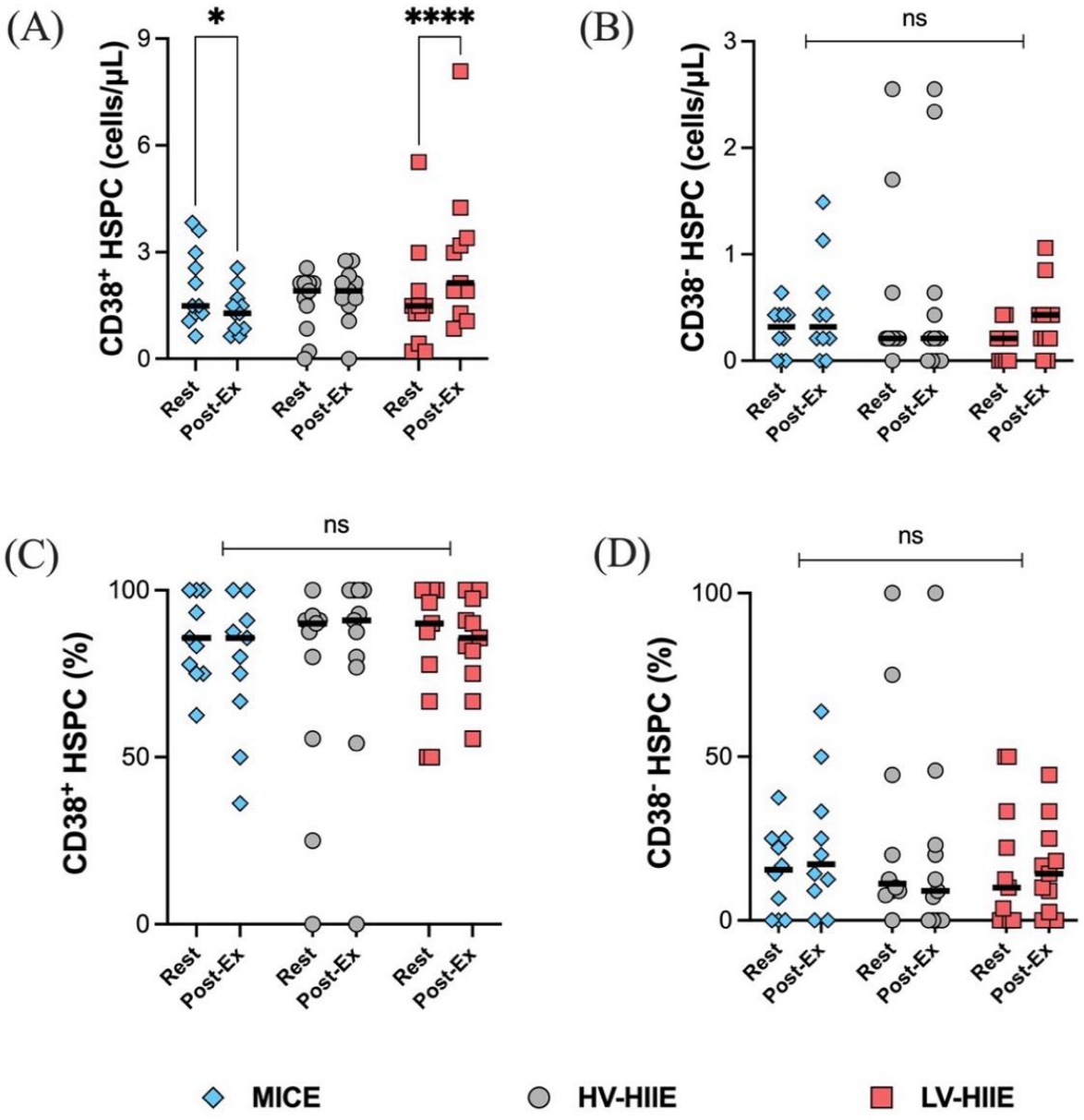

Figure 2.7 Changes in the peripheral blood concentration (A, B) and frequency (C, D) of $CD38^+$ and $CD38^-$ HSPCs between rest and Interval 4 (30 minutes) in MICE (blue bars), HV-HIIE (grey bars) and LV-HIIE (red bars). Data was obtained using SPFC analysis. Values are means ± SD. * indicates significant differences between Pre- and Post-Ex. *P < 0.05, ****P < 0.0001. Ns indicates no significant differences between timepoints or trials: P > 0.05. The 'Interval 4 (30 minutes)' timepoint is represented as 'Post-Ex'.

The concentration of $CD38^+$ HSPCs increased after LV-HIIE only (Rest: 1.66 ± 1.51 vs. Interval 4: 2.82 ± 2.04, *d* = 0.64, P < 0.0001), with no changes in $CD38^-$ HSPCs observed **(Figure 2.7A-B)**. The majority of circulating HSPCs were $CD38^+$ (95.23% ± 10.91) and the frequency of both $CD38^+$ and $CD38^-$ HSPCs did not change throughout MICE, HV-HIIE or LV-HIIE (P > 0.05, **Figure 2.7C-D**).

2.4.3 Immune Cell Subsets

Data obtained from automated haematology analysis and further phenotyping using flow cytometry indicated Time x Trial Interactions for peripheral blood concentrations of all immune cell subsets (full details and statistical output in **Table 2.3**). A comparison between Rest and Interval 4 (30 min) only indicated that the concentration of white blood cells was not significantly different across trials, but analysis of daughter populations revealed that monocyte (*d* = 0.82), lymphocyte (*d* = 0.97), and $CD56^{dim}$ NK cell (*d* = 1.65) concentrations were greater immediately after LV-HIIE compared to MICE.

Table 2.3 Statistical output of changes in peripheral blood concentrations of all immune cell subsets between Pre- and Post-Ex in all trials. The 'Interval 4 (30 minutes)' timepoint is represented as 'Post-Ex'.

Cell Subset	Timepoint	Cycling Trial			P Value
		MICE	HV-HIIE	LV-HIIE	
WBC	Pre	5620 ± 1273*	5457 ± 1112*	5520 ± 1491*	< 0.0001
	Post-Ex	6966 ± 1801*	8078 ± 1840*	8781 ± 2581*	
Neutrophils	Pre	2958 ± 695*	2912 ± 584*	3304 ± 1857*	0.05
	Post-Ex	3807 ± 1227*	4171 ± 1123*	4683 ± 2150*	
Lymphocytes	Pre	1882 ± 533*	1864 ± 587*	1847 ± 580*	< 0.0001
	Post-Ex	2315 ± 630[2,*]	3085 ± 1015*	3344 ± 1360[2,*]	
Monocytes	Pre	445 ± 105	416 ± 106	1790 ± 2629*	0.01
	Post-Ex	619 ± 167[2]	687 ± 204[3]	2547 ± 3336[2,3,*]	
T cells	Pre	1261 ± 417	1238 ± 434*	1187 ± 355*	0.03
	Post-Ex	1388 ± 441	1630 ± 678*	1715 ± 719*	
$CD56^{dim}$ NK	Pre	197 ± 87*	202 ± 85*	222 ± 88*	0.0002
	Post-Ex	433 ± 132[1,2,*]	817 ± 227[1,*]	943 ± 442[2,*]	
$CD56^{bright}$ NK	Pre	8.64 ± 3.62	7.38 ± 3.95*	8.05 ± 3.62*	0.02
	Post-Ex	10.33 ± 4.59	14.31 ± 7.20*	15.84 ± 9.23*	
HSPCs	Pre	2.15 ± 0.90	2.05 ± 0.86	1.84 ± 1.55*	< 0.0001
	Post-Ex	1.76 ± 0.82[2]	2.42 ± 1.04	3.21 ± 2.00[2,*]	

Data displayed as mean ± SD.

[1], significant difference between MICE and HV-HIIE ($P < 0.05$)

[2], significant difference between MICE and LV-HIIE ($P < 0.05$)

[3], significant difference between HV-HIIE and LV-HIIE ($P < 0.05$)

*, significant difference between Pre- and Post-Ex ($P < 0.05$)

Abbreviations: MICE, moderate intensity continuous exercise; HV-HIIE, high volume-high intensity interval exercise; LV-HIIE, low volume-high intensity interval exercise; WBC, white blood cell; NK, natural killer and HSPCs, haematopoietic stem and progenitor cells. The 'Interval 4 (30 minutes)' timepoint is represented as 'Post-Ex'.

The concentration of CD56^{dim} NK cells was greater after HV-HIIE > MICE, and for monocytes, was greater after LV-HIIE > HV-HIIE. Following adjustment of all cell concentrations for changes in blood volume, all Time effects remained significant, but there were no Time x Trial interaction effects noted for blood volume adjusted neutrophil, monocyte, and T cell concentrations. For visualisation of these changes across all immune cell subsets and trials, fold changes between Rest and Interval 4 (30 min) are depicted in **Figure 2.8**, and a comparison of the magnitude of change between cell subsets detailed in **Figure 2.9A-C**. Fold change of HSPCs was not greater than any other subset and mirrored the general leukocyte pattern across all trials.

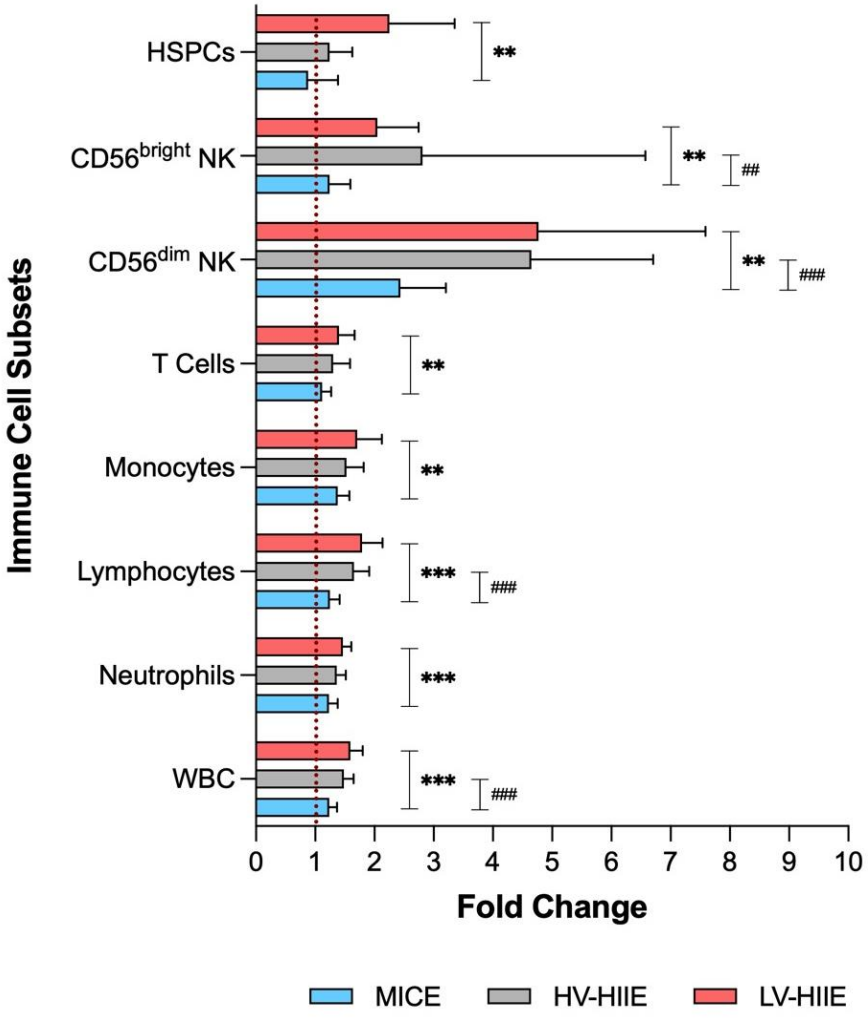

Figure 2.8 Fold change in immune cell subset concentrations (WBC, neutrophils, lymphocytes, monocytes, T cells, $CD56^{dim}$ NK cells, $CD56^{bright}$ NK cells and HSPCs) after Interval 4 (30 minutes) relative to rest in MICE (blue bars), HV-HIIE (grey bars) and LV-HIIE (red bars). * and # indicate significant differences between LV-HIIE vs. MICE and HV-HIIE vs. MICE respectively: **P < 0.01, ***P < 0.0001, ##P < 0.01, ###P < 0.0001.

In contrast, fold change of $CD56^{dim}$ NK cells was mostly greater than every subset across all trials (all P < 0.01), whereas fold change of $CD56^{bright}$ NK cells was significantly greater than neutrophils and T cells after LV-HIIE and HV-HIIE only (all P < 0.01). Finally, fold change of lymphocytes was greater than neutrophils after LV-HIIE and HV-HIIE only (all P < 0.01), and greater than monocytes after HV-HIIE only (P < 0.01).

A.

MICE	WBC	Neutrophils	Lymphocytes	Monocytes	T cells	$CD56^{dim}$ NK	$CD56^{bright}$ NK	HSPCs
Fold Change	1.24	1.23	1.25	1.38	1.12	2.44	1.24	0.88
WBC		##	ns	ns	##	**	ns	ns
Neutrophils			ns	*	ns	***	ns	ns
Lymphocytes				ns	###	***	ns	ns
Monocytes					##	**	ns	ns
T cells						***	ns	ns
$CD56^{dim}$ NK							###	##
$CD56^{bright}$ NK								ns

B.

HV-HIIE	WBC	Neutrophils	Lymphocytes	Monocytes	T cells	CD56^{dim} NK	CD56^{bright} NK	HSPCs
Fold Change	1.48	1.37	1.65	1.53	1.30	4.65	2.81	1.24
WBC		##	***	ns	##	***	**	ns
Neutrophils			**	ns	ns	***	***	ns
Lymphocytes				##	###	***	ns	ns
Monocytes					##	***	ns	ns
T cells						***	***	ns
CD56^{dim} NK							ns	###
CD56^{bright} NK								##

C.

LV-HIIE	WBC	Neutrophils	Lymphocytes	Monocytes	T cells	CD56^{dim} NK	CD56^{bright} NK	HSPCs
Fold Change	1.59	1.47	1.79	1.71	1.40	4.77	2.05	2.25
WBC		##	**	ns	##	***	ns	ns
Neutrophils			**	ns	ns	***	**	ns
Lymphocytes				ns	###	***	ns	ns
Monocytes					##	***	ns	ns
T cells						***	**	ns
CD56^{dim} NK							###	ns
CD56^{bright} NK								ns

Figure 2.9 A statistical comparison of the fold change (Interval 4 (30 minutes) vs. rest) between cell subsets (White blood cells (WBC), neutrophils, lymphocytes, monocytes, T cells, CD56^{dim} NK cells, CD56^{bright} NK cells and HSPCs) in MICE (A), HV-HIIE (B) and LV-HIIE (C). The grey area represents no comparison between row vs. column and vice versa. White boxes and # represent significant differences between table row vs. column. Red boxes and * represent significant differences between table column

vs. row. Blue boxes and ns indicate no significant differences between subsets. *P < 0.05, **P < 0.01, ***P < 0.001, ##P < 0.01, ###P < 0.001.

2.4.4 Bone Marrow Homing Potential of HSPCs

Changes in the peripheral blood concentration (cells/µL, **Figure 2.10A-B**) and frequency **(Figure 2.10C-D)** of CXCR-4^{+} and VLA-4^{+} HSPCs after each trial are reported in **Figure 2.10**. The cell surface expression of CXCR-4 and VLA-4 on gated HSPCs are depicted by a representative histogram **(Figure 2.10E-F)** and the average GeoMean data reported **(Figure 2.10G-H)**.

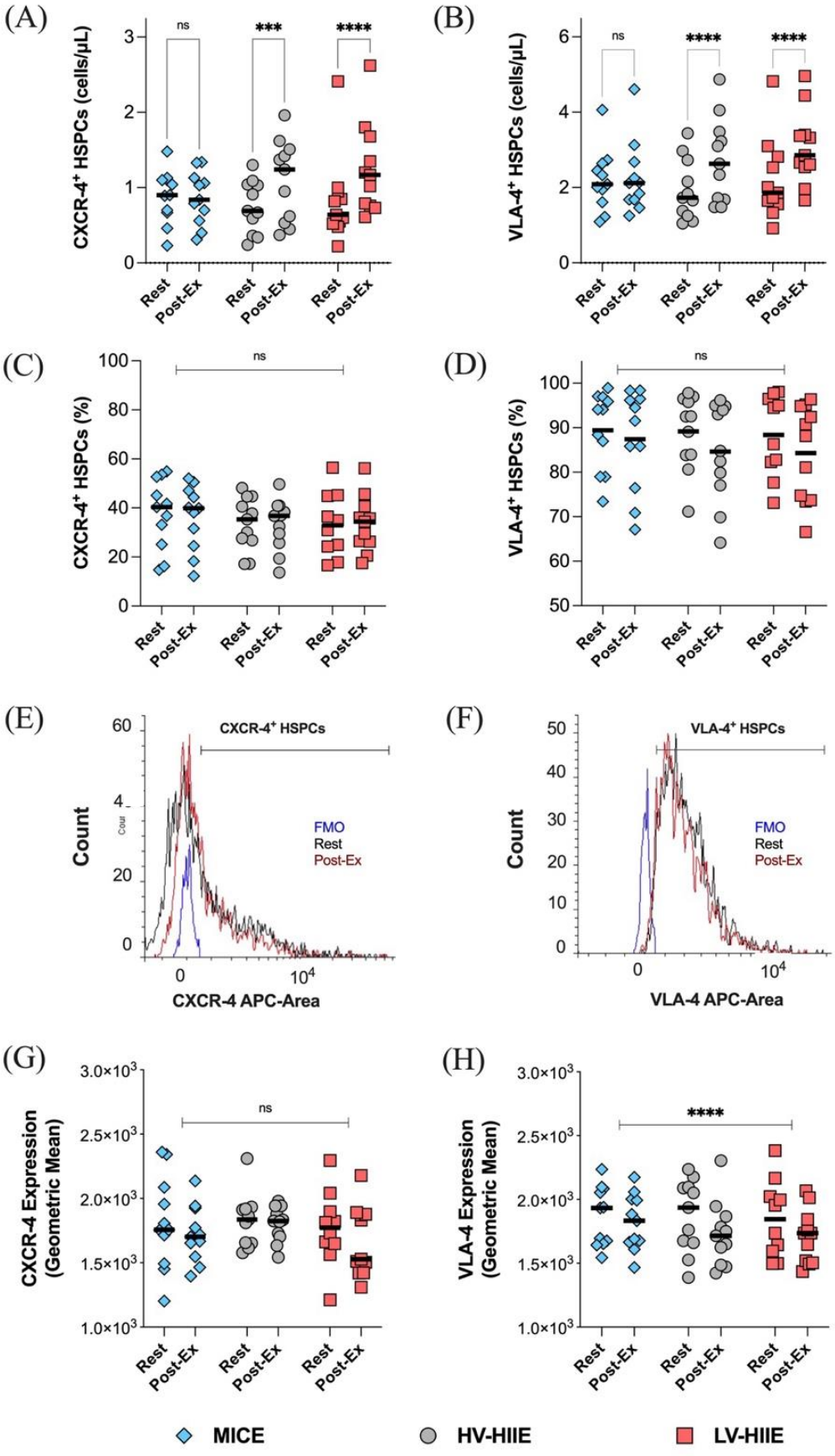
(A)
CXCR-4⁺ HSPCs (cells/µL)
ns
***
****
Rest
Post-Ex
(B)
VLA-4⁺ HSPCs (cells/µL)
ns
****
****
(C)
CXCR-4⁺ HSPCs (%)
ns
(D)
VLA-4⁺ HSPCs (%)
ns
(E)
CXCR-4⁺ HSPCs
Count
FMO
Rest
Post-Ex
CXCR-4 APC-Area
(F)
VLA-4⁺ HSPCs
Count
FMO
Rest
Post-Ex
VLA-4 APC-Area
(G)
CXCR-4 Expression (Geometric Mean)
ns
(H)
VLA-4 Expression (Geometric Mean)
****
MICE
HV-HIIE
LV-HIIE

Figure 2.10 Changes in the peripheral blood concentration (A, B), frequency (C, D) and cell surface expression (G, H) of CXCR-4 and VLA-4 on gated HSPCs between rest and Interval 4 (30 minutes) in MICE (blue bars), HV-HIIE (grey bars) and LV-HIIE (red bars). All data was obtained using DPFC and automated hematology analysis. The cell surface expression of CXCR-4 and VLA-4 on HSPCs at rest (black histogram) and Interval 4 (30 minutes) or 'Post-Ex' (red histogram) were established by determining the positive population with a fluorescence minus one (FMO) control (blue histogram) and then calculating the Geometric mean (E, F). Values are means ± SD. * indicates significant differences between Pre- and Post-Ex, representing pairwise comparisons in each trial (A, B) and in all trials (C, D, G, H): ***P < 0.001, ****P < 0.0001. Ns indicates no significant differences between timepoints or trials: P > 0.05. The 'Interval 4 (30 minutes)' timepoint is represented as 'Post-Ex'.

A repeated measures ANOVA revealed a significant Time x Trial interaction for CXCR-4^+ ($F(2, 30) = 8.17$, $P = 0.002$) and VLA-4^+ HSPC concentrations ($F(2, 30) = 7.46$, $P = 0.002$). *Post-hoc* analyses revealed that compared with rest, bone marrow homing potential of HSPC concentrations increased after LV-HIIE (CXCR-4^+: $d = 0.73$, $P < 0.0001$ and VLA-4^+: $d = 0.83$, $P < 0.0001$) and HV-HIIE (CXCR-4^+: $d = 0.76$, $P = 0.0008$ and VLA-4^+: $d = 0.82$, $P < 0.0001$), but not MICE (both $P > 0.05$). Within the HSPC population, there were no differences in the frequency of CXCR-4^+ or VLA-4^+ HSPCs in response to the trials ($P < 0.05$). When comparing changes in the cell surface expression levels of these receptors, there was a significant decrease in VLA-4 (Time Effect: $P < 0.0001$), but no change in CXCR-4 after all trials (Time Effect: $P = 0.66$).

2.4.5 Chemokine CXCL-12 and VCAM-1 Concentrations

Changes in plasma volume adjusted chemokine concentrations in response to each trial are presented in **Figure 2.11**. A repeated measures ANOVA revealed a significant effect of Time for CXCL-12 concentration (F (1, 29) = 10.18, P = 0.003), but no interaction effect (P=0.11). There were no changes in plasma VCAM-1 (P = 0.80) concentration in response to all cycling trials. There were no associations between changes in plasma chemokine and HSPC concentrations across any of the trials **(Figure 2.12A-B)**.

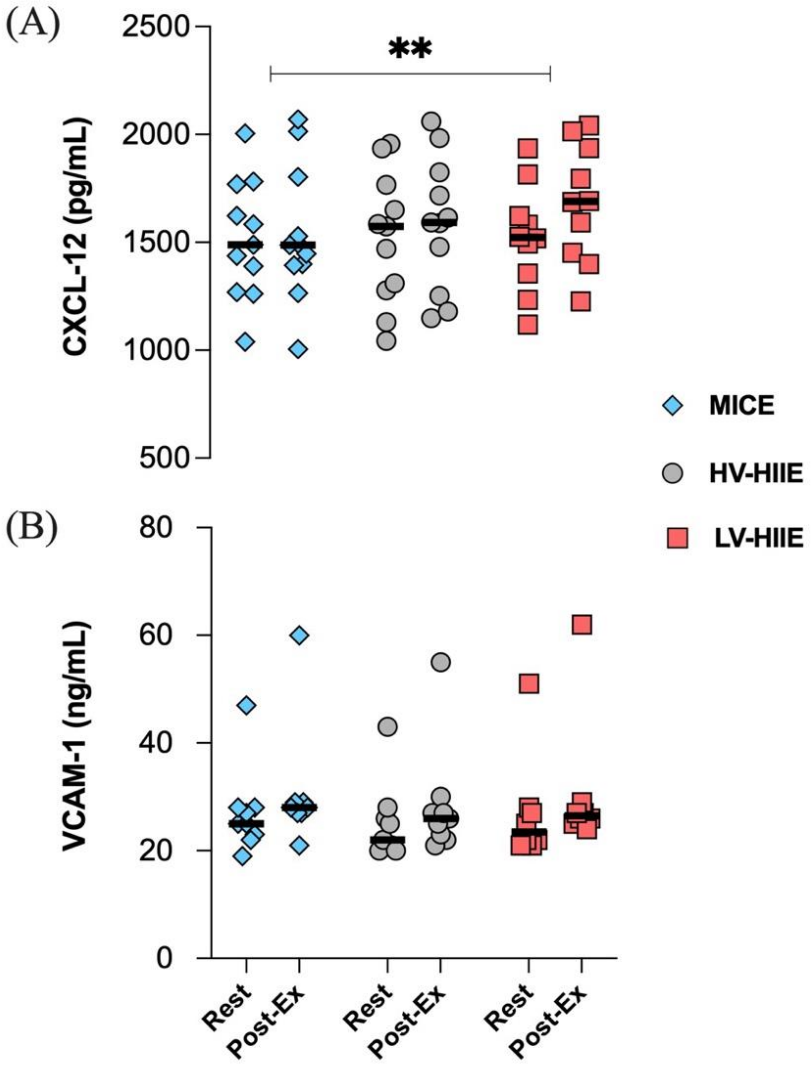

Figure 2.11 Changes in the plasma concentration of CXCL-12 (A) and VCAM-1 (B) between Rest and Interval 4 (30 minutes) of MICE (blue bars), HV-HIIE (grey bars) and LV-HIIE (red bars). Values are means ± SD. * indicates a significant effect of Time: **p < 0.01. The 'Interval 4 (30 minutes)' timepoint is represented as 'Post-Ex'.

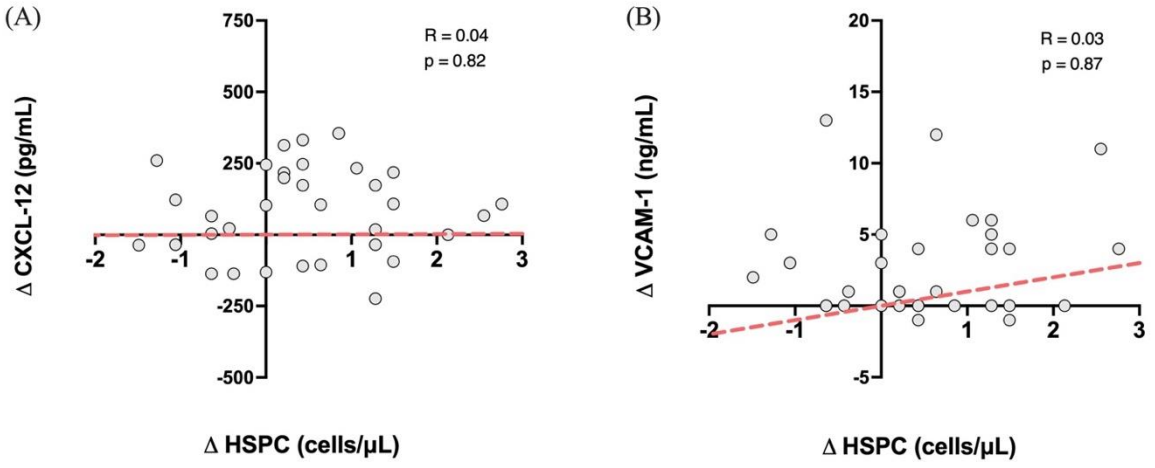

Figure 2.12 The relationship between HSPC mobilisation and changes in plasma chemokine concentrations between rest and Interval 4 (30 minutes) in all trials. The delta change (Δ) of HSPC concentration was plotted against Δ CXCL-12 (A) and Δ VCAM-1 (B), and Pearson and Spearman correlation coefficients determined respectively.

2.4.6 Comparison of Flow Cytometric Methods to Determine HSPC Concentrations

Changes in peripheral blood HSPC concentrations in response to trials determined by DPFC are shown in **Figure 2.13B**. A repeated measures ANOVA revealed a significant Time x Trial interaction effect (F (2, 30) = 10.27, P = 0.0004). *Post-hoc* analyses illustrated an increase in HSPC concentration after Interval 4 of LV-HIIE relative to rest

(Rest: 2.45 ± 1.09 vs. Interval 4: 3.72 ± 1.20, P < 0.0001) and HV-HIIE (Rest: 2.20 ± 0.88 vs. Interval 4: 3.26 ± 1.28, P < 0.0001), but not after MICE (Rest: 2.43 ± 0.85 vs. Interval 4: 2.57 ± 1.10, P > 0.99). There were significant differences in post-exercise HSPC concentrations between LV-HIIE and MICE (P = 0.04), but not HV-HIIE vs. MICE (P = 0.41) or LV-HIIE vs. HV-HIIE (P = 0.97).

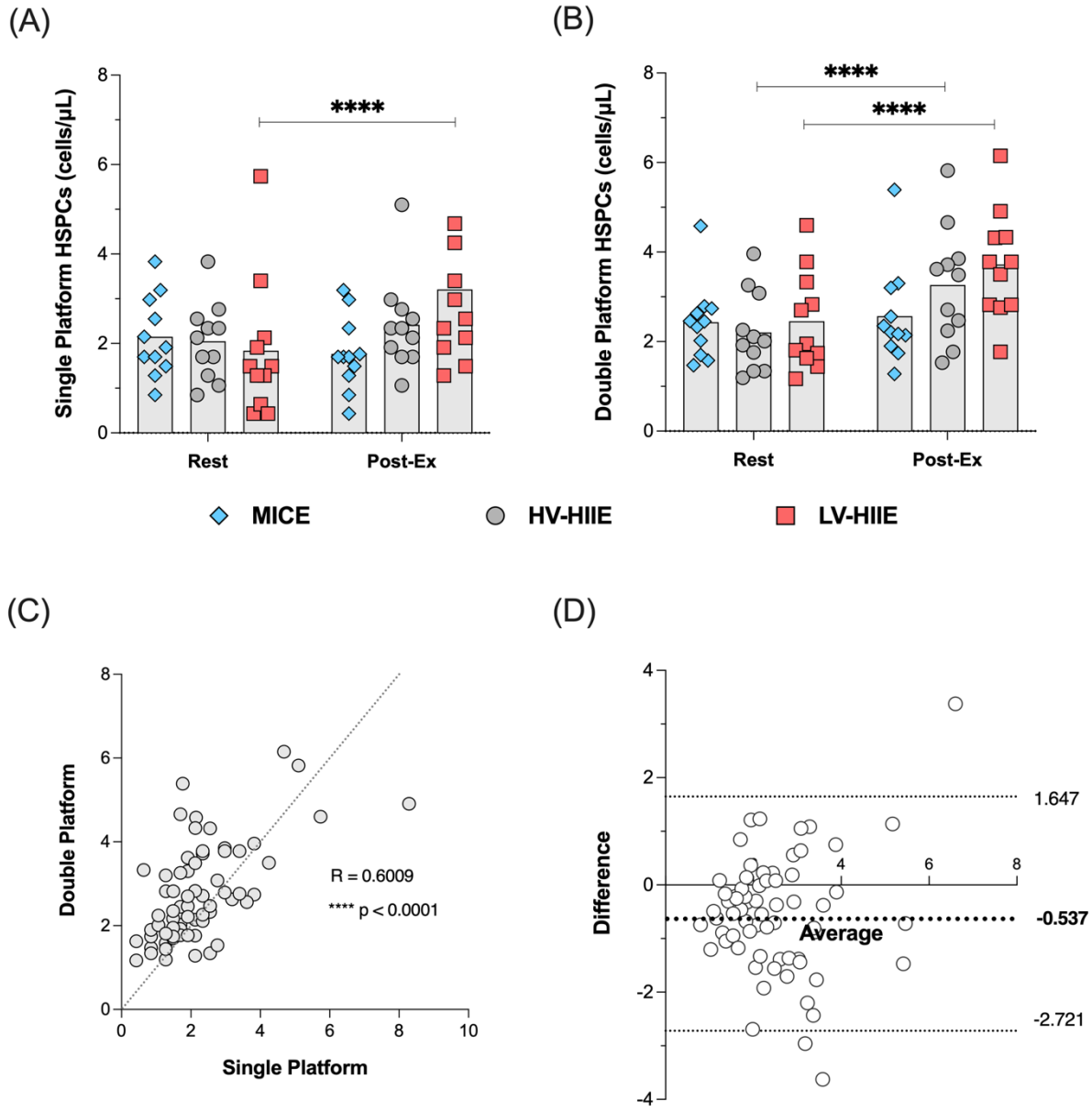

Figure 2.13 Changes in peripheral blood HSPC concentrations determined by (A) SPFC and (B) DPFC between Rest and Interval 4 (30 minutes) in MICE (blue bars), HV-HIIE (grey bars) and LV-HIIE (red bars). (C) The agreement between SPFC and DPFC was established by determining a Pearson correlation coefficient and (D) Bland-Altman plot. Values are means ± SD. * indicates significant differences between Pre- and Post-Ex: ****p < 0.0001. The 'Interval 4 (30 minutes)' timepoint is represented as 'Post-Ex'.

A Pearson's correlation indicated that there was a significantly positive relationship **(Figure 2.13C)** between SPFC and DPFC methods (R = 0.60, P < 0.0001). Furthermore, Bland-Altman analysis revealed no systemic differences between SPFC and DPFC methods. Figure 5D indicated that most differences (63 of 66 measurements) between SPFC and DPFC fell within the 'lower' (-2.721) and 'upper' (1.647) limits of agreement. The mean difference was -0.537 cells/μL between data pairs. A linear regression analysis between the mean of the data pairs vs. mean difference indicated no significant difference between methods (F (1, 64) = 1.28, P = 0.26). Moreover, main effects and *post hoc* analyses comparing HSPC concentration between Rest and Interval 4 across all 3 experimental trials revealed similar results from both methods.

2.5 Discussion

The results of the current study indicate that brief cycling intervals of high intensity (LV-HIIE and HV-HIIE), but not moderate intensity continuous cycling (MICE) mobilised HSPCs into peripheral blood of healthy young males. HSPC concentrations

determined by SPFC were elevated above rest after just two intervals of LV-HIIE (4 minutes) and three intervals of HV-HIIE (12 minutes). However, immediately following completion of Interval 4, HSPC concentration was only elevated above rest during LV-HIIE, returning to resting concentration within 5 minutes. These responses were exclusive to $CD38^{+}$ HSPCs, with no changes in the $CD38^{-}$ fraction observed. The frequency of HSPCs expressing bone marrow homing receptors CXCR-4 and VLA-4 were unaltered, but the cell surface expression of VLA-4 decreased after all cycling trials, indicating marginally altered bone marrow homing propensity of exercise-mobilised HSPCs. Accompanying these changes, both HIIE trials evoked more marked increases in the peripheral blood concentration of cytolytic $CD56^{dim}$ NK cells compared to MICE. Taken together, these data indicate that just 4–12 minutes of high intensity cycling intervals can enrich peripheral blood with more HSPCs and $CD56^{dim}$ NK cells compared to 30 minutes of moderate intensity continuous cycling. Given the importance of these cells in context of HSPC transplantation, and the low volume of cycling needed to evoke these changes, these findings provide a rationale to investigate the impact of interval cycling after prior G-CSF treatment to examine HSPC collection efficacy.

Previous studies have reported increases in peripheral blood HSPC concentrations after bouts of steady state exercise (25) and HIIE (4,44). Data supports ‘intensity’ to be a more prominent driver of HSPC mobilisation than ‘duration’ of a steady state exercise bout (24); however, the relationship between these variables when comparing bouts of HIIE is unclear. Whereas ‘all-out’ HIIE over a cumulative total of 120 seconds has been reported to increase HSPC concentration (27), 15 minutes of intervals at a

lower intensity (5 x 3 minutes at 90% of peak power) were needed to evoke a similar change (4), with 10 minutes not sufficient (10 x 1 minute at 90% of maximal heart rate) (19). Differences in participant demographics, timing between intervals, and criteria used to define exercise 'intensity' may partly explain some of the discrepancies noted between these studies. Moreover, studies to date have not directly compared how different volumes of HIIE impact HSPC mobilisation, which was a primary purpose of the current study. Given the potential translation of HIIE into a PBSC setting, the present study compared cycling protocols that aligned with criteria used to define clinical HIIE (32,33). We adopted the lower (85%) and upper intensity (95%) limits of these criteria for maximal heart rate to design HV-HIIE and LV-HIIE protocols respectively. A further novel element of the study was employing serial blood sampling to evaluate changes after each interval of HIIE and time-matched samples during MICE. This approach enabled us to determine that just 4 minutes of LV-HIIE and 12 minutes of HV-HIIE significantly increased HSPC concentrations compared to rest. Comparatively, no changes were observed across 7 timepoints over 30 minutes of moderate intensity continuous exercise (MICE), although total AUC between trials was not statistically different. Despite no statistically significant differences between LV-HIIE and HV-HIIE, HSPC concentrations were only greater after Interval 4 (30 min) of LV-HIIE vs. MICE and not HV-HIIE vs. MICE. Moreover, the lower volume of total work performed in LV-HIIE compared to HV-HIIE **(Table 2.2)** and more rapid initial increase in HSPCs indicate that the 'intensity' of HIIE is a more prominent determinant of HSPC mobilisation than 'duration'. The approximate 2-fold increase in HSPC concentration observed after LV-HIIE aligns with concentrations reported from previous studies evaluating intervals and steady state exercise of much longer duration (13,24,45).

Although maximal intensity cycling intervals can evoke HSPC mobilisation to this degree (44), our data indicate that low volume cycling at a more manageable intensity elicits a comparable increase.

In the present study, higher average power output, subjective exertion and HR_{peak} **(Table 2.2)** in LV- HIIE > HV-HIIE > MICE reflected greater physiological exertion that would likely elicit greater increases in systemic adrenaline concentration (3) and therefore HSPC mobilisation, corroborating previous work (24). The observed intensity-dependent changes in HSPCs were also observed across other immune cells subsets **(Table 2.3)**. Notably, the increased concentrations of lymphocytes and $CD56^{dim}$ NK cells were greater in response to LV-HIIE vs. MICE. The increased concentration of monocytes was greatest in LV-HIIE vs. HV-HIIE and MICE; however, this was driven by greater reductions in blood volume during LV-HIIE rather than greater cell mobilisation. It is well established that single bouts of exercise elicit non-uniform mobilisation of immune cells into peripheral blood, which is intensity dependent (13). Cells with high effector functions (e.g., non-classical monocytes, effector memory T cells and $CD56^{dim}$ NK cells are preferentially mobilised relative to naïve subsets under the actions of β2 adrenergic (6) and cytokine signalling (46). Although extensive phenotyping was not carried out in the present study, $CD56^{dim}$ NK cells had markedly higher ingress than any other cell subset **(Figure 2.8)**, illustrating preferential mobilisation of potent cytolytic cells, particularly during HIIE.

Perspectives and Clinical Considerations

The concept of implementing exercise in a PBSC setting has been proposed previously (47,48), and yet practical steps to facilitate this have not been taken. This first begins with providing empirical data to support an appropriate type of exercise for a broad range of autologous and allogeneic donors, before evaluating its clinical utility. The present study reports that HIIE can enrich peripheral blood with higher numbers of multiple immune cell subsets to a greater degree than MICE, most notably HSPCs and $CD56^{dim}$ NK cells. However, in line with previous studies (25), the increase in HSPC concentration observed was transient, with resting concentration restored within 5 minutes. PBSC collections take approximately 3–4-hours and the peak HSPC concentration of 3.2 ± 2.0 cells/μL during LV-HIIE **(Figure 2.6A)** reported herein falls short of the minimum collection threshold of 10 cells/μL following G-CSF treatment (49). Furthermore, when expressing HSPC data relative to body mass, despite a significant increase after LV-HIIE in the absence of G-CSF, HSPC dose after the trial was approximately 10-fold short of the 2 x 10^6 HSPCs/kg collection threshold required for successful engraftment after autologous transplantation (*data not shown*) (13). Therefore, bouts of exercise in isolation are insufficient to evoke clinically meaningful changes in HSPCs. Furthermore, $CD38^+$, but not $CD38^-$ HSPC concentrations increased after LV-HIIE in the present study **(Figure 2.7A-B)**. Although engraftment success is predicted clinically by $CD34^+$ count alone (50–52), a higher number and frequency of pluripotent $CD38^-$ HSPCs are mobilised from the bone marrow following G-CSF therapy (53) and predict more favourable engraftment success vs. $CD38^+$ HSPCs (54). It is noteworthy that the majority of circulating HSPCs in the present study were progenitor cells (≈95% at rest and after exercise, **Figure 2.7C-D**). Enrichment of

peripheral blood with $CD38^-$ HSPCs after G-CSF treatment results in a proportion of HSPCs residing in marginal pools of the circulation, thus not available for collection (48). Presently, it is unclear whether exercise could dislodge marginalised $CD38^+$ or $CD38^-$ HSPCs into the blood compartment during apheresis.

Beyond the importance of the harvested cell number, the engraftment potential of HSPCs and other collected cells are important. In the present study, engraftment potential of HSPCs was evaluated by quantifying cell surface expression of CXCR-4 and VLA-4. Although expression is known to be variable across individuals, our data aligned with mean $CXCR\text{-}4^+$ (≈40%) (55) and $VLA\text{-}4^+$ (≈68.5%) (56) HSPC frequencies in the absence of prior G-CSF treatment reported in other studies. The concentration, but not frequency of HSPCs expressing bone marrow homing receptors CXCR-4 and VLA-4 were increased after HIIE, but not MICE **(Figure 2.10A-D)**. Previous studies support these findings, reporting an increase in the concentration, but not frequency of peripheral blood $CXCR\text{-}4^+$ HSPCs (18), and $VLA\text{-}4^+$ T, B, NK cells (57) after steady state incline walking and resistance exercise respectively. Therefore, $CXCR\text{-}4^+$ and $VLA\text{-}4^+$ HSPC mobilisation during HIIE likely reflects non-specific demargination of these cells from marginal pools along with all leukocytes (58). Additionally, we observed a decrease in the cell surface expression of VLA-4, but not CXCR-4 after all cycling trials **(Figure 2.10G-H)**. The cell surface expression of CXCR-4 has been reported to be augmented on circulating T (59) and NK cells (60) after steady state exercise and associated with elevated tissue homing and subsequent lymphocytopenia. Expression changes of CXCR-4 and VLA-4 after bouts of exercise are evidently specific to each cell type and dependent on their microenvironment,

notably chemokine cues. We observed no relationship between the expression of these receptors with systemic changes in CXCL-12 and VCAM-1 concentrations, which displayed the reverse pattern **(Figure 2.11A-B)** (45), and thus local tissue chemokine cues might explain the decrease in VLA-4 expression on HSPCs. The latter implies that the bone marrow homing propensity of HSPCs was impaired after exercise relative to circulating HSPCs at rest; however, its impact on engraftment potential is presently unclear. Engraftment potential is also impacted by immune composition, notably $CD56^{dim}$ NK cells, which were ≈4-fold higher after HIIE vs. MICE **(Figure 2.8)**. Higher numbers of $CD56^{dim}$ NK cells have been reported to lower the risk of several clinical endpoints (e.g., post-transplant viral infections and GvHD) following allogenic HSPC transplantation by enhancing the recipient's adaptive immune responses (7).

Collectively, repeated intervals of LV-HIIE incrementally increased the concentration of peripheral blood HSPCs, albeit with a modulated bone marrow phenotype, to a greater degree than moderate intensity steady state cycling. These changes were accompanied by an increase in clinically relevant $CD56^{dim}$ NK cells in peripheral blood at the end of interval 4.

Comparison of SPFC and DPFC Methods

A secondary aim of the present study was to evaluate the relationship and systemic bias between SPFC and DPFC methods for enumerating HSPCs in peripheral blood before and after bouts of cycling. DPFC is more commonplace in studies evaluating changes in HSPC concentration after exercise, but high variability has been reported in some multi-site studies (31) whereas SPFC is the clinically accepted method used

during PBSC collections, established by ISHAGE (61). The same general pattern of response was observed between methods (**Figure 2.13A-B**), with the exception that post-exercise HSPC concentrations were significantly greater than rest after LV-HIIE and HV-HIIE vs. MICE using DPFC (**Figure 2.13B**), whereas this trend was only significant for LV-HIIE using SPFC (**Figure 2.13A**). A significant moderate correlation was observed between methods (**Figure 2.13C**), and there was no significant systemic bias between methods (**Figure 2.13D**). Whereas both quantitative methods appear acceptable depending on logistics of a research study design, a mean difference of -0.537 cells/μL might be considered clinically meaningful given that the collection threshold for initiating apheresis is > 10 cells/ μL (62). Regardless of method, these data collectively indicate that HIIE evoked greater mobilisation of HSPCs than MICE.

Strengths, Limitations and Future Perspectives

Using a randomised crossover design and serial blood sampling, this study employed internationally validated guidelines to enumerate peripheral blood HSPC concentrations after bouts of interval vs. continuous cycling; however, this study was not without limitations. A low recruitment rate following easing of COVID-19 restrictions resulted in our study population including only male participants, thus not biologically, socially or clinically representative. From a physiological perspective, our data indicate that just 4 minutes of LV-HIIE elicited an increase in peripheral blood HSPCs greater than 30 minutes steady state cycling, but at present, the translation of these findings are limited. It is evident that clinical trials are required to evaluate whether cycling during apheresis (with prior G-CSF) can improve HSPC collection efficacy. These trials should be preceded by studies first examining whether cycling throughout a PBSC

collection procedure (≈3 hours) sustains HSPC concentrations and the effect on immune composition. Beyond the physiological potential of exercise to maximise the number of these cells, future work is required to evaluate the feasibility and acceptability of such an approach for allogeneic and autologous donors undergoing G-CSF treatment. Cycling protocols such as LV-HIIE and HV-HIIE could be unfavourable for allogenic donors in the general population who do not exercise regularly and not recommended for autologous donors suffering with immunosuppressive disorders (63). Despite the physiological strain during LV-HIIE being markedly greater than MICE, the enjoyment level was equal across all exercise trials (**Table 2.2**). This provides some basic subjective data to support the use of these protocols in healthy young males, but implementation of these intervals over 3 hours in different population groups, albeit with longer rest periods, warrants investigation.

Conclusion

In conclusion, the present study revealed that 2 x 2-minute bouts of LV-HIIE and 3 x 4-minute bouts of HV-HIIE were sufficient to increase peripheral blood $CD38^{+}$ HSPC concentrations above rest, but not in response to 30 minutes of continuous cycling at moderate intensity. At the end of the trials, HSPC concentration was only elevated above rest in the LV-HIIE trial. Furthermore, peripheral blood was enriched with higher numbers of $CD56^{dim}$ NK cells after bouts of HIIE vs. MICE. Collectively, these data indicate that exercise intensity was a more prominent factor than duration in driving the mobilisation of immune cells with relevance to HSPC transplantation. With only 4 minutes of high intensity cycling intervals eliciting these changes, future studies should evaluate the clinical effectiveness of HIIE within a PBSC donation setting.

List of References

1. Walsh NP, Gleeson M, Shephard RJ, Jeffrey MG, Woods A, Bishop NC, et al. Position Statement: Immune Function of Exercise. Exerc Immunol Rev. 2011;17:6–63.

2. Simpson RJ, Kunz H, Agha N, Graff R. Exercise and the Regulation of Immune Functions. 1st ed. Vol. 135, Progress in Molecular Biology and Translational Science. Elsevier Inc.; 2015. 355–380 p.

3. Simpson RJ, Boßlau TK, Weyh C, Niemiro GM, Batatinha H, Smith KA, et al. Exercise and adrenergic regulation of immunity. Brain Behav Immun. 2021;97(June):303–18.

4. Krüger K, Pilat C, Schild M, Lindner N, Frech T, Muders K, et al. Progenitor cell mobilization after exercise is related to systemic levels of G-CSF and muscle damage. Scand J Med Sci Sports. 2015;25(3):e283–91.

5. Bonsignore MR, Morici G, Riccioni R, Huertas A, Petrucci E, Veca M, et al. Hemopoietic and angiogenetic progenitors in healthy athletes: Different responses to endurance and maximal exercise. J Appl Physiol. 2010;109(1):60–7.

6. Graff RM, Kunz HE, Agha NH, Baker FL, Laughlin M, Bigley AB, et al. β2-Adrenergic receptor signaling mediates the preferential mobilization of differentiated subsets of CD8+ T-cells, NK-cells and non-classical monocytes in response to acute exercise in humans. Brain Behav Immun. 2018;74:143–53.

7. Porrata LF, Gertz MA, Geyer SM, Litzow MR, Gastineau DA, Moore SB, et al. The dose of infused lymphocytes in the autograft directly correlates with clinical outcome after autologous peripheral blood hematopoietic stem cell transplantation in multiple myeloma. Leukemia. 2004;18(6):1085–92.

8. Giralt S, Costa L, Schriber J, DiPersio J, Maziarz R, McCarty J, et al. Optimizing autologous stem cell mobilization strategies to improve patient outcomes: Consensus guidelines and recommendations. Biology of Blood and Marrow Transplantation. 2014;20(3):295–308.

9. Carreras E, Dufour C, Mohty M, Kröger N. The EBMT Handbook: Hematopoietic stem cell transplantation and cellular therapies. The EBMT Handbook: Hematopoietic Stem Cell Transplantation and Cellular Therapies. 2018;1–702.

10. Henig I, Zuckerman T. Hematopoietic Stem Cell Transplantation—50 Years of Evolution and Future Perspectives. Rambam Maimonides Med J. 2014;5(4):e0028.

11. Sezer O, Possinger K, Metzner B, Illiger HJ, Wattad M, Fuss WHH, et al. Optimal CD34 + Cell Dose in Autologous Peripheral-Blood Stem-Cell Transplantation. J Clin Oncol. 2000;18(18):3319–20.

12. Maggs L, Kinsella F, Tracey Chan YL, Eldershaw S, Murray D, Nunnick J, et al. The number of CD56dim NK cells in the graft has a major impact on risk of disease relapse following allo-HSCT. Blood Adv. 2017;1(19):1589–97.

13. Baker JM, Nederveen JP, Parise G. Aerobic exercise in humans mobilizes HSCs in an intensity-dependent manner. J Appl Physiol. 2017;122(1):182–90.

14. Hénon PH, Sovalat H, Bourderont D. Importance of CD34+ cell subsets in autologous PBSC transplantation: the mulhouse experience using CD34+CD38- cells as predictive tool for hematopoietic engraftment. J Biol Regul Homeost Agents. 2001;15(1):62–7.

15. Felker S, Shrestha A, Bailey J, Pillis DM, Siniard D, Malik P. Differential CXCR4 expression on hematopoietic progenitor cells versus stem cells directs homing and engraftment. JCI Insight. 2022;7(9):1–17.

16. Potocnik AJ, Brakebusch C, Fässler R. Fetal and adult hematopoietic stem cells require b1 integrin function for colonizing. Immunity. 2000;12(6):653–63.

17. Asfour I, Afify H, Elkourashy S, Ayoub M, Kamal G, Gamal M, et al. CXCR4 (CD184) expression on stem cell harvest and CD34+ cells post-transplant. Hematology/ Oncology and Stem Cell Therapy [Internet]. 2017;10(2):63–9. Available from: http://dx.doi.org/10.1016/j.hemonc.2017.01.002

18. Taylor GS, Shaw A, Smith K, Capper TE, Scragg JH, Cronin M, et al. Type 1 diabetes patients increase CXCR4+ and CXCR7+ haematopoietic and endothelial progenitor cells with exercise, but the response is attenuated. Sci Rep. 2021;11(1):1–11.

19. Nederveen JP, Baker J, Ibrahim G, Ivankovic V, Percival ME, Parise G. Hematopoietic Stem and Progenitor Cell (HSPC) Mobilization Responses to Different Exercise Intensities in Young and Older Adults. Journal of Science in Sport and Exercise [Internet]. 2020;2(1):47–58. Available from: https://doi.org/10.1007/s42978-019-00050-4

20. Schmid M, Martins HC, Schratt G, Kröpfl JM, Spengler CM. MiRNA126 – RGS16 – CXCL12 Cascade as a Potential Mechanism of Acute Exercise-Induced Precursor Cell Mobilization. Front Physiol. 2021;12(December).

21. Brevetti G, De Caterina M, Martone VD, Ungaro B, Corrado F, Silvestro A, et al. Exercise increases soluble adhesion molecules ICAM-1 and VCAM-1 in patients with intermittent claudication. Clin Hemorheol Microcirc. 2001;24(3):193–9.

22. Emmons R, Niemiro GM, Owolabi O, De Lisio M. Acute exercise mobilizes hematopoietic stem and progenitor cells and alters the mesenchymal stromal cell secretome. J Appl Physiol. 2016;120(6):624–32.

23. Brzoska E, Kowalewska M, Markowska-Zagrajek A, Kowalski K, Archacka K, Zimowska M, et al. Sdf-1 (CXCL12) improves skeletal muscle regeneration via the mobilisation of Cxcr4 and CD34 expressing cells. Biol Cell. 2012;104(12):722–37.

24. Agha NH, Baker FL, Kunz HE, Graff R, Azadan R, Dolan C, et al. Vigorous exercise mobilizes CD34+ hematopoietic stem cells to peripheral blood via the β2-adrenergic receptor. Brain Behav Immun [Internet]. 2018;68:66–75. Available from: https://www.sciencedirect.com/science/article/pii/S0889159117304543

25. Schmid M, Kröpfl JM, Spengler CM. Correction to: Changes in Circulating Stem and Progenitor Cell Numbers Following Acute Exercise in Healthy Human Subjects: a Systematic Review and Meta-Analysis. Stem Cell Rev Rep. 2021;17(4):1511.

26. Barra NG, Fan IY, Gillen JB, Chew M, Marcinko K, Steinberg GR, et al. High Intensity Interval Training Increases Natural Killer Cell Number and Function in Obese Breast Cancer-challenged Mice and Obese Women. J Cancer Prev. 2017;22(4):260–6.

27. O'Carroll L, Wardrop B, Murphy RP, Ross MD, Harrison M. Circulating angiogenic cell response to sprint interval and continuous exercise. Eur J Appl Physiol. 2019 Mar 6;119(3):743–52.

28. Turner JE, Wadley AJ, Aldred S, Fisher JP, Bosch JA, Campbell JP. Intensive Exercise Does Not Preferentially Mobilize Skin-Homing T Cells and NK Cells. Med Sci Sports Exerc. 2016;48(7):1285–93.

29. Arroyo E, Tagesen EC, Hart TL, Miller BA, Jajtner AR. Comparison of the lymphocyte response to interval exercise versus continuous exercise in recreationally trained men. Brain Behav Immun Health. 2022;20(December 2021):100415.

30. Keeney M, Chin-Yee I, Weir K, Popma J, Nayar R, Robert Sutherland D. Single platform flow cytometric absolute CD34+ cell counts based on the ISHAGE guidelines. Communications in Clinical Cytometry. 1998;34(2):61–70.

31. Gratama JW, Kraan J, Keeney M, Sutherland DR, Granger V, Barnett D. Validation of the single-platform ISHAGE method for CD34+ hematopoietic stem and progenitor cell enumeration in an international multicenter study. Cytotherapy. 2003;5(1):55–65.

32. Weston KS, Wisløff U, Coombes JS. High-intensity interval training in patients with lifestyle-induced cardiometabolic disease: A systematic review and meta-analysis. Br J Sports Med. 2014;48(16):1227–34.

33. Taylor JL, Holland DJ, Spathis JG, Beetham KS, Wisløff U, Keating SE, et al. Guidelines for the delivery and monitoring of high intensity interval training in clinical populations. Prog Cardiovasc Dis. 2019;62(2):140–6.

34. Foster J. The General Practice Physical Activity Questionnaire (GPPAQ) A screening tool to assess adult physical activity levels , within primary care Updated May 2009. Nhs. 2009;(May):1–21.

35. Spielberger CD, Gonzalez-Reigosa F, Martinez-Urrutia A, Natalicio LFS, Natalicio DS. The State-Trait Anxiety Inventory. Revista Interamericana de Psicología/Interamerican Journal of Psychology. 2017 Jul 17;5(3 & amp; 4 SE-Articles).

36. Carney CE, Buysse DJ, Ancoli-Israel S, Edinger JD, Krystal AD, Lichstein KL, et al. The consensus sleep diary: Standardizing prospective sleep self-monitoring. Sleep. 2012;35(2):287–302.

37. Robert B, Brown EB. Psychophysical bases of perceived exertion. Med Sci Sports Exerc. 1982;14:377–81.

38. Hardy CJ, Rejeski WJ. Not What, but How One Feels: The Measurement of Affect during Exercise. J Sport Exerc Psychol. 2016;11(3):304–17.

39. Ettema G, Lorås HW. Efficiency in cycling: A review. Vol. 106, European Journal of Applied Physiology. 2009. p. 1–14.

40. R C Gagnon, J J Peterson. Estimation of confidence intervals for area under the curve from destructively obtained pharmacokinetic data. J Pharmacokinet Biopharm. 1998;26(1):87–102.

41. Matomäki P, Kainulainen H, Kyröläinen H. Corrected whole blood biomarkers – the equation of Dill and Costill revisited. Physiol Rep. 2018;6(12):1–3.

42. Dill DB, Costill DL. Calculation of percentage changes in volumes of blood, plasma, and red cells in dehydration. J Appl Physiol. 1974;37(2):247–8.

43. Cohen J. Statistical Power Analysis for the Behavioral Sciences, 2nd Edition. 1988.

44. O'Carroll L, Wardrop B, Murphy RP, Ross MD, Harrison M. Circulating angiogenic cell response to sprint interval and continuous exercise. Eur J Appl Physiol. 2019;119(3):743–52.

45. Niemiro GM, Parel J, Beals J, Van Vliet S, Paluska SA, Moore DR, et al. Kinetics of circulating progenitor cell mobilization during submaximal exercise. J Appl Physiol. 2017;122(3):675–82.

46. Bay ML, Heywood S, Wedell-Neergaard AS, Schauer T, Lehrskov LL, Christensen RH, et al. Human immune cell mobilization during exercise: effect of IL-6 receptor blockade. Exp Physiol. 2020;105(12):2086–98.

47. Emmons R, Niemiro GM, De Lisio M. Exercise as an Adjuvant Therapy for Hematopoietic Stem Cell Mobilization. Stem Cells Int. 2016;2016.

48. Simpson RJ, Bigley AB, Agha N, Hanley PJ, Bollard CM. Mobilizing immune cells with exercise for cancer immunotherapy. Exerc Sport Sci Rev. 2017;45(3):163–72.

49. Stroncek DF, Clay ME, Herr G, Smith J, Jaszcz WB, Ilstrup S, et al. The kinetics of G-CSF mobilization of CD34+ cells in healthy people. Transfusion Medicine. 1997;7(1):19–24.

50. Basquiera AL, Abichain P, Damonte JC, Ricchi B, Sturich AG, Palazzo ED, et al. The number of CD34+ cells in peripheral blood as a predictor of the CD34+ yield in patients going to autologous stem cell transplantation. J Clin Apher. 2006 Jul;21(2):92–5.

51. Allan DS, Keeney M, Howson-Jan K, Popma J, Weir K, Bhatia M, et al. Peripheral blood stem cells Number of viable CD34 + cells reinfused predicts engraftment in autologous hematopoietic stem cell transplantation. Bone Marrow Transplant [Internet]. 2002;29:967–72. Available from: www.nature.com/bmt

52. Duggan PR, Guo D, Luider J, Auer I, Klassen J, Chaudhry A, et al. Predictive factors for long-term engraftment of autologous blood stem cells [Internet]. Vol. 26, Bone Marrow Transplantation. 2000. Available from: www.nature.com/bmt

53. Bonig H, Papayannopoulou T. Mobilization of hematopoietic stem/progenitor cells: General principles and molecular mechanisms. Methods in Molecular Biology. 2012;904:1–14.

54. Astori G, Malangone W, Adami V, Risso A, Dorotea L, Falasca E, et al. A novel protocol that allows short-term stem cell expansion of both committed and pluripotent hematopoietic progenitor cells suitable for clinical use. Blood Cells Mol Dis. 2001;27(4):715–24.

55. Taylor GS, Shaw A, Smith K, Capper TE, Scragg JH, Cronin M, et al. Type 1 diabetes patients increase CXCR4+ and CXCR7+ haematopoietic and endothelial progenitor cells with exercise, but the response is attenuated. Sci Rep. 2021 Dec 1;11(1).

56. Bellucci R, Propris D, Buccisano F, Lisci A, Leone G, Tabilio A, et al. Modulation of VLA-4 and L-selectin expression on normal CD34 + cells during mobilization with G-CSF [Internet]. Vol. 23, Bone Marrow Transplantation. 1999. Available from: http://www.stockton-press.co.uk/bmt

57. Miles MP, Leach SK, Kraemer WJ, Dohi K, Bush JA, Mastro AM. Leukocyte adhesion molecule expression during intense resistance exercise. J Appl Physiol. 1998;84(5):1604–9.

58. Adams GR, Zaldivar FP, Nance DM, Kodesh E, Radom-Aizik S, Cooper DM. Exercise and leukocyte interchange among central circulation, lung, spleen, and muscle. Brain Behav Immun. 2011;25(4):658–66.

59. Okutsu M, Ishii K, Kai JN, Nagatomi R. Cortisol-induced CXCR4 augmentation mobilizes T lymphocytes after acute physical stress. Am J Physiol Regul Integr Comp Physiol. 2005;288(3 57-3):591–9.

60. Okutsu M, Ishii K, Niu K, Nagatomi R. Cortisol is not the primary mediator for augmented CXCR4 expression on natural killer cells after acute exercise. J Appl Physiol. 2014;117(3):199–204.

61. Sutherland DR, Anderson L, Keeney M, Nayar R, Chin-Yee I. The ISHAGE guidelines for CD34+ cell determination by flow cytometry. J Hematother Stem Cell Res. 1996;5(3):213–26.

62. Panch SR, Szymanski J, Savani BN, Stroncek DF. Sources of Hematopoietic Stem and Progenitor Cells and Methods to Optimize Yields for Clinical Cell Therapy. Biology of Blood and Marrow Transplantation. 2017;23(8):1241–9.

63. Baumann FT, Zopf EM, Nykamp E, Kraut L, Schüle K, Elter T, et al. Physical activity for patients undergoing an allogeneic hematopoietic stem cell transplantation: Benefits of a moderate exercise intervention. Vol. 87, European Journal of Haematology. 2011. p. 148–56.

Chapter 3: Method Development

3.1 Abstract

The field of immunometabolism has been significant in enhancing comprehension of how immune cells regulate their bioenergetics to perform crucial biological activities including glycolysis and mitochondrial respiration which are primarily responsible for energy production in T cells. These processes can be measured simultaneously utilising extracellular flux analysis (EFA) to investigate the metabolic characteristics and real-time response of the cells to activation. By conducting experiments to optimise an EFA assay using Jurkats and primary naïve T cells, this was then implemented in Chapter 4 of this thesis. After complications surrounding the work in Jurkats, conditions were optimised for enriched primary naïve $CD4^+$ and $CD8^+$ T cells (200 x 10^3 cells). Glucose (10 mM) and glutamine (2 mM) concentrations were optimised for a CD3/CD28 bead-induced activation assay using Seahorse XFe96 EFA. In order to accurately examine *in vivo* immunometabolic processes, blood collection procedures were then optimised. Real time changes in proton efflux rate (PER) were greater in naïve T cells after CD3/CD28 activation when naïve T cells was isolated immediately from sodium heparin blood tubes at room temperature. Moreover, the use of silicone inserts for cell seeding and standard assay media in EFA led to precise and improved alterations in PER following activation.

3.2 Introduction

Peripheral blood mononuclear cells (PBMCs) represent a diverse group of predominantly lymphocytes and monocytes that circulate between lymphatic organs

and other tissues to facilitate whole body immune responses. PBMCs are easily accessible from a venous blood draw and offer potential as markers of bioenergetic health given their susceptibility to various inflammatory and metabolic stimuli (8). For this reason, there has been increasing interest in the discipline of immunometabolism in the context of immune-driven disease pathology. For example, a study by La Rocca et al, 2017 reported aberrant T cell metabolic responses in people with multiple sclerosis vs. controls, which was defined by impaired changes in extracellular acidification rate (ECAR) and oxygen consumption rate (OCR) in response to activation (9). In people with autoimmune illness, upregulation of glucose metabolism in T cells enhances joint inflammation and autoantibody production in people with rheumatoid arthritis (10), and although basal OCR was higher in PBMCs isolated from individuals with rheumatoid arthritis, systemic lupus erythematosus and vasculitis, activation induced changes were attenuated vs. healthy individuals (8). The study of immunometabolism has therefore been central to developing understanding of how immune cells regulate their energy production to fulfil critical cell functions and provides an opportunity for therapeutic intervention by augmenting or inhibiting metabolic pathways using pharmaceutical or lifestyle (nutrition and exercise) approaches.

There are a plethora of quantitative methods available to evaluate immunometabolism. These include metabolomics to quantify specific metabolites using mass spectrometry (MS), isotope tracing to detect and quantify a targeted substrate *in vivo*, and single-cell RNA sequencing and proteomics to determine the gene and protein expression of cells respectively, indicating a metabolic phenotype. More recent technological advances have resulted in real time applications such as an EFA using Seahorse XF

analyser. EFA is automatic, user friendly, and now accessible for most laboratories. Moreover, Seahorse XF analyser can interrogate real-time metabolic assessment of cellular OCR and ECAR with small quantities of cells and provide flexibility to construct customisable experiments that enable exposure of bead-conjugated antibodies, ligands, inhibitors, and substrates to investigate various metabolic perturbations in PBMCs (9,11) or more specific T cell populations within the PBMC fraction (12,13).

Despite advances in the analytical methods used to evaluate immune cell energetics, there are obstacles taking place in the analysis such as the dynamic nature of cellular metabolism and differences in immune cell response to activation (14). This is particularly the case when studying immunometabolism using PBMCs. PBMCs are a heterogeneous population of cells, with diverse effector functions governed by unique metabolic pathways (15). In the context of exercise immunology, investigating the effects of single bouts of exercise in PBMC energetics presents further complications given the dynamic fluctuations in the number and type of immune cells within the PBMC fraction. As a proportion of PBMCs, T cells are the primary constituent that exhibit unique characteristics against pathogens and infected cells by producing a durable and highly specific immune response. To robustly evaluate the impact of exercise bouts on immunometabolic pathways in T cells, techniques must be adopted to first purify homogenous T cell populations (16,17). T cell subsets can be isolated from PBMCs with high purity using magnetic activated cell sorting (discussed in Chapter 4), which is a simple and fast separation method that does not compromise the viability of enriched target cells (18,19). This is essential for downstream applications such as the measurement of T cell energetics.

Glycolysis and mitochondrial respiration are the primary processes that are responsible for ATP production in T cells (20) which can be calculated simultaneously using EFA to evaluate shifts in metabolic phenotype. Furthermore, *ex vivo* T cell activation augments shifts in bioenergetic processes to fulfil the energy demands of the cell. These metabolic changes reflect T cells encountering pathogens *in vivo* (21). Hence, by evaluating the bioenergetics of single T cell populations through EFA (including real-time responses to activation), the effects of acute exercise on T cell energetics can be accurately examined.

To develop methods for use in subsequent chapters of this thesis, a Jurkat cell line was initially used to model a homogenous population of T cells, with the intention of conducting human serum exposure experiments from historical samples. The Jurkat cell line (Clone E6-1) is a leukemic T cell line derived from the peripheral blood of a 14-year-old male with acute leukemia. By optimising experimental conditions to expose Jurkat cells to serum isolated from human donors before and after bouts of exercise, this method will then evaluate the impact of exercise-induced fluctuations in serum metabolites on T cell energetics. For full transparency, this approach was adopted in light of the constraints imposed by COVID-19 restrictions. Planning for this experimental Chapter 4 started in January 2021 when there were significant delays with regards to gaining ethical and biological safety approvals. It was not possible to work with human participants and draw blood safely during this time. After restrictions were lifted and upon reflection of the data obtained from the initial Jurkat experiments,

the focus of subsequent experiments shifted to human primary T cells, more specifically, comparisons of bioenergetics in naïve vs. antigen-experienced T cells.

The aim of this chapter was to optimise methods to evaluate T cell energetics appropriate for implementation in human acute exercise studies carried out in experimental chapter 4 of this thesis. This section moreover provides the rationale and appropriate justification of the methods used.

3.3 Overview of Jurkat Methods

A Jurkat cell line (Clone E6-1) was used to model a homogenous T cell population, with the intention of then conducting human serum exposure experiments with samples from before and after bouts of exercise. Method development began with titrations of cell density for seeding the EFA plate **(section 3.2.3)** to determine the optimal cell number for the outcome measures of OCR and ECAR. This cell number was then applied to subsequent experiments measuring Proton Efflux Rate (PER) in response to T cell activation, with optimal glucose, glutamine, and T cell activation bead (CD3/CD28) concentrations within the EFA media determined **(section 3.2.4** and **3.2.5).** Given the high rates of basal PER observed in Jurkat cells, glucose starvation studies were then conducted with the intention of reducing basal PER prior to cell activation **(section 3.2.6)** and interleukin 2 (IL-2) secretion quantified in assay media as an indicator of cell activation.

The next two sections will first overview the method for culturing the Jurkat cell line **(section 3.3.1)** and generic details for the bioenergetic assays used to determine their

metabolic phenotype (Mito stress assay, **section 3.3.2.1**) and real-time responses to activation (Activation assay, **section 3.3.2.2**).

3.3.1 Jurkat Culture Method

Jurkats were cultured in complete media composed of glucose-containing RPMI (reference starvation studies below) supplemented with 10% fetal bovine serum (FBS), 2 mM L-glutamine and 100 U/mL penicillin-streptomycin. Initially, Jurkats were seeded into a T25 culture flask for 2-3 days (37ºC incubator with 5% CO_2) to improve cell viability. Cells were then seeded at a density of 1 x 10^5 - 1 x 10^6 cells/mL before passaging at 80% confluence (2.4 x 10^6 cells/mL). Culture media was replaced every 48 hours to achieve ≈90% viability by day 12.

3.3.2 Seahorse EFA

Experimental assays were carried out using the Seahorse XFe96 extracellular flux analyser and pre-designed using Seahorse analytics software 1.0.0-570 (*Agilent Technologies, USA*). A Mito stress assay was initially implemented to investigate the bioenergetic profile of Jurkats at different densities (via OCR and ECAR measurement) using an injection sequence of different cell respiration modulators (Oligomycin, BAM 15, Rotenone and Antimycin A) (21). An activation assay was then validated to evaluate real time bioenergetic changes to T cell activation, demonstrated by a rapid switch from mitochondrial respiration to glycolysis. This was measured via changes in PER after incubation of Jurkats with artificial human CD3/CD28 T cell activation beads, followed by injection of 2-DG (glycolytic inhibitor) (22,23).

3.3.2.1 Mito Stress Assay

Preparation

A Mito stress assay was carried out where a Seahorse XFe96 sensor cartridge was hydrated in 200 µL/well of XF Calibrant in a non-CO_2 incubator overnight at 37°C. The day after, Jurkats were suspended in 50 µL **(section 3.2.3)** of pre-warmed base Seahorse XF RPMI assay medium (10 mM glucose, 1 mM pyruvate, and 2 mM glutamine, pH = 7.4), following manufacture's standard protocols (*Agilent Technologies, USA*), and seeded onto a Seahorse XFe96 cell culture microplate (*Agilent Technologies, USA*). A total of 4 technical replicates were used for each assay. Each well was pre-coated with sterile Cultrex Poly-D-lysine (*Bio-techne, Minneapolis, USA*). The plate was centrifuged at 300 x *g* for 5 minutes at room temperature with the brake off and the plate rested for 1 hour in a non-CO_2 incubator at 37°C. Assay medium (130 µL) was added 15 minutes prior to starting the assay.

Assay Injection Strategy

Following assay preparation, 20 µL/well of injected reagents were prepared including 2 µg · mL^{-1} Oligomycin (*Sigma-Aldrich*, *Merck, UK*) in port A, 3 µM BAM 15 (*TOCRIS, Minneapolis, USA*) in port B and a mixture of 2 µM Rotenone + 2 µM Antimycin A (*Sigma-Aldrich*, *Merck, UK*) in port C for mitochondria stress (Mito stress) test in cell seeding density titration **(section 3.2.3)**. Seahorse XFe96 extracellular flux analyser was calibrated with pre-hydrated Seahorse XFe96 sensor cartridge for minimum 5 hours prior to assay start and followed by inserting the experimental plate into the analyser, and an induced real-time ATP rate (pmol · min^{-1}) assay was performed. Following the pre-design experimental assay, OCR (pmol · min^{-1}) and ECAR (mpH ·

min^{-1}) were measured 14 minutes after the assay begun reflecting the baseline measurement (3 cycles) and following each of 3 consecutive injections over a 40 measurement period **(Figure 3.1)**. Injections of Oligomycin (port A, 3 cycles) after 15–28 minutes, BAM 15 (port C, 3 cycles) after 29–41 minutes and a mixture of Rotenone + Antimycin A (port C, 3 cycles) after 42–54 minutes were implemented to provide the real-time mitochondria stress test for different cell number titrated.

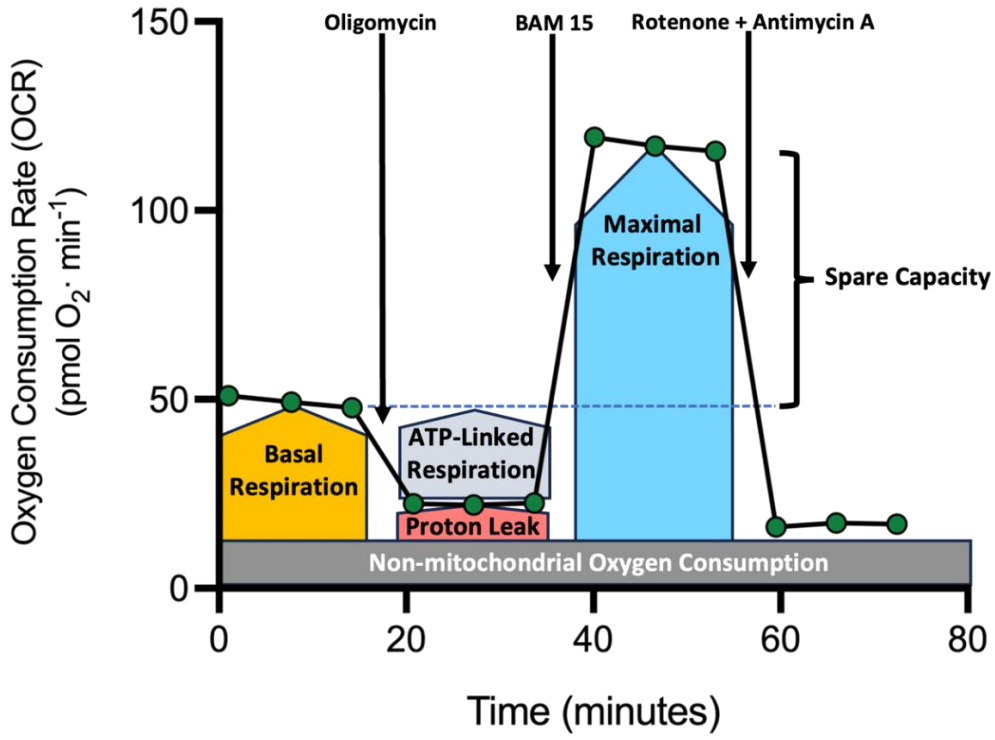

Figure 3.1 Seahorse XFe96 Mito Stress test profile. Kinetic trace of OCR in T cells during Mito Stress test, revealing essential parameters determining mitochondrial function and tested by the injection of drug modulators including Oligomycin, BAM 15, Rotenone, and Antimycin A.

3.3.2.2 T cell Activation Assay

A T cell activation assay followed identical preparation procedures to the Mito stress assay, differing only in assay media composition relating to titrations of glucose, glutamine **(section 3.2.2.4)** and activation bead concentrations **(section 3.2.2.5)** in metabolic assay media, and glucose concentration in growth media for the Jurkat glucose media starvation experiment **(section 3.2.2.6)**. The assay started with preparation of 20 µL/well of injected reagents including ImmunoCult human CD3/CD28 T-cell bead activator (*STEMCELL Technology, UK*) or assay medium for control well in port A and 50 mM 2-Deoxy-D-glucose (2-DG) (*Thermo Scientific, UK*) in port B. PER (pmol · min^{-1}) was measured 14 minutes after the assay baseline measurement (3 cycles) and following each of 2 consecutive injections over a 100 measurement period **(Figure 3.2)**. Activator or assay media for control samples (port A, 10 cycles) after 15–79 minutes and 2-DG (port B, 4 cycles) after 80–120 minutes were injected to provide the real-time glycolytic rate (through PER measurement) between control vs. experimental samples upon activation. PER is the number of protons exported by cells into the assay medium over time, expressed as pmol/min. The glucose analog 2-DG was also injected to inhibit glycolysis through competitive binding of glucose hexokinase, the first enzyme in the glycolytic pathway (24). The injection of 2-DG caused a rapid decrease in PER, thus providing confirmation that prior changes in PER were primarily due to glycolysis.

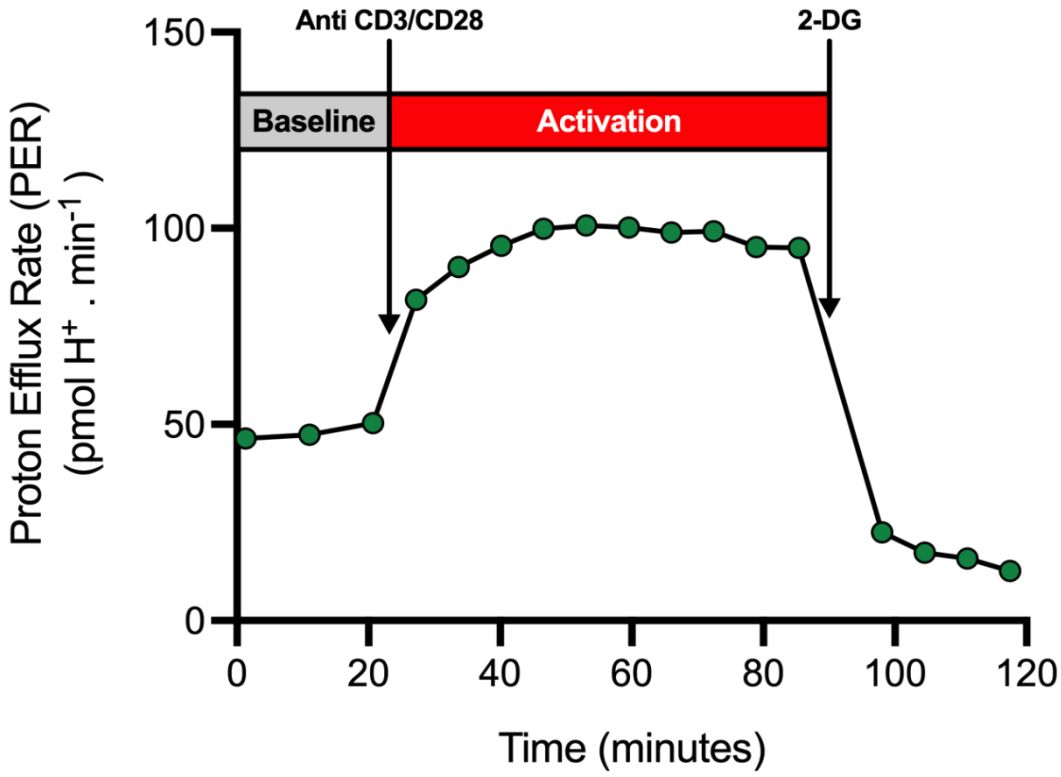

Figure 3.2 Seahorse XFe96 activation test profile. Kinetic trace of PER in T cells during activation assay, demonstrating an increase in PER upon injection of anti-CD3/CD28 bead activator relative to baseline, followed by an injection of 2-DG, which abrogates the activation-associated glycolytic increase.

3.3.2.3 Cell Seeding Density Titration

To accurately examine Jurkat bioenergetics using the Agilent Seahorse EFA, baseline and maximal OCR and ECAR of cells at different seeding densities was determined. Following manufacture's recommendation, overseeding cells should be avoided as it can lead to inadequate cell adhesion or cell clustering, which in turn results in false rate measurements. Optimal cell distribution (monolayer at 70-90% confluency) will generate metabolic rates in the desirable/ dynamic range of the Agilent Seahorse

XFe96 instrument, notably OCR (20 to 160 pmol/min) and ECAR (10 to 90 mpH/min). According to Agilent Seahorse EFA standard techniques, suspension cells such as Jurkats require 5 x 10^4 to 2 x10^5 cells/well. Therefore, the effect of 50, 100, 150, 200, 250 and 300 x 10^3 cells/well on basal and maximal OCR and ECAR throughout a Mitochondria Stress test was examined.

(A)

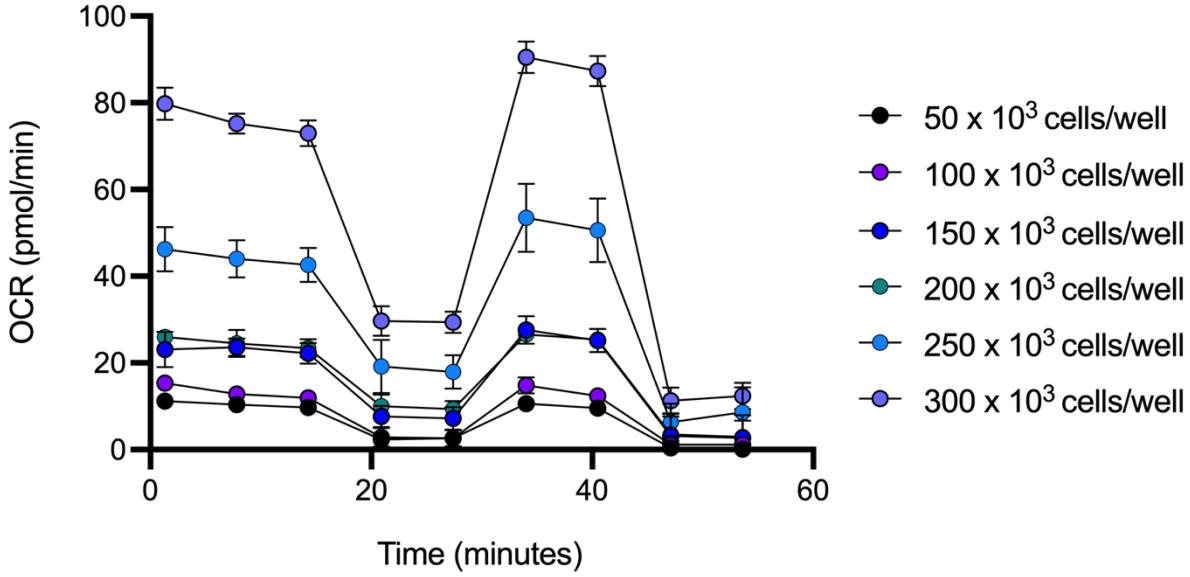

(B)

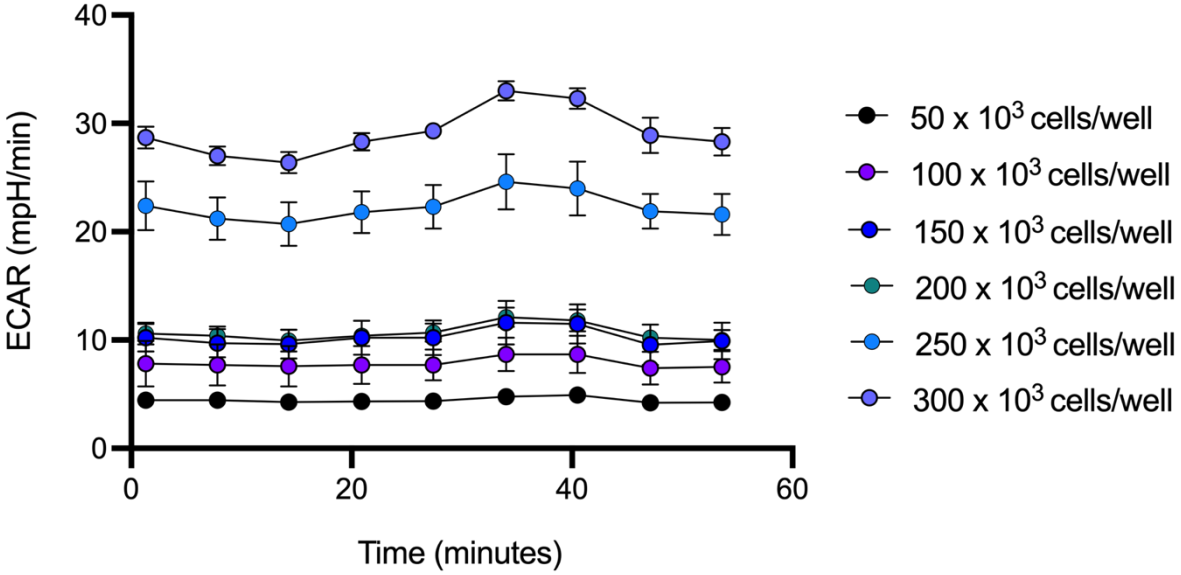

Figure 3.3 Kinetic traces of (A) OCR and (B) ECAR throughout a Mito stress test at different densities of Jurkats (cells/well). Data were absolute values from 4 replicate wells and presented as mean ± SD. $P > 0.05$.

Cell densities of 50 x 10^3 and 100 x 10^3 cells/well both exhibited basal OCR (<20 pmol/min) and ECAR (<10 mpH/min) values below the acceptable range owing to low confluency following manufacture's recommendation **(Figure 3.3)**. A marginal response to mitochondrial uncoupling was observed for cells at higher densities (≥ 200 x 10^3 cells/well), but there were no differences in basal and maximal respiration for cells at lower density (≤ 100 x 10^3 cells/well). This may have reflected high rates of basal glycolysis in an immortalised cell line such as Jurkats (confirmed in later experiments). A cell density of 200 x 10^3 cells/well resulted in accurate responses to each compound and more stabilised basal OCR and ECAR at 3 measurement points compared to 250 x 10^3 and 300 x 10^3 cells/well.

3.3.2.4 Titration of Glucose and Glutamine Concentrations in Assay Media

T cells demonstrate a profound metabolic shift upon activation to promote glycolysis > mitochondrial respiration for energy provision, for which nutrients such as glucose and glutamine availability are critical (25). Notably, these nutrients provide energy for T cell proliferation (25,26), activation and subsequent effector functions (27). Hence, the optimal concentrations of glucose and glutamine within the assay media to facilitate Jurkat activation in our experimental model was determined. Instead of using the base Seahorse XF RPMI assay medium with recommended supplements (used in **section 3.2.2.3**), glucose and glutamine concentration were titrated to determine the ideal

composition for maximising changes in PER following T cell activation. Therefore, assay media was supplemented with glucose and glutamine ranging from 0 – 10 mM and 0 – 2 mM, respectively. Assay media with 10 mM glucose or 2 mM glutamine served the highest concentrations as it is most commonly used in cell culture media (28) and 5 mM glucose (normal concentration) was used to reflect normal physiological glucose concentration in blood (29). Prior to the titration of human CD3/CD28 T cell activator **(section 3.2.2.5)**, manufacturer's instructions (1:1 dilution with assay media) were followed.

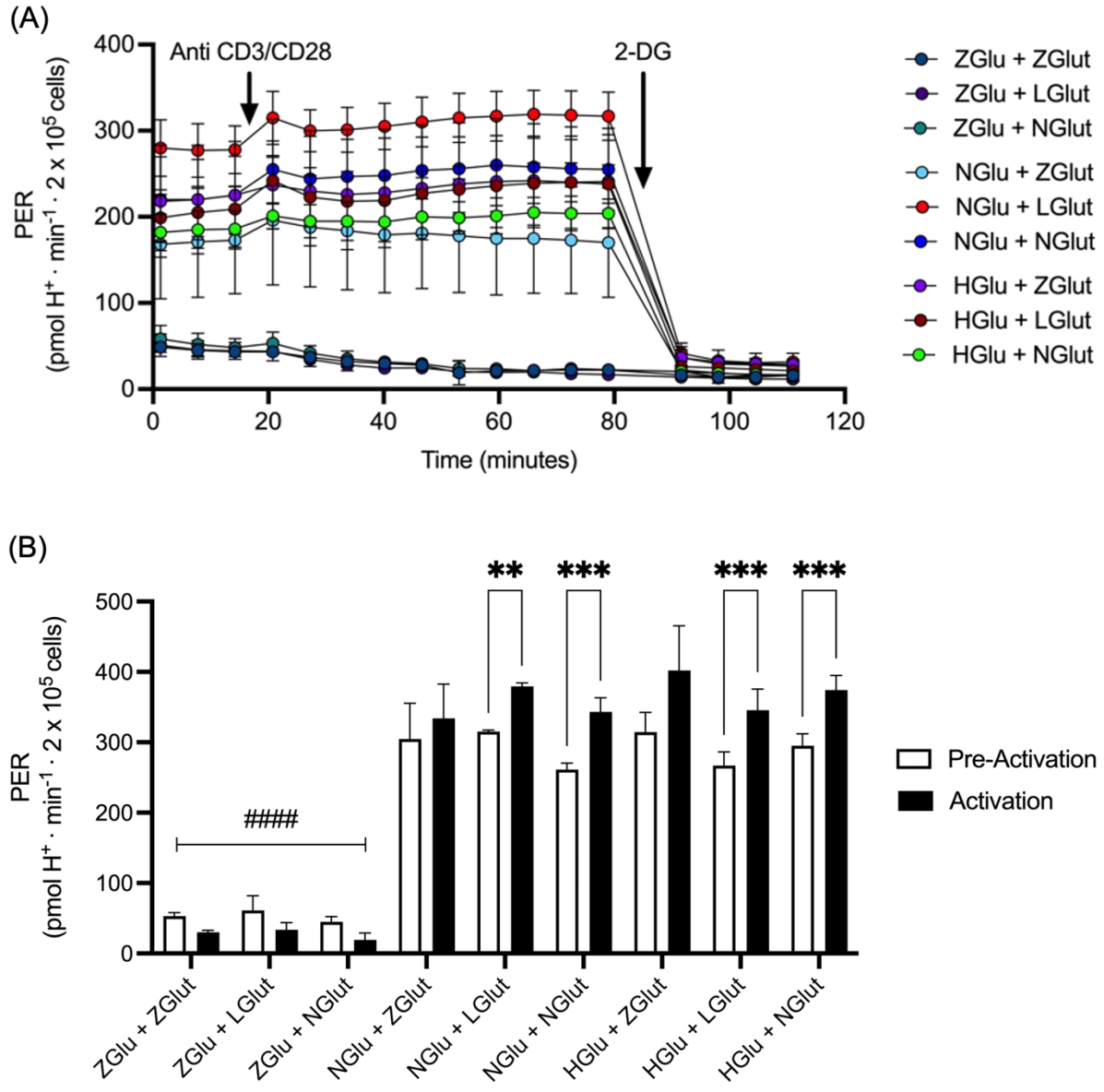

Figure 3.4 (A) Kinetic traces of PER in Jurkats (200 x 10^3 cells/well) exposed to CD3/CD28 activation beads and different media concentrations of Glucose and Glutamine. (B) Comparison of peak PER between pre-activation (basal, white bar) and activation (black bar) for different concentration of Glucose and Glutamine in assay media. ZGlu, 0 mM Glucose; NGlu, 5 mM Glucose; HGlu, 10 mM Glucose; ZGlut, 0 mM Glutamine; LGlut, 1 mM Glutamine and NGlut, 2 mM Glutamine. Data were absolute values from 4 replicate wells and presented as mean ± SD. **P < 0.01, ***P < 0.001. ####P < 0.0001, significant differences between assay media with ZGlu and NGlu or HGlu.

Jurkats supplemented no glucose (ZGlu) showed lower rates of basal PER and no change in PER in response to CD3/CD28 activation compared to cells supplemented with normal (NGlu) or high glucose (HGlu) **(Figure 3.4)**, independent of glutamine concentration. Uniformly flat PER traces over time were likely a consequence of a lack of glucose to facilitate T cell activation and thus changes in PER (30). Moreover, when no glutamine was added to the assay media in NGlu or HGlu, there was no significant change in PER, indicating the importance of glutamine in mediating T cell activation (31). There was a significant change in PER with NGlu vs. HGlu, but this was not significantly difference between assay medias. Therefore, HGlu and NGlut were selected to align with standard culture conditions and assay media used with previous EFA protocols (32).

3.3.2.5 Activator Dilution Comparison

T cell activation is initiated by the concurrent stimulation of the T cell receptor (TCR)/CD3 complexes and costimulatory receptors, such as CD28, by antigen-presenting cells (APC) (33). The Human CD3/CD28 T cell Activator is specifically formulated to stimulate and activate human T cells without the need for magnetic beads, feeder cells, or antigens. The T cell Activator is composed of soluble antibody complexes that specifically attach to CD3 and CD28 cell surface ligands which in turn provides the necessary primary and co-stimulatory signals for the activation of T cells (34). Given the high rates of glycolysis in Jurkats and marginal responses to activation reported in previous experiments, it was hypothesized that using more concentrated CD3/CD28 beads would maximize changes in PER for use in subsequent experiments.

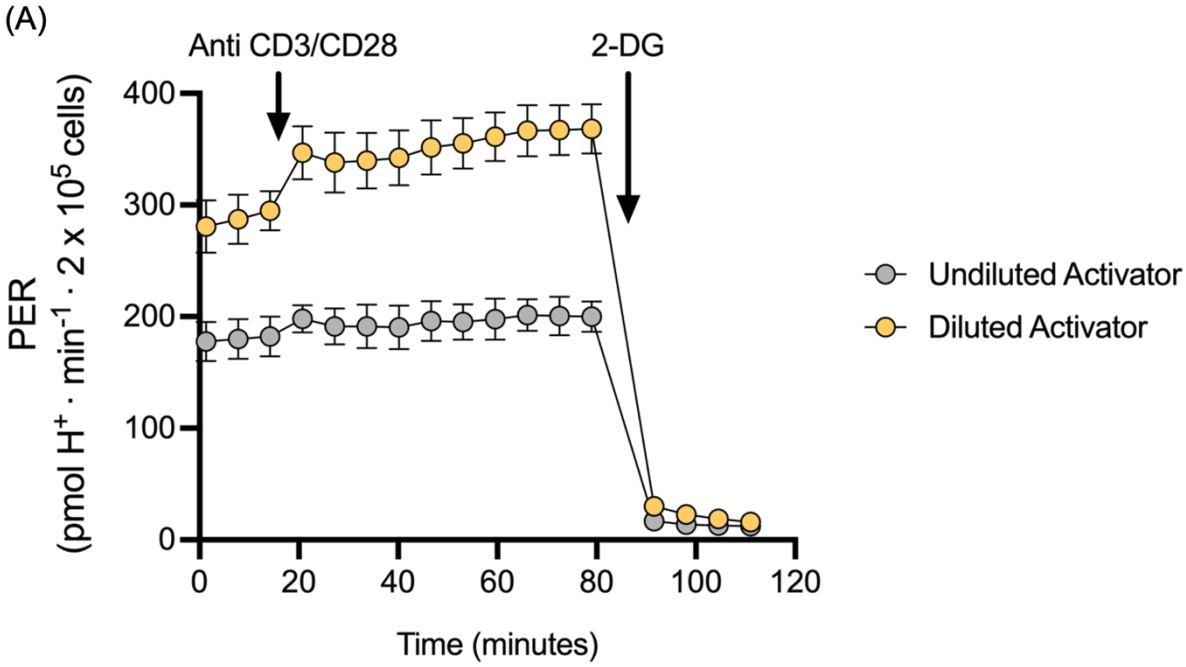

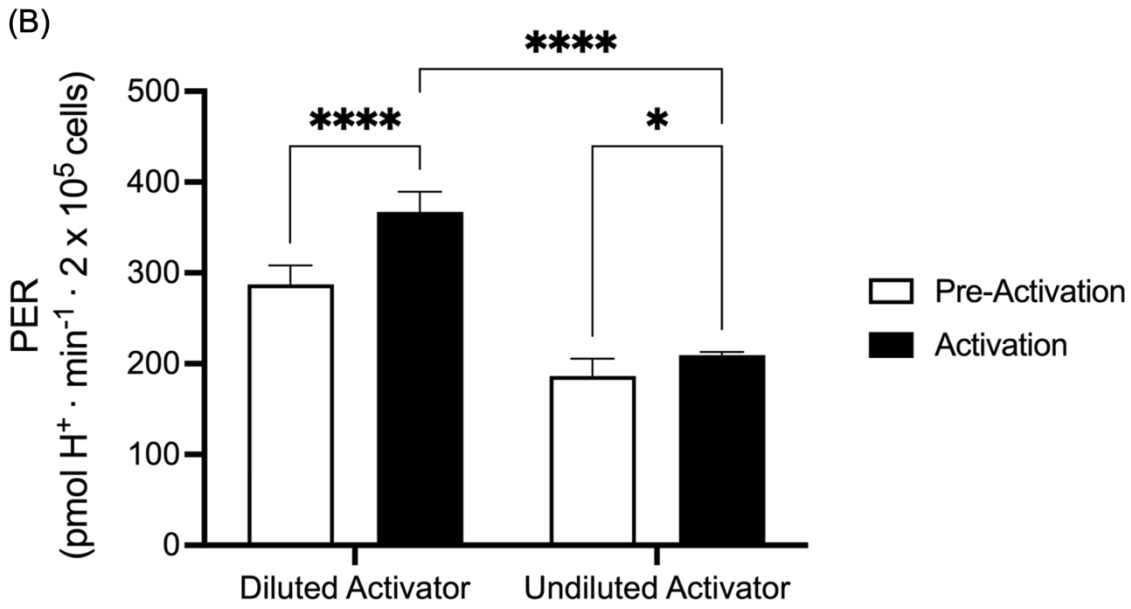

Figure 3.5 (A) Kinetic traces of PER in Jurkats (200 x 10^3 cells/well) in response to CD3/CD28 activation beads used at 5% (diluted) or 10% (undiluted) of the assay media composition. (B) Comparison of peak PER between pre-activation (basal, white bar) and activation (black bar) for undiluted and diluted activation beads. Data were absolute values from 4 replicate wells and presented as mean ± SD. *P < 0.05, ****P < 0.0001.

Although the magnitude of change in PER was greater using diluted vs. undiluted activation beads within the assay media, both promoted a significant increase in PER **(Figure 3.5)**. Like previous experiments, basal PER was high prior to activation and therefore to maximise stimulation to CD3 and CD28 cell surface receptors in Jurkats, undiluted activator was used for subsequent experiments.

3.3.2.6 Variance of Glucose Concentration in Culture Media

Due to differences in nutrient utilisation and higher rates of glycolysis, Jurkats exhibit metabolic requirements unique from non-cancerous T cells (35). As cancer cells, Jurkats upregulate the activity of glycolytic pathway to produce intermediates which are essential for synthesis of nucleic acids, proteins, and lipids to support cell growth and proliferation (35). Results from the previous experiments indicate that basal glycolysis was inherently high in Jurkats, thus potentially mitigating the impact of manipulating nutrient (i.e., glucose and glutamine) and/or activation bead concentrations on PER. To overcome this, culturing Jurkats in chronically low-glucose environment may provide a strategic approach to suppress basal glycolytic rate (30,36), thus optimising our experimental model. Hence, culture media with different glucose concentrations ranging from 2-10 mM were used to culture Jurkats for 14 days before the experimental assay started.

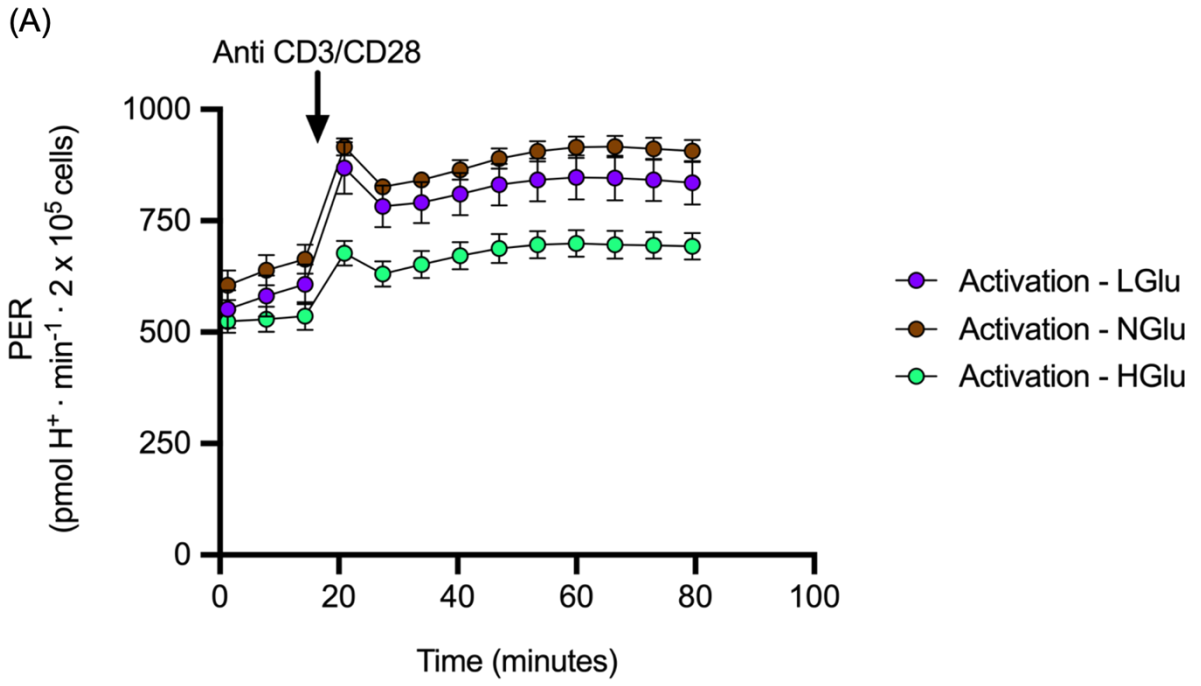

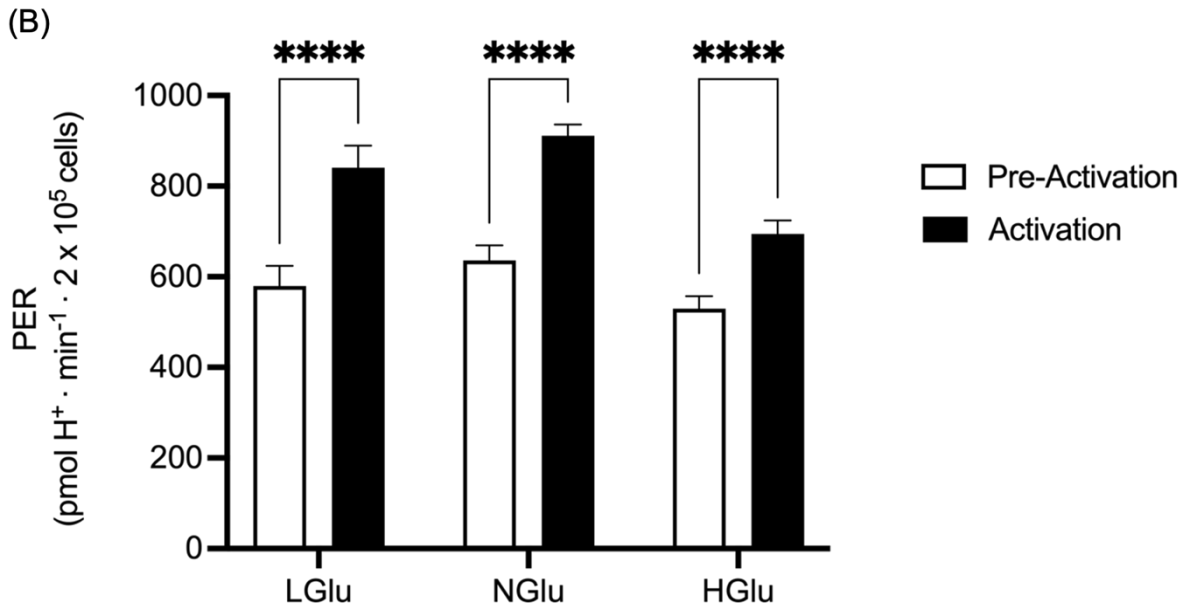

Figure 3.6 (A) Kinetic traces of PER after activation of Jurkats (200 x 10^3 cells/well) following 14-days of culture in low (LGlu, 2 mM), normal (NGlu, 5 mM), and high (HGlu, 10 mM) glucose concentrations. (B) Comparison of peak PER between pre-activation (basal, white bar) vs. activation (black bar) in LGlu, NGlu, and HGlu. Data were absolute values from 4 replicate wells and presented as mean ± SD. ****P < 0.0001.

Following CD3/CD28 activation, there was a significant increase in PER across all conditions. Surprisingly, there was a small decrease in PER after the initial peak (20-30 minutes) in all conditions, demonstrating unstable responses to activation **(Figure 3.6)**. Furthermore, high basal PER rendered the validity of using Jurkats to model T cell activation very low, due to the low spare respiratory capacity of these cells. To corroborate these findings, Interleukin (IL)-2 cytokine concentrations were quantified in metabolic assay media from control and activated Jurkats. T cell activation results in induction of the interleukin-2 receptor (IL-2R) and secretion of IL-2 (37).

Supernatants were isolated from the Seahorse EFA plate after the activation assay and centrifuged at 300 x *g* for 10 minutes before aspiration and subsequent analysis in duplicate using high sensitivity (>0.066 pg · mL^{-1}) enzyme-linked immunosorbent assay (ELISA) kits (*Bio-techne*, *Minneapolis, USA*), with values obtained from a standard curve of known IL-2 concentration. No IL-2 was detectable in the metabolic assay media after activation or control.

Interim Conclusion

In summary, a cell density of 200 x 10^3 Jurkats/well resulted in accurate and enhanced stability of basal OCR and ECAR in responses to a Mito stress test. Moreover, Jurkats cultured in assay media supplemented with 10% CD3/CD28 activation beads, 10 mM glucose and 2 mM glutamine exhibited the most optimal change in PER in response to activation across experiments. Despite chronically starving Jurkats of glucose for a 14-day period, basal rates of PER remained high in this experimental model. Following the lifting of COVID-19 restrictions (e.g., no collecting of blood and expired gases from humans), the validation of protocols in primary human T cells was prioritised and optimisation of this Jurkat model ceased.

3.4 Overview of Primary Cell Methods

Protocols were developed with the purpose of investigating the impact of prolonged moderate intensity exercise on T cell energy metabolism in purified naive T cells vs. total peripheral blood mononuclear cells (PBMCs) isolated from humans **(Chapter 4)**. Method development began with optimising a flow cytometry protocol (cell density and antibody titrations) to confirm high purity **(3.3.1)** of enriched naive $CD4^+$ and $CD8^+$ T

cells isolated from PBMCs using magnetic activated cell sorting (MACS) (discussed in **Chapter 4**). Following this, a T cell activation assay was developed for naive $CD4^+$ and $CD8^+$ T cells using seahorse EFA **(3.3.2)**, initially including titrations of cell seeding density, seeding conditions (standard vs. silicone well inserts) and activation bead (CD3/CD28) concentration. Finally, the influence of blood collection tube anticoagulant (EDTA vs. sodium heparin) and transit time between blood collection and analysis were determined.

3.4.1 Flow Cytometry

Flow cytometry is a distinct method that uses standard laser-based technology to analyse single cells in a heterogenous mixture of biological cells. It is a rapid, unbiased, and quantitative analytical tool for measuring the size and shape of cells through light scatter, coupled to fluorescence signals that identify molecules unique to individual cells (38). The principal of flow cytometry was applied in chapter 3 and 4 to confirm the purity of naïve $CD4^+$ and $CD8^+$ T cells before and after MACS using specific fluorescence-conjugated antibodies that target cell surface molecules (e.g., CD markers) (39). Flow Cytometry data acquisition was undertaken using a CytoFlex-S flow cytometer (*Beckman Coulter, California, USA*) and data analysed and presented with CytExpert v2.5 Software (*Beckman Coulter, California, USA*). All antibodies were purchased from BioLegend (*San Diego, CA*), gates were formed using fluorescence minus one (FMO) controls, and compensation was applied using single stained controls. Dead cells were excluded using a viability exclusion dye.

3.4.1.1 Gating Strategy of Naïve T cell

A gating strategy is a delineation in flow cytometry analysis **(Figure 3.7)**, either in numerical or graphical form, that serves to establish the specific attributes of cell population that are to be considered for subsequent analysis. The gating process involves the selection of a specific region on the scatter or histogram plot created during the flow experiment to choose which cells should be further analysed (38).

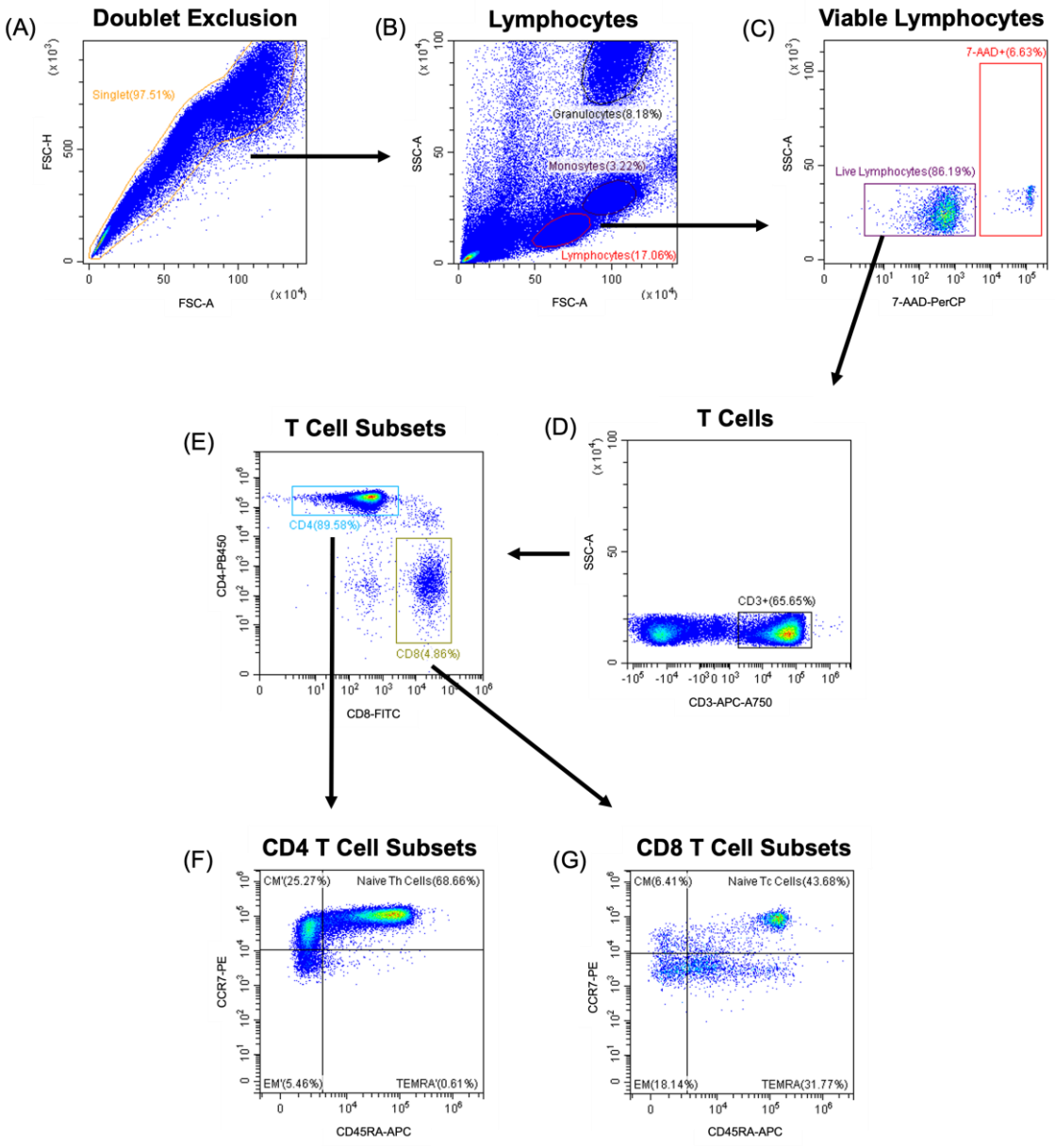

Figure 3.7 Schematic overview of naïve T cells gating strategy. Gating strategy was used to enumerate Naïve CD8 and CD4 T Cells Enumeration in PBMCs (200 x 10^3 cells). (A) Doublets were discriminated using forward side scatter-area (FSC-A) vs. forward side scatter-height (FSC-H). (B) Lymphocytes were gated on fully stained PBMCs. (C) Viable cells were acquired by using 7-AAD Exclusion. (D) Live CD3+ T cell events. (E) Lymphocyte subsets were identified using a CD8 PB450-Area vs. CD4 PE-Area bivariate plot. (F) CD4 subsets or (G) CD8 subsets were identified using a CD45RA FITC-Area vs. CCR7 APC-Area bivariate plot. Abbreviation: 7-AAD, 7-Aminoactinomycin D; CM, Central Memory; EM, Effector Memory; TEMRA, T Effector Memory Re-expressing CD45RA.

3.4.1.2 Antibody Titration and Cell Density

Titrations of cell number and antibody volume were conducted to determine the optimal conditions for flow cytometry analysis of naïve T cell purity. Eight volumes (0, 0.3125, 0.625, 1.25, 2.5, 5, 10 and 20 µL) of CD3, CD4, CD8, CD45RA and CCR7 antibodies were each added to 100 x 10^3 or 200 x 10^3 PBMCs (50 µL). A stain index (SI) was calculated for the titrated volumes of each antibody. SI represents the level of separation between positive and negative cell populations and is calculated by dividing the difference between the median fluorescence intensity (MFI) of positive and negative populations by 2 times the standard deviation of the negative population. Below, CD3-APC-A750 was used as a representative example.

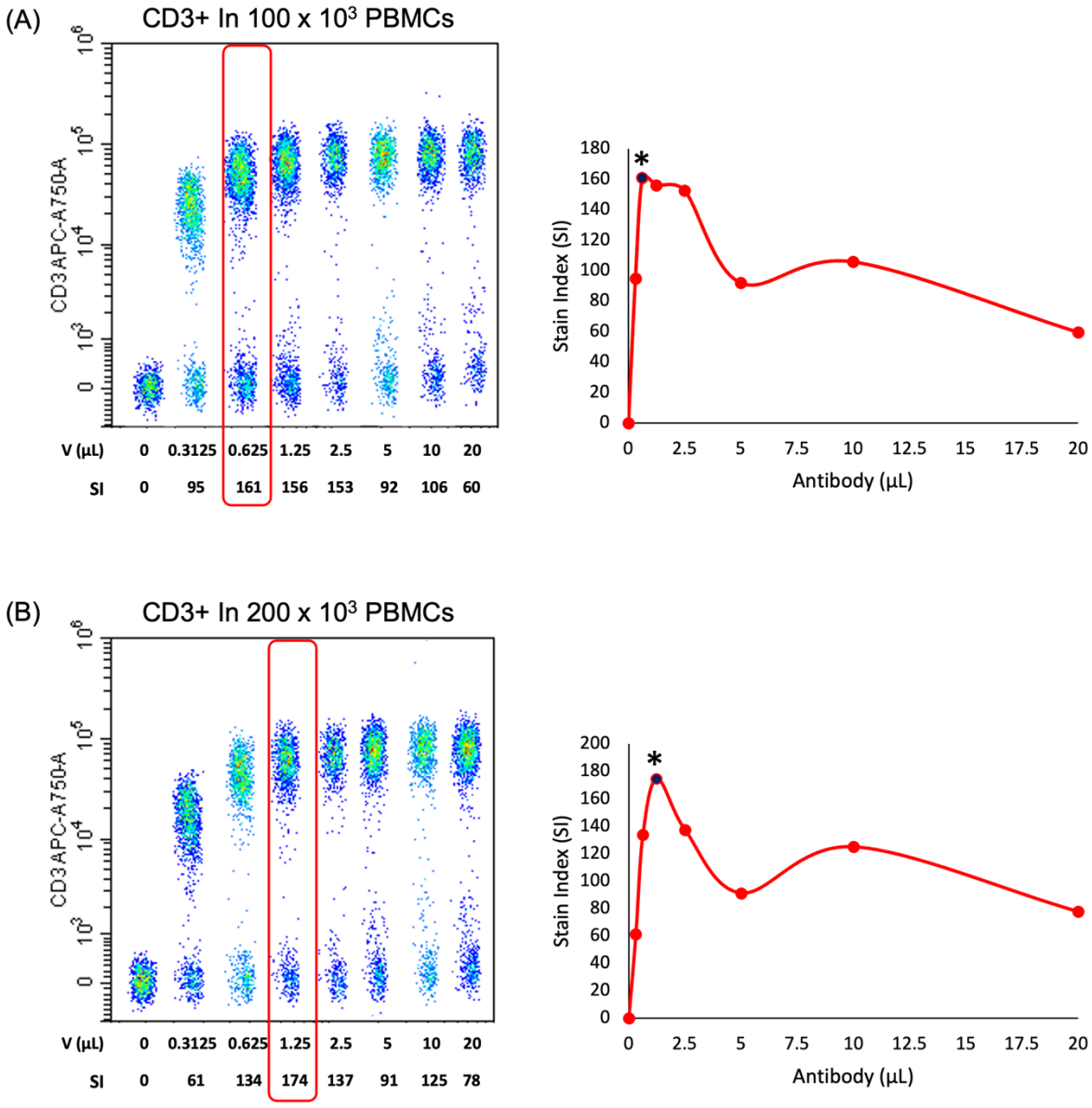

Figure 3.8 Antibody titration for (A) 100 x 10^3 vs. (B) 200 x 10^3 PBMCs stained with 0, 0.3125, 0.625, 1.25, 2.5, 5, 10 and 20 µL of CD3-APC-A750. The dot plots (left) display the separation between CD3+ and CD3- cells and the line graph the stain index of each antibody volume (right).

The red boxes and * in the dot and line graphs respectively indicate the volume of CD3-APC-A750 that gave the highest SI and therefore, optimal separation between CD3+

and CD3- populations **(Figure 3.8)**. The SI was 0.625 µL and 1.25 µL for 100 x 10^3 and 200 x 10^3 PBMCs stained with CD3-APC-A750, respectively. Moreover, SI evidenced that applying more antibodies did not serve a better separation between positive and negative cell population. Optimal volumes of CD4, CD8, CD45RA, and CCR7 based on SI are indicated in **Table 3.1**. Collectively, it was decided that 200 x 10^3 PBMCs was optimal for subsequent flow cytometry analysis.

Table 3.1 Volumes of each antibody validated for flow cytometry analysis using 200 x 10^3 PBMCs.

Antibody	Fluorescence	Validated Volume (µl)
CD3	APC-A750	1.25
CD4	PB450	0.625
CD8	FITC	1.25
CD45RA	APC	5
CCR7	PE	5

3.4.1.3 Antibody Isotype Control Validation

Isotype controls are primary antibodies that correspond to the class and type of the primary antibody used in the application but do not possess target specificity to bind to cell target. The isotype control serves to help distinguish the primary antibody signal from non-specific background signal (40). Moreover, as the binding or effect of the primary antibodies is specific, using isotype antibody controls ensures non-specific interactions with the Fc receptor or with other proteins on the cell surface are identified. Non-specific background is an important variable that needs to be controlled (40). By

configuring the relevant isotype antibody controls to identify non-specific binding, it is attainable to minimise the occurrence of false positive results and precisely examine true antigen-antibody interactions.

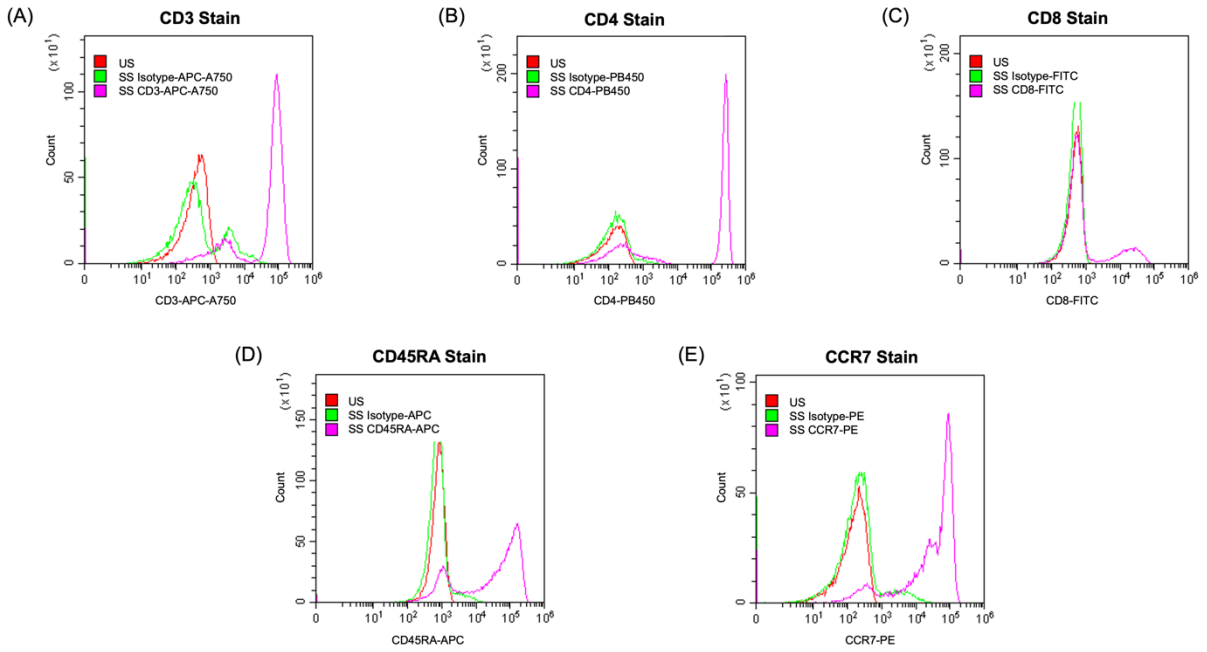

Figure 3.9 Histograms displaying specificity of titrated (A) CD3-APC-A750 (B) CD4-PB450 (C) CD8-FITC (D) CD45RA-APC and (E) CCR7-PE. US, unstained lymphocytes (red); SS, single stained lymphocytes with mouse IgG anti-human isotype control (green) or single stained lymphocytes with anti-human antibody (violet).

Figure 3.9 depicts minimal overlap between all signals from positive stained cell populations (violet) and corresponding Isotype antibody controls (green). This indicates that all primary antibodies were highly specific and exhibited a fluorescent signal distinct from non-specific binding.

3.4.2 Metabolic assay

The same assay procedures were followed for EFA of primary T cells as Jurkats **(section 3.2.2)**, but optimisation only carried out for real-time responses to activation (section 3.2.2.2). Method development began with titrations of cell density for seeding the EFA plate **(3.3.3.1)** to find an optimal cell number based on measurements of PER. This cell number was then applied to determine optimal human T cell activation bead (CD3/CD28) concentrations within the EFA media **(3.3.3.2)**, the use of standard seahorse well design vs. with silicone inserts **(3.3.3.3)** and the influence of anticoagulant (K_2EDTA vs. Sodium Heparin) within the blood collection vacutainer **(3.3.3.4)**. Finally, given the timely logistics of conducting human based exercise studies **(chapter 4)**, the impact of time from blood collection to analysis (immediately vs. 4 hours) was examined to elucidate the optimal conditions to preserve naïve T cell viability and measure representative *in vivo* bioenergetic responses to activation.

3.4.2.1 Naïve T Cell Seeding Density Titration

The impact of seeding 100 x 10^3 vs. 200 x 10^3 enriched naïve $CD4^+$ and $CD8^+$ T cells/well (MACS protocol overviewed in **Chapter 4**) on changes in PER after CD3/CD28 bead activation was examined. There was a significant increase in PER for 200 x 10^3 naïve T cells/well activated with CD3/CD28 beads, but not 100 x 10^3 naïve T cells/well **(Figure 3.10)**. Hence, a cell density of 200 x 10^3 cells/well was implemented for subsequent protocols to ensure optimal and stable responses to each measurement point after CD3/CD28 bead activation.

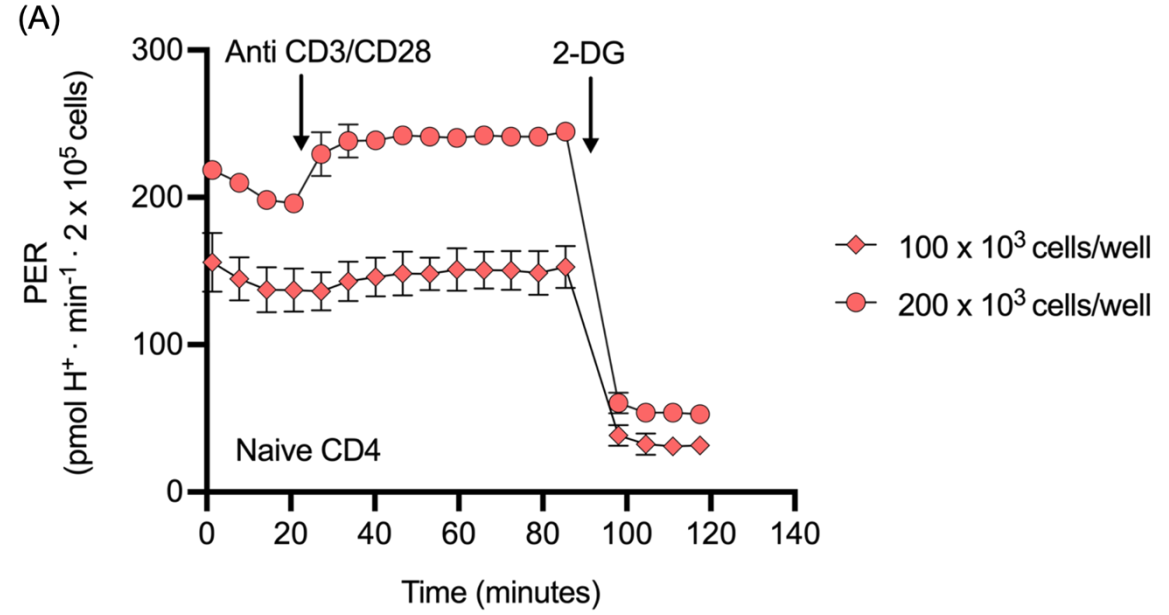
(A)
Anti CD3/CD28
2-DG
PER
(pmol H+ · min-1 · 2 x 10^5 cells)
300
200
100
0
Naive CD4
0
20
40
60
80
100
120
140
Time (minutes)
100 x 10^3 cells/well
200 x 10^3 cells/well

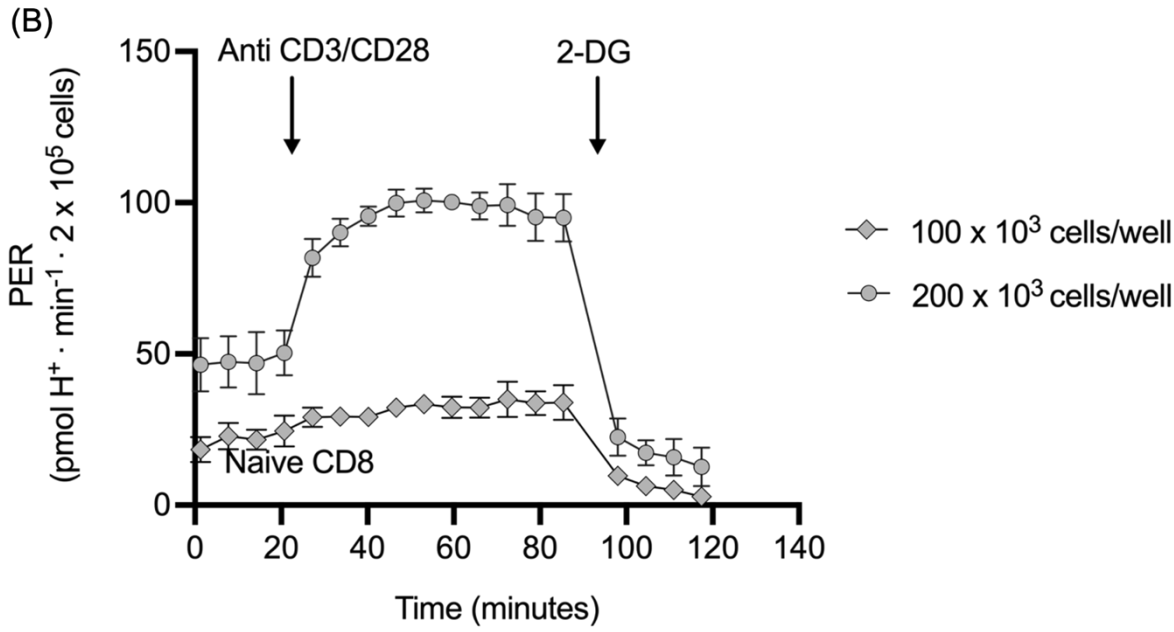
(B)
Anti CD3/CD28
2-DG
PER
(pmol H+ · min-1 · 2 x 10^5 cells)
150
100
50
0
Naive CD8
0
20
40
60
80
100
120
140
Time (minutes)
100 x 10^3 cells/well
200 x 10^3 cells/well

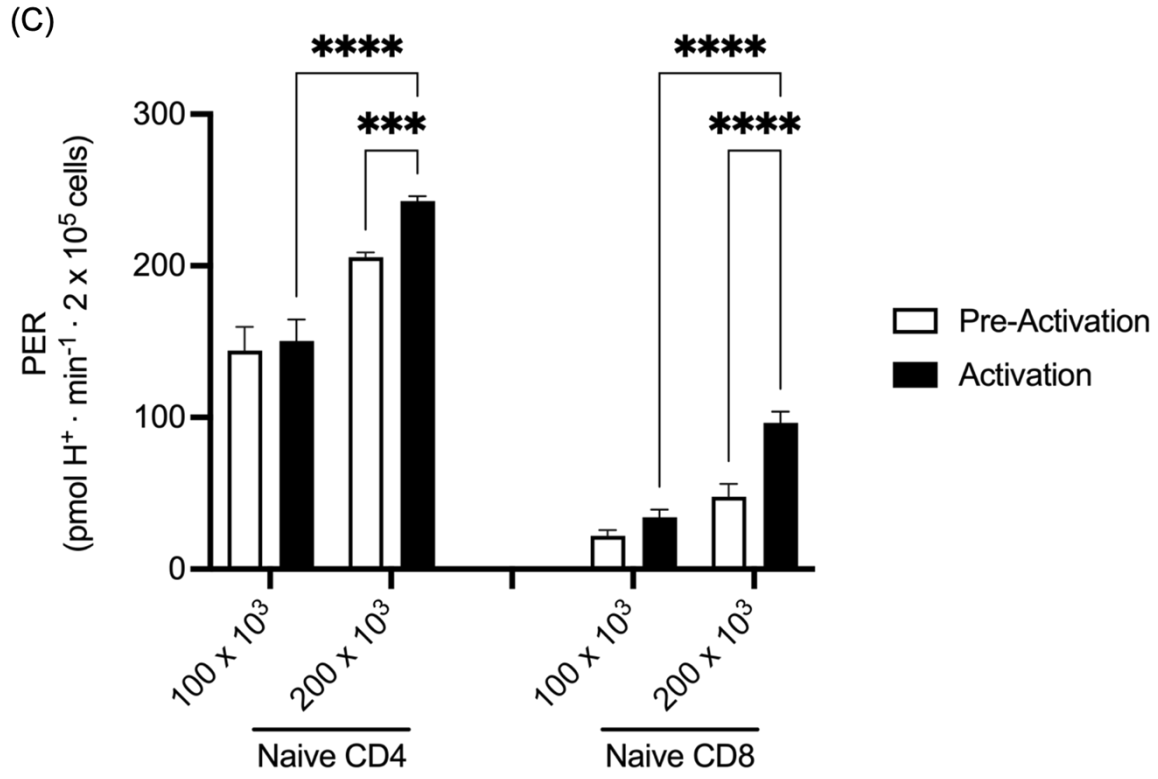

Figure 3.10 Kinetic traces of PER for 100 x 10^3 and 200 x 10^3 naïve (A) $CD4^+$ and (B) $CD8^+$ T cells in response to CD3/CD28 bead activation. (C) Comparison of peak PER between pre-activation (basal, white bar) vs. activation (black bar) for all conditions. Data were from 4 replicate wells and presented as mean ± SD. ***P < 0.001, ****P < 0.0001.

3.4.2.2 Standard vs. Silicone Well Comparison

Seahorse XFe96 EFA well plates are manufactured without silicone inserts as standard but used to facilitate cell seeding in 8-well EFA plates, such that the cell monolayer is located directly underneath sensor cartridges of the Seahorse EFA. This may in turn enhance measurements of PER during the assay, although this has yet to

be investigated in a 96-well format. **Figure 3.11** visually depicts that cells were more concentrated within wells using silicon inserts vs. standard wells. Furthermore, following injection of CD3/CD28 activation beads, naïve $CD4^+$ T cells seeded in the Seahorse EFA plate with a silicone insert exhibited more stable and greater increases in PER compared to cells seeded in standard wells, whereby there was no significant response to activation **(Figure 3.11B+D)**. The same pattern was observed for naïve $CD8^+$ T cells, but this didn't reach statistical significance **(Figure 3.11C+D)**.

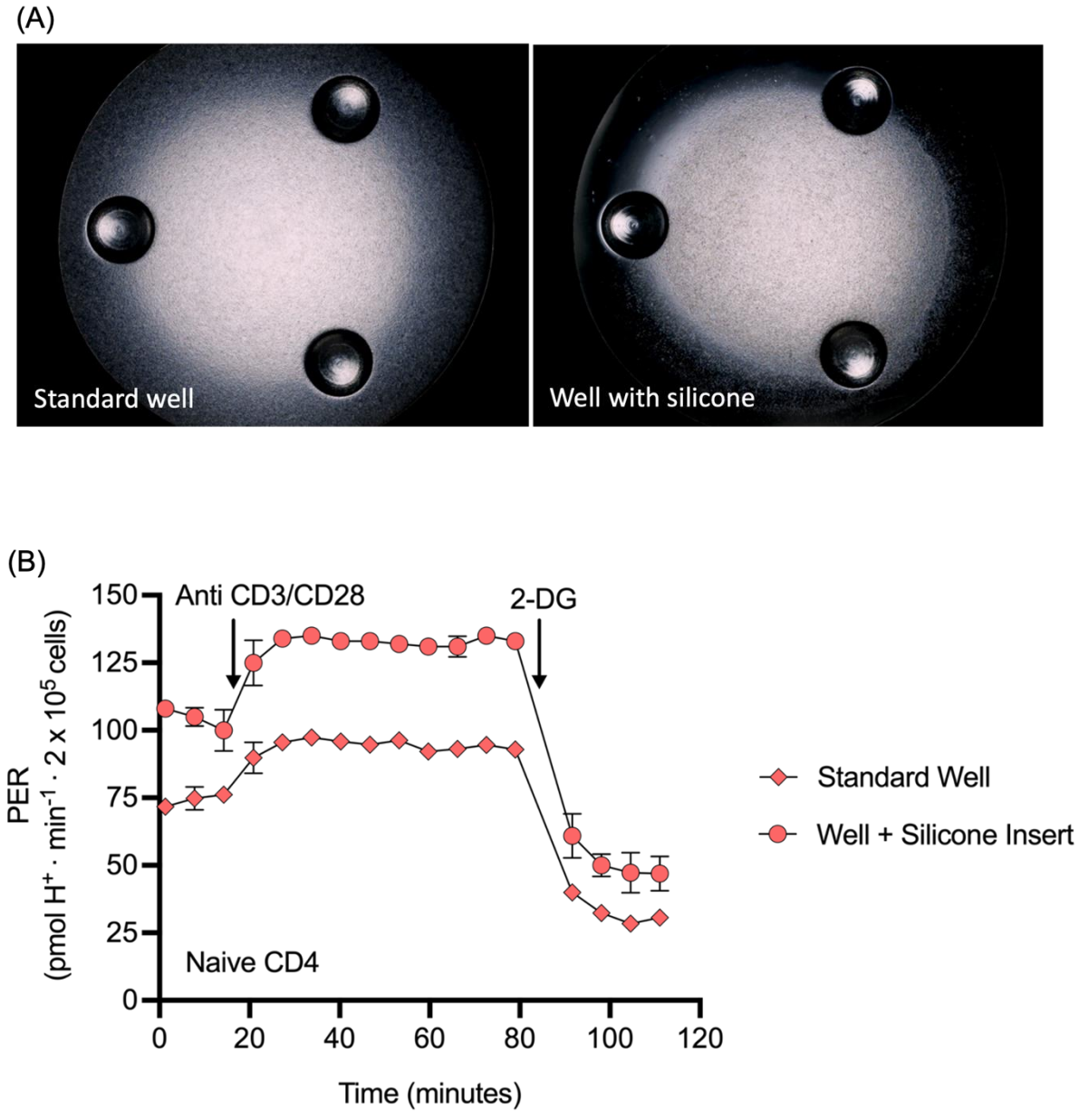

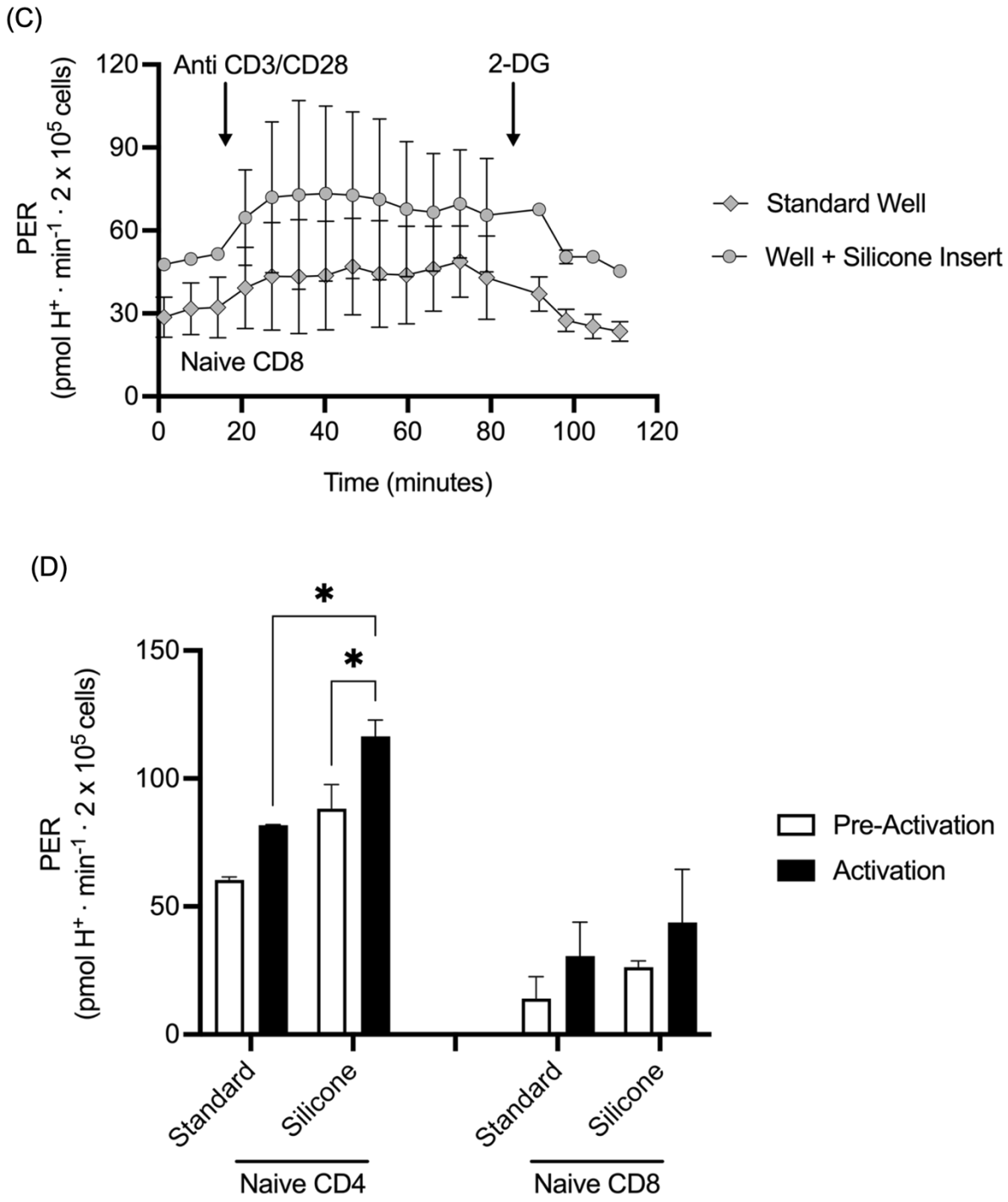

Figure 3.11 (A) Representative images of Seahorse XFe96 EFA wells with (left) or without (right) silicone insert added for seeding naïve T cells. Kinetic traces of PER for 200 x 10^3 (B) naïve $CD4^+$ and (C) $CD8^+$ T cells/well in response to CD3/CD28 bead

activation for silicon insert vs. standard wells. (D) Comparison of peak PER between pre-activation (basal, white bar) and activation (black bar) for naïve CD4+ and CD8+ T cells seeded in silicon insert vs. standard wells. Data were from 4 replicate wells and presented as mean ± SD. *P < 0.05.

3.4.2.3 Blood Anticoagulant Comparison

Anticoagulants are used to inhibit the process of blood coagulation or the clotting of blood proteins in order evaluate aspects of plasma or immune cell samples. EDTA, heparin, and citrates are the most frequently used anticoagulants, with EDTA and sodium heparin used most commonly for functional immune assays (41). To our knowledge, there is no data directly comparing the impact of these anticoagulants on PBMC bioenergetics (42,43). This experiment was conducted to determine the impact of EDTA vs. sodium heparin anticoagulants in blood collection tubes on real-time metabolic responses to T cell activation.

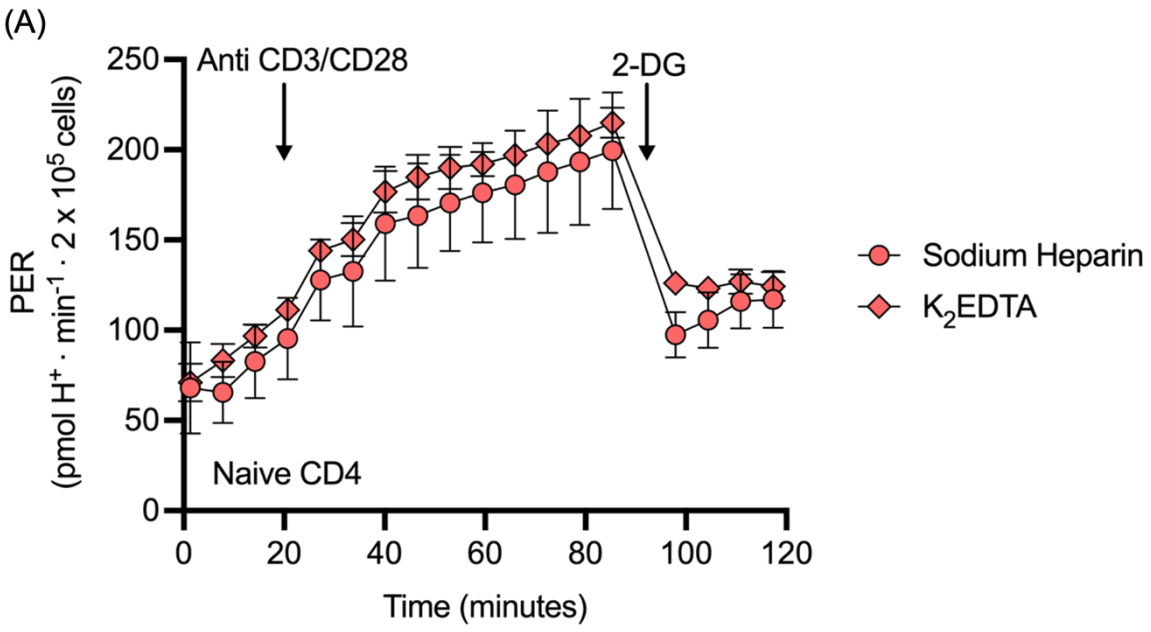

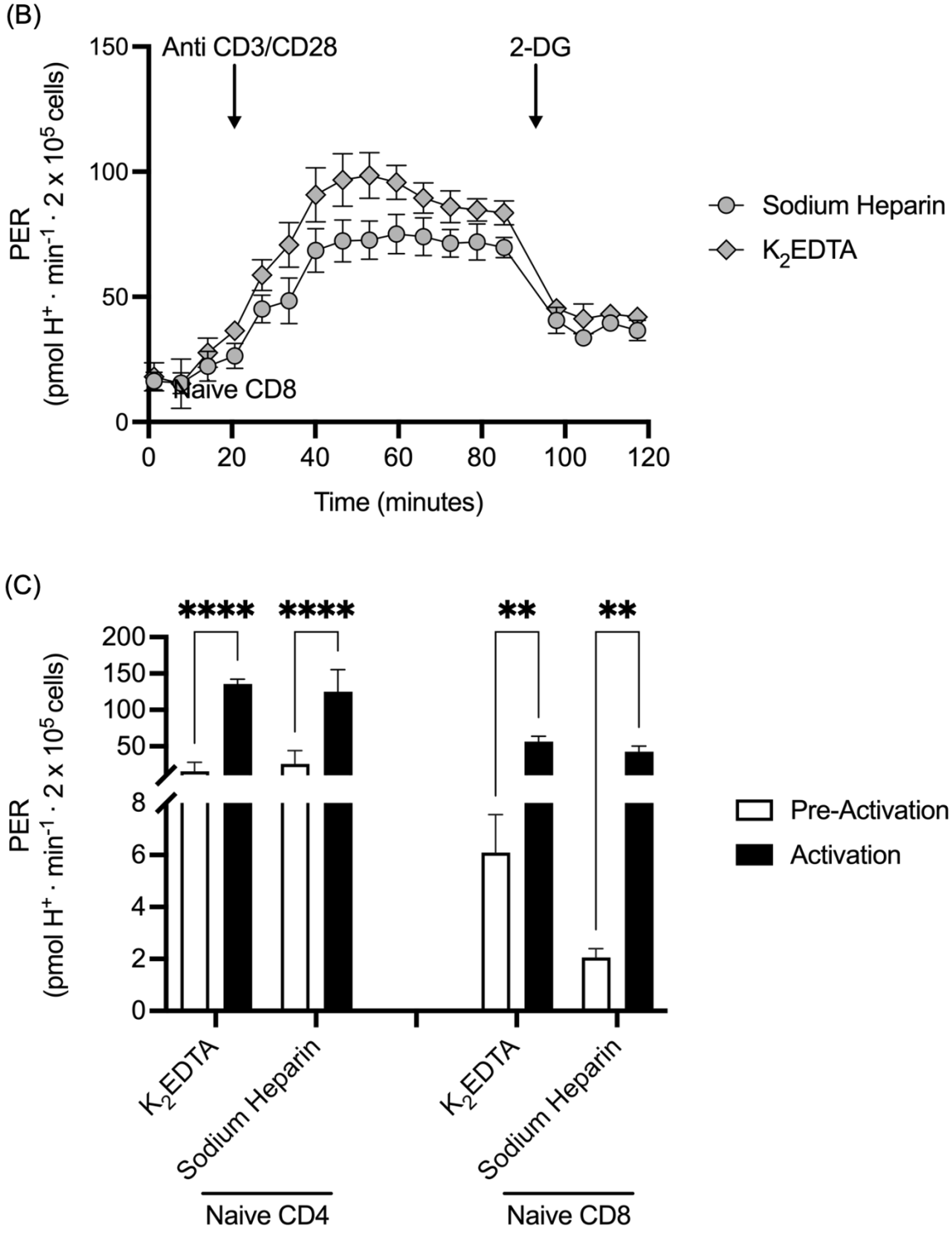

Figure 3.12 Kinetic traces of PER for 200 x 10^3 (A) naïve CD4+ and (B) CD8+ T cells/well isolated from blood collection tubes containing EDTA and sodium heparin in response to CD3/CD28 bead activation. (C) Comparison of peak PER between pre-

activation (basal, white bar) and activation (black bar) for naïve $CD4^+$ (left) and $CD8^+$ (right) T cells collected in EDTA and sodium heparin. Data were from 4 replicate wells and presented as mean ± SD. **P < 0.01, ****P < 0.0001.

There were significant increases in PER following CD3/CD28 bead activation for all cell types, collected with blood collection tubes using both EDTA and sodium heparin anticoagulants, with no differences between conditions. Naïve T cells (specifically naïve CD8 T cells) mixed with sodium heparin exhibited marginally higher and stable PER values compared to EDTA after activation **(Figure 3.12)**. EDTA chelates enzyme cofactors such as calcium, copper, zinc, or magnesium and may therefore alter cofactor-dependent activity of metabolic enzymes (42). Sodium heparin is the preferred anticoagulant for numerous clinical chemistry studies due to its modest chelating characteristics and limited impact on the osmotic balance of cells (44). A metabolomic study conducted by Jennie *et all.* (2021) demonstrated that sodium heparin better maintained the availability of metabolites for cells compared to multiple anticoagulants, including EDTA (43). Hence, vacutainers containing sodium heparin were used for blood collection in chapter 4 of this thesis.

3.4.2.4 Naïve T cell Isolation Time Delay Comparison

Initially, the experimental design for chapter 4 included the withdrawal 3 blood samples over 4 hours – at rest (0 minutes), immediately after prolonged cycling (120 minutes) and in recovery (240 minutes). In addition, this 4-hour trial would be repeated with identical blood sampling, but under resting conditions. The initial approach was to cryopreserve PBMCs and isolated naïve $CD4^+$ and $CD8^+$ T cells before

immunometabolic profiling proceeded. However, we found that cell recovery was too low for seeding enough replicates to obtain accurate data (*data not shown*).

To profile immune cells on the day of peripheral blood collection also presented challenges. The logistics of coordinating a 4-hour human exercise trial (with feeding) in conjunction with cell isolation and EFA analysis was extremely challenging for 3 blood samples. Moreover, to even achieve this, the stability of bioenergetic measures within PBMCs and naïve T cells over a 4-hour period warranted investigation. Notably, if naïve T cell isolation for all blood samples were to start at the end of the cycling trial (after collection of the Recovery sample) a time delay of 4 hours would have occurred prior to isolation of the resting sample. Importantly, staggered isolation and analysis of these blood samples was not permissible. Hence, the impact of blood sitting time (0 vs. 4 hours) on changes in PER after CD3/CD28 bead activation were examined in $CD4^+$ and $CD8^+$ naïve T cells.

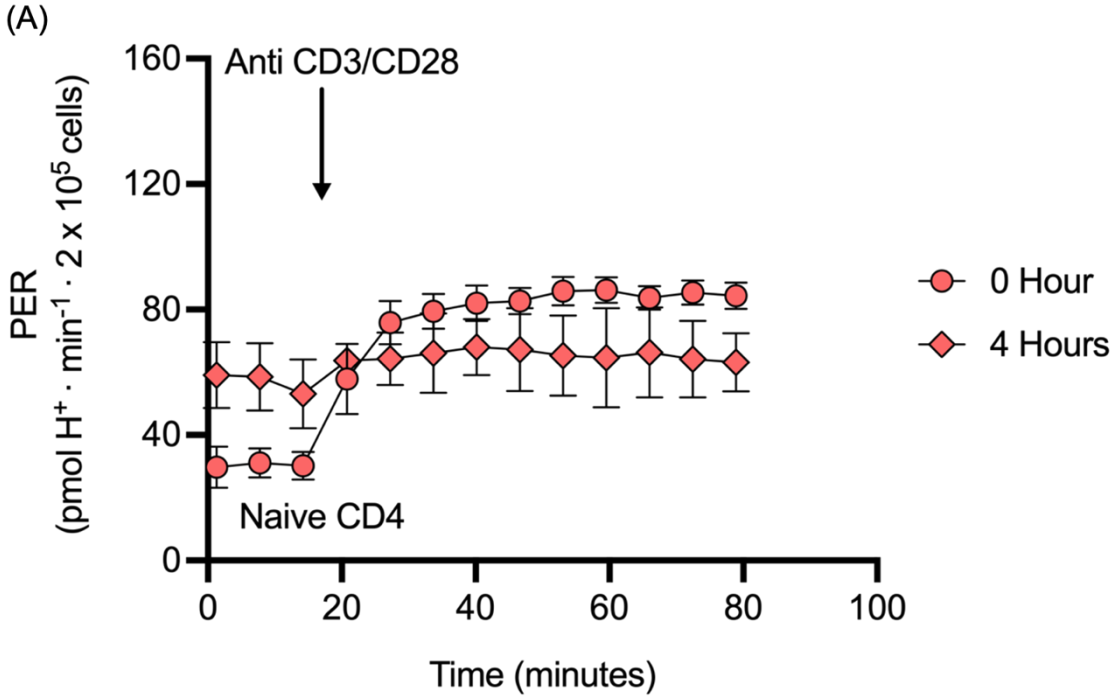
(A)
Anti CD3/CD28
PER
(pmol H+ · min-1 · 2 x 10^5 cells)
160
120
80
40
0
Naive CD4
0
20
40
60
80
100
Time (minutes)
0 Hour
4 Hours

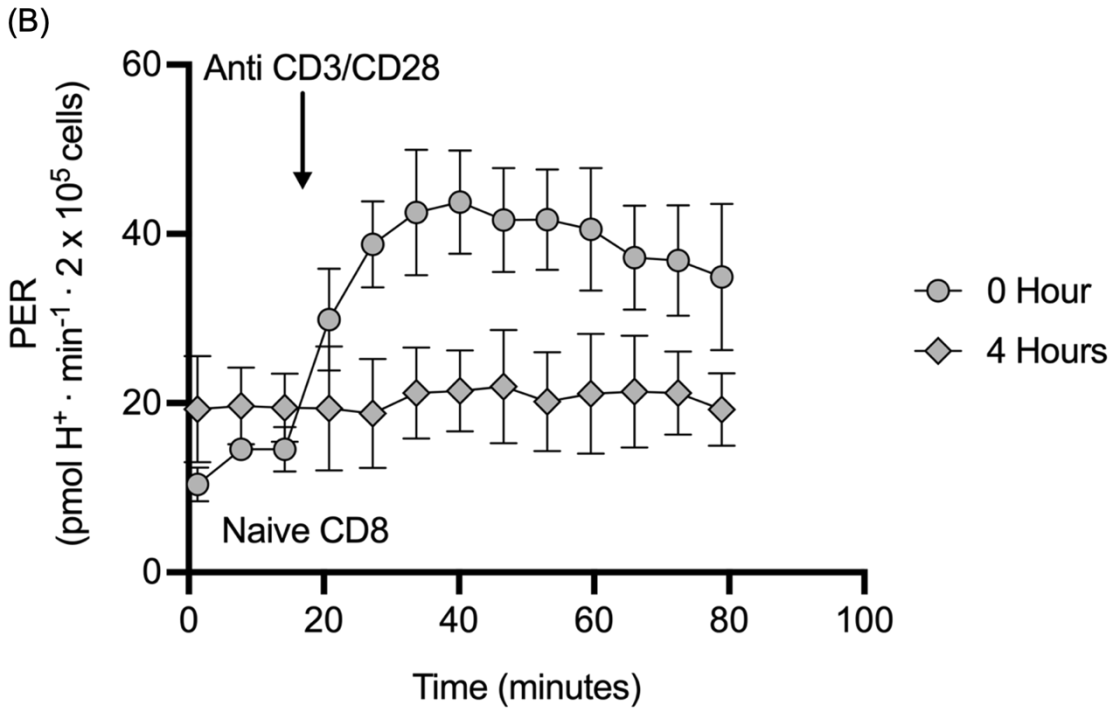
(B)
Anti CD3/CD28
PER
(pmol H+ · min-1 · 2 x 10^5 cells)
60
40
20
0
Naive CD8
0
20
40
60
80
100
Time (minutes)
0 Hour
4 Hours

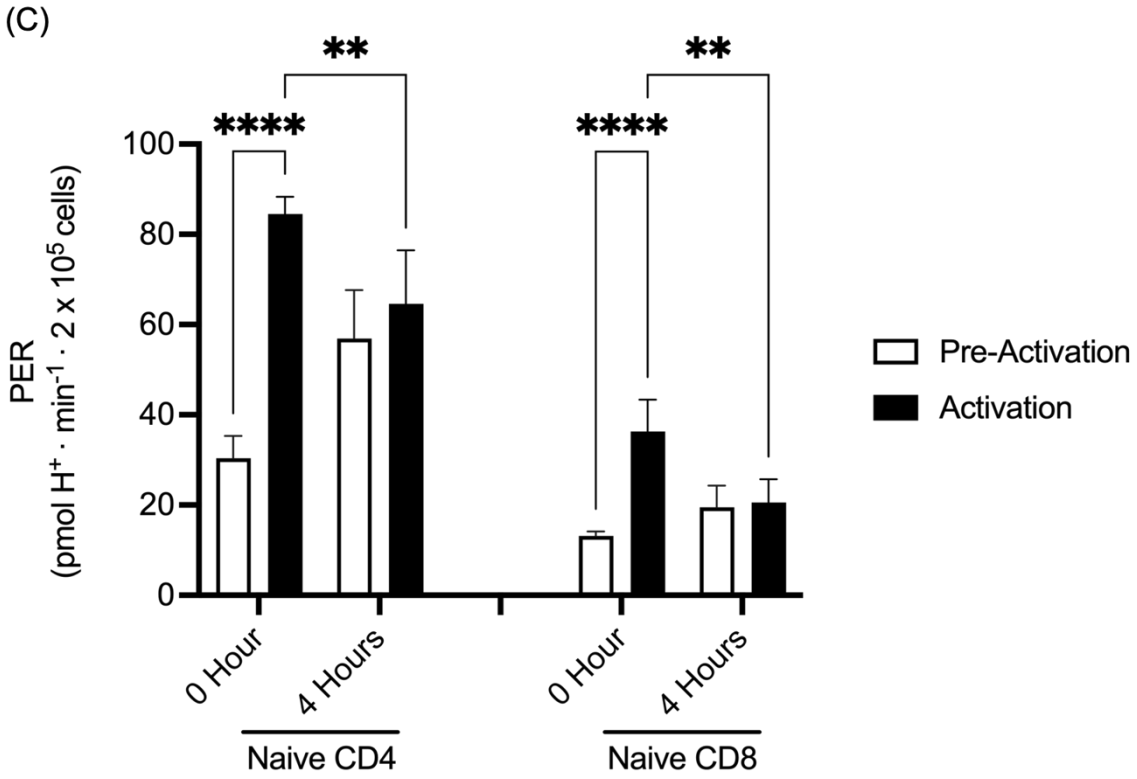

Figure 3.13 Kinetic traces of PER for 200 x 10^3 (A) naïve CD4 and (B) CD8 T cells cells/well isolated from heparin-blood immediately vs. after 4 hours in response to activation. (C) Comparison of peak PER between pre-activation (basal, white bar) vs. activation (black bar). Data were from 4 replicate wells and presented as mean ± SD. **P < 0.01, ****P < 0.0001.

The results in **Figure 3.13** indicate that peripheral blood CD4+ and CD8+ naïve T cells isolated after a 4-hour delay exhibited reduced changes in PER after CD3/CD28 bead activation compared to cells isolated immediately. Therefore, it was decided to isolate naïve T cells immediately after each timepoint and this resulted in modifications to our original exercise protocol (outlined in Chapter 4).

Discussion

The study of immunometabolism has played a key role in advancing understanding of how immune cells modulate their bioenergetics to carry out important T cell functions. Glycolysis and mitochondrial respiration are the main processes that generate ATP in T cells and both can be quantified simultaneously using EFA to establish a metabolic phenotype and real time responses to activation. To establish an experimental model to investigate the impact of exercise on T cell metabolism (Chapter 4), this chapter aimed to optimise EFA assays, firstly using a Jurkat cell line, and subsequently primary PBMCs vs. isolated T cells.

This method development chapter initially indicated that Jurkats and primary naïve T cells (200 x 10^3 cells), required appropriate amounts of nutrients (glucose and glutamine) to facilitate CD3/CD28 bead-induced activation on Seahorse XFe96 EFA. To optimise blood collection procedures, data in this chapter indicated that the immediate vs. delayed (4 hours) isolation of naïve T cells from peripheral blood samples in sodium heparin vs. EDTA blood collection tubes at room temperature resulted in different response to activation whereby peak PER values were higher in naïve T cells isolated immediately into sodium heparin blood collection tubes. For EFA, the use of silicone inserts for cell seeding and standard assay media resulted in accurate and enhanced changes in PER after activation. Collectively, the results of this chapter provide a set of optimised protocols to implement in Chapter 4.

List of References

1. Jones GE. Cellular signaling in macrophage migration and chemotaxis [Internet]. Available from: http://www.jleukbio.org

2. Pixley FJ, Stanley ER. CSF-1 regulation of the wandering macrophage: Complexity in action. Vol. 14, Trends in Cell Biology. 2004. p. 628–38.

3. Kotsias F, Cebrian I, Alloatti A. Antigen processing and presentation. In: International Review of Cell and Molecular Biology. Elsevier Inc.; 2019. p. 69–121.

4. Pishesha N, Harmand TJ, Ploegh HL. A guide to antigen processing and presentation. Vol. 22, Nature Reviews Immunology. Nature Research; 2022. p. 751–64.

5. Guy CS, Vignali KM, Temirov J, Bettini ML, Overacre AE, Smeltzer M, et al. Distinct TCR signaling pathways drive proliferation and cytokine production in T cells. Nat Immunol. 2013;14(3):262–70.

6. Li X, Jiang S, Tapping RI. Toll-like receptor signaling in cell proliferation and survival. Vol. 49, Cytokine. 2010. p. 1–9.

7. Russell JH, Ley TJ. Lymphocyte-mediated cytotoxicity. Vol. 20, Annual Review of Immunology. 2002. p. 323–70.

8. Kuhnke A, Burmester GR, Krauss S, Buttgereit F. Bioenergetics of immune cells to assess rheumatic disease activity and efficacy of glucocorticoid treatment. Ann Rheum Dis. 2003 Feb 1;62(2):133–9.

9. La Rocca C, Carbone F, De Rosa V, Colamatteo A, Galgani M, Perna F, et al. Immunometabolic profiling of T cells from patients with relapsing-remitting multiple sclerosis reveals an impairment in glycolysis and mitochondrial respiration. Metabolism. 2017 Dec 1;77:39–46.

10. Abboud G, Choi SC, Kanda N, Zeumer-Spataro L, Roopenian DC, Morel L. Inhibition of glycolysis reduces disease severity in an autoimmune model of rheumatoid arthritis. Front Immunol. 2018 Sep 3;9(SEP).

11. Scharping NE, Menk A V., Moreci RS, Whetstone RD, Dadey RE, Watkins SC, et al. The Tumor Microenvironment Represses T Cell Mitochondrial Biogenesis to Drive Intratumoral T Cell Metabolic Insufficiency and Dysfunction. Immunity. 2016;45(2):374–88.

12. Curtis KD, Smith PR, Despres HW, Snyder JP, Hogan TC, Rodriguez PD, et al. Glycogen Metabolism Supports Early Glycolytic Reprogramming and Activation in Dendritic Cells in Response to Both TLR and Syk-Dependent CLR Agonists. Cells. 2020 Mar 14;9(3).

13. Zeisbrich M, Yanes RE, Zhang H, Watanabe R, Li Y, Brosig L, et al. Hypermetabolic macrophages in rheumatoid arthritis and coronary artery disease due to glycogen synthase kinase 3b inactivation. Ann Rheum Dis. 2018 Jul 1;77(7):1053–62.

14. Forlin R, James A, Brodin P. Making human immune systems more interpretable through systems immunology. Vol. 44, Trends in Immunology. Elsevier Ltd; 2023. p. 577–84.

15. Green KJ, Rowbottom DG, Mackinnon LT. Exercise and T-lymphocyte function: A comparison of proliferation in PBMC and NK cell-depleted PBMC culture. J Appl Physiol. 2002;92(6):2390–5.

16. Campbell JP, Turner JE. Debunking the Myth of Exercise-Induced Immune Suppression: Redefining the Impact of Exercise on Immunological Health Across the Lifespan. Front Immunol [Internet]. 2018 Apr 16;9(APR):1–21. Available from: http://journal.frontiersin.org/article/10.3389/fimmu.2018.00648/full

17. Campbell JP, Turner JE. There is limited existing evidence to support the common assumption that strenuous endurance exercise bouts impair immune competency. Vol. 15, Expert Review of Clinical Immunology. Taylor and Francis Ltd; 2019. p. 105–9.

18. Semple JW, Allen D, Chang W, Castaldi P, Freedman J. Rapid separation of CD4+ and CD19+ lymphocyte populations from human peripheral blood by a magnetic activated cell sorter (MACS). Cytometry. 1993;14(8):955–60.

19. McDermott AB, Spiegel HML, Irsch Johannes, Ogg GS, Nixon DF. A simple and rapid magnetic bead separation technique for the isolation of tetramer-positive virus-specific CD8 T cells. AIDS. 2001;15(6):810–2.

20. Chapman NM, Shrestha S, Chi H. Metabolism in Immune Cell Differentiation and Function. In: Advances in Experimental Medicine and Biology [Internet]. 2017. p. 1–85. Available from: http://link.springer.com/10.1007/978-94-024-1170-6_1

21. Mercier-Letondal P, Marton C, Godet Y, Galaine J. Validation of a method evaluating T cell metabolic potential in compliance with ICH Q2 (R1). J Transl Med. 2021 Dec 1;19(1).

22. Jones N, Cronin JG, Dolton G, Panetti S, Schauenburg AJ, Galloway SAE, et al. Metabolic adaptation of human CD4+ and CD8+ T-cells to T-cell receptor-mediated stimulation. Front Immunol. 2017;8(NOV).

23. Nicoli F, Papagno L, Frere JJ, Cabral-Piccin MP, Clave E, Gostick E, et al. Naïve CD8+ t-cells engage a versatile metabolic program upon activation in humans and differ energetically from memory CD8+ T-cells. Front Immunol. 2018;9(December):1–12.

24. Sottnik JL, Lori JC, Rose BJ, Thamm DH. Glycolysis inhibition by 2-deoxy-d-glucose reverts the metastatic phenotype in vitro and in vivo. Clin Exp Metastasis. 2011 Dec;28(8):865–75.

25. Calder PC, Dimitriadis G, Newsholme P. Glucose metabolism in lymphoid and inflammatory cells and tissues.

26. Cruzat V, Rogero MM, Keane KN, Curi R, Newsholme P. Glutamine: Metabolism and immune function, supplementation and clinical translation. Vol. 10, Nutrients. MDPI AG; 2018.

27. Mohan R. Kaadige, Marc G. Elgort, Donald E. Ayer. Coordination of glucose and glutamine utilization by an expanded Myc network [Internet]. 2010. Available from: www.landesbioscience.com

28. Wang L, Li JJ, Guo LY, Li P, Zhao Z, Zhou H, et al. Molecular link between glucose and glutamine consumption in cancer cells mediated by ctbp and sirt4. Oncogenesis. 2018;7(3).

29. Koobotse MO, Schmidt D, Holly JMP, Perks CM. Glucose concentration in cell culture medium influences the brca1-mediated regulation of the lipogenic action of igf-i in breast cancer cells. Int J Mol Sci. 2020 Nov 2;21(22):1–18.

30. Khajah MA, Khushaish S, Luqmani YA. Glucose deprivation reduces proliferation and motility, and enhances the anti-proliferative effects of paclitaxel and doxorubicin in breast cell lines in vitro. PLoS One. 2022 Aug 1;17(8 August).

31. Carr EL, Kelman A, Wu GS, Gopaul R, Senkevitch E, Aghvanyan A, et al. Glutamine Uptake and Metabolism Are Coordinately Regulated by ERK/MAPK during T Lymphocyte Activation. The Journal of Immunology. 2010 Jul 15;185(2):1037–44.

32. Desousa BR, Kim KK, Jones AE, Ball AB, Hsieh WY, Swain P, et al. Calculation of ATP production rates using the Seahorse XF Analyzer. EMBO Rep. 2023 Oct 9;24(10).

33. Dimeloe S, Burgener AV, Grählert J, Hess C. T-cell metabolism governing activation, proliferation and differentiation; a modular view. Immunology. 2017 Jan;150(1):35–44.

34. Arneth BM. Activation of CD4 and CD8 T cell receptors and regulatory T cells in response to human proteins. PeerJ [Internet]. 2018 Mar 9;6(3):e4462. Available from: https://peerj.com/articles/4462

35. Cairns RA, Harris IS, Mak TW. Regulation of cancer cell metabolism. Vol. 11, Nature Reviews Cancer. 2011. p. 85–95.

36. Graham NA, Tahmasian M, Kohli B, Komisopoulou E, Zhu M, Vivanco I, et al. Glucose deprivation activates a metabolic and signaling amplification loop leading to cell death. Mol Syst Biol. 2012;8.

37. Isakov N, Bleackley RC, Shaw J, Altman A. The tumor promoter teleocidin induces IL 2 receptor expression and IL 2-independent proliferation of human peripheral blood T cells. The Journal of Immunology [Internet]. 1985 Oct 1;135(4):2343–50. Available from: https://doi.org/10.4049/jimmunol.135.4.2343

38. McKinnon KM. Flow cytometry: An overview. Curr Protoc Immunol. 2018 Feb 1;2018:5.1.1-5.1.11.

39. Dingley S, Chapman KA, Falk MJ. Fluorescence-activated cell sorting analysis of mitochondrial content, membrane potential, and matrix oxidant burden in human lymphoblastoid cell lines. Methods in Molecular Biology. 2012;837:231–9.

40. Hulspas R, O'Gorman MRG, Wood BL, Gratama JW, Robert Sutherland D. Considerations for the control of background fluorescence in clinical flow cytometry. Vol. 76, Cytometry Part B - Clinical Cytometry. 2009. p. 355–64.

41. Kotikalapudi R, Patel RK. Comparative Study of The Influence of EDTA and Sodium Heparin on Long Term Storage of Cattle DNA Citation: Kotikalapudi R, Patel RK. Comparative study of the influence of EDTA and sodium heparin on long term storage of cattle DNA. Vol. 17, CELL JOURNAL(Yakhteh). 2015.

42. Baskin L, Dias V, Chin A, Abdullah A, Naugler C. Effect of Patient Preparation, Specimen Collection, Anticoagulants, and Preservatives on Laboratory Test Results. In: Accurate Results in the Clinical Laboratory: A Guide to Error Detection and Correction. Elsevier Inc.; 2013. p. 19–34.

43. Sotelo-Orozco J, Chen SY, Hertz-Picciotto I, Slupsky CM. A Comparison of Serum and Plasma Blood Collection Tubes for the Integration of Epidemiological and Metabolomics Data. Front Mol Biosci. 2021 Jul 8;8.

44. O'Keane MP, Cunningham SK. Evaluation of three different specimen types (serum, plasma lithium heparin and serum gel separator) for analysis of certain analytes: Clinical significance of differences in results and efficiency in use. Clin Chem Lab Med. 2006 May 1;44(5):662–8.

Chapter 4: Immunometabolic profiling of isolated and mixed T cell populations in response to prolonged moderate intensity cycling in humans

Work presented within this chapter has been prepared for publication:

Pradana, **F.,** Barlow, J.P., Shayler, J., Dimeloe, S.K., Gudgeon, N., Podlogar, T., Wallis, G.A., Wadley, A.J., (2024). Immunometabolic profiling of isolated and mixed T cell populations in response to prolonged moderate intensity cycling in humans. *Exercise Immunology Review (In preparation).*

4.1 Abstract

Single bouts of exercise evoke the mobilisation of T cells that may modulate their substrate metabolism to govern remodelling of the immune system in recovery. There is currently a dearth of literature examining immunometabolic responses to prolonged moderate intensity exercise, particularly with single cell resolution. The current study was designed to examine the metabolic phenotypes and real-time responses to activation of enriched naïve $CD4^+$ and $CD8^+$ T cells, and PBMCs in response to prolonged moderate intensity cycling. Ten healthy males and females (mean ± SD: age 21 ± 1 years; body mass index: 21.5 ± 2.0 kg · m^{-2}) undertook a 2-hour bout of continuous-cycling at a power output eliciting 95% lactate threshold-1. Blood samples were collected at rest, immediately after and 2 hours after cycling completion. $CD4^+$ and $CD8^+$ T cells were enriched from PBMCs using magnetic-activated cell sorting (MACS) and bioenergetic profiles examined using an injection sequence of cell respiration modulators and a CD3/CD28 activation assay. There was no change in the metabolic phenotypes of naïve $CD4^+$ and $CD8^+$ T cells, or PBMCs immediately after

and 2 hours into recovery, relative to rest. Moreover, absolute and relative measures of mitochondrial respiration, glycolytic flux and ATP synthesis rate were similar across all timepoints. The contribution of mitochondrial respiration to ATP production was greater than glycolysis in naïve T cells across all timepoints; however, the contribution was equal in PBMCs 2 hours into recovery. In addition, there were no differences in cellular bioenergetic responses in response to *ex vivo* activation in all cell types isolated before, immediately after or 2 hours into recovery. These data indicate that the metabolic phenotype and *ex vivo* responses to activation of the total PBMC fraction and isolated naïve T cells were unaltered within 2 hours of prolonged moderate intensity cycling.

4.2 Introduction

Single bouts of exercise promote the preferential mobilisation of effector lymphocytes primed for migration to peripheral tissues. The trafficking of these cells is believed to facilitate remodelling of these tissues and the immune system; however, the underpinning mechanisms are unclear. In 1958, it was first reported using respirometry that moderate intensity exercise increased peripheral blood mononuclear cell (PBMC) oxygen consumption (1). More recently, real-time extracellular flux analysis has determined that maximal and reserve oxygen consumption rate (OCR) increased in PBMCs (2) and isolated natural killer (NK) cells (3) after exhaustive exercise. There is consequently growing interest in whether modulation of lymphocyte substrate metabolism during exercise mediates this cell trafficking. Although these studies were insightful, PBMC and NK cell fractions are composed of diverse sub-populations of cells with unique functions and distinct metabolic profiles. Moreover, bouts of exercise

evoke an immediate increase in peripheral blood T and NK cell concentrations, followed by a decrease in recovery (≈1-3 hours) as effector lymphocytes leave the bloodstream. This presents a challenge when sampling cells for evaluation of their metabolism and many conclusions have been drawn from mixed cell populations (4). For this reason, the discipline of exercise immunometabolism is still in its infancy and notably, relatively little attention has been paid to T cells, namely Helper ($CD4^+$) and Cytotoxic ($CD8^+$) T cells.

$CD4^+$ T cells serve broadly to orchestrate immune response via cytokine signalling (e.g., interleukin (IL)-2), whereas $CD8^+$ T cells eliminate cancerous or virus infected cells through the release of cytotoxic molecules. The metabolic pathways used to generate ATP in T cell subsets are dependent on the degree of antigen experience (5). Naïve T cells are antigen inexperienced cells generated in the thymus that mostly rely on mitochondrial respiration to fulfil their primary function of identifying novel pathogens (6). Upon T cell receptor (TCR) engagement, CD28 ligation is a costimulatory signal that evokes a pronounced glycolytic shift that facilitates T cell effector functions and subsequent differentiation into memory T cells (7–9). Antigen encounters therefore result in central memory (CM), effector memory (EM) and terminally differentiated effector memory (TEMRA) T cells exhibiting increasingly greater reliance on glycolysis than naive T cells for basal respiration (TEMRA > EM > CM > naïve). Enrichment of peripheral blood with antigen experienced T cells with higher basal respiration may therefore, in part, underpin the heightened metabolic activity of the PBMC fraction during exercise, rather than individual T cell changes *per se* (4). However, a recent study employing single cell RNA sequencing reported that

genes associated with metabolic regulation were enriched in $CD4^+$ and $CD8^+$ T cells after maximal exercise, most notably in EM, rather than CM or naïve subsets (10). These changes were aligned with upregulation of genes associated with cell migration, antigen binding, and cytokine production. With other data indicating that T cells mobilised during exercise are primed to uptake energy substrates (e.g., glucose and fatty acids) (11), it is intuitive to suggest that their metabolic activity is modulated to fulfil these effector functions.

Much of the literature examining immunometabolic responses to exercise have evaluated changes in mixed cell populations immediately after maximal exercise, whereby fluctuations in T cell concentrations are substantial. Exercise performed at low-moderate intensity results in more stable T cell concentrations, but a recent scoping review reported that there is a dearth of literature examining resultant immunometabolic responses, particularly in isolated immune cell populations (12). Furthermore, studies have largely used physiological (e.g., fixed percentage of $\dot{V}O_{2max}$) rather than metabolic thresholds (e.g., lactate threshold, LT) to prescribe exercise intensity. Given that metabolic thresholds occur at variable proportions of $\dot{V}O_{2max}$ (13), this approach may not account for inter-individual variability in substrates that feed immunometabolic response to exercise (13).

The current study was designed to evaluate the metabolic sensitivity of mixed vs. isolated T cell fractions in response to prolonged moderate intensity exercise. Given the abundance and differing basal metabolic profiles of naïve vs. antigen experienced T cells (CM, EM, and TEMRA), a direct comparison of their metabolic responses was

undertaken alongside changes in circulating T cell substrates (glucose, glutamine, and triglycerides). Accordingly, the aim of this study was to determine the metabolic phenotypes of naïve $CD4^+$ and $CD8^+$ T cells compared to the PBMC fraction at rest (Pre-Ex), immediately after and in the recovery from a 2-hour bout of cycling at 95% of LT-1. In addition, real-time metabolic responses to CD3/CD28 activation in these cell populations and subsequent IL-2 production were determined.

4.3 Materials and Methods

4.3.1 Participants

Ten participants (5 males and 5 females) gave written informed consent to take part in this study (mean ± SD: age 21 ± 1 years; body mass index: 21.5 ± 2.0 kg · m^{-2}). The study was given favourable ethical opinion by the Science, Technology, Engineering and Mathematics ethical committee at the University of Birmingham (ERN_19-1574PA3). Participants underwent screening prior to enrolment to include individuals who were physically active as defined by the General Practice Physical Activity Questionnaire (GPPAQ) (14), and exceeded an aerobic fitness threshold (males: 50 ml · kg^{-1} · min^{-1} and females: 35 ml · kg^{-1} · min^{-1}) (15). For female participants, all experimental visits were performed in the same phase of the menstrual cycle to mitigate the potential impact of estrogen on immunometabolic parameters (16). Participants were excluded if they were smokers, currently taking medication/s, eating a ketogenic diet, had donated blood in the last 3 months, or had a history of cardiovascular, metabolic, neurological, or inflammatory disease.

4.3.2 Study Design

The study was a randomised crossover design, comprising four morning visits at the School of Sport, Exercise and Rehabilitation Sciences at the University of Birmingham, conforming to the Declaration of Helsinki (2). After an initial screening visit to determine lactate threshold (LT) and maximal oxygen consumption ($\dot{V}O_{2max}$), participants undertook three randomised visits, consisting of two identical cycling trials (CT-1 and CT-2) and one rest trial (RT), each separated by 7 days **(Figure 4.1)**. Our preliminary data indicated greater induction of glycolysis in response to activation of T cells isolated from an identical blood sample processed and analysed immediately vs. 4 hours at 21°C or 37°C after collection (refer to chapter 3). Given that T cell metabolism was to be examined over a 4-hour period in response to prolonged exercise, the study protocol was designed to equalise time spent preparing T cell metabolic assays and eliminate the effect of blood sitting time. Therefore, to evaluate the immunometabolic responses to prolonged cycling, the primary blood samples were collected on different trials at rest (RT), immediately after (CT-1), and 2 hours after (CT-2) cycling and processed immediately. CT-1 and CT-2 were differentiated only by the timing of these blood sample withdrawals after cycling cessation, and conducted under identical conditions, with the aim of eliciting comparable physiological and immunological responses. The latter was confirmed by drawing secondary blood samples at every timepoint throughout CT-1 and CT-2. Between all trials, lifestyle factors that might influence immunity were subjectively monitored, including illness symptoms, anxiety, and sleep quality.

All visits started at the same time of day for each participant (range: 6:30–8.00 AM) and were conducted under stable climatic conditions (temperature (ºC): 21.0 ± 0.6, humidity (%): 39.1 ± 10.0 and barometric pressure (hPa): 1002.1 ± 12.7). Participants were asked to refrain from vigorous exercise, and the consumption of caffeine and alcohol for 48 hours prior to attending each visit. Furthermore, to standardise nutrition, participants were asked to record their food intake for 24 hours before the first visit and to replicate this diet for all subsequent visits, as well undertaking an overnight fast from 10pm, consuming only water (ad libitum) during this period. Participants were provided with a breakfast of oats mixed with semi-skimmed milk (normalised for carbohydrate content: 1 g · kg^{-1} body mass) (18,19) to ensure the energy and macronutrient intake across trials and between participants was standardised.

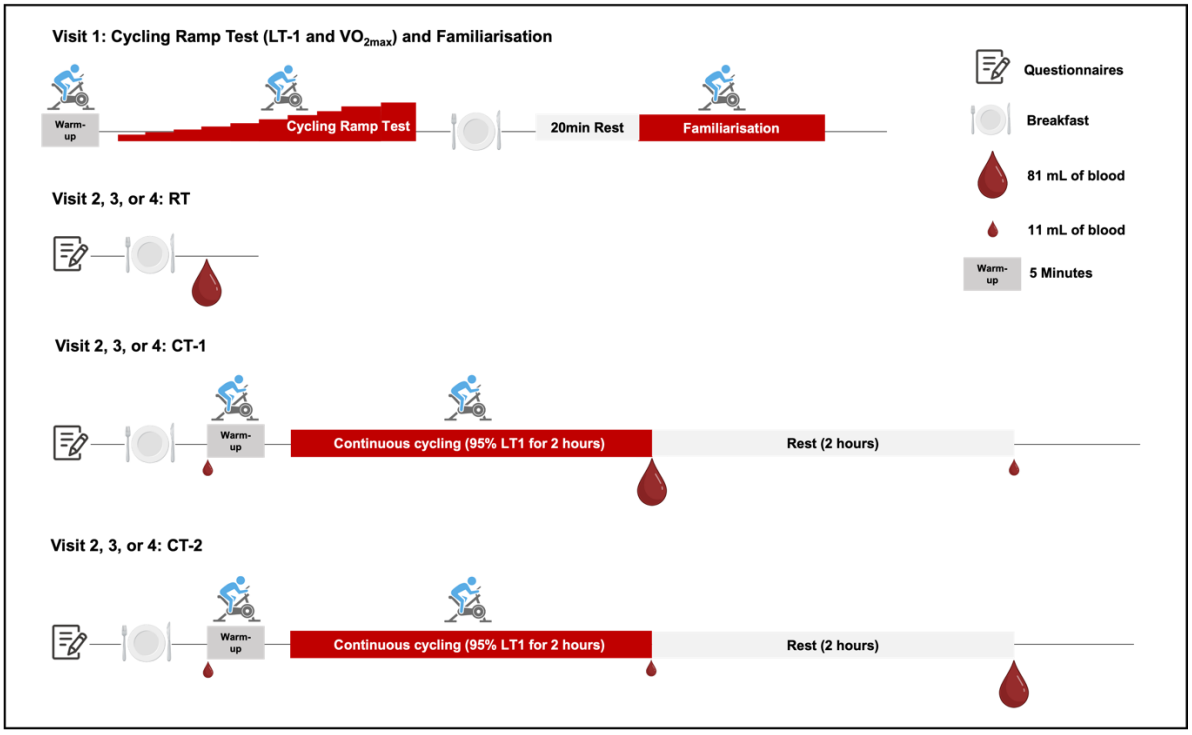

Figure 4.1 Study design illustrating a time axis of the completion of questionnaires, breakfast, 5 minute warmup, rest or steady state cycling (2 hours), and recovery cycling periods (2 hours) for the 4 laboratory visits and 3 randomised trials: RT (rest trial) and

2 identical steady-state cycling trials (CT-1 and CT-2). Blood sampling is indicated with small droplets (11 mL) for whole blood and plasma analyses and large droplets (81 mL) for whole blood, plasma and PBMC analyses. Created with BioRender.com.

4.3.3 Preliminary Testing (Visit 1)

Participants attended the laboratory for screening and determination of LT and $\dot{V}O_{2max}$. Body mass (*Ohaus CD31, New Jersey, USA*) and height (*Seca Alpha, Hamburg, Germany*) were recorded and then participants rested for a period of 5 minutes before measurement of resting heart rate and blood pressure (*Thuasne BP 3W1-A, Taipei, Taiwan*). An exercise tolerance test was then conducted on an electromagnetically braked cycle ergometer (*Excalibur, Lode, The Netherlands*). After a warm-up for 5 minutes at a rating of perceived exertion (RPE) of 8–10 using the Borg scale (20), participants commenced cycling at 70 watts and then 30 watt increments were added every 4 minutes until volitional exhaustion. A breath-by-breath system (*Vyntus, Vyaire Medical, IL, US*) and heart rate monitor (*H10, Polar Electro, Finland*) were used for continuous measurement of oxygen uptake and heart rate (HR, *H10, Polar Electro, Finland*) respectively, and fingertip blood lactate measurements were made at the end of every 4-minute stage (*Lactate Pro 2, Arkray, Kyoto, Japan*). Participants were asked to maintain a pedal cadence >60 and encouragement was given by the research team. A respiratory exchange ratio (VCO_2/VO_2) >1.1, plateau in participant oxygen consumption or a maximal heart rate >220 beats min^{-1} – age were all factors used collectively with an RPE of 20 to indicate $\dot{V}O_{2max}$ (21). The test was then terminated and $\dot{V}O_{2max}$ determined and expressed relative to body weight ($ml \cdot kg^{-1} \cdot min^{-1}$). Participants were provided with breakfast and during this time, an online LT software

(www.exphyslab.com), was used to determine the power output that elicited a 0.5 mmol · L^{-1} increase in lactate above baseline value, thus defining LT-1 (22,23). A 15-minute familiarisation was then conducted at a power output eliciting 95% of LT-1 and a final blood lactate measurement made to confirm the correct intensity for subsequent trials.

4.3.4 Experimental Trials (Visits 2-4)

In the morning of each trial (RT, CT-1, and CT-2), participants were asked to complete questionnaires evaluating illness symptoms (24), state and trait anxiety (25) and sleep efficiency (percentage of time asleep relative to the amount of time spent in bed) (26) during a 30-minute period of rest (Pre-Ex). During this time, blood pressure and body mass were also measured. A standardised breakfast was provided and then a catheter (*Becton, Dickson & Company, Oxford, UK*) inserted into the antecubital vein of the forearm to obtain a resting blood sample 15 minutes after feeding. Each exercise trial commenced with a 5-minute warm-up at a RPE of 8–10, followed by 2-hours of continuous-cycling at a power output eliciting 95% LT1 (CT-1 or CT-2). Every 15 minutes during CT-1 and CT-2, exercise intensity was confirmed by measuring HR and $\dot{V}O_2$ uptake for 3 minutes and RPE. Additionally, the affective response to exercise were measured using the Feeling Scale (27). Following completion of the CT-1 and CT-2, participants remained seated in the laboratory for a 2-hour recovery period.

4.3.5 Blood Sampling

A total of seven blood samples were taken across the 3 trials, including a single blood draw during RT (Pre-Ex) and 3 blood draws during CT-1 and CT-2 (Pre-Ex, Post-Ex,

and Recovery). The catheter was kept patent through regular flushes with saline (0.9% NaCl*, Becton, Dickson & Company, Oxford, UK*). The volumes of blood drawn at each timepoint varied depending on the trial. During RT (Pre-Ex), immediately after CT-1 (Post-Ex) and 2 hours post-exercise in CT-2 (Recovery), 70 mL of blood was collected into sodium heparin vacutainers (*Becton, Dickson & Company, Oxford, UK*) for isolation of peripheral blood mononuclear cells (PBMCs). Additionally, 6 mL of blood was collected into K_2EDTA vacutainers (*Becton, Dickson & Company, Oxford, UK*) and 4 mL into clotting vacutainers (*Becton, Dickson & Company, Oxford, UK*) for isolation of plasma and serum at these 3 timepoints, respectively. Across all seven timepoints, 1 mL of blood was collected into K_2EDTA vacutainers (*Greiner Bio-One, Frickenhausen, Germany*) to obtain a complete blood cell count using an automated haematology analyser (*Yumizen H500, Horiba, Kyoto, Japan*). These data were obtained to ensure comparable leukocyte counts at rest (RT vs. CT-1 vs. CT-2) and in response to prolonged cycling (CT-1 vs. CT-2).

4.3.6 Blood Processing

PBMCs were isolated by gradient density centrifugation by diluting whole blood in 1:1 ration with Dulbecco's phosphate-buffered saline (*D-PBS, Thermo Fisher Scientific, Massachusetts, USA*). Diluted blood was gently loaded into sterile Leucosep tubes (*Greiner Bio-One, Frickenhausen, Germany*) that were pre-filled with room temperature Histopaque-1077 separating medium (*Sigma Aldrich, Missouri, USA*) and centrifuged for 10 min, at 1000 x *g* (brake off) at 21^{o}C. After carefully removing platelet rich plasma, PBMCs were harvested and washed 3 times with D-PBS. An aliquot of cells was stained 1:1 with acridine orange/propidium iodide (AO/PI) to obtain a viable

cell count using a Cellometer 2000 dual fluorescence cell counter (*Nexcelom Bioscience, Massachusetts, USA*). Whole blood in clotting tubes was left for 15 minutes at room temperature and then both plasma and serum isolated by centrifugation for 10 minutes at 1,525 x *g* at 4^{o}C and stored at -80^{o}C.

4.3.7 Naïve T-cell Purification

Naïve $CD4^+$ and $CD8^+$ T cells were enriched from PBMCs using magnetic activated cell sorting (MACS) human naïve $CD4^+$ and $CD8^+$ T cell microbead isolation kits (*Miltenyi Biotec, Bergisch Gladbach, Germany*). Following manufacturer's recommendations of staining up to 10^7 cells, harvested PBMCs were centrifuged at 300 x *g* for 10 minutes and cell pellets resuspended in 40 µL of de-gassed, sterile filtered (0.2 µm) column buffer (D-PBS, 2 mM EDTA, and 0.5% BSA). A naive $CD8^+$ T cell biotin-antibody cocktail (10 µL) was added to the cell suspension and incubated for 10 minutes at 4^{o}C, followed by 30 µL of column buffer and 20 µL of anti-biotin microbeads for an additional 15 minutes at 4^{o}C. Cells were washed and then resuspended in 500 µL of column buffer and applied onto a pre-equilibrated LD column. The column was washed 2 times with 1 mL of column buffer to elute the unlabelled cell fraction (naïve T cells) via negative selection using a QuadroMACS system (*Miltenyi Biotec, Bergisch Gladbach, Germany*). Unlabelled cells were washed and then processed as above but stained with CD8 microbeads to isolate naïve $CD8^+$ T cells by positive selection using an OctoMACS system (*Miltenyi Biotec, Bergisch Gladbach, Germany*). The flowthrough fraction was then stained with CD4 MicroBeads to isolate naïve $CD4^+$ T cells by positive isolation (OctoMACS).

The purity of $CD4^+$ and $CD8^+$ T cell fractions was confirmed through immunophenotyping using a CytoFlex-S flow cytometer (*Beckman Coulter, California, USA*) **(Figure 4.2)**. Cell fractions (2×10^5) were stained with anti-human CD3-PerCP (clone HIT3a), anti-human CD8-FITC (clone SK1), anti-human CD45RA-APC (clone HI100), and anti-human CCR7-PE (clone G043H7) and incubated on ice, in the dark for 30 minutes. Cells were then washed three times in FACS buffer (D-PBS, 2 mM EDTA, 0.1% Sodium Azide, and 1 mM FBS) for 5 minutes at 500 x *g* at 4ºC before data acquisition. All antibodies used were purchased from BioLegend (*San Diego, CA*) and data were analysed using CytExpert v2.5 Software (*Beckman Coulter, California, USA*).

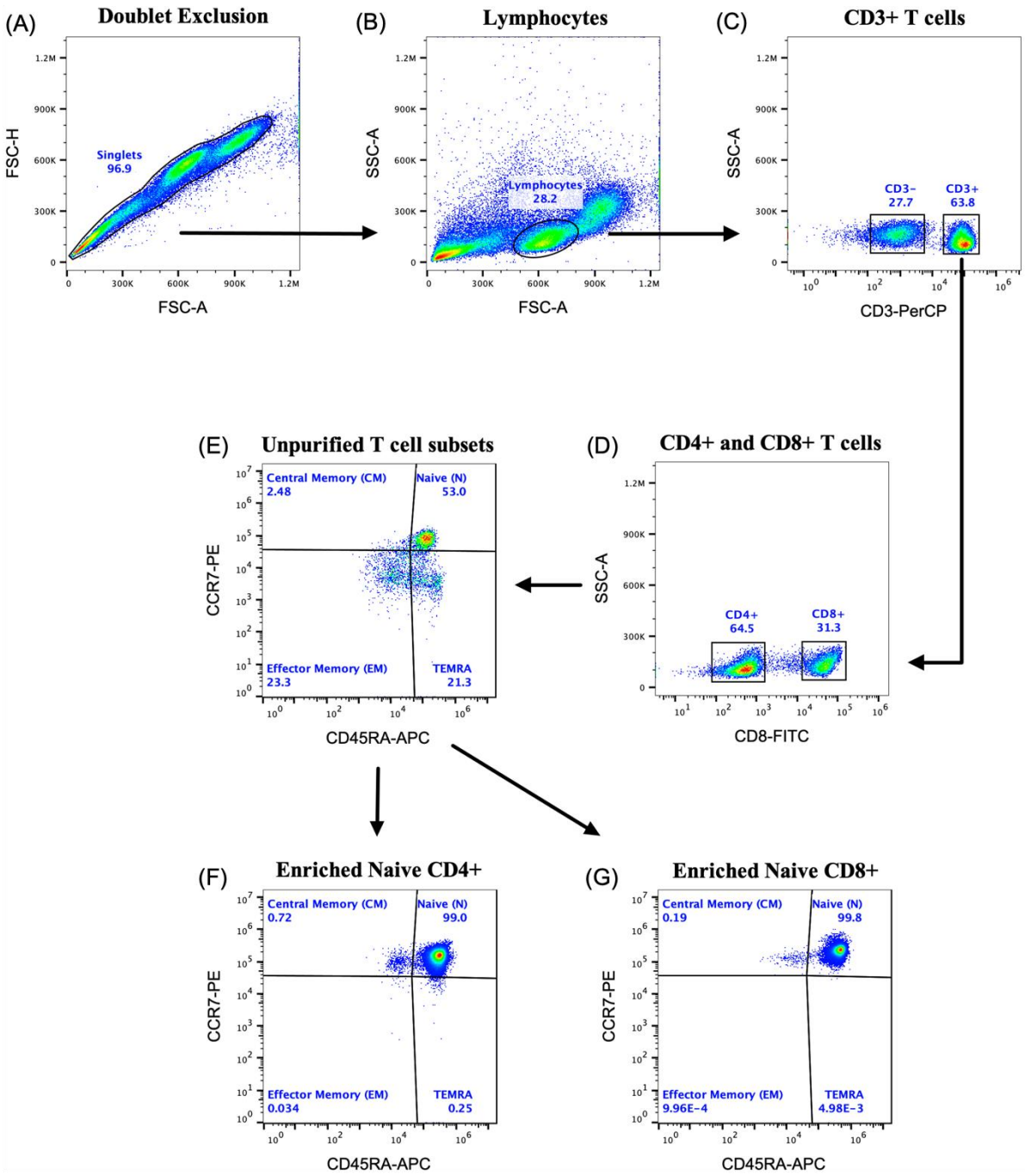

Figure 4.2 Representative gating strategy for naïve T cells within PBMCs (200 x 10^3 cells). (A) Doublets were discriminated using forward side scatter-area (FSC-A) vs. forward side scatter-height (FSC-H), (B) lymphocytes identified on FSC-A vs. side scatter-area (SSC-A) and then (C) CD3+ T lymphocytes by plotting CD3-PerCP vs SSC-A. (D) CD4+ and CD8+ T cell populations were gated using a CD8-FITC vs. SSC-

A plot and their (E) naïve, central memory, effector memory and TEMRA subsets identified using a bivariate plot of CD45RA-APC vs. CCR7-PE (not enriched). Examples of (F) naïve CD4+ and (G) naïve CD8+ T cell enrichment using MACS are displayed using a CD45RA-APC vs. CCR7-PE bivariate plot. Abbreviation: TEMRA, T Effector Memory Re-expressing CD45RA.

The frequency of naïve $CD4^+$ and $CD8^+$ T cells was determined by first sequentially identifying singlets, viable cells, and $CD3^+$ T cells, and then using a bivariate quadrant gate to enumerate $CD45RA^+$ and $CCR7^+$ cells. A minimum of 6×10^4 naïve CD4 or CD8 T cells events were acquired in the final gate. Gating strategy presentation was carried out using FlowJo™ v10.9 Software (*Becton, Dickson & Company, Ashland, USA*).

4.3.8 Real-Time Cell Metabolic Profiling

The optimisation of metabolic assay protocols using extracellular flux analysis (EFA) was established in Method Development **(Chapter 3)** using Seahorse XFe96 and then implemented in the **Chapter 4** for immunometabolic profiling with details of final method presented below. Experimental assay was pre-designed using Seahorse analytics software 1.0.0-570 and carried out on Seahorse XFe96 extracellular flux analyser (*Agilent Technologies, USA*). A Seahorse XFe96 sensor cartridge was hydrated in 200 µL/well of XF Calibrant in a non-CO_2 incubator overnight at 37°C. The day after, 20 µL/well of injected reagents were prepared including ImmunoCult human CD3/CD28 T-cell activator (*STEMCELL Technology, UK*) for experimental well or assay medium for control well in port A, 2 $\mu g \cdot mL^{-1}$ Oligomycin (*Sigma-Aldrich*, *Merck,*

UK) in port B, 3 µM BAM 15 (*TOCRIS, Minneapolis, USA*) in port C and a mixture of 2 µM Rotenone + 2 µM Antimycin A (*Sigma-Aldrich*, *Merck, UK*) + 25 µM Monensin (*Invitrogen, Thermo Fisher Scientific, UK*) in port D for each well involved.

PBMCs, enriched naïve $CD4^+$ and $CD8^+$ T cells (2 x 10^5 cells/well) were suspended in 50 µL of pre-warmed Seahorse XF RPMI assay medium (supplemented with 10 mM glucose, 1 mM pyruvate, and 2 mM glutamine, pH = 7.4, *Agilent Technologies, USA*) and seeded onto a Seahorse XFe96 cell culture microplate (*Agilent Technologies, USA*). For each sample, 4 technical replicates were used for both activated and non-activated (control) PBMCs, enriched naïve $CD4^+$ and $CD8^+$ T cells. Each well was pre-coated with sterile Cultrex Poly-D-lysine (*Bio-techne, Minneapolis, USA*) and contained silicone cell-seeding inserts (*Agilent Technologies, USA*) to concentrate the plated cell in the middle of each well for better interaction with the cartridge sensor. The plate was centrifuged at 300 x *g* for 5 minutes at room temperature with the brake off, each silicon insert removed from the wells, and the plate rested for 1 hour in a non-CO_2 incubator at 37°C. Assay medium (130 µL) was added 15 minutes prior to starting the assay.

Equilibrated Seahorse XFe96 extracellular flux analyser was calibrated with pre-hydrated Seahorse XFe96 sensor cartridge followed by inserting the experimental plate into the analyser and an induced real-time ATP rate (pmol · min^{-1}) assay was performed. Following the pre-design experimental assay, OCR (pmol · min^{-1}) and PER (pmol · min^{-1}) were measured 1–2 minutes after the assay begun reflecting the baseline measurement (3 cycles) and following each of four consecutive injections over a 124 measurement period. Injections of activator or assay medium (port A, 10

cycles) after 14–20 minutes, Oligomycin (port B, 3 cycles) after 78–85 minutes, BAM 15 (port C, 3 cycles) after 98–105 minutes and a mixture of Rotenone + Antimycin A + Monensin (port D, 3 cycles) after 118–124 minutes were implemented to provide a detailed metabolic profile for each sample. The mean of 3 measurement cycles after each reagent injected was used to calculate OCR and the final 3 measurement cycles after activator bead injected was used to calculate PER. The calculation detail of respiratory parameters is provided in **Table 4.1**. OCR is applied to the real-time mitochondria stress test of control samples and PER is used as variable to compare the real-time glycolytic rate between control vs. experimental samples upon activation.

Table 4.1 Calculation of respiratory parameters measured by Seahorse extracellular flux analyser

Parameter	Calculation
Basal respiration	Initial OCR measurements subtracted by non-mitochondrial respiration
Proton leak	The OCR after Oligomycin injection subtracted by non-mitochondrial respiration
Maximal respiration	The highest OCR after injection of BAM15
Reserve respiratory capacity	The difference between the maximal and basal respiratory capacity
ATP-linked respiration	Basal respiration subtracted by proton leak

Non-mitochondrial respiration	The OCR after the injection of Rotenone + Antimycin A + Monensin
Mitochondrial PER	OCR multiplied by 0.61 (CO_2 contribution factor)
Glycolytic PER	Total PER subtracted by mitochondrial PER

Abbreviations: OCR, oxygen consumption rate; ATP, adenosine triphosphate; PER, proton efflux rate.

4.3.9 Ex Vivo T-cell Stimulation

Under sterile conditions, PBMCs and enriched naïve $CD4^+$ and $CD8^+$ cells (2 x 10^5 cells/well) were suspended in 180 µL of pre-warmed ImmunoCult-XF T-cell expansion medium (*STEMCELL Technology, UK*) and seeded onto a non-treated 96-well round bottomed microplate (*Fisher Scientific, UK*). Into each well, 20 µL of ImmunoCult human CD3/CD28 T-cell activator (*STEMCELL Technology, UK*) or 20 µL of expansion medium (control well) was gently mixed with the cells and incubated for 12 hours at 37ºC (5% CO_2). All cell suspensions were centrifuged at 300 x *g* for 5 minutes at room temperature to harvest cells for measurement of post-activation diameter using a dual fluorescence cell counter, and the supernatant was stored at -80ºC for future quantification of interleukin 2 (IL-2).

4.3.10 Nutrient Quantification and Enzyme-Linked Immunosorbent Assays

The concentrations of glucose and glutamine in plasma, and triglyceride in serum were quantified using bioluminescent rapid assay kits (*Promega, Madison, USA*). The concentration of Interleukin (IL)-2 in supernatants harvested from activated naïve T cells was determined using high sensitivity (0.066 pg · mL^{-1}) enzyme-linked immunosorbent assay (ELISA) kits (assay sensitivity: 0.066 pg · mL^{-1}), *Bio-techne*,

Minneapolis, USA). All samples were analysed in duplicate and concentrations were obtained from a standard curve of known IL-2 concentration. The manufacturer reported intra- (2.13%) and inter-assay (6.57%) variability that aligned with our laboratory.

4.3.11 Statistical Analysis

GraphPad Prism 10.2.2 analysis software (*San Diego, CA*) was used to perform any statistical analysis and graph creation. Data at three timepoints of each trial were assessed for normal distribution via the Shapiro-Wilk test. Data that weren't normally distributed were analysed using Wilcoxon or Kruskal-Wallis's test. However, normally distributed variables were analysed each timepoint (Pre-Ex, Post-Ex, and Recovery) and across exercise trials (RT, CT-1, and CT-2) by mixed-effects two-way analysis of variance (Two-way ANOVA). *Post hoc* analyses of any interaction effects (Time x cell type) were performed by a test of multiple comparisons, with either Tukey test, depending on variable normality, and one-way analysis of variance (One-way ANOVA) was used to compare data between timepoints (Pre-Ex, Post-Ex, and Recovery) to assist effect sizes calculation. Statistical significance was accepted at the $P < 0.05$ level. All values are presented as means ± standard deviation (SD). 95% confidence intervals (CI) are presented when describing significant differences in metabolic profiling **(section 4.4.5 and 4.4.6)** identified in *post hoc* testing, and effect sizes (Cohen's *d*) were computed to aid in evaluating the practical significance of the results. An effect size of 0.2 was considered the minimal value for a meaningful difference. Effect sizes of 0.5 and 0.8 were considered moderate and large respectively (28,29).

4.4 Results

4.4.1 Participant Characteristics, Sleep Efficiency and Anxiety

Mean participant characteristics including anthropometrics, cardiorespiratory fitness, maximal power output and LT1 are reported in **Table 4.2**.

Table 4.2 Participant characteristics

Variable	All (n = 10)
Age (years)	20.70 ± 1.06
Height (cm)	175.25 ± 12.03
Body mass (kg)	65.85 ± 8.06
BMI ($kg \cdot m^2$)	21.48 ± 2.04
$\dot{V}O_{2max}$ ($mL \cdot kg^{-1} \cdot min^{-1}$)	53.94 ± 9.78
Maximum Power output (W)	262.44 ± 53.35
LT-1 (mmol/L)	2.09 ± 0.39

Data displayed as mean ± SD.

Abbreviations: BMI, body mass index; $\dot{V}O_{2max}$, maximum rate of oxygen uptake; LT, lactate threshold.

Fluctuations in sleep quality and levels of anxiety in the weeks between trials might perturb immunometabolic parameters. A repeated measures ANOVA showed no significant differences in sleep efficiency ($F(1.25, 11.26) = 1.87$, $P = 0.20$), state anxiety ($F(1.62, 14.62) = 0.69$, $P = 0.49$) or trait anxiety ($F(1.91, 17.17) = 0.23$, $P =$

0.79) (**Table 4.3**). Sleep efficiency and anxiety were therefore not included as covariates in subsequent statistical analyses of primary and secondary variables.

Table 4.3 Sleep efficiency and state and trait anxiety score prior to each experimental trial

	Experimental Trial			
Variable	**RT**	**CT-1**	**CT-2**	**P-Value**
Sleep Efficiency (%)	83.80 ± 11.74	83.83 ± 8.06	88.60 ± 4.48	> 0.05
Anxiety State ($S_{anxiety}$)	44.40 ± 2.07	45.80 ± 4.87	45.40 ± 3.41	> 0.05
Anxiety Trait ($T_{anxiety}$)	45.00 ± 5.50	45.10 ± 5.26	44.20 ± 3.97	> 0.05

Data displayed as mean ± SD. P > 0.05 indicates no significant differences between trials.

Abbreviations: RT, rest trial; CT-1, cycling trial 1; CT-2, cycling trial 2.

4.4.2 Physiological and Subjective Responses

Physiological data in response to CT-1 and CT-2 are presented in **Table 4.4**. A repeated measures ANOVA revealed no significant differences in HR at rest between the three trials (F (1.54, 13.82) = 1.67, P = 0.22). Similarly, average HR (F (1.13, 10.20) = 178.40, P = 0.70), absolute $\dot{V}O_2$ uptake (F (2, 18) = 420.00, P = 0.89), relative $\dot{V}O_2$ uptake (F (2, 27) = 176.90, P = 0.96) and total energy expenditure (F (1.34, 12.08) = 403.40, P = 0.92) during exercise were not significantly different between CT-1 and CT-2. For subjective perceptions, there was no significant difference in the affective response (F (1.29, 11.65) = 49.39, P = 0.23), or RPE (F (1.57, 14.16) = 65.14, P = 0.84) between CT-1 and CT-2.

Table 4.4 Mean physiological responses during identical cycling trials

Experimental Trial			
Variable	**CT-1**	**CT-2**	**P-Value**
HR (bpm)	137 ± 16	135 ± 16	> 0.05
RPE	11.05 ± 1.92	10.84 ± 1.54	> 0.05
Affective Response	2.10 ± 1.13	2.50 ± 0.64	> 0.05
Average $\dot{V}O_2$ Uptake ($mL \cdot min^{-1}$)	2311 ± 337	2268 ± 333	> 0.05
Total Energy Expenditure (kcal)	1363 ± 207	1351 ± 198	> 0.05
Relative $\dot{V}O_2$ Uptake ($\%\dot{V}O_{2max}$)	67 ± 11	66 ± 11	> 0.05
Respiratory Exchange Ratio	0.89 ± 0.03	0.90 ± 0.02	> 0.05
Carbohydrate Oxidation (g/min)	1.86 ± 0.36	1.86 ± 0.38	> 0.05
Fat Oxidation (g/min)	0.41 ± 0.16	0.38 ± 0.12	> 0.05

Data displayed as mean ± SD. P > 0.05 indicates no significant differences between trials.

Abbreviations: CT-1, cycling trial 1; CT-2, cycling trial 2; HR, heart rate; RPE, rating of perceived exertion; $\dot{V}O_2$, rate of oxygen uptake.

4.4.3 Immune Cell Concentrations

Blood volume adjusted immune cell concentrations at Pre-Ex, Post-Ex and Recovery during CT-1 and CT-2 are displayed in **Table 4.5**. Total WBC (cells/µL, Pre-Ex: 5700 ± 1080 vs. Post-Ex: 9330 ± 1937, P < 0.001), neutrophil (Pre-Ex: 2913 ± 794 vs. Post-Ex: 6056 ± 1782, P < 0.001) and monocyte (Pre-Ex: 490 ± 137 vs. Post-Ex: 691 ± 220, P < 0.01) concentrations significantly increased immediately after CT-1 and CT-2 and

remained elevated at Recovery. Lymphocyte concentration increased immediately after CT-1 and CT-2, but this did not reach statistical significance (cells/µL, Pre-Ex: 1960 ± 457 vs. Post-Ex: 2222 ± 582, P = 0.33). There was a significant decrease in lymphocyte concentration at Recovery, relative to the end of CT-1 and CT-2 (Post-Ex: 2222 ± 582 vs. Recovery: 1803 ± 508, P < 0.01), but this was not different to Pre-Ex (P = 0.30). When comparing concentrations of WBC's, neutrophils, monocytes and lymphocytes between CT-1 and CT-2, there were no significant differences in either trial or at any timepoint (all Time x Trial interactions, P > 0.05).

Table 4.5 Differences in Peripheral Blood Immune Cell Concentrations

	Experimental Trial			
Immune cell subset (cells/µL)	**Pre-Ex**	**Post-Ex**	**Recovery**	**P-Value**
WBCs	5700 ± 1080[1,2]	9330 ± 1937[1]	9463 ± 1135[2]	< 0.001
Neutrophils	2913 ± 794[1,2]	6056 ± 1782[1]	6852 ± 1135[2]	< 0.001
Lymphocytes	1960 ± 457	2222 ± 582[3]	1803 ± 508[3]	< 0.01
Monocytes	490 ± 137[1,2]	691 ± 220[1]	577 ± 127[2]	< 0.01
T cells	701 ± 501[1]	1248 ± 507[1,3]	546 ± 462[3]	< 0.05
$CD4^+$ T cells	435 ± 364	722 ± 304[3]	300 ± 279[3]	< 0.001
N	283 ± 280	430 ± 230[3]	177 ± 184[3]	< 0.001
CM	53 ± 35[1]	108 ± 47[1,3]	42 ± 32[3]	< 0.05
EM	92 ± 52	172 ± 135	76 ± 61	> 0.05

	TEMRA	7 ± 5	12 ± 6[3]	5 ± 6[3]	< 0.05
$CD8^+$ T cells		183 ± 140[1]	348 ± 165[1,3]	139 ± 107[3]	< 0.01
	N	98 ± 75[1]	171 ± 95[1,3]	70 ± 48[3]	< 0.05
	CM	7 ± 7	11 ± 7[3]	5 ± 4[3]	< 0.05
	EM	63 ± 59[1]	116 ± 77[1,3]	49 ± 51[3]	< 0.05
	TEMRA	15 ± 14[1]	50 ± 44[1,3]	15 ± 15[3]	< 0.05

Data displayed as mean ± SD. P > 0.05 indicates no significant differences between trials.
[1], significant difference between Pre-Ex and Post-Ex (P < 0.05)
[2], significant difference between Pre-Ex and Rec-Ex (P < 0.05)
[3], significant difference between Post-Ex and Rec-Ex (P < 0.05)

Abbreviations: Pre-Ex, pre-exercise; Post-Ex, post-exercise; Rec-Ex, Recovery-Exercise; WBC, white blood cell; N, Naïve; CM, central memory; EM, effector memory; TEMRA, terminally differentiated effector memory.

To further examine the composition of the lymphocyte population, specifically T cell memory subsets, flow cytometry was subsequently employed. Blood volume adjusted concentrations of $CD4^+$ and $CD8^+$ T cells and their daughter populations (N, CM, EM, and TEMRA) at Pre-Ex, Post-Ex and Recovery are reported across the 3 trials in **Table 4.5** (see study design, **section 4.3.2**). There were increases in total $CD3^+$ (Pre-Ex: 701 ± 501 vs. Post-Ex: 1248 ± 507, P = 0.03), $CD8^+$ (Pre-Ex: 183 ± 140 vs. Post-Ex: 348 ± 165, P = 0.008), and $CD4^+$ (Pre-Ex: 435 ± 363.54 vs. Post-Ex: 722 ± 303.90, P = 0.07) T cell concentrations, but the latter did not reach statistical significance. Within the $CD8^+$ population, these changes were driven by naïve (Pre-Ex: 98 ± 75 vs. Post-Ex: 171 ± 95, P = 0.05), EM $CD8^+$ (Pre-Ex: 63 ± 59 vs. Post-Ex: 116 ± 77, P = 0.03), and TEMRA $CD8^+$ (Pre-Ex: 15 ± 14 vs. Post-Ex: 50 ± 44, P = 0.02), but not CM T cells

(Pre-Ex: 7.14 ± 7.48 vs. Post-Ex: 10.90 ± 6.57, P = 0.33). The concentrations of $CD3^+$ (546 ± 462, P = 0.0006), $CD4^+$ (300 ± 279, P = 0.0006) and $CD8^+$ (139 ± 107, P = 0.0002) T cells significantly decreased at Recovery relative to Post-Ex, but these were not different to Pre-Ex across all T cell subsets (P > 0.05).

4.4.4 Changes in the Metabolic Phenotype of PBMCs vs. Isolated Naïve T cells in Response to Prolonged Cycling

Absolute and relative changes in the metabolic phenotype of PBMCs and naïve $CD4^+$ and $CD8^+$ T cells immediately after and 2 hours into recovery from prolonged cycling are presented in **Figure 4.3** and **Figure 4.4** respectively. EFA data was coupled to cell proportions determined by flow cytometry to calculate the contribution of naïve $CD4^+$ and $CD8^+$ T cells to each parameter within the PBMC fraction. To interpret these findings, data on the composition of the PBMC fraction **(4.4.4.1)** and purity of the naïve $CD4^+$ and $CD8^+$ T cell populations **(4.4.4.2)** are first presented.

4.4.4.1 Composition of PBMC Fraction

Given the dynamic changes in the concentrations of T cell subsets in response to prolonged cycling (4.4.4), the composition of seeded PBMCs used to measure metabolic phenotype were first examined. A repeated measures ANOVA indicated significant differences in the frequency of immune cell subsets across timepoints (Time x cell subset Interaction: F (24, 234) = 7.14, P < 0.0001). *Post-hoc* analysis revealed an increase in the proportions of monocytes (Pre-Ex %: 20.25 ± 5.15 vs. Post-Ex %: 23.86 ± 5.02, P = 0.01) and total $CD8^+$ T cells (Pre-Ex %: 7.28 ± 4.39 vs. Post-Ex %:

11.09 ± 3.52, P = 0.01) in Post-Ex relative to Pre-Ex, with the latter driven $CD8^+$ TEMRA (Pre-Ex %: 0.61 ± 0.50 vs. Post-Ex %: 1.62 ± 1.31, P = 0.01) **(Figure 4.3C-D)**. Between Post-Ex and Recovery timepoints, there was a significant decrease in the proportion of $CD3^+$ T cells (Post-Ex %: 40.45 ± 11.25 vs. Recovery %: 21.33 ± 14.10, P = 0.0003), driven by naïve $CD4^+$ (Post-Ex %: 14.13 ± 6.51 vs. Recovery %: 7.09 ± 6.40, P < 0.0001), $CD4^+$ CM (Post-Ex %: 3.60 ± 1.46 vs. Recovery %: 1.70 ± 1.08, P = 0.001), naïve $CD8^+$ (Post-Ex %: 5.48 ± 2.54 vs. Recovery %: 2.89 ± 1.77, P < 0.0001), and CD8+ TEMRA (Post-Ex %: 1.62 ± 1.31 vs. Recovery %: 0.56 ± 0.45, P = 0.02) T cells.

4.4.4.2 Purity of Enriched $CD4^+$ and $CD8^+$ Naïve T cells

The purity of naïve T cells was confirmed by flow cytometry. Prior to enrichment, the average frequency of naïve $CD4^+$ and naïve $CD8^+$ T cell within the PBMC fraction was 67.15 ± 16.08 and 52.12 ± 14.69 respectively. After MACS enrichment, there were no significant differences in the purity (%) of naïve $CD4^+$ (98.85 ± 1.18, P = 0.39) and naïve $CD8^+$ (99.84 ± 0.14, P = 0.11) T cells across participants or experimental trials.

4.4.4.3 Absolute Changes in Metabolic Parameters

Live-cell absolute measurements of OCR in response to modulators of mitochondrial respiration (Mito Stress assay) are presented in **(Figure 4.3A-B)** and used to calculate parameters of mitochondrial function **(Figure 4.3E)**. There were no significant differences in basal, ATP-linked, maximal respiration, proton leak and spare respiratory capacity in naïve $CD4^+$ and $CD8^+$ T cells, and PBMCs between Pre-Ex, Post-Ex and Recovery (P > 0.05). The Mito stress assay can also provide real-time measurements of glycolytic flux by measuring PER (**Figure 4.3F)** and energy

phenotype by determining the contributions of glycolysis and mitochondrial respiration to ATP synthesis (**Figure 4.3G**). There were no significant changes in glycolytic PER or ATP synthesis rates in naïve $CD4^+$ and $CD8^+$ T cells, and PBMCs across timepoints. Across all absolute measurements, a two-way ANOVA revealed that OCR, glycolytic PER and ATP synthesis rates were significantly greater in PBMCs than naïve CD4+ and CD8+ T cells for Pre-Ex, Post-Ex and Recovery samples ($P < 0.0001$).

Given the logistical challenges of conducting lengthy laboratory analysis on fresh human samples (≈14 hours per trial day), this study maybe underpowered. To assist with data interpretation, 95% confidence intervals of the mean differences and effect sizes (Cohen's *d*) were calculated and presented in **Table 4.6**. There were consistent trends for an increase in all metabolic variables between Pre-Ex and Post-Ex for all cell subsets, demonstrating small (0.2 - 0.5) to moderate (0.5 – 0.8) effect sizes. Furthermore, there were consistent trends for a decrease in the same variables between Pre-Ex and Recovery, demonstrating moderate (0.5 – 0.8) to large effect sizes (> 0.8). However, the large confidence intervals spanning negative and positive values for the mean differences indicate variable responses between participants within our participant cohort.

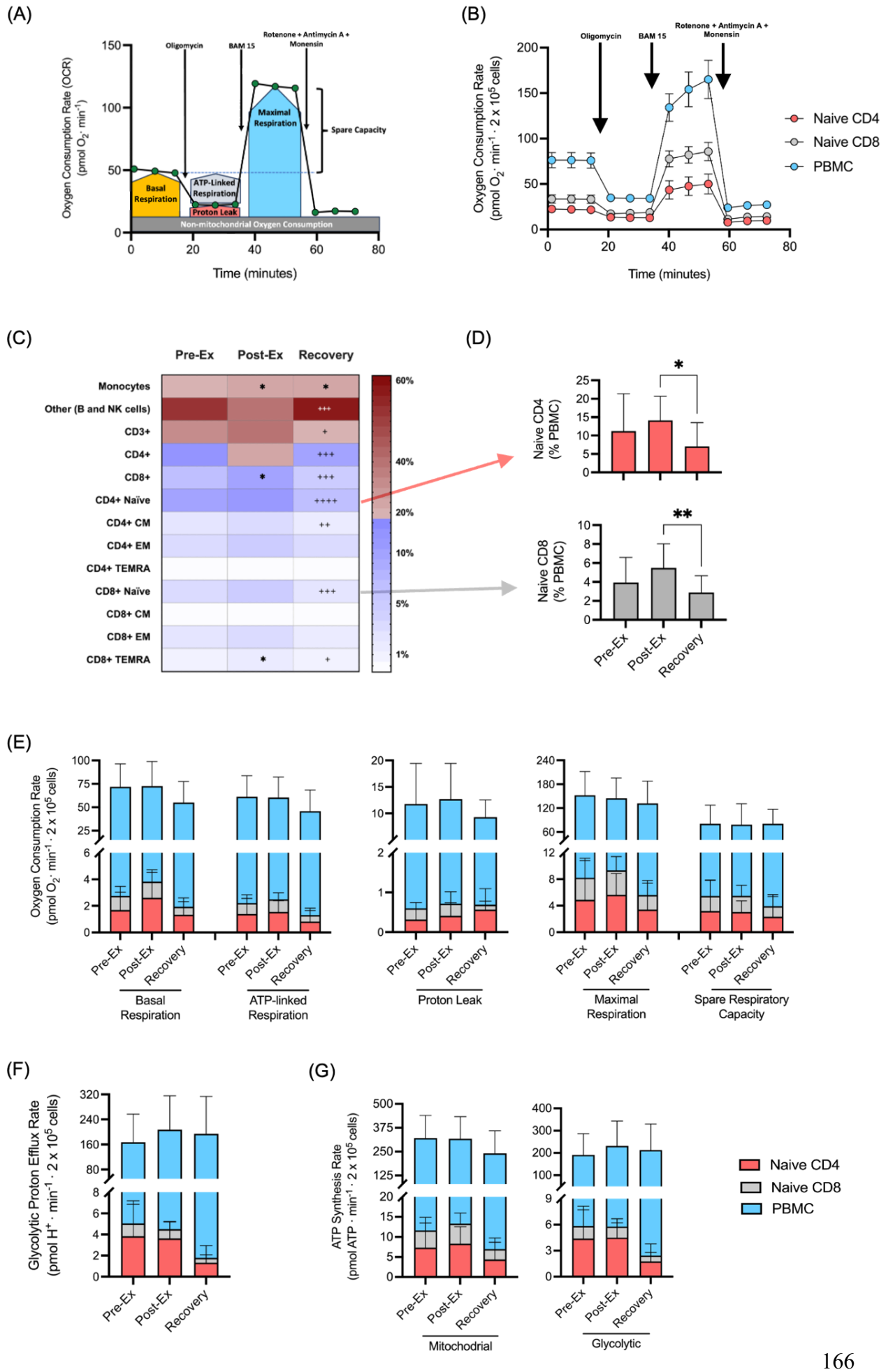
(A)
Oxygen Consumption Rate (OCR)
(pmol O2 · min-1)
Oligomycin
BAM 15
Rotenone + Antimycin A + Monensin
Maximal Respiration
Spare Capacity
Basal Respiration
ATP-Linked Respiration
Proton Leak
Non-mitochondrial Oxygen Consumption
Time (minutes)
(B)
Oxygen Consumption Rate
(pmol O2 · min-1 · 2 x 10^5 cells)
Oligomycin
BAM 15
Rotenone + Antimycin A + Monensin
Time (minutes)
Naive CD4
Naive CD8
PBMC
(C)
Pre-Ex
Post-Ex
Recovery
Monocytes
Other (B and NK cells)
CD3+
CD4+
CD8+
CD4+ Naïve
CD4+ CM
CD4+ EM
CD4+ TEMRA
CD8+ Naïve
CD8+ CM
CD8+ EM
CD8+ TEMRA
60%
40%
20%
10%
5%
1%
(D)
Naive CD4
(% PBMC)
Naive CD8
(% PBMC)
Pre-Ex
Post-Ex
Recovery
(E)
Oxygen Consumption Rate
(pmol O2 · min-1 · 2 x 10^5 cells)
Pre-Ex
Post-Ex
Recovery
Basal Respiration
ATP-linked Respiration
Proton Leak
Maximal Respiration
Spare Respiratory Capacity
(F)
Glycolytic Proton Efflux Rate
(pmol H+ · min-1 · 2 x 10^5 cells)
(G)
ATP Synthesis Rate
(pmol ATP · min-1 · 2 x 10^5 cells)
Mitochodrial
Glycolytic
Naive CD4
Naive CD8
PBMC

Figure 4.3 Mitochondrial profile of naïve $CD4^+$ and $CD8^+$ T cells within 200 x 10^3 seeded PBMCs/well. (A) Schematic representation of changes in oxygen consumption rate (OCR) monitored using a Seahorse XFe96 Analyzer when oligomycin, BAM 15 and rotenone + antimycin A + monensin were injected. Basal (yellow), ATP-linked (grey), maximal respiration (blue), proton leak (red), and spare respiratory capacity (blue) were calculated (B) Representative live traces of OCR in naïve $CD4^+$ (red circles) and $CD8^+$ T cells (grey circles) and total PBMCs (blue circles). OCR was measured continuously throughout the experimental period at baseline followed by the addition of the 3 indicated drugs, (C). A heat map presents the proportions of immune cell populations determined using flow cytometry within Pre-Ex, Post-Ex and Recovery PBMC samples. N.B. monocyte, B cell and NK cell frequencies were calculated from negative populations acquired during flow cytometry analysis and not directly using antibody conjugates. (D) Frequencies of naïve $CD4^+$ and $CD8^+$ T cells in seeded PBMCs from each timepoint for OCR measurement are graphically depicted. (E) Basal, ATP-linked, maximal respiration, proton leak, and spare respiratory capacity (F) Glycolytic PER, (G) Mitochondrial and Glycolytic ATP production rate are presented for naïve $CD4^+$ T cells (red stacked bars), $CD8^+$ T cells (grey stacked bars) and PBMCs (total bar). N.B. Blue stacked bars represent values for 'PBMC – naïve $CD4^+$ and $CD8^+$ T cells'. Data were presented as the mean ± SD of 10 participants x 3 timepoints. * indicates significant differences between Pre-Ex and Post-Ex or Recover, and + indicates significant differences between Post-Ex and Recovery: $P > 0.05$, $^*P < 0.05$, $^{**}P < 0.01$, $^{+}P < 0.05$, $^{++}P < 0.01$, $^{+++}P < 0.001$, $^{++++}P < 0.0001$.

Table 4.6 Descriptive statistics of the effect sizes (Cohen's *d*) in listed variables and cell types between timepoints with threshold:

Positive Effect	< 0.2 − 0	0.2 − 0.5	0.5 − 0.8	> 0.8
Negative Effect	> -0.2 − 0	-0.2 − -0.5	-0.5 − -0.8	< -0.8

Panel E (OCR) - Basal Respiration

Cell Type	Mean			STDev.			Comparison	P-Value	Mean Diff.	Confidence Interval (95%)	Pooled STDev.	Effect Size Cohen's d
	Pre-Ex	Post-Ex	Recovery	Pre-Ex	Post-Ex	Recovery						
Naïve CD4⁺ T cells	1.68	2.61	1.33	1.35	2.11	1.26	Pre-Ex VS. Post-Ex	0.42	-0.93	-2.73 to 0.87	1.77	0.52
							Pre-Ex VS. Rec	0.88	0.35	-1.45 to 2.15	1.31	-0.27
							Post-Ex VS. Rec	0.20	1.28	-0.52 to 3.07	1.74	-0.74
Naïve CD8⁺ T cells	1.07	1.22	0.60	0.71	0.69	0.37	Pre-Ex VS. Post-Ex	0.85	-0.15	-0.82 to 0.53	0.70	0.21
							Pre-Ex VS. Rec	0.22	0.47	-0.21 to 1.15	0.57	-0.82
							Post-Ex VS. Rec	0.08	0.62	-0.06 to 1.29	0.55	-1.11
PBMCs	69.06	68.78	53.09	24.58	26.23	22.39	Pre-Ex VS. Post-Ex	0.10	0.28	-26.83 to 27.39	25.42	-0.01
							Pre-Ex VS. Rec	0.33	15.97	-11.14 to 43.08	23.51	-0.68
							Post-Ex VS. Rec	0.34	15.69	-11.42 to 42.80	24.39	-0.64

Panel E (OCR) - ATP-linked Respiration

Cell Type	Mean			STDev.			Comparison	P-Value	Mean Diff.	Confidence Interval (95%)	Pooled STDev.	Effect Size Cohen's d
	Pre-Ex	Post-Ex	Recovery	Pre-Ex	Post-Ex	Recovery						
Naïve CD4+ T cells	1.39	1.55	0.82	1.17	0.84	1.02	Pre-Ex VS. Post-Ex	0.94	-0.16	-1.28 to 0.97	1.02	0.15
							Pre-Ex VS. Rec	0.43	0.57	-0.55 to 1.70	1.10	-0.52
							Post-Ex VS. Rec	0.26	0.73	-0.40 to 1.86	0.93	-0.78
Naïve CD8+ T cells	0.82	0.94	0.49	0.62	0.50	0.33	Pre-Ex VS. Post-Ex	0.85	-0.12	-0.67 to 0.43	0.56	0.22
							Pre-Ex VS. Rec	0.32	0.33	-0.22 to 0.88	0.50	-0.66
							Post-Ex VS. Rec	0.13	0.45	-0.10 to 1.00	0.43	-1.06
PBMCs	58.90	57.90	44.51	22.59	21.94	22.64	Pre-Ex VS. Post-Ex	0.99	1.01	-23.82 to 25.83	22.27	-0.04
							Pre-Ex VS. Rec	0.34	14.39	-10.44 to 39.21	22.62	-0.64
							Post-Ex VS. Rec	0.39	13.38	-11.45 to 38.21	22.29	-0.60

Panel E (OCR) - Proton Leak

Cell Type	Mean			STDev.			Comparison	P-Value	Mean Diff.	Confidence Interval (95%)	Pooled STDev.	Effect Size Cohen's d
	Pre-Ex	Post-Ex	Recovery	Pre-Ex	Post-Ex	Recovery						
Naïve CD4+ T cells	0.32	0.411	0.57	0.27	0.33	0.53	Pre-Ex VS. Post-Ex	0.86	-0.09	-0.54 to 0.35	0.30	0.31
							Pre-Ex VS. Rec	0.34	-0.25	-0.69 to 0.19	0.42	0.60
							Post-Ex VS. Rec	0.67	-0.16	-0.60 to 0.29	0.44	0.36
Naïve CD8+ T cells	0.28	0.31	0.12	0.15	0.30	0.09	Pre-Ex VS. Post-Ex	0.96	-0.03	-0.24 to 0.19	0.23	0.11
							Pre-Ex VS. Rec	0.19	0.16	-0.06 to 0.38	0.12	-1.31
							Post-Ex VS. Rec	0.11	0.18	-0.04 to 0.40	0.22	-0.84
PBMCs	11.19	11.99	8.59	7.65	6.74	3.26	Pre-Ex VS. Post-Ex	0.96	-0.80	-7.65 to 6.05	7.21	0.11
							Pre-Ex VS. Rec	0.62	2.60	-4.25 to 9.46	5.88	-0.44
							Post-Ex VS. Rec	0.45	3.40	-3.45 to 10.25	5.29	-0.64

Panel E (OCR) - Maximal Respiration

Cell Type	Mean			STDev.			Comparison	P-Value	Mean Diff.	Confidence Interval (95%)	Pooled STDev.	Effect Size Cohen's d
	Pre-Ex	Post-Ex	Recovery	Pre-Ex	Post-Ex	Recovery						
Naïve CD4+ T cells	4.87	5.65	3.42	5.92	3.20	4.39	Pre-Ex VS. Post-Ex	0.92	-0.78	-5.92 to 4.36	4.76	0.16
							Pre-Ex VS. Rec	0.77	1.45	-3.69 to 6.59	5.21	-0.28
							Post-Ex VS. Rec	0.54	2.24	-2.91 to 7.37	3.84	-0.58
Naïve CD8+ T cells	3.34	3.67	2.19	2.92	2.10	1.79	Pre-Ex VS. Post-Ex	0.95	-0.33	-2.90 to 2.24	2.54	0.13
							Pre-Ex VS. Rec	0.52	1.15	-1.42 to 3.72	2.42	-0.48
							Post-Ex VS. Rec	0.34	1.48	-1.09 to 4.05	1.95	-0.76
PBMCs	144.20	135.30	126.20	59.23	51.18	55.86	Pre-Ex VS. Post-Ex	0.93	8.95	-52.62 to 70.51	55.35	-0.16
							Pre-Ex VS. Rec	0.75	18.03	-43.53 to 79.59	57.57	-0.31
							Post-Ex VS. Rec	0.93	9.08	-52.48 to 70.65	53.57	-0.17

Panel E (OCR) - Spare Respiratory Capacity

Cell Type	Mean			STDev.			Comparison	P-Value	Mean Diff.	Confidence Interval (95%)	Pooled STDev.	Effect Size Cohen's d
	Pre-Ex	Post-Ex	Recovery	Pre-Ex	Post-Ex	Recovery						
Naïve CD4+ T cells	3.19	3.04	2.33	4.63	1.69	3.33	Pre-Ex VS. Post-Ex	0.99	0.15	-3.67 to 3.97	3.48	-0.04
							Pre-Ex VS. Rec	0.85	0.85	-3.07 to 4.78	4.03	-0.21
							Post-Ex VS. Rec	0.90	0.71	-3.22 to 4.63	2.64	-0.27
Naïve CD8+ T cells	2.27	2.45	1.59	2.41	1.59	1.45	Pre-Ex VS. Post-Ex	0.97	-0.18	-2.25 to 1.89	2.04	0.09
							Pre-Ex VS. Rec	0.70	0.68	-1.39 to 2.75	1.99	-0.34
							Post-Ex VS. Rec	0.57	0.86	-1.21 to 2.93	1.52	-0.56
PBMCs	75.17	73.09	76.86	46.64	52.29	36.06	Pre-Ex VS. Post-Ex	0.99	2.08	-48.37 to 52.53	49.55	-0.04
							Pre-Ex VS. Rec	0.99	-1.69	-52.14 to 48.76	41.69	0.04
							Post-Ex VS. Rec	0.98	-3.77	-54.22 to 46.68	44.91	0.08

Panel F - Glycolytic PER

Cell Type	Mean			STDev.			Comparison	P-Value	Mean Diff.	Confidence Interval (95%)	Pooled STDev.	Effect Size Cohen's d
	Pre-Ex	Post-Ex	Recovery	Pre-Ex	Post-Ex	Recovery						
Naïve CD4⁺ T cells	3.83	3.63	1.32	3.36	1.61	1.63	Pre-Ex VS. Post-Ex	0.98	0.20	-2.40 to 2.80	2.63	-0.08
							Pre-Ex VS. Rec	0.06	2.51	-0.09 to 5.11	2.64	-0.95
							Post-Ex VS. Rec	0.09	2.31	-0.29 to 4.91	1.62	-1.43
Naïve CD8⁺ T cells	1.22	0.88	0.47	1.81	0.68	0.28	Pre-Ex VS. Post-Ex	0.79	0.33	-0.92 to 1.58	1.37	-0.24
							Pre-Ex VS. Rec	0.32	0.74	-0.51 to 1.99	1.30	-0.57
							Post-Ex VS. Rec	0.68	0.41	-0.81 to 1.63	0.52	-0.79
PBMCs	162.20	203.10	192.60	90.14	108.20	119.30	Pre-Ex VS. Post-Ex	0.67	-40.87	-159.00 to 77.29	99.58	0.41
							Pre-Ex VS. Rec	0.80	-30.40	-148.60 to 87.76	105.73	0.29
							Post-Ex VS. Rec	0.97	10.47	-107.70 to 128.60	113.89	-0.09

Panel G – Mitochondrial ATP Synthesis Rate

Cell Type	Mean			STDev.			Comparison	P-Value	Mean Diff.	Confidence Interval (95%)	Pooled STDev.	Effect Size Cohen's d
	Pre-Ex	Post-Ex	Recovery	Pre-Ex	Post-Ex	Recovery						
Naïve CD4⁺ T cells	7.32	8.32	4.38	6.12	4.23	5.34	Pre-Ex VS. Post-Ex	0.91	-1.00	-6.87 to 4.86	5.26	0.19
							Pre-Ex VS. Rec	0.44	2.94	-2.93 to 8.80	5.75	-0.51
							Post-Ex VS. Rec	0.24	3.94	-1.93 to 9.81	4.82	-0.82
Naïve CD8⁺ T cells	4.32	4.97	2.57	3.26	2.66	1.73	Pre-Ex VS. Post-Ex	0.84	-0.65	-3.56 to 2.26	2.97	0.22
							Pre-Ex VS. Rec	0.31	1.75	-1.16 to 4.66	2.61	-0.67
							Post-Ex VS. Rec	0.12	2.40	-0.51 to 5.31	2.24	-1.07
PBMCs	309.60	304.50	234.20	118.00	115.30	117.90	Pre-Ex VS. Post-Ex	0.99	5.07	-124.80 to 134.90	116.66	-0.04
							Pre-Ex VS. Rec	0.33	75.39	-54.44 to 205.20	117.95	-0.64
							Post-Ex VS. Rec	0.38	70.32	-59.51 to 200.10	116.61	-0.60

Panel G - Glycolytic ATP Synthesis Rate

Cell Type	Mean			STDev.			Comparison	P-Value	Mean Diff.	Confidence Interval (95%)	Pooled STDev.	Effect Size Cohen's d
	Pre-Ex	Post-Ex	Recovery	Pre-Ex	Post-Ex	Recovery						
Naïve CD4+ T cells	4.39	4.50	1.76	3.74	1.70	2.02	Pre-Ex VS. Post-Ex	0.99	-0.11	-3.04 to 2.83	2.91	0.04
							Pre-Ex VS. Rec	0.09	2.63	-0.30 to 5.56	3.01	-0.87
							Post-Ex VS. Rec	0.07	2.74	-0.20 to 5.67	1.87	-1.47
Naïve CD8+ T cells	1.45	1.29	0.67	1.88	0.90	0.36	Pre-Ex VS. Post-Ex	0.95	0.17	-1.19 to 1.52	1.47	-0.11
							Pre-Ex VS. Rec	0.34	0.78	-0.57 to 2.13	1.35	-0.58
							Post-Ex VS. Rec	0.51	0.62	-0.74 to 1.97	0.69	-0.89
PBMCs	185.30	226.10	210.40	95.70	111.50	117.40	Pre-Ex VS. Post-Ex	0.68	-40.77	-161.20 to 79.64	103.90	0.39
							Pre-Ex VS. Rec	0.86	-25.07	-145.50 to 95.34	107.10	0.23
							Post-Ex VS. Rec	0.94	15.70	-104.70 to 136.1	114.49	-0.14

4.4.4.4 Relative Changes in Metabolic Parameters

Measurements of OCR and PER in response to modulators of mitochondrial respiration were used to calculate the relative contributions of mitochondrial parameters within naïve CD4 + and CD8 + T cells and PBMCs **(Figure 4.4)**. There were no significant differences in coupling efficiency (% basal OCR) in naïve CD4 + ($F(2, 20) = 0.88$, $P = 0.43$), naïve CD8 + ($F(2, 23) = 1.28$, $P = 0.30$) T cells and PBMCs ($F(2,24) = 1.31$, $P = 0.29$) or spare respiratory capacity (% maximal OCR) in naïve CD4 + ($F(2, 25) = 0.44$, $P = 0.65$), naïve CD8 + ($F(2, 26) = 1.14$, $P = 0.34$) T cells and PBMCs ($F(2, 25) = 0.87$, $P = 0.43$) across timepoints **(Table 4.7 and Figure 4.4A-B)**. Similarly, there were no changes observed in the proportional contributions of proton leak (naïve CD4 + ($F(2, 24) = 1.37$, $P = 0.27$), naïve CD8 + ($F(2, 26) = 0.57$, $P = 0.57$) T cells and PBMCs ($F(2, 23) = 0.05$, $P = 0.95$), ATP-linked respiration (naïve CD4 + ($F(2, 24) = 2,56$, $P = 0.10$), naïve CD8 + ($F(2, 26) = 0.82$, $P = 0.45$) T cells and PBMCs ($F(2, 23) = 0.62$, $P = 0.55$), and spare respiratory capacity (naïve CD4 + ($F(2, 24) = 0.13$, $P = 0.88$), naïve CD8 + ($F(2, 26) = 1.14$, $P = 0.34$) T cells and PBMCs ($F(2, 23) = 0.55$, $P = 0.58$) in any cell type or between timepoints **(Table 4.7 and Figure 4.4C)**. When comparing the relative contribution of glycolysis and mitochondrial respiration to ATP synthesis rates, total ATP production was driven by mitochondrial respiration relative to glycolysis across all cell types ($F(1, 18) = 97.07$, $P < 0.0001$), with the contribution greater in naïve T cells vs. PBMCs ($F(2, 27) = 10.52$, $P = 0.0004$) **(Table 4.8)**. This pattern was present across all timepoints, except PBMCs at recovery ($P = 0.78$) **(Figure 4.4D)**. Although this indicates a shift in metabolic energy phenotype at this timepoint, there were no differences in mitochondrial or glycolytic driven ATP

production between timepoints for naïve CD4 + (P = 0.87), naïve CD8 + (P = 0.61) T cells or PBMCs (P = 0.29).

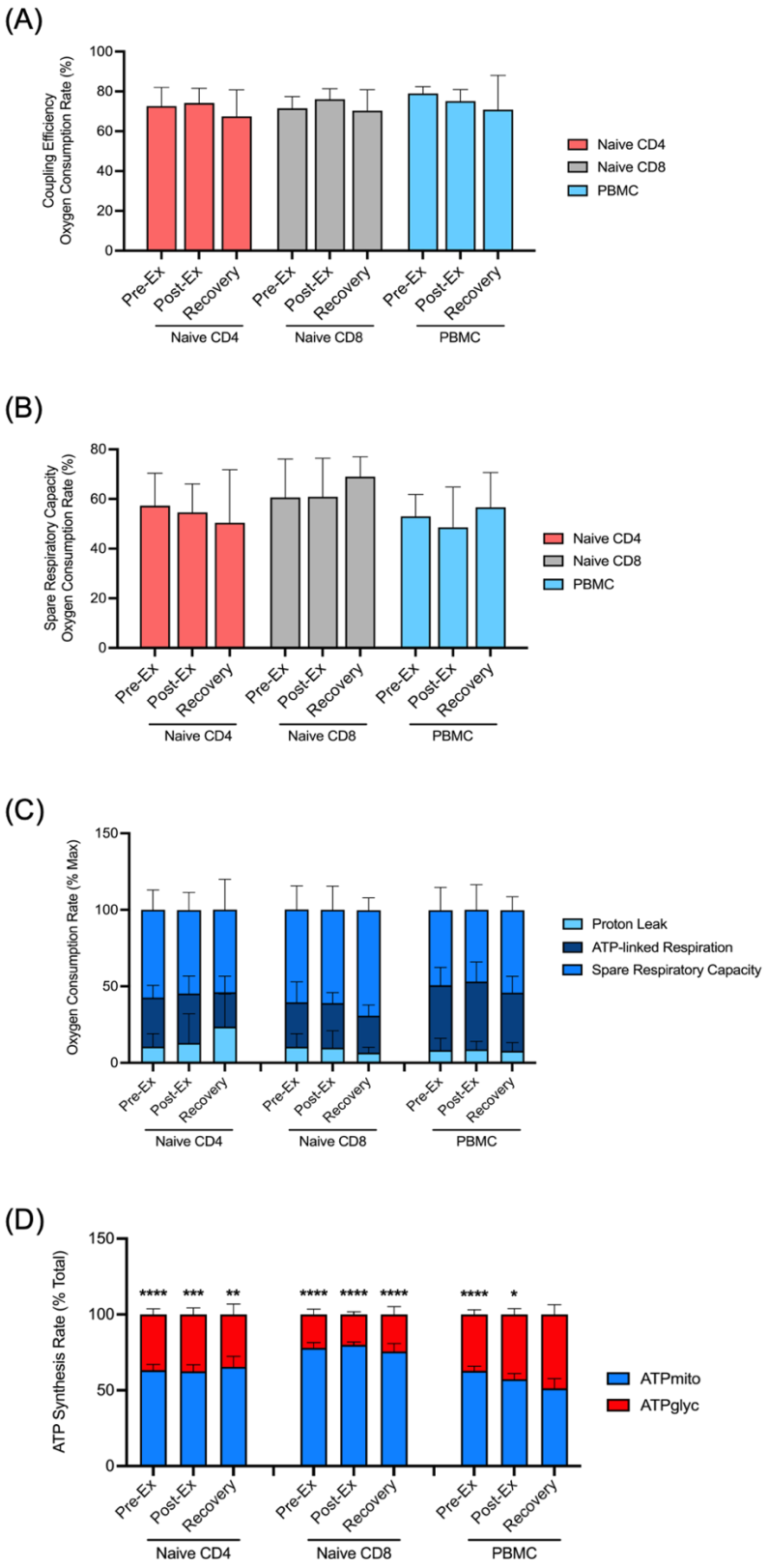

Figure 4.4 Relative data (% maximal OCR) on changes in metabolic parameters in isolated naïve $CD4^+$ and $CD8^+$ T cells vs. PBMCs in response to prolonged cycling. (A) Coupling Efficiency. (B) Spare Respiratory Capacity. (C) Differences in proton leak, ATP-linked respiration, and spare respiratory capacity in mitochondrial respiration. (D) ATP synthesis rate (% total). Data were presented as the mean ± SD of 10 participants. * indicates significant differences between ATPmito and ATPglyc: $P > 0.05$, $*P < 0.05$, $**P < 0.01$, $***P < 0.001$, $****P < 0.0001$.

Table 4.7 Descriptive statistics of the effect sizes (Cohen's *d*) in listed variables and cell types between timepoints with threshold:

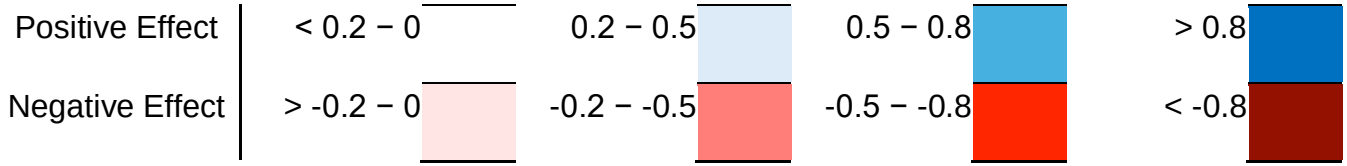

Panel A - Coupling Efficiency (% Basal OCR)

Cell Type	Mean			STDev.			Comparison	P-Value	Mean Diff.	Confidence Interval (95%)	Pooled STDev.	Effect Size Cohen's d
	Pre-Ex	Post-Ex	Recovery	Pre-Ex	Post-Ex	Recovery						
Naïve CD4⁺ T cells	72.63	74.22	67.5	9.43	7.31	13.25	Pre-Ex VS. Post-Ex	0.94	-1.60	-13.66 to 10.47	8.43	0.19
							Pre-Ex VS. Rec	0.61	5.13	-8.29 to 18.54	11.50	-0.45
							Post-Ex VS. Rec	0.42	6.72	-6.37 to 19.81	10.70	-0.63
Naïve CD8⁺ T cells	71.5	76.13	70.4	5.88	5.22	10.44	Pre-Ex VS. Post-Ex	0.48	-4.63	-14.44 to 5.19	5.56	0.83
							Pre-Ex VS. Rec	0.95	1.10	-8.22 to 10.41	8.47	-0.13
							Post-Ex VS. Rec	0.29	5.73	-3.59 to 15.04	8.25	-0.69
PBMCs	79.00	75.11	70.89	3.46	5.80	17.12	Pre-Ex VS. Post-Ex	0.72	3.89	-8.62 to 16.40	4.78	-0.81
							Pre-Ex VS. Rec	0.26	8.11	-4.40 to 20.62	12.35	-0.66
							Post-Ex VS. Rec	0.68	4.22	-8.29 to 16.73	12.78	-0.33

Panel B - Spare Respiratory Capacity (% Maximal OCR)

Cell Type	Mean			STDev.			Comparison	P-Value	Mean Diff.	Confidence Interval (95%)	Pooled STDev.	Effect Size Cohen's d
	Pre-Ex	Post-Ex	Recovery	Pre-Ex	Post-Ex	Recovery						
Naïve CD4+ T cells	57.33	54.60	50.44	13.01	11.47	21.39	Pre-Ex VS. Post-Ex	0.92	2.73	-15.29 to 20.75	12.26	-0.22
							Pre-Ex VS. Rec	0.63	6.89	-11.60 to 25.38	17.70	-0.39
							Post-Ex VS. Rec	0.83	4.16	-13.87 to 22.18	17.16	-0.24
Naïve CD8+ T cells	60.60	60.90	69.00	15.49	15.5	8.03	Pre-Ex VS. Post-Ex	0.99	-0.30	-15.46 to 14.86	15.50	0.02
							Pre-Ex VS. Rec	0.39	-8.40	-23.97 to 7.17	12.34	0.68
							Post-Ex VS. Rec	0.41	-8.10	-23.67 to 7.47	12.34	0.66
PBMCs	53.00	48.56	56.70	8.83	16.3	13.94	Pre-Ex VS. Post-Ex	0.76	4.44	-11.31 to 20.20	13.11	-0.34
							Pre-Ex VS. Rec	0.82	-3.70	-19.06 to 11.66	11.67	0.32
							Post-Ex VS. Rec	0.40	-8.14	-23.50 to 7.211	15.17	0.54

Panel C - Proton Leak (% Maximal OCR)

Cell Type	Mean			STDev.			Comparison	P-Value	Mean Diff.	Confidence Interval (95%)	Pooled STDev.	Effect Size Cohen's d
	Pre-Ex	Post-Ex	Recovery	Pre-Ex	Post-Ex	Recovery						
Naïve CD4+ T cells	10.67	13	23.63	8.41	19.11	21.31	Pre-Ex VS. Post-Ex	0.95	-2.33	-21.98 to 17.31	14.76	0.16
							Pre-Ex VS. Rec	0.28	-12.96	-33.73 to 7.82	16.20	0.80
							Post-Ex VS. Rec	0.40	-10.63	-30.90 to 9.65	20.24	0.53
Naïve CD8+ T cells	10.60	9.90	6.67	8.46	11.12	3.57	Pre-Ex VS. Post-Ex	0.98	0.70	-8.70 to 10.10	9.88	-0.07
							Pre-Ex VS. Rec	0.58	3.93	-5.72 to 13.59	6.49	-0.61
							Post-Ex VS. Rec	0.69	3.23	-6.42 to 12.89	8.26	-0.39
PBMCs	8.30	8.75	7.75	7.68	5.26	5.57	Pre-Ex VS. Post-Ex	0.99	-0.45	-8.05 to 7.15	6.58	0.07
							Pre-Ex VS. Rec	0.98	0.55	-7.05 to 8.15	6.71	-0.08
							Post-Ex VS. Rec	0.95	1.00	-7.01 to 9.01	5.42	-0.18

Panel C - ATP-linked Respiration (% Maximal OCR)

Cell Type	Mean			STDev.			Comparison	P-Value	Mean Diff.	Confidence Interval (95%)	Pooled STDev.	Effect Size Cohen's d
	Pre-Ex	Post-Ex	Recovery	Pre-Ex	Post-Ex	Recovery						
Naïve CD4+ T cells	32.00	32.30	22.50	7.94	11.49	10.52	Pre-Ex VS. Post-Ex	0.99	-0.30	-11.93 to 11.33	9.87	0.03
							Pre-Ex VS. Rec	0.15	9.50	-2.80 to 21.80	9.32	-1.02
							Post-Ex VS. Rec	0.12	9.80	-2.21 to 21.81	11.02	-0.89
Naïve CD8+ T cells	29.00	29.20	24.11	13.44	6.84	7.01	Pre-Ex VS. Post-Ex	0.99	-0.20	-10.97 to 10.57	10.66	0.02
							Pre-Ex VS. Rec	0.52	4.89	-6.17 to 15.95	10.72	-0.46
							Post-Ex VS. Rec	0.51	5.09	-5.97 to 16.15	6.93	-0.73
PBMCs	42.40	44.50	38.13	11.69	12.66	10.67	Pre-Ex VS. Post-Ex	0.92	-2.10	-16.00 to 11.80	12.18	0.17
							Pre-Ex VS. Rec	0.72	4.28	-9.63 to 18.18	11.19	-0.38
							Post-Ex VS. Rec	0.53	6.38	-8.28 to 21.03	11.71	-0.54

Panel C - Spare Respiratory (% Maximal OCR)

Cell Type	Mean			STDev.			Comparison	P-Value	Mean Diff.	Confidence Interval (95%)	Pooled STDev.	Effect Size Cohen's d
	Pre-Ex	Post-Ex	Recovery	Pre-Ex	Post-Ex	Recovery						
Naïve CD4+ T cells	57.33	54.60	54.00	13.01	11.47	19.82	Pre-Ex VS. Post-Ex	0.92	2.73	-14.30 to 19.77	12.26	-0.22
							Pre-Ex VS. Rec	0.89	3.33	-14.68 to 21.35	16.76	-0.20
							Post-Ex VS. Rec	0.99	0.60	-16.98 to 18.18	16.19	-0.04
Naïve CD8+ T cells	60.60	60.90	69.00	15.49	15.50	8.03	Pre-Ex VS. Post-Ex	0.99	-0.30	-15.46 to 14.86	15.50	0.02
							Pre-Ex VS. Rec	0.39	-8.40	-23.97 to 7.17	12.34	0.68
							Post-Ex VS. Rec	0.41	-8.10	-23.67 to 7.47	12.34	0.66
PBMCs	49.10	46.75	53.88	14.88	16.44	8.86	Pre-Ex VS. Post-Ex	0.93	2.35	-14.14 to 18.84	15.68	-0.15
							Pre-Ex VS. Rec	0.75	-4.78	-21.27 to 11.72	12.24	0.39
							Post-Ex VS. Rec	0.57	-7.13	-24.51 to 10.26	13.20	0.54

Table 4.8 Comparative data between mitochondrial vs. glycolytic ATP synthesis rate

Cell Type	Timepoints	Mean (%) and STDev. Comparison (ATPmito vs. ATPglyc)	P-Value
Naïve $CD4^+$ T cells	Pre-Ex	63.30 ± 11.60 vs. 36.70 ± 11.55	< 0.0001
	Post-Ex	62.50 ± 13.72 vs. 37.50 ± 13.73	0.0007
	Recovery	65.44 ± 25.02 vs. 34.56 ± 25.01	0.006
Naïve $CD8^+$ T cells	Pre-Ex	78.00 ± 11.13 vs. 22.00 ± 10.99	< 0.0001
	Post-Ex	80.00 ± 5.45 vs. 20.00 ± 5.52	< 0.0001
	Recovery	75.60 ± 16.18 vs. 24.40 ± 16.15	< 0.0001
PBMCs	Pre-Ex	62.80 ± 9.69 vs. 37.20 ± 9.73	< 0.0001
	Post-Ex	57.30 ± 11.76 vs. 42.70 ± 11.83	0.01
	Recovery	51.30 ± 20.26 vs. 48.70 ± 20.35	0.78

4.4.5 Effect of Prolonged Cycling on *Ex vivo* T cell Metabolic Profile upon Activation

4.4.5.1 Composition of PBMC Fraction

To determine real-time metabolic responses to T cell activation in collected blood samples, enriched naïve T cells and PBMCs were incubated with CD3/CD28 beads. All samples were seeded at 200 x 10^3 cells per well, thus enriched naïve $CD4^+$ and $CD8^+$ T cell numbers were equal across Pre-Ex, Post-Ex and Recovery. However,

given the fluctuations in T cell concentrations throughout prolonged cycling **(Figure 4.5A-B)**, the numbers of T cell subsets may vary within the 200 x 10^3 PBMCs that were seeded and therefore these numbers were calculated using flow cytometry data.

A repeated measures ANOVA showed significant differences in the number of T cell subsets within the PBMC fraction across timepoints (Time x cell subset Interaction: $F(24, 234) = 6.78$, $P < 0.0001$). *Post-hoc* analysis revealed that relative to Pre-Ex, there were greater numbers of $CD4^+$ CM (Pre-Ex: 4,362.25 ± 2,697.09 vs. Post-Ex: 7,200.77 ± 2928.60, $P < 0.03$) and both $CD8^+$ EM (Pre-Ex: 4,888.71 ± 3724.54 vs. Post-Ex: 7,260.22 ± 4351.20, $P < 0.04$) and $CD8^+$ TEMRA (Pre-Ex: 1,227.14 ± 1000.43 vs. Post-Ex: 3,241.03 ± 2620.02, $P < 0.01$) Post-Ex, but lower numbers in Recovery ($CD4^+$ CM: 3,408.03 ± 2150.57, $P = 0.001$, $CD8^+$ EM: 3,565.91 ± 2940.79, $P = 0.02$, $CD8^+$ TEMRA: 1,112.80 ± 898.41, $P = 0.02$). Moreover, total T cell number was significant higher Post-Ex vs. Recovery (Post-Ex: 69,592.28 ± 21,199.11 vs. Recovery: 34,897.79 ± 23,682.26, $P < 0.0001$) but not vs. Pre-Ex (49,516.98 ± 33,522.09, $P = 0.08$). **(Figure 4.5A)**.

4.4.5.2 Absolute Changes in Metabolic Parameters upon Stimulation

There were significant differences in PER **(Table 4.9** and **Figure 4.5D)** at each time point between control vs. activated naïve $CD4^+$ T cells and $CD8^+$ T cells, and PBMCs, but there was no main effect of time ($P = 0.06$) observed across cell types naïve $CD4^+$ ($F(2, 27) = 2.41$, $P = 0.11$) and $CD8^+$ ($F(2, 27) = 0.33$, $P = 0.72$) T cells, and PBMCs ($F(2, 27) = 0.42$, $P = 0.66$) which resulted in significant increases in glycolytic ATP synthesis rate after activation across all timepoints for naïve $CD4^+$ T cells (Pre-Ex,

Control: 42.03 ± 20.94 vs. Activation: 96.94 ± 37.11, P < 0.0001, Post-Ex, Control: 35.67 ± 12.81 vs. Activation: 70.14 ± 26.10, P = 0.003, Recovery, Control: 27.12 ± 15.51 vs. Activation: 71.45 ± 28.84, P = 0.0002) and Naïve $CD8^+$ T cells (Pre-Ex, Control: 32.69 ± 26.54 vs. Activation: 53.65 ± 31.18, P = 0.04, Post-Ex, Control: 23.19 ± 8.50 vs. Activation: 44.72 ± 21.06, P = 0.03, Recovery, Control: 28.51 ± 19.48 vs. Activation: 52.99 ± 18.69, P = 0.02), but not PBMCs **(Figure 4.5F)**. Absolute PER was significantly greater in PBMCs vs naïve T cells (F (2, 54) = 79.67, P < 0.0001).

Table 4.9 Comparative PER data between Control and Activation

Cell Type	Timepoints	Mean and STDev. Comparison (Control vs. Activation)	P-Value
Naïve $CD4^+$ T cells	Pre-Ex	36.04 ± 20.02 vs. 87.21 ± 37.66	< 0.0001
	Post-Ex	29.39 ± 13.58 vs. 61.13 ± 24.17	0.0002
	Recovery	20.85 ± 16.36 vs. 61.68 ± 29.05	< 0.0001
Naïve $CD8^+$ T cells	Pre-Ex	26.03 ± 26.97 vs. 43.92 ± 30.34	0.0002
	Post-Ex	15.64 ± 7.01vs. 36.82 ± 20.14	0.0001
	Recovery	21.12 ± 20.52 vs. 43.74 ± 20.60	< 0.0001
PBMCs	Pre-Ex	162.25 ± 90.14 vs. 257.14 ± 153.24	0.01
	Post-Ex	203.12 ± 108.19 vs. 302.81 ± 142.49	0.008
	Recovery	192.65 ± 119.32 vs. 270.15 ± 100.67	0.03

Moreover, the significant differences in glycolytic ATP synthesis rate co-changed mitochondrial ATP synthesis which altered ATP-linked respiration rate, but the changes were significantly greater in activated naïve $CD4^+$ T cells at Recovery between Control: 11.21 ± 6.66 vs. Activation: 17.87 ± 5.59, (P = 0.03) only **(Figure 4.5E).** No differences in ATP synthesis rate were observed across cell types and timepoints **(Figure 4.5F)** in response to activation (Naïve $CD4^+$ (P = 0.06), Naïve $CD8^+$ (P =0.49), PBMCs (P = 0.26) or mitochondrial respiration and Glycolysis (Naïve $CD4^+$ (P = 0.31), Naïve $CD8^+$ (P =0.43), PBMCs (P = 0.32).

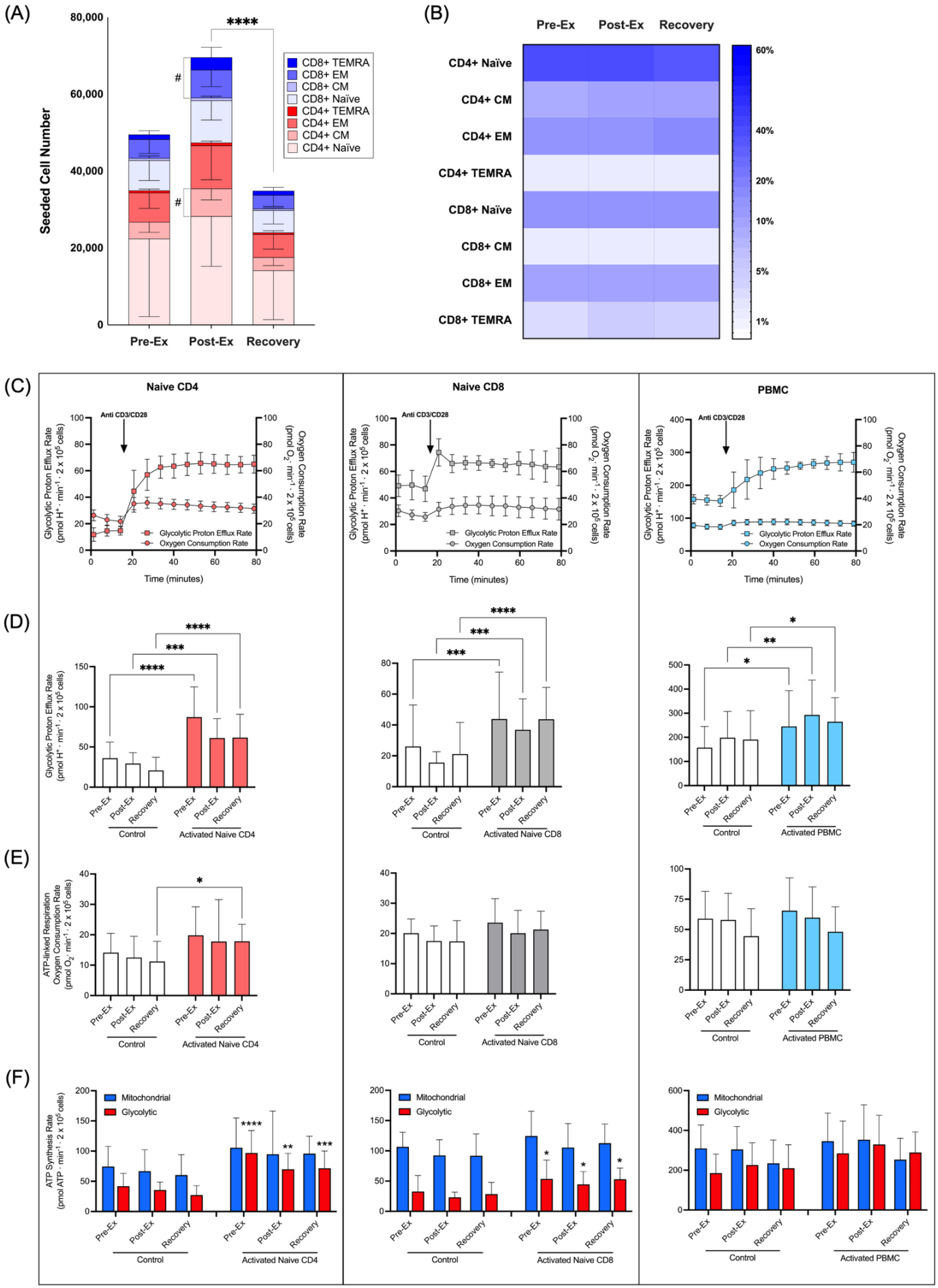
(A)
Seeded Cell Number
80,000
60,000
40,000
20,000
0
****
#
#
CD8+ TEMRA
CD8+ EM
CD8+ CM
CD8+ Naïve
CD4+ TEMRA
CD4+ EM
CD4+ CM
CD4+ Naïve
Pre-Ex
Post-Ex
Recovery
(B)
Pre-Ex
Post-Ex
Recovery
CD4+ Naïve
CD4+ CM
CD4+ EM
CD4+ TEMRA
CD8+ Naïve
CD8+ CM
CD8+ EM
CD8+ TEMRA
60%
40%
20%
10%
5%
1%
(C)
Naive CD4
Naive CD8
PBMC
Anti CD3/CD28
Glycolytic Proton Efflux Rate
(pmol H+ · min-1 · 2 x 10^5 cells)
Oxygen Consumption Rate
(pmol O2 · min-1 · 2 x 10^5 cells)
Glycolytic Proton Efflux Rate
Oxygen Consumption Rate
Time (minutes)
(D)
Glycolytic Proton Efflux Rate
(pmol H+ · min-1 · 2 x 10^5 cells)
Pre-Ex
Post-Ex
Recovery
Control
Activated Naive CD4
Activated Naive CD8
Activated PBMC
(E)
ATP-linked Respiration
Oxygen Consumption Rate
(pmol O2 · min-1 · 2 x 10^5 cells)
(F)
ATP Synthesis Rate
(pmol ATP · min-1 · 2 x 10^5 cells)
Mitochondrial
Glycolytic

Figure 4.5 Real-time metabolic responses to CD3/CD28 activation in enriched naïve CD4 $^{+}$and naïve CD8 $^{+}$T cells, and PBMCs. (A) a stacked graph presents the numbers and (B) a heat map shows the frequency of T cell subsets within the seeded PBMC fraction for the activation assay. (C) Representative traces of Glycolytic PER vs. Mitochondrial OCR upon activation were recorded with a Seahorse XFe96 Analyzer. CD3/CD28 activation beads were injected at 14 – 20 minutes, and PER was measured continuously throughout the experimental period after 3 measurements at baseline. (D) PER (E) ATP-linked respiration of activated naïve CD4 $^{+}$(red bars), naïve CD8^{+} (grey bars) T cells, and PBMCs (blue bars) vs. control (white bars) were then calculated. (F) Differences in ATP synthesis rate between mitochondrial respiration (blue bars) and glycolysis (red bars). Data were presented as the mean ± SD of 10 participants. $^{\#}$ indicates significant differences between Pre-Ex and Post-Ex, and * indicates significant differences between timepoints or condition: P > 0.05, $^{\#}$P < 0.05, *P < 0.05, **P < 0.01, ***P < 0.001, ****P < 0.0001.

4.4.6 Prolonged *Ex Vivo* T-cell Stimulation

Two further indicators of naïve T cell activation upon stimulation are an increase in cell diameter (30), and secretion of IL-2, measured in the cell supernatant (31) and these data are presented in **Figure 4.6**. In response to a 12-hour incubation (prolonged activation) with CD3/CD28 beads, the mean diameter (μm) of naïve CD4^{+} (control: 6.37 ± 0.49 vs. activation: 7.50 ± 0.53, Main Effect of Condition: P < 0.0001) and CD8^{+} (control: 6.05 ± 0.59 vs. activation: 7.95 ± 0.54, Main Effect of Condition: P < 0.0001) T cells significantly increased across all timepoints, but there was no differences between timepoints (P = 0.13). The concentration of IL-2 (pg/mL) measured in the

supernatant isolated from naïve CD4$^+$ and naïve CD8$^+$ T cells was greater after activation across all timepoints, but this did not reach statistical significance (F (2, 20) = 0.29, P = 0.75 and F (2, 29) = 0.20, P = 0.82). There were no significant differences across timepoints (P = 0.18) and no correlation between changes in IL-2 concentration and PER within naïve CD4$^+$ or naïve CD8$^+$ T cells across timepoints **(Figure 4.6)**.

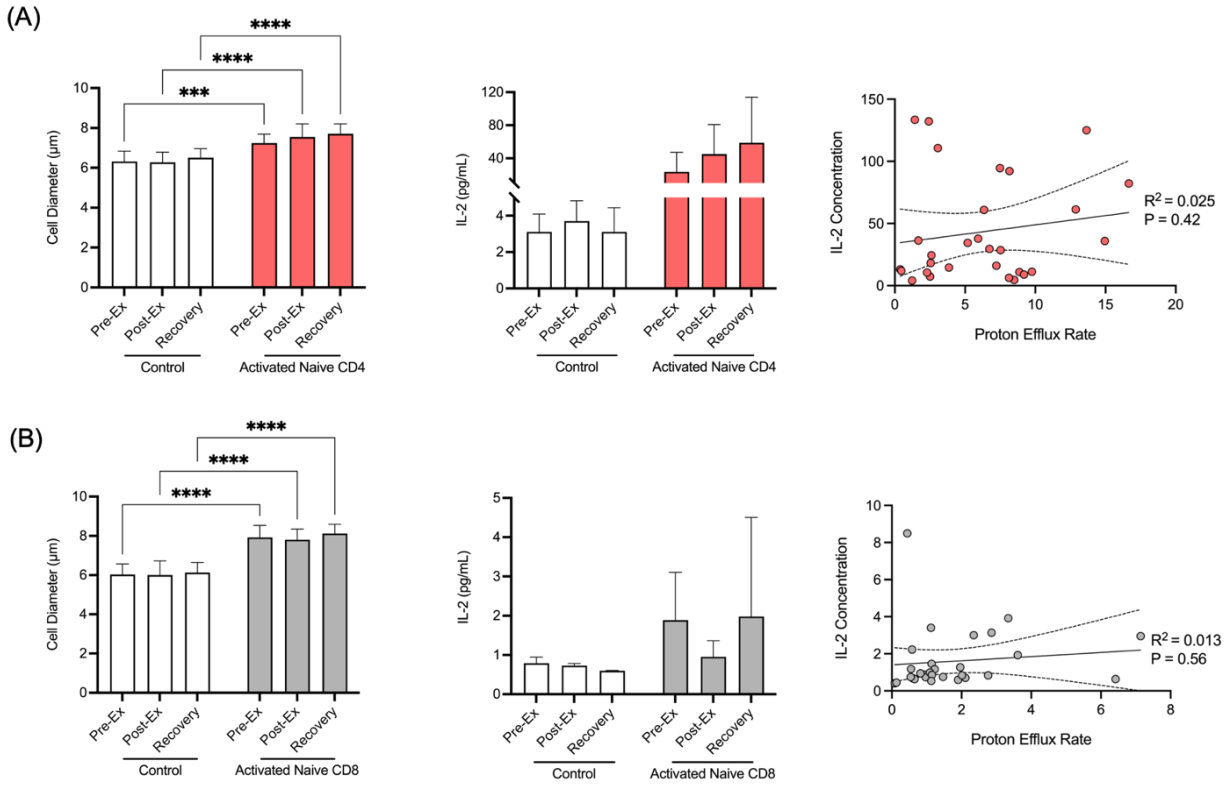

Figure 4.6 (A) Different cell diameters and mean IL-2 concentrations of naïve CD4 $^+$T cells (red bar) vs. controls after prolonged-activation, and Correlation between IL-2 concentration and PER (B) Different cell diameters and mean IL-2 concentrations of naïve CD8 $^+$T cells (grey bar) vs. controls after prolonged-activation, and the IL-2 concentration was plotted against PER of naïve CD4 $^+$or CD8 $^+$T cells, and Pearson and Spearman correlation coefficients determined. Data were presented as the mean

± SD of 10 participants. * indicates significant differences between control and activation: P > 0.05, ***P < 0.001, ****P < 0.0001.

To evaluate changes in circulating nutrient availability in response to prolonged moderate-intensity cycling, the concentrations of glucose, glutamine, and triglycerides were quantified **(Figure 4.7A-C)**. There were no differences in glucose ($F(2, 27) = 1.89$, $P = 0.17$) and triglyceride ($F(2, 25) = 2.17$, $P = 0.14$) concentrations across timepoints, but glutamine concentration **(Figure 4.7B)** significantly decreased at Recovery compared to Pre-Ex (Pre-Ex: 331.50 ± 56.00 vs. Recovery: 255.50 ± 52.56, $P = 0.02$). Moreover, there were no significant correlations between changes in plasma glucose, glutamine or triglyceride concentration and metabolic parameters in all cell types across any timepoints.

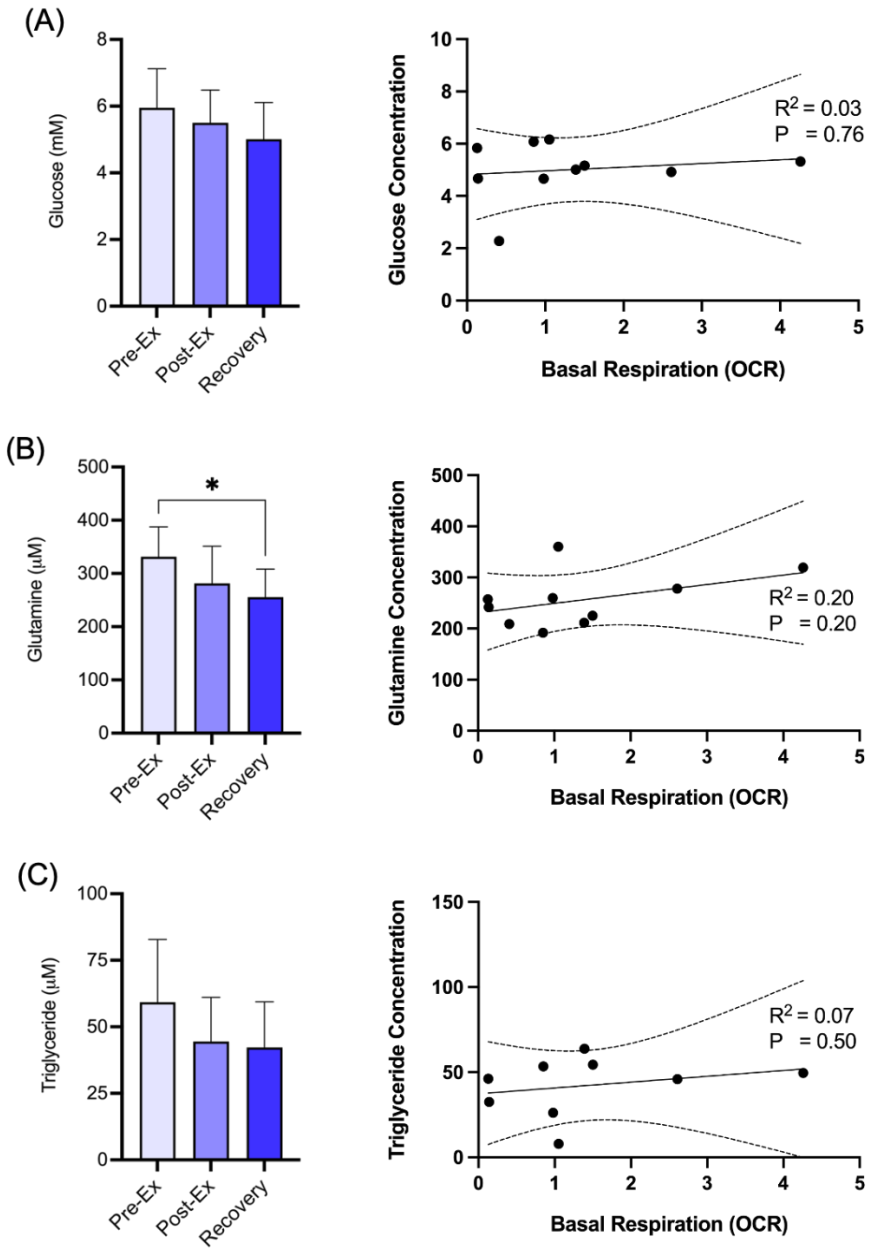

Figure 4.7 Changes in the concentrations of (A) glucose, (B) glutamine, and (C) triglycerides in response to prolonged cycling. A representative correlation between the individual nutrient and basal respiration is provided. Data were presented as the mean ± SD of 10 participants. * indicates significant differences between timepoints: P > 0.05, *P < 0.05.

4.5 Discussion

This study investigated changes in the bioenergetic profiles of isolated naïve $CD4^+$ and $CD8^+$ T cells vs. PBMCs in response to prolonged moderate intensity cycling. The primary finding was that relative to rest, 2 hours of cycling at 95% LT-1 elicited no change to the metabolic phenotypes of naïve $CD4^+$ and $CD8^+$ T cells, and PBMCs immediately after and 2 hours into recovery. Absolute and relative measures of mitochondrial respiration, glycolytic flux and ATP synthesis rate were similar across all timepoints. The contribution of mitochondrial respiration to ATP production was greater than glycolysis in naïve T cells across all timepoints; however, the contribution was not different in PBMCs 2 hours into recovery. In addition, there were no differences in cellular bioenergetic responses to *ex vivo* activation in all cell types isolated before, immediately after or 2 hours into recovery. Collectively, these data indicate that the metabolic phenotype and *ex vivo* responses to activation of the total PBMC fraction and isolated naïve T cells were unaltered within 2 hours of prolonged moderate intensity cycling.

The current study demonstrated an expected exercise-induced lymphocytosis (32–35), with significantly greater concentrations of CM $CD4^+$ (+204%), and naïve (+174%), EM (+184%) and TEMRA $CD8^+$ T cells (+333%) in peripheral blood immediately after prolonged cycling at 95% LT-1, relative to rest. A pattern of preferential mobilisation of antigen experienced T cells was present for $CD8^+$ (TEMRA > EM > N), but not $CD4^+$ T cells. The mobilisation of antigen experienced T cells during bouts of exercise has been a reproducible finding in the field of exercise immunology (34,36,37). The subsequent redeployment of these cells from the circulation is believed to govern

immunosurveillance during recovery (35,38,39) and shifts in cellular metabolism likely facilitate this (4,10,33,40,41). Recent studies have examined immunometabolic changes within circulating PBMCs after exhaustive exercise, sampling immediately following the bout (4,11). Data from the present study indicates no statistically significant difference in the bioenergetic profile of the total PBMC fraction immediately after prolonged moderate intensity cycling. This corroborates previous data indicating no effect of moderate-to-vigorous intensity cycling (30 minutes at 65–70% $\dot{V}O_{2max}$) (11) or maximal swimming (4) on the mitochondrial respiratory function of PBMCs. Analysis of PBMCs 2 hours into recovery was a novel element of the present study design. Our data indicate modulation of energy phenotype at this timepoint, whereby the contribution of mitochondrial respiration and glycolysis to ATP production were equal **(Figure 4.4D)**. Before and immediately after prolonged cycling, the contribution of mitochondrial respiration to ATP production was significantly greater than glycolysis in PBMCs, and across all timepoints in naïve T cells. This finding is challenging to interpret within a mixed cell population and results either from shifts in the composition of cells or cell-by-cell shifts in bioenergetics.

A conundrum persists when evaluating changes in immunity after single bouts of exercise in PBMCs, such that the exchange of cells between the peripheral blood compartment and tissues may hinder analysis of the cells of interest. To overcome these challenges, the present study employed immunomagnetic separation to enrich naïve T cells from the PBMC fraction and examine metabolic phenotype. The differing patterns of N, CM, EM and TEMRA mobilisation observed in peripheral blood **(Table 4.5)** underpin the importance of providing single cell resolution on measures of cellular

bioenergetic responses to acute exercise. This was exemplified by the substantially higher rates of OCR **(Figure 4.3E)** and PER **(Figure 4.5D)** in PBMCs vs. naïve T cells. These differences are independent of any effect of exercise, making interpretation of changes within the mixed PBMC fraction challenging due to distinct metabolic profiles between T cell subsets (4). However, like PBMCs, there were no statistically significant differences in the bioenergetic profiles of naïve $CD4^+$ and $CD8^+$ T cells both immediately and 2 hours after cessation of cycling. Specifically, absolute and relative OCR measures of basal, maximal and ATP-linked respiration, proton leak and spare respiratory capacity were unaltered **(Figures 4.3E)**. Furthermore, rates of glycolysis and the contribution of both this and mitochondrial respiration to ATP production were not different across timepoints **(Figures 4.3F-G)**. Common trends with moderate to large effects sizes **(Table 4.6)** were observed for all metabolic variables in naïve T cells, but not PBMCs, and these changes appeared to mirror changes in naïve T cell concentrations, namely 1) an increase in OCR and PER from Pre-Ex to Post-Ex and 2) a decrease in OCR and PER from Rest to Recovery. Naive T cell concentrations increased immediately after cycling (% difference relative to rest, $CD4^+$: +51.9, P = 0.10 and $CD8^+$: +74.5, P = 0.05) and there was a decrease (% difference relative to rest, $CD4^+$: -37.5, P = 0.40 and $CD8^+$: -28.6, P = 0.32) to marginally below resting values within 2 hours of recovery **(Table 4.5)**, although not all of these changes were statistically significant (42). Circulating metabolites that support T cell function were also examined and although glucose and triglyceride concentrations remained stable throughout the trial, there was a significant decrease in glutamine concentration in Recovery, relative to Rest (**Figure 4.7**). Given the role of glutamine in regulating multiple aspects of T cell function (43,44), this may in part, explain the lower OCR and

PER values in recovery compared to Rest. However, no associations were found between changes in naïve T cell concentrations or glutamine after prolonged cycling with changes in any metabolic variable. Regardless this is speculative given that no statistically significant differences in OCR and PER variables were observed and the large confidence intervals indicate variable responses between participants. More importantly, whereas the decrease in glutamine levels was observed following exercise, this did not affect immune cell biologically as previous studies showed that the concentration remains significantly higher than the minimum levels required for optimal lymphocyte function (45–48).

To determine the impact of prolonged cycling on functional metabolic changes in naïve and antigen experienced T cells (CM, EM and TEMRA), their real-time metabolic responses to activation were examined *ex vivo* using CD3/CD28 activation beads (**Figure 4.5D**). This approach enabled specific T cell responses to be examined within PBMCs and enriched naïve T cells. In response to *ex vivo* activation, there was an increase in maximal glycolytic flux defined by PER, cell diameter and IL-2 production ($P > 0.05$); however, there were no differences observed between timepoints. This indicates preserved metabolic reprogramming of T cells in the recovery from prolonged cycling. An ongoing narrative in the exercise immunology literature purports that prolonged arduous exercise may impair aspects of immune function (49–53). For the current study population of aerobically trained males and females, 2 hours at a moderate intensity (~65% $\dot{V}O_{2max}$) was subjectively perceived as 'fairly light' (RPE: 11.1 ± 1.9) and 'fairly good' (affective response: 2.5 ± 0.6) for physical exertion and enjoyment respectively. Although not arduous, there is no evidence presented herein

to indicate impairment of immune function (with single cell resolution) within 2 hours of continuous exercise in healthy and young males and females.

Collectively, these data indicate that the bioenergetic profile and metabolic responses to activation of naïve $CD4^+$ and $CD8^+$ T cells and the total PBMC fraction were unaltered in response to prolonged moderate intensity cycling. These analyses included measurements both immediately and 2 hours into recovery under controlled laboratory conditions, whereby nutrition and rest were controlled. It is noteworthy that recent studies employing single cell RNA sequencing have revealed pro-glycolytic shifts within mobilised EM T cells after bouts of exhaustive exercise (10), independent of shifts in cell composition. This study directly examined naïve T cells, due to their high proportion within the PBMC fraction (section 4.4.4.2) and ease of isolation compared to antigen experienced T cells which are at a lower frequency (CM, EM, and TEMRA). Although significant mobilisation of $CD8^+$ naïve T cells was reported in the present study, the preferential mobilisation of TEMRA > EM > CM > N (34,36) warrants bioenergetic examination of antigen experienced T cell subsets, and other cell types (e.g., NK cells, monocytes and B cells) after exercise bouts of different intensity.

Many previous studies examining immunometabolic responses to bouts of exercise have mostly defined 'intensity' based on a proportion of $\dot{V}O_{2max}$ (13), which doesn't account for inter-individual variation in metabolic thresholds that occur at different stages of $\dot{V}O_{2max}$ (13). The current study therefore used 95% LT-1 to prescribe a metabolically controlled bout of cycling near aerobic threshold. At this intensity, exercise can be sustained for prolonged durations with minimal fatigue and metabolite

(such as lactate) accumulation (54,55). However, an increase in intensity above LT-1, may only sustain exercise for a short period (~15 minutes) (54,56) which differed from 2-hour cycling protocol applied in the current study. Nonetheless, our data adds to the growing body of literature examining immunometabolic responses to exercise bouts of moderate intensity, notably changes at the single cell level (12).

In conclusion, this was the first study to examine the effect of a metabolically controlled bout of moderate intensity cycling on the bioenergetic phenotype and acute metabolic responses to activation of naïve T cells. These data indicate no perturbations in naïve T cell bioenergetics either immediately or 2 hours after cycling and a similar pattern was observed within the total PBMC fraction. The moderate physiological strain aerobically trained individuals may, in part, explain these findings.

List of References

1. Bisset S. Effect of Muscular Activity prior to Venepuncture on the Respiration of Leucocytes in vitro. 1958.

2. Janssen JJE, Lagerwaard B, Porbahaie M, Nieuwenhuizen AG, Savelkoul HFJ, Van Neerven RJJ, et al. Extracellular flux analyses reveal differences in mitochondrial PBMC metabolism between high-fit and low-fit females. Am J Physiol Endocrinol Metab. 2022 Feb 1;322(2).

3. Lin ML, Hsu CC, Fu TC, Lin YT, Huang YC, Wang JS. Exercise Training Improves Mitochondrial Bioenergetics of Natural Killer Cells. Med Sci Sports Exerc. 2022 May 1;54(5):751–60.

4. Stampley JE, Cho E, Wang H, Theall B, Johannsen NM, Spielmann G, et al. Impact of maximal exercise on immune cell mobilization and bioenergetics. Physiol Rep [Internet]. 2023 Jun 13;11(11):1–10. Available from: https://physoc.onlinelibrary.wiley.com/doi/10.14814/phy2.15753

5. Rangel Rivera GO, Knochelmann HM, Dwyer CJ, Smith AS, Wyatt MM, Rivera-Reyes AM, et al. Fundamentals of T Cell Metabolism and Strategies to Enhance Cancer Immunotherapy. Vol. 12, Frontiers in Immunology. Frontiers Media S.A.; 2021.

6. Nicoli F, Papagno L, Frere JJ, Cabral-Piccin MP, Clave E, Gostick E, et al. Naïve CD8+ t-cells engage a versatile metabolic program upon activation in humans and differ energetically from memory CD8+ T-cells. Front Immunol. 2018;9(December):1–12.

7. Gubser PM, Bantug GR, Razik L, Fischer M, Dimeloe S, Hoenger G, et al. Rapid effector function of memory CD8+ T cells requires an immediate-early glycolytic switch. Nat Immunol. 2013;14(10):1064–72.

8. Rathmell JC, Heiden MG Vander, Harris MH, Frauwirth KA, Thompson CB. In the Absence of Extrinsic Signals, Nutrient Utilization by Lymphocytes Is Insufficient to Maintain Either Cell Size or Viability. Mol Cell. 2000;6:683–92.

9. van der Windt GJW, Everts B, Chang CH, Curtis JD, Freitas TC, Amiel E, et al. Mitochondrial Respiratory Capacity Is a Critical Regulator of CD8 + T Cell Memory Development. Immunity. 2012 Jan 27;36(1):68–78.

10. Batatinha H, Diak DM, Niemiro GM, Baker FL, Smith KA, Zúñiga TM, et al. Human lymphocytes mobilized with exercise have an anti-tumor transcriptomic profile and exert enhanced graft-versus-leukemia effects in xenogeneic mice. Front Immunol [Internet]. 2023 Apr 3;14(April):1–14. Available from: https://www.frontiersin.org/articles/10.3389/fimmu.2023.1067369/full

11. Theall B, Stampley J, Cho E, Granger J, Johannsen NM, Irving BA, et al. Impact of acute exercise on peripheral blood mononuclear cells nutrient sensing and mitochondrial oxidative capacity in healthy young adults. Physiol Rep. 2021 Dec 1;9(23).

12. Rothschild-Rodriguez D, Causer AJ, Brown FF, Collier-Bain HD, Moore S, Murray J, et al. The effects of exercise on complement system proteins in humans: a systematic scoping review. 2022.

13. Lei TH, Wang IL, Chen YM, Liu XH, Fujii N, Koga S, et al. Critical power is a key threshold determining the magnitude of post-exercise hypotension in non-hypertensive young males. Exp Physiol. 2023 Nov 1;108(11):1409–21.

14. Foster J. The General Practice Physical Activity Questionnaire (GPPAQ) A screening tool to assess adult physical activity levels , within primary care Updated May 2009. Nhs. 2009;(May):1–21.

15. Toth MJ, Goran MI, Ades PA, Howard DB, Poehlman ET. Examination of data normalization procedures for expressing peak VO, data [Internet]. Vol. 75, Appl. Physiol. 1993. Available from: www.physiology.org/journal/jappl

16. Oertelt-Prigione S. Immunology and the menstrual cycle. Vol. 11, Autoimmunity Reviews. 2012.

17. World Medical Association Declaration of Helsinki: ethical principles for medical research involving human subjects. J Am Coll Dent. 2014;81(3):14–8.

18. Burke LM, Hawley JA, Wong SHS, Jeukendrup AE. Carbohydrates for training and competition. J Sports Sci. 2011;29(SUPPL. 1).

19. Thomas DT, Erdman KA, Burke LM. Nutrition and Athletic Performance. Med Sci Sports Exerc. 2016;48(3):543–68.

20. Robert B, Brown EB. Psychophysical bases of perceived exertion. Med Sci Sports Exerc. 1982;14:377–81.

21. Howley ET, Bassett Jr DR, Welch HG. Criteria for maximal oxygen uptake: review and commentary. Medicine & Science in Sports & Exercise, 27(9),. 1995;27(9):1292–1301.

22. Berg A, Jakob E, Lehmann M, Dickhuth HH, Huber G, Keul J. [Current aspects of modern ergometry]. Pneumologie. 1990 Jan;44(1):2–13.

23. Zoladz JA, Rademaker AC, Sargeant AJ. Non-linear relationship between O2 uptake and power output at high intensities of exercise in humans. J Physiol. 1995;488(1):211–7.

24. Nieman DC, Henson DA, Dumke CL, Lind RH, Shooter LR, Gross SJ. Relationship between salivary IgA secretion and upper respiratory tract

infection following a 160-km race. J Sports Med Phys Fitness. 2006 Mar;46(1):158–62.

25. Spielberger CD, Gonzalez-Reigosa F, Martinez-Urrutia A, Natalicio LFS, Natalicio DS. The State-Trait Anxiety Inventory. Revista Interamericana de Psicología/Interamerican Journal of Psychology. 2017 Jul 17;5(3 & amp; 4 SE-Articles).

26. Carney CE, Buysse DJ, Ancoli-Israel S, Edinger JD, Krystal AD, Lichstein KL, et al. The consensus sleep diary: Standardizing prospective sleep self-monitoring. Sleep. 2012;35(2):287–302.

27. Hardy CJ, Rejeski WJ. Not What, but How One Feels: The Measurement of Affect during Exercise. J Sport Exerc Psychol. 2016;11(3):304–17.

28. Cohen J. Statistical power analysis for the behavioral sciences. Routledge. 2013;

29. Lovakov A, Agadullina ER. Empirically derived guidelines for effect size interpretation in social psychology. Eur J Soc Psychol. 2021 Apr 1;51(3):485–504.

30. Tasnim H, Fricke GM, Byrum JR, Sotiris JO, Cannon JL, Moses ME. Quantitative measurement of naïve T cell association with dendritic cells, FRCs, and blood vessels in lymph nodes. Front Immunol. 2018 Jul 26;9(JUL).

31. Cantrell DA, Smith KA. The Interleukin-2 T-Cell System: A New Cell Growth Model [Internet]. Vol. 18. 2015. Available from: www.sciencemag.org

32. Turner JE, Wadley AJ, Aldred S, Fisher JP, Bosch JA, Campbell JP. Intensive Exercise Does Not Preferentially Mobilize Skin-Homing T Cells and NK Cells. Med Sci Sports Exerc. 2016;48(7):1285–93.

33. Graff RM, Kunz HE, Agha NH, Baker FL, Laughlin M, Bigley AB, et al. β2-Adrenergic receptor signaling mediates the preferential mobilization of differentiated subsets of CD8+ T-cells, NK-cells and non-classical monocytes in response to acute exercise in humans. Brain Behav Immun. 2018;74(July):143–53.

34. Campbell JP, Riddell NE, Burns VE, Turner M, van Zanten JJCSV, Drayson MT, et al. Acute exercise mobilises CD8+ T lymphocytes exhibiting an effector-memory phenotype. Brain Behav Immun [Internet]. 2009;23(6):767–75. Available from: http://dx.doi.org/10.1016/j.bbi.2009.02.011

35. Rooney B V., Bigley AB, LaVoy EC, Laughlin M, Pedlar C, Simpson RJ. Lymphocytes and monocytes egress peripheral blood within minutes after cessation of steady state exercise: A detailed temporal analysis of leukocyte extravasation. Physiol Behav [Internet]. 2018;194(June):260–7. Available from: https://doi.org/10.1016/j.physbeh.2018.06.008

36. Hunt RM, Elzayat MT, Markofski MM, Laughlin M, LaVoy EC. Characterization of transitional memory CD4+ and CD8+ T-cell mobilization during and after an acute bout of exercise. Front Sports Act Living. 2023;5.

37. Wadley AJ, Cullen T, Vautrinot J, Keane G, Bishop NC, Coles SJ. High intensity interval exercise increases the frequency of peripheral PD-1+ CD8+ central memory T-cells and soluble PD-L1 in humans. Brain Behav Immun Health [Internet]. 2020;3(January):100049. Available from: https://doi.org/10.1016/j.bbih.2020.100049

38. Simpson RJ, Boßlau TK, Weyh C, Niemiro GM, Batatinha H, Smith KA, et al. Exercise and adrenergic regulation of immunity. Brain Behav Immun. 2021;97(June):303–18.

39. Krüger K, Lechtermann A, Fobker M, Völker K, Mooren FC. Exercise-induced redistribution of T lymphocytes is regulated by adrenergic mechanisms. Brain Behav Immun. 2008;22(3):324–38.

40. Nieman DC, Lila MA, Gillitt ND. Immunometabolism: A Multi-Omics Approach to Interpreting the Influence of Exercise and Diet on the Immune System. Annu Rev Food Sci Technol. 2019;10:341–63.

41. Jones N, Piasecka J, Bryant AH, Jones RH, Skibinski DOF, Francis NJ, et al. Bioenergetic analysis of human peripheral blood mononuclear cells. Clin Exp Immunol. 2015 Oct 1;182(1):69–80.

42. Kakanis MW, Peake J, Brenu EW, Simmonds M, Gray B, Hooper SL, et al. The open window of susceptibility to infection after acute exercise in healthy young male elite athletes.

43. Lai AG, Forde D, Chang WH, Yuan F, Zhuang X, Rubio CO, et al. Glucose and glutamine availability regulate HepG2 transcriptional responses to low oxygen . Wellcome Open Res. 2018;3.

44. Cruzat V, Rogero MM, Keane KN, Curi R, Newsholme P. Glutamine: Metabolism and immune function, supplementation and clinical translation. Vol. 10, Nutrients. MDPI AG; 2018.

45. Salleh M, Ardawi M, Newsholme EA. Glutamine metabolism in lymphocytes of the rat. Vol. 212, Biochem. J. 1983.

46. Newsholme EA, Crabtree B, Ardawi MSM. GLUTAMINE METABOLISM IN LYMPHOCYTES: ITS BIOCHEMICAL, PHYSIOLOGICAL AND CLINICAL IMPORTANCE. Quarterly Journal of Experimental Physiology. 1985 Oct 10;70(4):473–89.

47. Brand K, Fekl W, Von Hintzenstern J, Langer K, Luppa P, Schoerner C. Metabolism of Glutamine in Lymphocytes.

48. Cruzat V, Rogero MM, Keane KN, Curi R, Newsholme P. Glutamine: Metabolism and immune function, supplementation and clinical translation. Vol. 10, Nutrients. MDPI AG; 2018.

49. Nieman DC, Johanssen LM, Lee JW, Arabatzis K. Infectious episodes in runners before and after the Los Angeles Marathon. Journal of Sports Medicine and Physical Fitness. 1990;30(3):316–28.

50. Nieman DC, Henson DA, Dumke CL, Lind RH, Shooter LR, Gross SJ. Relationship between salivary IgA secretion and upper respiratory tract infection following a 160-km race. J Sports Med Phys Fitness. 2006 Mar;46(1):158–62.

51. Nieman DC. Is infection risk linked to exercise workload? Med Sci Sports Exerc. 2000;32(7 SUPPL.).

52. Simpson R, Campbell J, Gleeson M, Krüger K, Nieman D, Pyne D, et al. Can exercise affect immune function to increase susceptibility to infection? J Appl Sport Psychol. 2015;27(2):216–34.

53. Campbell JP, Turner JE. Debunking the Myth of Exercise-Induced Immune Suppression: Redefining the Impact of Exercise on Immunological Health Across the Lifespan. Front Immunol [Internet]. 2018 Apr 16;9(APR):1–21. Available from: http://journal.frontiersin.org/article/10.3389/fimmu.2018.00648/full

54. Iannetta D, Inglis EC, Mattu AT, Fontana FY, Pogliaghi S, Keir DA, et al. A Critical Evaluation of Current Methods for Exercise Prescription in Women and Men. Med Sci Sports Exerc. 2020 Feb 1;52(2):466–73.

55. Cannon DT, White AC, Andriano MF, Kolkhorst FW, Rossiter HB. Skeletal muscle fatigue precedes the slow component of oxygen uptake kinetics during exercise in humans. Journal of Physiology. 2011 Feb;589(3):727–39.

56. Barstow TJ, Mole PA. Linear and nonlinear characteristics of oxygen uptake kinetics during heavy exercise [Internet]. 1991. Available from: www.physiology.org/journal/jappl

Chapter 5: General Discussion

The overarching theme of this thesis was to explore the effect of single sessions of exercise on the number and function of immune cells in peripheral blood, with two primary aims:

1. To establish whether low and high-volume interval cycling increased peripheral blood HSPC and $CD56^{dim}$ NK cell concentrations to a greater degree than continuous cycling **(Chapter 2)**.

2. To investigate the effect of prolonged moderate intensity exercise (defined by 95% LT-1) on the metabolic phenotypes and real-time responses to activation of naïve $CD4^+$ and $CD8^+$ T cells compared to the peripheral blood mononuclear cell (PBMC) fraction **(Chapter 4)**.

The General Discussion chapter will provide a concise summary of the key findings presented in each experimental chapter. Subsequent sections will discuss a more comprehensive analysis of each chapter, specifically examining how the chapters align with the aforementioned objectives, and common themes and concepts that link the experimental chapters. The thesis will also address study limitations and provide recommendations for further research.

5.1 Summary of Key Findings

Chapter 2 compared the effect of high-intensity interval exercise (HIIE) of both low volume (LV-HIIE) and high volume (HV-HIIE) vs. moderate-intensity continuous exercise (MICE) on the peripheral blood concentrations of HSPCs and $CD56^{dim}$ NK cells after each of 4 bouts of LV-HIIE and HV-HIIE. The data in this chapter revealed that performing 2 x 2-minute bouts of LV-HIIE and 3 x 4-minute bouts of HV-HIIE were effective in elevating the peripheral blood concentration of $CD38^{+}$ HSPCs compared to rest. However, there was no significant increase in $CD38^{+}$ HSPC concentrations throughout MICE. Following MICE and the 4^{th} bout of HIIE, the concentration of HSPCs was only higher than at rest in LV-HIIE. Moreover, following all trials, there was a small reduction in the expression of bone marrow homing receptor VLA-4, but no change in the expression of CXCR-4 on exercise-induced mobilised HSPCs. In addition, the number of $CD56^{dim}$ NK cells in peripheral blood was markedly higher after bouts of LV-HIIE and HV-HIIE compared to MICE. Overall, these data indicate that exercise intensity is a prominent driver for stimulating the movement of immune cells into peripheral blood that are relevant to HSPC transplantation.

Chapter 3 optimised experimental methods to examine immunometabolic processes in T cells for implementation in Chapter 4 by conducting EFA assays in a Jurkat cell line and enriched primary naïve $CD4^{+}$ and $CD8^{+}$ T cells. The choice of Jurkat cells was taken in light of the COVID-19 pandemic. Despite best endeavours, the high rates of basal glycolysis in these cells made it challenging to manipulate glycolytic rates after CD3/CD28 bead activation and thus efforts were halted when COVID-19 restrictions were lifted. Chapter 3 showed that primary naïve $CD4^{+}$ and $CD8^{+}$ T cells (200 x 10^{3}

cells) required a specific quantities of nutrients, namely as glucose and glutamine to maximise PER following CD3/CD28 bead-induced activation using Seahorse XFe96 EFA. Moreover, Chapter 3 demonstrated that activation induced changes in glycolysis (defined by PER) in naïve $CD4^+$ and $CD8^+$ T cells were significantly greater when PBMCs and naive T cells were isolated and analysed immediately from sodium heparin blood collection tubes at room temperature. Finally, the utilisation of silicone inserts for cell seeding and standard assay media in EFA resulted in accurate and enhanced changes in PER following activation.

In conjunction with the development of methods in Chapter 3, Chapter 4 employed a novel human study design and methodology to elucidate the effect of prolonged moderate intensity exercise on T cell bioenergetics, providing single cell resolution for naïve CD4+ and CD8+ T cell subsets. This chapter demonstrated that 2-hours of moderate intensity cycling at a power output eliciting 95% lactate threshold-1 did not alter the metabolic phenotypes of naïve $CD4^+$ and $CD8^+$ T cells, or PBMCs immediately after and into recovery, relative to rest. Absolute and relative measures of mitochondrial respiration, glycolytic flux and ATP synthesis rate were similar across all timepoints. The contribution of mitochondrial respiration to ATP production was greater than glycolysis in naïve T cells across all timepoints; however, the contribution balanced in PBMCs 2 hours into recovery. In addition, in response to *ex vivo* activation, there were no differences in cellular bioenergetic responses in all cell types isolated before, immediately after or 2 hours into recovery.

5.2 The Link between Experimental Chapters

Supporting findings from previous studies, our data in Chapter 2 showed that exercise-induced leukocytosis was intensity-dependent (1). Exercise-induced leukocytosis was likely driven by increases in haemodynamic shear stress and β2-adrenergic (β2-AR) signalling (1,2), which drives preferential mobilisation of effector immune cells such as cytolytic NK cells ($CD56^{dim}$) (2,3). When comparing exercise-induced leukocytosis between cycling protocols used in Chapters 2 and 4, both HIIE protocols applied in Chapter 2 resulted in greater fold increases in lymphocytes (HV-HIIE: +1.39 and LV-HIIE: +1.47) and NK cells (HV-HIIE: +4.60 and LV-HIIE: +4.83) than 2 hours of cycling at a power output eliciting 95% LT-1. This was likely driven by a higher exercise intensity used in Chapter 2 vs. 4, exemplified by greater objective and subjective physiological responses such as HR (+37.12%) and RPE (+55.39%) respectively. Both Chapters employed acute cycling studies, with similarities with regards to study design, control of confounding variables (e.g., environmental conditions, monitoring of illness, sleep quality, anxiety, restriction of alcohol and caffeine intake prior to trials) and participant characteristics (except biological sex), including sample size, age, fitness level. Collectively, data in this thesis confirms the most reproducible finding in exercise immunology, namely a rapid exercise intensity-dependent induced leukocytosis. These responses were then used as a model to examine our two primary research questions, outlined above.

With regards to the outcome measures examined in Chapters 2 and 4 of this thesis, Chapter 4 examined immune function using more sophisticated analytical methods such as real-time bioenergetic profiling. Chapter 2 measured cell surface marker

expression on immune cell subsets to perform cell counts and phenotyping, focussing primarily on the peripheral blood concentration of HSPCs and the bone marrow homing potential of these cells. Although more basic, this chapter had a very applied approach, which was novel.

5.3 Novelty of Methodological Approaches in Experimental Studies

Chapter 2 was the first study to comprehensively investigate changes in peripheral blood HSPC concentrations over a detailed timecourse for bouts of HIIE of different volumes. The broader aim of this chapter was to establish a feasible and safe cycling protocol suitable for use in a PBSC donation setting. To design high and low-volume HIIE procedures, we adopted the lower (85%) and upper intensity (95%) thresholds for maximal heart rate respectively, to align with clinical HIIE guidelines (4,5). A further novel aspect of the study was applying serial blood sampling during and post-exercise to explore detailed changes over time in HSPC mobilisation into the bloodstream following each interval of HIIE vs. time-matched samples during MICE. This was novel, given that many studies simply examine changes before and after the complete exercise bout. We were therefore able to establish that just 4 minutes of LV-HIIE and 12 minutes of HV-HIIE significantly increased HSPC concentrations compared to rest. At the end of the cycling bouts, there were significantly greater numbers of $CD56^{dim}$ NK cells in peripheral blood compared to steady state cycling. Collectively, these findings indicate that compared to duration, the mobilisation of HSPCs and $CD56^{dim}$ NK cells were more determined by exercise intensity with only 4 minutes HIIE significantly increasing these cell concentrations in peripheral blood.

The International Society of Hematotherapy and Graft Engineering (ISHAGE) established a reliable method for measuring the concentration of HSPCs in whole blood in 1998 (6) and this is used clinically for PBSC donations and HSCTs. When comparing studies that have examined changes in HSPCs in response to exercise, the reported variance between studies is marked and this gold standard method outlined by ISHAGE has not been used. High variance across studies can possibly be attributed to the selection of either whole blood or purified PBMCs for the labelling of cell surface antibodies and the utilisation of quantitative single or double platform methodologies. The ISHAGE single platform method utilises whole blood to quantify HSPCs and demonstrates intra- and inter- laboratory variance > 5% and > 9%, respectively (6) but the double platform method has been reported to have inter-laboratory variance as high as 21% (7). With a validated Boolean gating strategy applied under ISHAGE guidance, Chapter 2 employed this method to precisely enumerate $CD34^+$ HSPCs.

A recent scoping review found a lack of research examining immunometabolic responses of isolated immune cell subsets to exercise (8). In addition, most of the studies have predominantly set the intensity based on the fraction of $\dot{V}O_{2max}$ or HR_{max}, rather than use metabolic thresholds like the LT to determine the appropriate exercise intensity (9). Since metabolic thresholds occur at different fractions of $\dot{V}O_{2max}$ (10), this method may result in a different metabolic stimulus between participants of the study (9). The cycling protocol in Chapter 4 therefore employed a hybrid test, combining LT and $\dot{V}O_{2max}$ measurements to define individual fitness level where LT was used to set exercise intensity and $\dot{V}O_2$ uptake data in corresponding recorded LT was used to monitor workload during 2-hour exercise protocol.

Engaging in exercise at a low-moderate intensity leads to more stable peripheral blood concentrations of T cells. Most of studies examining immunometabolic responses to exercise have evaluated changes in the heterogenous PBMC fraction immediately after maximal exercise. The substantial fluctuations that acute exercise exerts on peripheral blood immune cell composition and the unique metabolic profiles that different cells, such as T cells possess, renders examination of the PBMC bioenergetic profile limited. Therefore, enrichment of peripheral blood with antigen experienced T cells with higher basal respiration may, in part, underpin the heightened metabolic activity of the PBMC fraction during exercise, rather than individual T cell changes *per se* (11). A recent study conducted by Batatinha *et al.,* (2023) employing single cell RNA sequencing reported that genes associated with metabolic regulation were enriched in $CD4^+$ and $CD8^+$ T cells after maximal exercise, most notably in EM, rather than CM or naïve subsets (12). Chapter 4 of this thesis, therefore employed single cell analysis to provide better understanding on exercise-induced regulation of immune cell bioenergetics.

Ex vivo T cell activation augments shifts in bioenergetic processes to fulfil the energy demands of the cell. These metabolic changes reflect T cells encountering pathogens *in vivo* (13). Investigating the effects of exercise on *ex vivo* T cell activation permits modelling of how bouts of exercise influence functional metabolic regulation of T cells in response to a challenge. Metabolic pathways such as glycolysis and mitochondrial respiration that are responsible for ATP production in T cells (14) can be measured simultaneously using EFA. The Seahorse XF analyser interrogates real-time metabolic

assessments of cellular OCR and ECAR using small quantities of cells and provides flexibility to construct customisable experiments that enable exposure of bead-conjugated antibodies, ligands, inhibitors, and substrates to robustly evaluate the metabolic phenotype of different cells. By employing these methods, data from this chapter has shown that in response to 2 hours of moderate intensity cycling, the metabolic profiles of naïve $CD4^+$ and $CD8^+$ T cells were unaltered immediately after, and 2 hours into recovery, relative to rest.

5.4 Limitations

Although the study population in Chapter 4 included both male and female participants (n = 10), experimental Chapter 2 (n = 11) included only male participants due to constraints in recruitment following lifting of COVID-19 restrictions. Hence, sample size and population in both experimental studies, from a biological standpoint were low in numbers and not representative with regards to biological sex for Chapter 2. Another limitation was the limited control over participants' activities and diets prior to laboratory visits in all experimental sessions. In Chapter 2 and 4, participants were asked to refrain from vigorous exercise 48 hours before each trial to prevent alterations in resting immune function and to replicate their diet before undertaking an overnight fast before the laboratory visits in the morning, but there was no supervision or monitoring of these procedures. Objectively monitoring participants' activity using accelerometery and providing meals would have reduced any potential influence of these factors on immunity.

5.5 Future Work and Conclusions

Chapter 2 offers preliminary evidence to justify the utilisation of HIIE protocols in a PBSC donation setting, but at present, only in healthy young males. Physiologically, our data show that only 4 minutes of LV-HIIE resulted in a greater increase in peripheral blood HSPCs compared to 30 minutes of continuous cycling. However, the application of these findings is currently limited. Clinical trials are necessary to examine if intermittent cycling during apheresis (with prior G-CSF administration) is safe and can increase the harvest of HSPCs and whether this promotes better engraftment and health outcomes (survival and relapse) for patients. However, prior to conducting these trials, it is necessary to first investigate whether implementing HIIE throughout a typical PBSC collection period, which is approximately 3 hours can maximise HSPC concentrations in peripheral blood. If HSPC concentrations can be maintained over this time, then this provides compelling evidence to explore cycling during apheresis. The impact of this approach on immune composition, notably NK cells is equally important given the importance of these cells in offsetting GvHD following allogenic transplantation (15). Notably, our data revealed a striking increase (+324.63%) in $CD56^{dim}$ NK cells after just 8 minutes of interval cycling. It is conceivable that spacing intervals over 3 hours (with adequate rest periods) could sustain concentrations of these cells in peripheral blood. In addition to the physiological potential of exercise to optimise the quantity of HSPC, further research is needed to evaluate the feasibility and acceptability of such an approach for both allogeneic and autologous donors who are undergoing G-CSF treatment. A recent study conducted by Kuehl et at., (2023) reported that patients undertaking HIIE as prehabilitative care (for future cancer treatment) prior to allogeneic HSCT had very high adherence (92%) over 4-12 weeks

(16). This data is highly encouraging to support the concept of HIIE in clinical populations that might benefit from cycling during apheresis.

Chapter 3 provides a robust protocol design which worked well in experimental chapter 4. However, chapter 4 demonstrated that prolonged moderate intensity cycling protocol applied did not alter the metabolic phenotypes of naïve $CD4^+$ and $CD8^+$ T cells, or PBMCs immediately after and 2 hours into recovery, relative to rest. This indicate that the physiological strain may be insufficient to create changes in the metabolic phenotype of immune cells. Therefore, future studies are needed to apply the series of validated assays with more intense bouts of exercise or periods of intensified training/overtraining to investigate exercise effect on immunometabolic profiles.

Conclusion

The main objective of the thesis was to investigate the impact of single bouts of cycling on the number and function of peripheral blood immune cells. Chapter 2 revealed that interval cycling evokes greater changes in peripheral blood haematopoietic stem and progenitor and cytolytic natural killer cell concentrations than continuous cycling. For HSPCs, this was apparent after just 2 x 2-minute bouts of LV-HIIE and 3 x 4-minute bouts of HV-HIIE, and not 30 minutes of continuous cycling. Chapter 4 reports that a 2-hour bout of moderate intensity cycling does not alter the metabolic phenotypes of naïve $CD4^+$ and $CD8^+$ T cells or the mixed PBMC fraction within 2 hours of recovery. This thesis presents mechanistic data to advance knowledge of the acute immune response to exercise (Chapters 3 and 4) and data to support future applied work that may exploit acute changes in clinically relevant immune cells for patient benefit

(Chapter 2). Collectively, these studies support the growing area of exercise immunology and its emerging applications in multiple areas of human health.

List of References

1. Agha NH, Baker FL, Kunz HE, Graff R, Azadan R, Dolan C, et al. Vigorous exercise mobilizes CD34+ hematopoietic stem cells to peripheral blood via the β2-adrenergic receptor. Brain Behav Immun [Internet]. 2018;68:66–75. Available from: https://www.sciencedirect.com/science/article/pii/S0889159117304543

2. Graff RM, Kunz HE, Agha NH, Baker FL, Laughlin M, Bigley AB, et al. β2-Adrenergic receptor signaling mediates the preferential mobilization of differentiated subsets of CD8+ T-cells, NK-cells and non-classical monocytes in response to acute exercise in humans. Brain Behav Immun. 2018;74(July):143–53.

3. Simpson RJ, Kunz H, Agha N, Graff R. Exercise and the Regulation of Immune Functions [Internet]. 1st ed. Vol. 135, Progress in Molecular Biology and Translational Science. Elsevier Inc.; 2015. 355–380 p. Available from: http://dx.doi.org/10.1016/bs.pmbts.2015.08.001

4. Weston KS, Wisløff U, Coombes JS. High-intensity interval training in patients with lifestyle-induced cardiometabolic disease: A systematic review and meta-analysis. Br J Sports Med. 2014;48(16):1227–34.

5. Taylor JL, Holland DJ, Spathis JG, Beetham KS, Wisløff U, Keating SE, et al. Guidelines for the delivery and monitoring of high intensity interval training in clinical populations. Prog Cardiovasc Dis [Internet]. 2019;62(2):140–6. Available from: https://doi.org/10.1016/j.pcad.2019.01.004

6. Keeney M, Chin-Yee I, Weir K, Popma J, Nayar R, Robert Sutherland D. Single platform flow cytometric absolute CD34+ cell counts based on the ISHAGE guidelines. Communications in Clinical Cytometry. 1998;34(2):61–70.

7. Gratama JW, Kraan J, Keeney M, Sutherland DR, Granger V, Barnett D. Validation of the single-platform ISHAGE method for CD34+ hematopoietic stem and progenitor cell enumeration in an international multicenter study. Cytotherapy. 2003;5(1):55–65.

8. Rothschild-Rodriguez D, Causer AJ, Brown FF, Collier-Bain HD, Moore S, Murray J, et al. The effects of exercise on complement system proteins in humans: a systematic scoping review. 2022.

9. Iannetta D, Inglis EC, Mattu AT, Fontana FY, Pogliaghi S, Keir DA, et al. A Critical Evaluation of Current Methods for Exercise Prescription in Women and Men. Med Sci Sports Exerc. 2020 Feb 1;52(2):466–73.

10. Lei TH, Wang IL, Chen YM, Liu XH, Fujii N, Koga S, et al. Critical power is a key threshold determining the magnitude of post-exercise hypotension in non-hypertensive young males. Exp Physiol. 2023 Nov 1;108(11):1409–21.

11. Stampley JE, Cho E, Wang H, Theall B, Johannsen NM, Spielmann G, et al. Impact of maximal exercise on immune cell mobilization and bioenergetics. Physiol Rep [Internet]. 2023 Jun 13;11(11):1–10. Available from: https://physoc.onlinelibrary.wiley.com/doi/10.14814/phy2.15753

12. Batatinha H, Diak DM, Niemiro GM, Baker FL, Smith KA, Zúñiga TM, et al. Human lymphocytes mobilized with exercise have an anti-tumor transcriptomic profile and exert enhanced graft-versus-leukemia effects in xenogeneic mice. Front Immunol [Internet]. 2023 Apr 3;14(April):1–14. Available from: https://www.frontiersin.org/articles/10.3389/fimmu.2023.1067369/full

13. Mercier-Letondal P, Marton C, Godet Y, Galaine J. Validation of a method evaluating T cell metabolic potential in compliance with ICH Q2 (R1). J Transl Med. 2021 Dec 1;19(1).

14. Chapman NM, Shrestha S, Chi H. Metabolism in Immune Cell Differentiation and Function. In: Advances in Experimental Medicine and Biology [Internet]. 2017. p. 1–85. Available from: http://link.springer.com/10.1007/978-94-024-1170-6_1

15. Porrata LF, Gertz MA, Geyer SM, Litzow MR, Gastineau DA, Moore SB, et al. The dose of infused lymphocytes in the autograft directly correlates with clinical outcome after autologous peripheral blood hematopoietic stem cell transplantation in multiple myeloma. Leukemia. 2004;18(6):1085–92.

16. Kuehl R, Feyer J, Limbach M, Pahl A, Stoelzel F, Beck H, et al. Prehabilitative high-intensity interval training and resistance exercise in patients prior allogeneic stem cell transplantation. Sci Rep. 2023 Dec 1;13(1).